



HAL
open science

Design of DDF protocols for plug-and-play relays

Mélanie Plainchault

► **To cite this version:**

Mélanie Plainchault. Design of DDF protocols for plug-and-play relays. Other. Télécom ParisTech, 2012. English. NNT : 2012ENST0023 . pastel-00958365

HAL Id: pastel-00958365

<https://pastel.hal.science/pastel-00958365>

Submitted on 12 Mar 2014

HAL is a multi-disciplinary open access archive for the deposit and dissemination of scientific research documents, whether they are published or not. The documents may come from teaching and research institutions in France or abroad, or from public or private research centers.

L'archive ouverte pluridisciplinaire **HAL**, est destinée au dépôt et à la diffusion de documents scientifiques de niveau recherche, publiés ou non, émanant des établissements d'enseignement et de recherche français ou étrangers, des laboratoires publics ou privés.



École doctorale n°130 : 2012 ENST 023

Doctorat ParisTech

T H È S E

pour obtenir le grade de docteur délivré par

Télécom ParisTech

Spécialité : Électronique et Communications

présentée et soutenue publiquement par

Mélanie PLAINCHAULT

le 9 mai 2012

**Conception de protocoles DDF pour le
déploiement de relais auto-configurables.**

Directeur de thèse : **Ghaya REKAYA BEN-OTHTMAN**, Télécom ParisTech

Co-encadrement de la thèse : **Nicolas GRESSET**, Mitsubishi Electric R&D Center Europe

Jury

M. Mérouane **DEBBAH**, Professeur, Supélec, France
M. **Joseph BOUTROS**, Professeur, Texas A&M University, Qatar
M. **David GESBERT**, Professeur, Eurécom, France
M. **Jean-Claude BELFIORE**, Professeur, Télécom ParisTech, France
M. **Ahmed SAADANI**, Orange Labs, France

Président du jury
Rapporteur
Rapporteur
Examinateur
Examinateur

**T
H
È
S
E**

Télécom ParisTech

école de l'Institut Télécom – membre de ParisTech

Remerciements

Je souhaite tout d'abord remercier les membres du jury d'avoir accepté d'évaluer mes travaux de thèse, ainsi que pour leurs nombreuses et intéressantes questions lors de ma soutenance.

Un grand merci ensuite à Ghaya et Nicolas, mes encadrants sans qui cette thèse n'aurait jamais vu le jour, pour leur patience et leurs conseils. Tout particulièrement, merci Nicolas pour ces longues heures passées au téléphone ou sur gtalk, ces moments de réflexions privilégiés lors de mes séjours à MERCE qui ont fait que j'ai toujours aimé venir m'exiler à Rennes. Pourvu que ces échanges continuent, ils sont tellement enrichissants.

Merci à tous mes collègues de MERCE, Cristina, Loïc, David, Mourad, Magali, Jacqueline, Marie, et les autres, qui sont eux aussi des passionnés de la recherche, de m'avoir donné la foi dans ces travaux de longue haleine. Merci de m'avoir si bien accueilli à chaque fois que je suis venue travailler au labo.

Je tiens ensuite à remercier du fond du coeur mes parents, mes frères, Laurent qui ont été à mes côtés pendant ces trois années où l'ascenseur émotionnel subi par tout thésard, m'a sûrement rendue insupportable. Vraiment, merci.

Je pense aussi à tous mes amis, de Télécom, Franck, Pierre, Sébastien, Chadi, Germain ... et d'ailleurs, Nico, Iponie, Rémi, Flo, Mathieu et Olivia ... d'avoir rendu ces années bien agréables. Je suis sûre que vous serez aussi là pour les suivantes, heureusement que notre amitié ne se termine pas avec le point final de cette thèse !

Un grand Merci à tous.

Abstract

Relaying has been proposed as an efficient solution to increase transmission reliability by providing spatial diversity, and to increase transmission efficiency. Among the wide variety of existing relaying protocols proposed for the relay channel, we are interested in the Dynamic Decode and Forward (DDF) protocol as it outperforms all previously defined forwarding strategies in terms of Diversity Multiplexing Tradeoff. When using the DDF protocol, the relay assists the transmission only if it correctly decodes the sent message before the destination.

We propose a practical implementation of this DDF protocol based on channel coding for hybrid automatic repeat request. Then, we define and study two relaying schemes for the relay channel that can be used when the source is relay-unaware: the Monostream scheme and the Distributed Alamouti scheme. The performance of these proposed relaying schemes for the DDF protocol are derived for open-loop and closed-loop transmissions. After defining the macro diversity order achieved by a transmission, we derived upper bounds on the achievable macro and micro diversity orders of these DDF protocols when the transmitting nodes use finite symbol alphabet.

We proposed a so-called Patching technique in order to increase this achievable macro diversity order still guaranteeing that the source is relay-unaware. This Patching technique aims at increasing the number of bits transmitted by the relay up to the number of information bits in the message. This technique is also combined with Space Time Block Codes in order to improve both the achievable macro and micro diversity orders.

This Patching technique has also been applied over the Interference Relay Channel where we introduce the use of a precoded DDF protocol at a relay shared by several source/destination pairs. We use the Patching technique in order to increase the achieved performance.

The gain resulting from the use of these various derivations of the DDF protocol are finally observed at the system level for two scenarios: a macro cellular network over urban area and an indoor network, combined with two applications: a unicast transmission, e.g., web browsing, and a broadcasting transmission, e.g., video broadcasting. The results show that the Monostream relaying scheme for the DDF protocol provides good performance while allowing both the source and the destination to be relay-unaware. Consequently, the Monostream DDF is a promising protocol for the deployment of plug-and-play relays in wireless systems.

Contents

List of Figures	xi
List of Acronyms	xiv
List of Notations	xvi
Résumé de la thèse en Français	xix
Introduction	xix
Chapitre 1 : Méthode d'évaluation des performances des transmissions sans fil	xxi
1 Evaluation lien : définitions des canaux basiques et métriques	xxi
2 Evaluation système : application, déploiement et modèles de propagation	xxiii
3 Conclusion	xxiv
Chapitre 2 : Ordre de macro diversité atteignable en utilisant le protocole DDF	xxv
1 Le protocole DDF	xxv
2 Définitions et bornes pour la diversité	xxvi
3 Implémentation pratique du protocole DDF	xxvi
4 Conclusion	xxviii
Chapitre 3 : Techniques de Patching et rotations distribuées pour le canal à relais	xxix
1 Technique de Patching	xxix
2 Rotations Distribuées	xxix
3 D'autres méthodes pour améliorer les ordres de diversité	xxx
4 Conclusion	xxxi
Chapitre 4 : Techniques de Patching pour le canal à interférence et relais	xxxii
1 Adaptation du protocole DDF au canal à interférence et relais	xxxii
2 Combinaison du précodage et de la technique de Patching	xxxiii
3 Conclusion	xxxiv
Chapitre 5 : Evaluations système des protocoles DDF	xxxv
1 Transmission Unicast	xxxv
2 Diffusion	xxxv
3 Conclusion	xxxvii
Conclusion	xxxviii
Introduction	xl

1	Modus operandi for wireless transmissions evaluation	3
	Introduction	3
1.1	Link level evaluation : basic channel models and metrics	4
1.1.1	All begins with a point to point transmission	4
1.1.2	Relay channel	11
1.1.3	Multiple Access channel	17
1.1.4	Broadcast channel	17
1.1.5	Interference channel	17
1.2	System level evaluation : application, deployment and propagation models	18
1.2.1	Application	18
1.2.2	Deployment	19
1.2.3	Propagation models	20
1.2.4	Metrics of interest for system level evaluation	22
1.3	Examples	22
	Conclusion	23
2	Achievable macro diversity order using the DDF protocol	25
	Introduction	25
2.1	The DDF protocol	25
2.1.1	Original protocol	25
2.1.2	Derived versions of the DDF protocol	27
2.2	Definitions and bounds for diversity	29
2.2.1	Macro diversity	29
2.2.2	Definition of the macro diversity order	30
2.2.3	Recovering diversity with channel coding	31
2.3	Practical implementation of the DDF protocol	35
2.3.1	DDF implementation based on HARQ principles	36
2.3.2	Metrics of performance	37
2.4	Monostream DDF protocol	39
2.4.1	Monostream scheme	39
2.4.2	Equivalent channels analysis	40
2.4.3	Analytic analysis	41
2.5	Distributed Alamouti DDF protocol	46
2.5.1	DA relaying scheme	46
2.5.2	Equivalent channels analysis	47
2.5.3	Analytic analysis	48
2.6	Simulation results	50
2.6.1	Outage probability	50
2.6.2	Spectral Efficiency	56
	Conclusion	57
3	Patching technique and Distributed Rotations for the relay channel	59
	Introduction	59
3.1	Patching technique	59
3.1.1	Definition of the Patching technique	59
3.1.2	Generating hypersymbols of QAM from the combination of QPSK symbols	60

3.1.3	Patched Monostream DDF protocol	64
3.1.4	Patched Space-Time Blocks Codes for the DDF protocol	66
3.1.5	Strategy to maximize the achievable diversity orders	69
3.2	Distributed rotations	69
3.2.1	Equivalent channels analysis	70
3.2.2	Analytic analysis	71
3.2.3	Comparison with the Monostream DDF and the DA DDF	72
3.3	Other methods to improve the achievable diversity orders	73
3.3.1	Spatial Division Multiplexing DDF	73
3.3.2	Modulation adaptation	74
3.4	Simulation results	74
3.4.1	Outage probability	74
3.4.2	Spectral Efficiency	78
3.4.3	Transmission strategies for practical systems	79
Conclusion	80
4	Patching technique for the Interference Channel with Relay	83
Introduction	83
4.1	Dealing with interference	83
4.2	Precoding for the DDF protocol	88
4.2.1	DDF protocol for the IRC	88
4.2.2	Precoding DDF for the IRC	89
4.2.3	Adaptation to a half duplex relay	89
4.2.4	Simulation results	90
4.3	Combining Patching and precoding	92
4.3.1	Generalization to the n-pair case	92
4.3.2	Two interfering pairs	93
4.3.3	Adaptation to a half duplex relay	94
4.3.4	Simulation results	94
Conclusion	95
5	System level evaluation of the DDF protocols	97
Introduction	97
5.1	Unicast transmission	97
5.1.1	Dedicated relays	97
5.1.2	Typical urban macro cellular network	97
5.1.3	Unicast for indoor small cells	106
5.2	Broadcasting	109
5.2.1	When users can become relays	109
5.2.2	Broadcast in a macrocellular network	112
Conclusion	114
Conclusion and perspectives		116

A Recovering diversity from channel coding	119
A.1 Diversity bound for the uncorrelated block-fading channel	119
A.2 Diversity upper bound for the Matryoshka channel	120
Bibliography	121
List of Publications	126

List of Figures

1	Le canal à relais.	xxii
2	Le canal à interférences.	xxiii
3	Génération d'un mot de code.	xxvi
4	Structure d'un mot de code et transmission pendant le protocole DDF.	xxvii
5	Principe de la technique de Patching.	xxix
6	Couples (ρ_{SD}, ρ_{RD}) qui permettent d'atteindre une efficacité spectrale cible pour $\rho_{SR} = 10dB$, et plusieurs version du protocole Monostream DDF.	xxx
7	Le canal IRC à deux paires considéré ainsi que la structure de trame des mots de code.	xxxii
8	Efficacité spectrale moyenne à D maximisée sur les différents rendements de codage possibles en fonction du SINR, $P_R/P_S = 6dB$, $N_r = 1$ pour $(M_S, M_I) \in \{(1, 1), (5, 5)\}$ et tous les instants M_S lorsque $M_I = 3$. Le relais utilise le protocole DDF avec précodeur optimisé.	xxxiii
9	Efficacité spectrale moyenne à D maximisée sur les différents rendements de codage possibles en fonction du SINR, $P_R/P_S = 6dB$, $N_r = 1$ pour $M_S = M_I \in \{1, 2, 3, 4, 5\}$. Le relais utilise le protocole DDF avec précodeur optimisé ou bien le protocole DDF avec Patching et précodeur optimisé.	xxxiv
10	Efficacité spectrale (bpcu) lorsque des femto cellules dans les bâtiments de Mitsubishi Electric R&D Center Europe (points noirs) sont assistées par des relais (points blancs).xxxvi	
1.1	Point to point channel, the source carries N_{tx} antennas and the destination carries N_{rx} antennas.	4
1.2	Different modulations, the circle represents points of unit energy.	5
1.3	Mutual information and capacity of the SISO channel According to ρ_{SD}	7
1.4	DMT of different MIMO schemes.	12
1.5	The relay channel.	12
1.6	A taxonomy of current technologies for Type 2 layer 2 relays.	13
1.7	DMT of different AF and DF protocols.	16
1.8	Two basic channels.	17
1.9	The interference channel.	18
1.10	Map of SNR in dB between the BS and the UEs in an isolated cell according to the shadowing model. The axes values represent the distance in meter from the base station.	21
1.11	Basic channels in a cellular system.	23
2.1	DMT of the DDF protocol with 1, 2 or 4 relays.	27

2.2	BF channel of N blocks with correlated fading coefficients (correlation A).	32
2.3	Block fading channel of three blocks with correlated fading coefficients (correlation B).	34
2.4	Matryoshka channel of N blocks.	35
2.5	Codeword generation.	36
2.6	Codeword details and details on the DDF transmission.	36
2.7	Outage regions according to r values.	45
2.8	DMT of the Monostream DDF protocol matching the DMT of the DDF protocol proposed by Azarian.	46
2.9	Outage probability of the Monostream DDF protocol, for fixed instants of correct decoding at the relay and Gaussian symbol alphabet according to $\rho_{SD} = \rho_{RD}$. . .	51
2.10	Codeword composed of 5 sub-frames, the first one being three time longer than the others and containing only information bits.	51
2.11	Outage probability of the Monostream DDF according to ρ_{SD} and the instant of correct decoding at the relay. $R_{c1} = 1, m_S = 2$	52
2.12	Pairs of SNR (ρ_{SD}, ρ_{RD}) achieving the target outage probability of 10^{-3} according to the instant of correct decoding at the relay for the Monostream DDF. $R_{c1} = 1$. .	52
2.13	Couples of SNR (ρ_{SD}, ρ_{RD}) achieving the target outage probability of 10^{-3} according to the instant of correct decoding at the relay for the Monostream DDF and the DA DDF. $N_{rx} = 2, R_{c1} = 1$	54
2.14	Outage probability of the Monostream DDF when $\rho_{SD} = \rho_{RD}$ for several ρ_{SR} values.	55
2.15	Couples (ρ_{SD}, ρ_{RD}) achieving the target outage probability of 10^{-3} for the Monostream DDF (black line) and the DA DDF (blue line).	55
2.16	Spectral efficiency of the Monostream DDF protocol according to ρ_{SD} and ρ_{RD} when $\rho_{SR} = 30$ dB.	56
2.17	Couples of SNRs achieving several target spectral efficiencies for $\rho_{SR} = 30$ dB when the relay uses the Monostream DDF (full line) or the DA DDF (dotted line). . . .	57
3.1	Patching principle.	60
3.2	Linear combination of two QPSK, $\alpha = 0.2143$	62
3.3	The QPSK mapping, and the mapping of the 16 QAM resulting from the linear combination of the two QPSKs with $\alpha = 0.5$	63
3.4	A_2 symbols resulting from the combination of 2 QPSKs.	63
3.5	Codeword composed of 2 sub-frames, the first one being twice longer than the other and containing only information bits.	74
3.6	Performance of the Monostream DDF, the Patched Monostream DDF and the Monostream with modulation adaptation. $N_{rx} = 2, m_S = 2$	75
3.7	Codeword composed of 5 sub-frames, the first one being three time longer than the others and containing only information bits.	76
3.8	Couples of SNR (ρ_{SD}, ρ_{RD}) achieving the target outage probability of 10^{-3} according to the instant of correct decoding at the relay for the Monostream DDF, the Patched Monostream DDF with minimal use and medium use, the Monostream with adapted modulation. $N_{rx} = 2, R_{c1} = 1$	76
3.9	Outage probability of distinct DDF protocol using the Alamouti relaying scheme. .	77

3.10	Couples (ρ_{SD}, ρ_{RD}) achieving an outage probability of 10^{-3} for several ρ_{SR} . The green curves represents $\rho_{SR} = -8\text{dB}$, the black ones $\rho_{SR} = -6\text{dB}$, the blues ones $\rho_{SR} = -5\text{dB}$ and the purple one represents $\rho_{SR} = -3\text{dB}$	78
3.11	Couples (ρ_{SD}, ρ_{RD}) achieving distinct target spectral efficiencies for a $\rho_{SR} = 10\text{dB}$, and several Monostream schemes.	79
4.1	The Interference channel with relay.	84
4.2	The considered 2-pair IRC.	87
4.3	Impact of the precoder optimization on the average QSPK input mutual information between the source and destination according to the SINR observed at D , P_R/P_S , for $n = 2$, $N_r = 1$ and $N_t=2$	88
4.4	IRC with precoding at the relay.	89
4.5	Average outage probability at D according to the SINR, $P_R/P_S = 6\text{dB}$, $N_r = 1$. The relay uses DDF protocol with optimized precoder.	90
4.6	Average spectral efficiency at D maximized over the available coding rates, according to the SINR, $P_R/P_S = 6\text{dB}$, $N_r = 1$ for $(M_S, M_I) \in \{(1, 1), (5, 5)\}$ and all possible M_S for $M_I = 3$. The relay uses the DDF protocol with an optimized precoder. . .	91
4.7	Average outage probability at D according to the SINR, $P_R/P_S = 6\text{dB}$, $N_r = 1$ for $M_S = M_I \in \{1, 2, 3, 4\}$. The relay uses the optimized precoder for the DDF protocol or the Patched DDF protocol.	94
4.8	Average spectral efficiency maximized over the coding rates, according to the SINR observed at D , $P_R/P_S = 6\text{dB}$, $N_r = 1$ for $M_S = M_I \in \{1, 2, 3, 4, 5\}$. The relay uses the optimized precoder for the DDF protocol or the Patched DDF protocol.	95
5.1	Long term SINR at the mobiles over the considered area for two deployment of BSs, considering no shadowing.	99
5.2	Map of SNR between the BS and the UEs in an isolated cell and the relays positions (stars).	100
5.3	Cdf of throughput of the users in an isolated cell containing 8 relays. Comparison of the Monostream relaying scheme and the DA relaying scheme according to the deployment of relays.	102
5.4	Throughput according to the number of relays in the cell, and the minimum distance guaranteed between them.	103
5.5	Performance over the macro cellular network.	105
5.6	Satellite view of MERCE lab (source: google maps).	107
5.7	Throughput (bpcu) for indoor pico cells (black dots) assisted by femto relays (white dots).	108
5.8	Throughput (bpcu) for indoor femto cells (black dots) assisted by femto relays (white dots).	110
5.9	Probability of first correct decoding according to the sub-frame index.	111
5.10	Performance achieved when the MSs use the systematic activation mode.	113
5.11	Performance achieved when the MSs using the Monostream relaying scheme and different activation modes.	115

List of Acronyms

AF	Amplify and Forward
ARQ	Automatic Repeat reQuest
AWGN	Additive White Gaussian Noise
BF	block-fading
bpcu	bit per channel use
BS	Base Station
BRC	Broadcast Relay Channel
cdf	cumulative distribution function
CF	Compress and Forward
CRC	Cyclic Redundancy Check
CSI	Channel State Information
DA	Distributed Alamouti
DDF	Dynamic Decode and Forward
DF	Decode and Forward
DMT	Diversity Multiplexing Trade off
DR	Distributed Rotation
FS	Femto Station
HARQ	Hybrid Automatic Repeat reQuest
HARQ-CC	Hybrid Automatic Repeat reQuest with Chase Combining
HARQ-IR	Hybrid Automatic Repeat reQuest with Incremental Redundancy
IC	Interference Channel
IRC	Interference Channel with Relay
ISI	Inter Symbol Interference
LTW	DF Laneman Tse Wornell Decode and Forward
MAC	Multiple Access Channel
MAP	Maximum A Posteriori
MARC	Multiple Access Channel with Relay
MCS	Modulation and Coding Scheme
MIMO	Multiple Input Multiple Output
MISO	Multiple Input Single Output
ML	Maximum Likelihood
MMSE	Minimum Mean Square Error
MRC	Maximum Ratio Combining
MS	Mobile Station
NAF	Non-Orthogonal Amplify and Forward
NBK	DF Nabar Bolcskei Kneubehler Decode and Forward

OAF	Orthogonal Amplify and Forward
OFDM	Orthogonal Frequency Division Multiplexing
PS	Pico Station
PSK	Phase Shift Keying
QAM	Quadrature Amplitude Modulation
QoS	Quality of Service
RS	Relay Station
SDF	Sequential Decode and Forward
SDM	Spatial Division Multiplexing
SIMO	Single Input Multiple Output
SINR	Signal to Interference plus Noise Ratio
SISO	Single Input Single Output
SNR	Signal to Noise Ratio
ST	Space Time

List of Notations

\mathbb{R}	Set of real numbers
\mathbb{R}^{+*}	Set of strictly positive real numbers
x	Scalar
$\mathcal{R}(x)$	Real part of x
$\mathcal{I}(x)$	Imaginary part of x
$(x)^+$	The maximum of x and 0
$\mathbb{E}_b(\cdot)$	Expected values over the variable b
\mathbf{x}	Vector
\mathbf{M}	Matrix
\mathbf{I}_n	Identity matrix of size n
\mathbf{M}^t	Transpose of the matrix \mathbf{M}
\mathbf{M}^*	Conjugate of the matrix \mathbf{M}
\mathbf{M}^\dagger	Conjugate transpose of the matrix \mathbf{M}
$\det(\mathbf{M})$	Determinant of the matrix \mathbf{M}

Résumé de la thèse en Français

Introduction

Puisqu'une transmission sans fil se diffuse naturellement dans l'espace, tous signaux émis par une source pour une destination donnée peuvent être reçus par d'autres noeuds présents dans le système. Ces noeuds peuvent avoir différents objectifs quant à ces données reçues. Certains d'entre eux peuvent être des noeuds espions ayant pour but d'intercepter le message et/ou de perturber la transmission entre la source et la destination. D'autres noeuds appelés relais ont pour but d'aider la transmission en introduisant de la diversité spatiale pour palier les effets des évanouissements, et en augmentant la puissance de signal utile reçue à la destination. Les relais sont actuellement introduits dans des normes de communications telles que la version 10 du LTE pour augmenter les débits et étendre la couverture des réseaux sans fil.

Les opérations effectuées par les relais sur les signaux reçus ainsi que le planning temporel utilisé pour transmettre ces données à la destination définissent un protocole de relayage. Parmi la pluralité de protocoles connus, le protocole Dynamic Decode and Forward (DDF) atteint le meilleur compromis diversité - gain de multiplexage à très forts rapports signal sur bruit (SNR). Les performances de ce protocole de relayage ont uniquement été étudiées via des métriques de théorie de l'information pour le canal à relais, composé de trois noeuds: une source, une destination et un relais, en supposant que les trois liens de communication: source-relais, source-destination, et relais-destination ont le même rapport signal à bruit.

Par conséquent, nous proposons dans ce travail une implémentation pratique du protocole Dynamic Decode and Forward satisfaisant 2 hypothèses.

Tout d'abord, nous supposons que la source n'a pas conscience du fait qu'il y a un relais dans le système. Cela permet de concevoir des protocoles nécessitant peu de signalisation dédiée au relayage, et complètement distribués. De plus, cette hypothèse permet aux anciens équipements de profiter des avantages offerts par les techniques de relayage sans avoir besoin d'aucune mise à jour, cela s'appelle la rétro-compatibilité des protocoles.

Enfin, nous imposons le fait que la destination n'ait pas de capacité de décodage supplémentaire par rapport au cas où il n'y a pas de relais dans le système de façon à garantir la rétro-compatibilité des protocoles conçus.

Les performances de cette implémentation pratique du protocole DDF sont décrites pour des rapports signal sur bruit différents sur chaque lien. Cette nouvelle description des performances donne lieu à la définition d'une nouvelle métrique d'évaluation appelée *ordre de macro diversité*.

Nous présenterons tout d'abord la méthodologie utilisée dans ces travaux pour caractériser les performances d'une transmission. Il s'agit d'une évaluation en deux étapes : la première est

l'évaluation au niveau lien, et la seconde l'évaluation au niveau système. Ces deux étapes ainsi que les métriques de l'état de l'art associées sont décrites dans le Chapitre 1.

Dans le second Chapitre, après une analyse de l'état de l'art lié au protocole DDF, nous nous focalisons sur la définition de nouveaux outils d'évaluation: nous définissons l'ordre de macro diversité atteint lors d'une transmission, et nous définissons des bornes supérieure sur les ordres de macro et micro diversité atteignables sur certains modèles de canal. De plus, nous proposons une implémentation pratique du protocole DDF lorsque la source n'a pas conscience du fait qu'il y ait un relais dans le système. Nous analysons les performances atteintes par deux schémas de relayage particuliers : le protocole Monostream DDF et le protocole DDF avec Alamouti Distribué (DA DDF).

Nous proposons dans le Chapitre 3 une technique appelée Patching dont le but est d'augmenter l'ordre de macro diversité atteignable lors d'une transmission avec DDF tout en garantissant que la source n'a pas conscience de la présence du relais. Cette technique de Patching est aussi combinée avec des codes spatio-temporels de façon à augmenter les ordres de macro et de micro diversité atteints par la transmission. Lorsque la contrainte de source non consciente du relais peut être relâchée, nous proposons d'autres méthodes pour améliorer les ordres de diversité telles que l'adaptation de modulation. Enfin, les rotations distribuées sont combinées au protocole DDF pour améliorer le gain de codage par rapport au Monostream DDF.

Dans le Chapitre 4 nous nous concentrons sur un autre type de canal : le canal à interférence et relais. Après avoir décrit les techniques de gestion de l'interférence de l'état de l'art pour ce canal, nous introduisons l'emploi d'un protocole DDF avec précodage par un relais partagé par plusieurs paires source-destination. Ce protocole est ensuite combiné à la technique de Patching de façon à améliorer ses performances.

Enfin, dans le dernier Chapitre, ces différentes versions du protocole DDF sont étudiées au niveau système pour deux applications: une transmission unicast, par exemple du téléchargement sur internet, et de la diffusion, par exemple de la diffusion de vidéo, et pour deux types de déploiements : un environnement urbain macro cellulaire, et un déploiement à l'intérieur des bâtiments (indoor).

Chapitre 1 : Méthode d'évaluation des performances des transmissions sans fil

L'évaluation des technique de communication sans fil utilisée pour ces travaux de thèse est décrite dans ce premier chapitre.

Il s'agit d'une évaluation en deux étapes, la première étape est une évaluation au niveau lien. C'est à dire que l'évaluation se fait en considérant un système appelé canal basique : le système le plus simple possible faisant apparaitre le problème à résoudre. Les métriques associées à ces canaux sont des métriques de la théorie de l'information, par exemple la capacité, la probabilité de coupure, ou encore l'efficacité spectrale. Si cette première étape d'évaluation permet de montrer certains gains par rapport aux systèmes de transmission de l'état de l'art, une seconde étape d'évaluation est nécessaire. Cette seconde étape est appelée évaluation au niveau système ayant pour but d'évaluer les performances de la technique de communication dans un système complet qui peut être vu comme le système résultant de multiples duplications du canal basique étudié. Pour ce type d'évaluation, les performances sont généralement décrites par les fonctions de répartition d'une métrique donnée.

Nous rappellerons dans la première partie de ce chapitre les différents canaux de base ainsi que les métriques d'évaluation associées. Dans une seconde partie, nous traiterons les différentes étapes nécessaires à l'évaluations système ainsi que les métriques associées.

1 Evaluation lien : définitions des canaux basiques et métriques

Nous présentons 5 canaux basiques : le canal point à point, le canal à relais, le canal à interférence et le canal à accès multiple.

1.1 Canal point à point

Le premier système de transmission sans fil étudié a été le canal point à point. Il s'agit d'un canal comportant deux noeuds : une source et une destination. En fonction du nombres d'antennes à chaque noeud, ce canal prend différentes appellations. Nous serons particulièrement intéressés par le canal à entrées et sorties multiples (Multiple Input Multiple Output, MIMO) où la source et la destinations ont chacune plusieurs antennes. Sur ce canal, la théorie de l'information définit la quantité maximale d'information qui peut être transmise avec une fiabilité aussi grande que l'on souhaite comme la capacité du canal.

Il est donc nécessaire de définir cette notion de fiabilité que l'on traduit par la **probabilité d'erreur** moyenne atteinte par un schéma de transmission, ou encore par la **probabilité de coupure** sur ce canal. Ces métriques sont très intéressantes pour caractériser les performances des transmissions en boucle ouverte, c'est à dire quand il n'y a pas de lien de retour de la destination vers la source. Dans la littérature, on trouve plusieurs façons d'améliorer ces métriques telles que le codage correcteur d'erreur (aussi appelé codage canal) ou le codage spatio-temporel.

Lorsque le lien de retour existe, la transmission est caractérisée par son **efficacité spectrale**, c'est à dire la quantité de ressources (temps/ fréquence) nécessaire à la réception correcte de toute l'information à la destination. Dans ce cas, on peut améliorer les performances obtenues de plusieurs façons : la première en utilisant un mécanisme d'Automatic Repeat reQuest (ARQ) au cours du quel la destination demande des retransmissions entières de la trame émise jusqu'à l'avoir correctement décodée, la deuxième solution consiste à utiliser de l'Hybrid Automatic Repeat re-

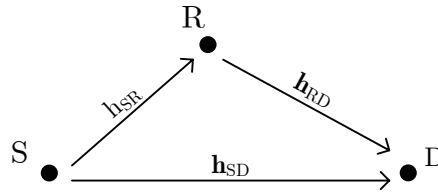


Figure 1: Le canal à relais.

Quest (HARQ) qui consiste à demander à la source de transmettre de la redondance supplémentaire (Incremental Redundancy) de façon à ce que la destination ait de plus en plus de facilité à décoder le message. C'est cette technique de transmission de redondance incrémentale qui servira de base à notre implémentation pratique du protocole DDF.

Une dernière métrique de la théorie de l'information utilisée pour décrire les performances d'un système sans fil est appelée *compris diversité/gain de multiplexage* (DMT), qui caractérise pour des rapports signal à bruit asymptotiquement grands le niveau de fiabilité des données décodées en fonction du débit que l'on transmet.

1.2 Canal à relais

La combinaison de trois noeuds : une source S , un relais R et une destination D forme un autre canal basique utile à l'évaluation lien appelé canal à relais présenté sur la figure Fig. 1. Du point de vue de la destination, ce canal est un canal MIMO virtuel car elle reçoit de l'information de deux antennes affectées par deux coefficients d'évanouissement différents. Ce canal basique a été introduit en 1971 par Van Der Meulen [1] pour deux raisons. D'un coté, il permet d'augmenter la fiabilité de la transmission en apportant de la diversité spatiale. D'un autre coté, ce canal permet d'augmenter l'efficacité spectrale de la transmission et donc le débit à la destination.

Une classification des relais est donnée dans le chapitre 1 suivant plusieurs caractéristiques. Dans cette thèse, nous nous focaliserons sur l'emploi de relais de type 2 et de layer 2 tels qu'ils seront introduits dans les futures versions du LTE et ayant les caractéristiques suivantes : causal, utilisant la même ressource fréquentielle que la source, non-orthogonal, et half-duplex. Ainsi, l'utilisation de ce type de relais permet de ne pas utiliser plus de ressource que dans un cas sans relais.

Nous décrivons dans ce chapitre les protocoles de relayage de l'état de l'art : "amplifie et transfère" (AF), "décode et transfère" (DF), ainsi que leurs différentes versions et performances.

Nous nous focaliserons sur le protocole "décode de façon dynamique et transfère" (DDF) puisque, parmi cette pluralité de protocoles de relayage, il permet d'atteindre le meilleur *compris diversité-gain de multiplexage*.

1.3 Canal à interférence

Un troisième canal basique présenté dans cette thèse est le canal à interférence, il est représenté sur la figure Fig. 2. Il est composé de plusieurs paires source-destination utilisant les mêmes ressources temps-fréquences, interférant donc les unes sur les autres.

Nous nous intéresserons particulièrement dans ce travail à une version de ce canal dans laquelle les transmissions sont assistées par un relais, il s'agit alors d'un canal basique appelé canal à interférence et relais.

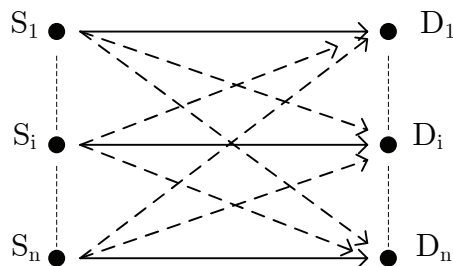


Figure 2: Le canal à interférences.

1.4 Autres canaux basiques

Deux autres canaux basiques sont présentés dans le chapitre 1 appelé canal à accès multiple et canal à diffusion.

2 Evaluation système : application, déploiement et modèles de propagation

Lorsque les protocoles étudiés sur les canaux basiques montrent des performances améliorées par rapport à l'état de l'art, il est nécessaire de compléter cette étude par une évaluation des protocoles au niveau système. En effet, il est possible que les plages de rapport signal à bruit sur lesquelles les améliorations sont visibles au niveau lien, ne soient pas celles qui soient les plus courantes au niveau système affaiblissant l'intérêt de ces protocoles.

Ces évaluations système sont généralement faites via un simulateur système pour une application donnée, un certain déploiement de noeuds, et des modèles de propagation adaptés à la zone considérée dans le simulateur.

Nous décrivons donc dans cette deuxième partie du chapitre 1 ces notions d'application, de déploiement et de modèle de propagation nécessaires aux évaluations système ainsi que les métriques associées.

2.1 Application

L'application d'une transmission décrit son objectif. Par exemple, il peut s'agir de diffusion (broadcast) d'un programme télévisé auquel cas toutes les destinations écoutent la même ressource temps / fréquence pour récupérer l'information, ou encore d'une transmission unicast dans le cas d'un téléchargement sur internet : chaque paire source / destination utilise une ressource temps / fréquence distincte.

2.2 Déploiement

Après avoir défini l'application pour laquelle les transmissions sont utilisées, le déploiement considéré pour l'évaluation système est mis en place dans le simulateur système. Il définit 3 caractéristiques environnementales pour les transmissions se font : le type de zone géographique (zone urbaine, rurale, à l'intérieur d'un bâtiment...), les familles de noeuds utilisés (station de base, capteurs, relais, mobiles...) et la position, i.e. la topologie, des noeuds dans la zone considérée.

On notera l'importance de garder une cohérence forte avec la réalité des déploiements physiques par exemple, il paraît peu probable d'avoir à déployer des stations de base à l'intérieur d'un bâtiment.

2.3 Modèles de propagation

Après avoir spécifié l'application du système de transmission, et le déploiement sur la zone géographique considérée, la simulation système permet de calculer les rapports signal à interférence plus bruit (SINR) instantanés sur les différents liens simulés.

Ce calcul se fait en deux étapes grâce à l'utilisation de modèles de propagation qui sont issus de résultats théoriques et heuristiques [33]. La première étape consiste à calculer la puissance moyenne, par rapport au temps, reçue à chaque destination à partir d'un modèle de propagation long-terme. Cette puissance dépend principalement de la distance entre la source et la destination et du type de zone géographique. La seconde étape consiste à moduler cette puissance reçue par un coefficient d'évanouissement court-terme représentant les petites variations temporelles de cette puissance sur des échelles de temps et de distance très petites.

2.4 Métriques

Suite à ces étapes de déploiement et de calcul de SINR, les métriques représentatives des performances du système simulés peuvent être dérivées.

Elles dépendent du type d'application considérées. Par exemple, pour un service de diffusion d'un programme TV, chaque utilisateur reçoit la même information et souhaite avoir une certaine qualité de service. Il est donc intéressant sur la zone considérée de mesurer la performance en terme de couverture, c'est à dire en pourcentage de la zone sur laquelle cette qualité de service est atteinte. Par contre, pour un service unicast, les utilisateurs souhaitent recevoir leur information avec un minimum de délai et une grande fiabilité. Il est donc intéressant de mesurer l'efficacité spectrale de chaque lien source/destination, et de traduire toutes ces performances via une fonction de répartition de l'efficacité spectrale.

Il faut toute fois noter que ce ne sont que des exemples, il faut, pour chaque système simulé trouver la meilleure façon de présenter les performances de façon à traduire de façon pertinente les paramètres et les effets qu'on souhaite présenter.

3 Conclusion

Dans ce chapitre sont **présentées les deux étapes nécessaires à l'évaluation de protocoles de transmission: l'évaluation lien et l'évaluation système**. Nous avons **rappelé les différentes métriques généralement associées à ces deux étapes pour caractériser les performances**.

Nous avons montré l'intérêt des technologies de relaying pour augmenter la fiabilité des transmissions. Dans toute la suite de ces travaux, nous considérerons un système comportant des relais en supposant que

- les noeuds sont parfaitement synchronisés,
 - aucune source ne sera au courant de la présence de relais dans le système,
 - les protocoles de relaying conçus n'imposent pas de capacité de décodage plus élevées à la destination par rapport au cas sans relais.
-

Chapitre 2 : Ordre de macro diversité atteignable en utilisant le protocole DDF

Dans ce second chapitre, après une étude bibliographique du protocole DDF, nous proposons une implémentation pratique de ce protocole satisfaisant les hypothèses définies dans le chapitre 1. Nous introduisons une nouvelle métrique appelée ordre de macro diversité permettant de refléter l'utilité du relaying dans une transmission.

1 Le protocole DDF

Le protocole DDF a été proposé en 2005 simultanément dans [27] et [28] pour le canal à relais, lorsque les relais sont half-duplex.

Ce protocole se compose de deux phases. Lors de la première phase, la source transmet le mot de code que la destination et le relais reçoivent. Cette phase se termine lorsqu'un critère prédéfini, appelé règle de décision, est satisfait au relais. Par exemple, dans [27], cette règle de décision est équivalente au fait que le relais a correctement décodé le message lorsque la source utilise un alphabet gaussien et que le mot de code est très long.

Ce protocole est dit dynamique pour deux raisons : la durée de cette phase dépend du coefficient d'évanouissement court-terme subi au relais, et le relais vérifie après chaque symbole reçu si la règle de décision est satisfaite.

Pendant la seconde phase du protocole, le relais connaît parfaitement les bits d'information contenus dans le message. Il transmet ainsi cette information sur la même ressource temps/fréquence que la source. Cette phase se termine lorsque la source a terminé sa transmission ou lorsque la destination a correctement décodé le message.

Il a été prouvé que ce protocole atteint le meilleur compromis diversité-gain de multiplexage parmi tous les protocoles de relaying de l'état de l'art et qu'il est optimal pour les gains de multiplexage compris entre 0.5 et 1.

Cependant, le protocole DDF tel qu'il a été défini dans [27] présente plusieurs inconvénients:

- la source et le relais utilisent des alphabets gaussiens ;
- les mots de code sont infiniment longs ;
- le protocole demande une très grande complexité de décodage et une grande vitesse de calcul;
- le protocole demande un décodeur capable de travailler sur plusieurs flux indépendants codant pour la même information.

Nous rappelons dans ces travaux plusieurs versions dérivées de ce protocole DDF originel. Plus particulièrement, nous avons trouvé intéressante l'idée de concevoir un codage espace-temps d'Alamouti pendant la seconde phase du protocole DDF [37] qui permet de réduire la complexité de décodage à la destination tout en garantissant la performance en terme de DMT, ainsi que l'idée de créer un protocole DF séquencé via les mécanismes d'HARQ [43] permettant au relais de vérifier s'il a correctement décodé le message ou non.

Pour ces raisons, notre implémentation pratique du protocole DDF est basée sur du codage canal et de l'HARQ à redondance incrémentale tout en satisfaisant deux hypothèses : la source n'a pas conscience de la présence du relais dans le système et la destination a de faibles possibilités en terme de décodage.

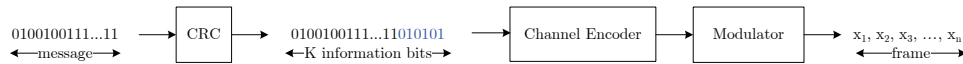


Figure 3: Génération d'un mot de code.

2 Définitions et bornes pour la diversité

2.1 Définition de la macro diversité

Dans ces travaux de thèse, nous définissons une nouvelle métrique appelée macro diversité. Elle représente le fait que plusieurs sources transmettant la même information vers une destination subissant des SNR long-terme indépendants permet d'améliorer le SNR long-terme à la destination. Plus particulièrement, on parle de diversité puisque lorsque l'un de ces liens est très mauvais, les autres sont présents pour satisfaire la transmission.

Dans le cas nous intéressant d'une transmission assistée par un relais causal utilisant le protocole DDF, le relais ne transmet pas l'ensemble du message émis par la source. Deux questions se posent alors : est-il possible d'obtenir de la macro diversité ? Quelles sont les conditions à satisfaire par la transmission pour qu'elle soit pleinement profitable à la destination ?

Nous définissons alors l'ordre de macro diversité atteint à une destination comme le nombre minimal de liens long-terme vers la destination qu'il faut couper de façon à ce que la performance ciblée ne soit plus atteignable (cf Section 2.2.2).

Par opposition, nous utilisons le vocabulaire *micro diversité* pour traduire la diversité apportée par les coefficients d'évanouissement court-terme.

2.2 Diversité atteignable et codage canal

Suite à cette définition, nous dérivons une série de résultats indiquant l'ordre de diversité atteignable en fonction du rendement de codage utilisé pour transmettre et du nombre de bits d'information dans le message, pour certains modèles de canal (canal à évanouissement par blocs, avec ou sans corrélation, canal Matryoshka).

Les modèles de canal considérés seront ensuite reliés à notre implémentation pratique du protocole DDF, et les résultats nous permettront d'expliquer les comportements de notre protocole DDF en terme de macro et micro diversité.

3 Implémentation pratique du protocole DDF

La génération des mots de code transmis par la source selon l'implémentation pratique du protocole DDF est résumée sur la Fig. 3. Elle se compose de 3 étapes :

- Les bits de CRC sont ajoutés pour que le relais puisse vérifier s'il a décodé le message correctement ;
- le codage canal permet au relais d'essayer de décoder l'information avant la fin de la transmission par la source. Plus particulièrement, il est possible que ce codeur canal soit un turbo-code associé à un algorithme de rate matching. Cela permet de mimer un mécanisme d'HARQ avec redondance incrémentale ;
- ces bits codés sont ensuite modulés en utilisant un alphabet discret (par exemple une 16 QAM) et les symboles générés forment une trame.

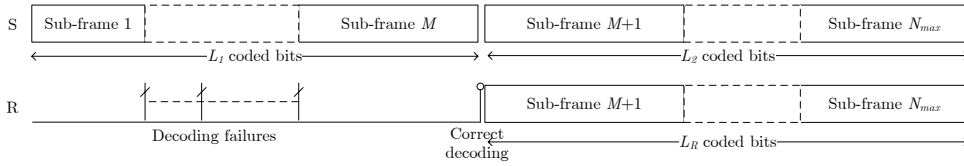


Figure 4: Structure d'un mot de code et transmission pendant le protocole DDF.

En utilisant cette construction des mots de code, une transmission où le relais utilise le protocole DDF se passe comme illustré sur la Fig. 4 : le relais essaie de décoder le message après chaque sous-trame émise par la source jusqu'à ce que les bits décodés satisfassent le CRC. Lorsque c'est le cas, le relais émet en utilisant la même ressource temps/fréquence que la source.

La question qui se pose alors consiste à définir explicitement ce que le relais transmet pendant cette deuxième phase du protocole DDF.

Nous proposons dans ce chapitre 2, deux schémas de relayage possible n'augmentant pas la complexité de décodage à la destination. Le premier schéma de relayage est appelé "Monostream" et le second "Alamouti Distribué".

3.1 DDF avec Monostream

Après avoir correctement décodé le message, le relais connaît parfaitement les bits d'information, le schéma d'encodage et de modulation utilisés par la source. Il est donc capable de reconstruire parfaitement la trame émise par la source, et surtout les sous-frames qui vont être émises pendant la seconde phase du protocole DDF.

Lorsque le relais utilise le schéma de relayage appelé "Monostream", il se contente d'émettre exactement les mêmes symboles que la source sur la même ressource temps/fréquence.

De cette façon, du point de vue de la destination, l'ensemble de cette transmission consiste à recevoir un mot de code affecté par deux coefficients d'atténuation corrélés : pendant la première phase, il s'agit du coefficient d'atténuation entre la source et la destination, et pendant la seconde phase du protocole, il s'agit de la somme des coefficients d'atténuation source-destination et relais-destination.

Nos résultats sur les comportements en diversité montrent que cette transmission atteint un ordre de macro diversité maximal lorsque la seconde phase du protocole permet de transmettre un nombre de bits supérieur au nombre de bits d'information, et un ordre de micro diversité maximal lorsque la plus courte phase du protocole permet de transmettre un nombre de bits supérieur au nombre de bits d'information.

Ces résultats sont ensuite confirmés par une étude de probabilité d'erreur par paire dans le but de dériver le gain de codage, ainsi que par une étude de probabilité de coupure dans le but de dériver le gain de coupure du protocole Monostream DDF. De plus, nous montrons que le Monostream DDF permet d'atteindre la DMT du protocole DDF originel.

3.2 DDF avec Alamouti Distribué

Lorsque le relais, après avoir correctement décodé le message transmet les symboles de façon à générer des mots de code d'Alamouti distribué avec ceux émis par la source, le schéma de relayage est appelé "Alamouti Distribué". Il est décrit dans [37] et est étudié en terme de DMT.

Nos résultats sur les comportements en diversité montrent que cette transmission atteint un ordre de macro diversité et un ordre de micro diversité maximum lorsque la seconde phase du protocole permet de transmettre un nombre de bits supérieur au nombre de bits d'information.

Ces résultats sont ensuite confirmés par une étude de probabilité d'erreur par paire dans le but de dériver le gain de codage.

4 Conclusion

Après avoir **défini une nouvelle métrique appelée ordre de macro diversité**, nous avons **proposé une implémentation pratique du protocole DDF et deux schémas de relayage (le Monostream et l'Alamouti Distribué) pour cette implémentation**, nous avons **étudié leurs performances**. Ces deux schémas atteignent les mêmes ordres de diversité, l'Alamouti Distribué apportant un gain de codage par rapport au Monostream.

Les comportements en diversité sont fortement impactés par l'instant de décodage correct au relais : le plus tôt le relais transmet, meilleur est l'ordre de diversité atteint. Cependant, puisque la source n'a pas conscience de la présence du relais dans le système, elle ne peut pas adapter son débit à la qualité du lien source-relais. Nous proposons donc dans le chapitre suivant une méthode appelée "Patching" permettant de résoudre cette difficulté.

Chapitre 3 : Techniques de Patching et rotations distribuées pour le canal à relais

1 Technique de Patching

La technique de Patching consiste à virtuellement transférer des bits de la première phase du protocole DDF dans la seconde phase de façon à créer à la destination un canal équivalent dans lequel le relais aurait décodé le message correctement plus tôt qu'il ne le fait réellement.

Cette technique dont le principe est illustré sur la figure Fig. 5 se compose de deux étapes.

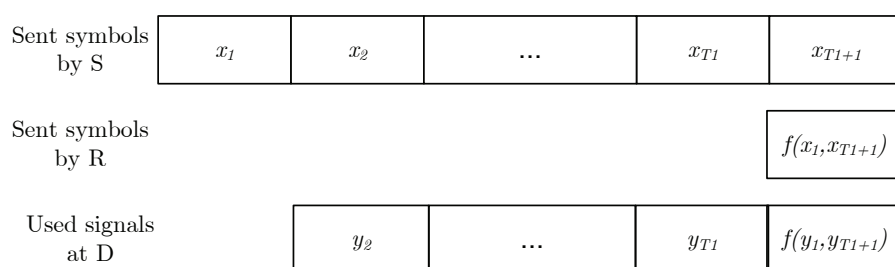


Figure 5: Principe de la technique de Patching.

La première étape se fait au relais : il transmet des combinaisons linéaires de symboles déjà émis par la source lors de la première phase et de symboles que la source va transmettre dans la seconde phase.

La seconde étape se fait à la destination : elle combine les signaux reçus en utilisant la même combinaison linéaire que le relais.

En concevant de façon intéressante cette combinaison linéaire, il est possible de conserver une complexité de décodage raisonnable à la destination (pas d'augmentation par rapport au cas sans relais). Nous montrons par exemple qu'à partir de deux symboles de QPSK, il est possible de générer tous les symboles d'une 16QAM. Cette relation est étendue dans ce chapitre à la combinaison linéaire d'une pluralité de symboles de QPSK.

Cette technique de Patching fonctionne quelque soit le schéma de relaying utilisé : le Monostream, l'Alamouti Distribué. Nous proposons aussi, via cette technique d'utiliser d'autres codes spatio-temporels tels que le Golden Code ou le Silver Code (Patched DSTBC) tout en garantissant que la source n'a pas conscience de la présence du relais dans le système. Les différentes combinaisons linéaires utilisées dans ce cas au relais sont décrites dans le tableau Tab. 3.2.

Nous montrons cependant que ce gain en terme de diversité apporté par la technique de Patching est à nuancer car cette technique apporte aussi une perte en terme de gain de codage due à l'augmentation de la taille de la constellation.

2 Rotations Distribuées

Après avoir proposé la technique de Patching pour améliorer les ordres de diversité atteints pendant une transmission utilisant le protocole DDF, nous démontrons que l'introduction de rotations distribuées permettent d'améliorer le gain de codage.

Ce schéma a été proposé dans [38] et il a été montré qu'il permet d'atteindre la DMT du protocole DDF originel mais il n'a pas été comparé au protocole Monostream DDF. Nous démontrons

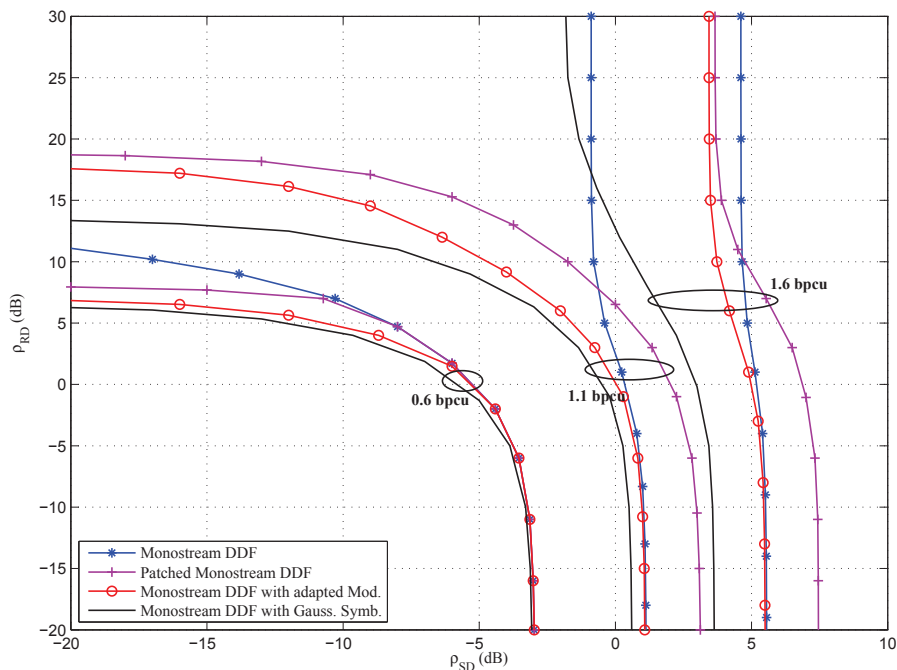


Figure 6: Couples (ρ_{SD}, ρ_{RD}) qui permettent d'atteindre une efficacité spectrale cible pour $\rho_{SR} = 10dB$, et plusieurs version du protocole Monostream DDF.

donc ici que les deux schémas de relayage permettent d'atteindre les mêmes ordres de macro et micro diversité, et que les rotations distribuées n'apportent que du gain de codage.

3 D'autres méthodes pour améliorer les ordres de diversité

Dans les cas où la contrainte de faible complexité de décodage à la destination peut être relâchée, nous proposons une technique appelée "Spatial Division Multiplexing DDF" permettant d'augmenter les ordres de diversité atteints par la transmission. Elle consiste à faire émettre par le relais la redondance que la source générerait après l'ensemble de la trame initiale. La modulation et la quantité de bits générée au relais sont adaptées de façon à ce qu'il transmette un nombre de bits supérieur au nombre de bits d'information dans le message.

De plus, quand la source est au courant de la présence du relais dans le système (imaginable par exemple lorsque la source est une station de base), il est possible d'utiliser une technique d'adaptation de modulation. Dans ce cas, la source et le relais adaptent de façon similaire le nombre de bits de redondance générés ainsi que la modulation utilisée pour qu'au moins un nombre de bits égal au nombre de bits d'information soit transmis pendant la seconde phase du protocole DDF.

Nous montrons dans la Fig. 6 les couples de SNR long-terme permettant d'atteindre des efficacités spectrales cibles pour plusieurs versions du Monostream DDF : sans Patching, avec Patching, avec adaptation de modulation et avec des symboles Gaussiens (meilleure performance atteignable). Nous observons l'effet d'un ordre de macro diversité maximal : lorsque le lien source-destination est très mauvais, le lien relais-destination permet d'atteindre la performance cible. Cette figure montre aussi les gains du Patching et de l'adaptation de modulation.

4 Conclusion

Nous montrons donc dans ce chapitre que notre technique de **Patching permet d'améliorer l'ordre de macro diversité** atteint lors d'une transmission utilisant notre implémentation pratique du protocole DDF lorsque la source n'a pas conscience de la présence du relais dans le système. Cette technique peut être **combinée avec des codes spatio-temporel ce qui permet de d'augmenter l'ordre de micro diversité atteint**.

Nous démontrons aussi que l'ajout de rotations distribuées dans le protocole DDF permet d'augmenter le gain de codage par rapport au Monostream DDF.

Nos résultats de simulations permettent de comprendre que les gains maximaux apportés par la macro diversité sont observés à faibles ρ_{SD} et fort ρ_{RD} . Cette remarque permet de comprendre où les relais doivent être déployés dans le réseau cellulaire : en bordure de cellule. **Cependant, ils accroitraient alors l'interférence générée sur les autres cellules**. Pour cette raison, nous proposons dans le chapitre suivant une implémentation pratique du protocole DDF permettant de gérer l'interférence et de profiter aux utilisateurs de bords de cellule.

Chapitre 4 : Techniques de Patching pour le canal à interférence et relais

Nous proposons dans ce chapitre d'utiliser le protocole DDF, initialement conçu pour le canal à relais, sur le canal à interférences et relais. Sur ce canal, plusieurs paires sources-destinations utilisent la même ressource temps/fréquence pour transmettre différents messages interférant donc les unes sur les autres.

Nous commençons par faire un tour d'horizon des différentes techniques de gestion d'interférences avec et sans relais. Nous avons été particulièrement intéressé par une technique de précodage [60] conçue dans le cas où le relais était non causal.

1 Adaptation du protocole DDF au canal à interférence et relais

Dans un canal à interférence et relais, plusieurs paires source / destination tentent de communiquer en utilisant l'aide d'un seul relais.

Nous souhaitons que le relais utilise notre implémentation pratique du protocole DDF. Si la construction des mots de code par les sources reste identique à celle définie au chapitre 2, les algorithmes de décodage utilisés au relais sont nécessairement différents, et il est nécessaire de définir précisément la règle de décision à utiliser au relais. Nous détaillons dans ce chapitre différentes possibilités de règles de décision en fonction du type de duplexage au relais.

Dans tous les cas, lorsque le relais va transmettre, il a la possibilité

- d'augmenter la puissance affectée au signal voulu à la destination D_i de façon à le faire ressortir de l'interférence subie cette destination, au détriment des autres destinations qui subissent alors plus d'interférence,
- d'annihiler l'interférence subie cette destination, au détriment des autres destinations qui reçoivent alors moins de signal utile.

C'est dans le but de gérer ces compromis que nous nous sommes intéressé au précodeur défini dans [60] : il a pour but de maximiser la plus petite capacité sur tous les liens source-destination garantissant ainsi un critère d'équité entre toutes les paires.

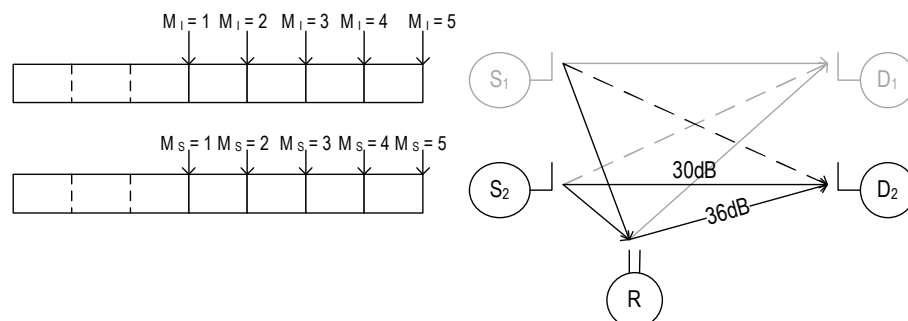


Figure 7: Le canal IRC à deux paires considéré ainsi que la structure de trame des mots de code.

Par exemple, en considérant un canal à interférence et relais comportant deux paires source / destination ainsi que la structure de trame des mots de code présentés sur la figure Fig. 7, les performances obtenues en terme d'efficacité spectrale sont présentées sur la figure Fig. 8 en fonction

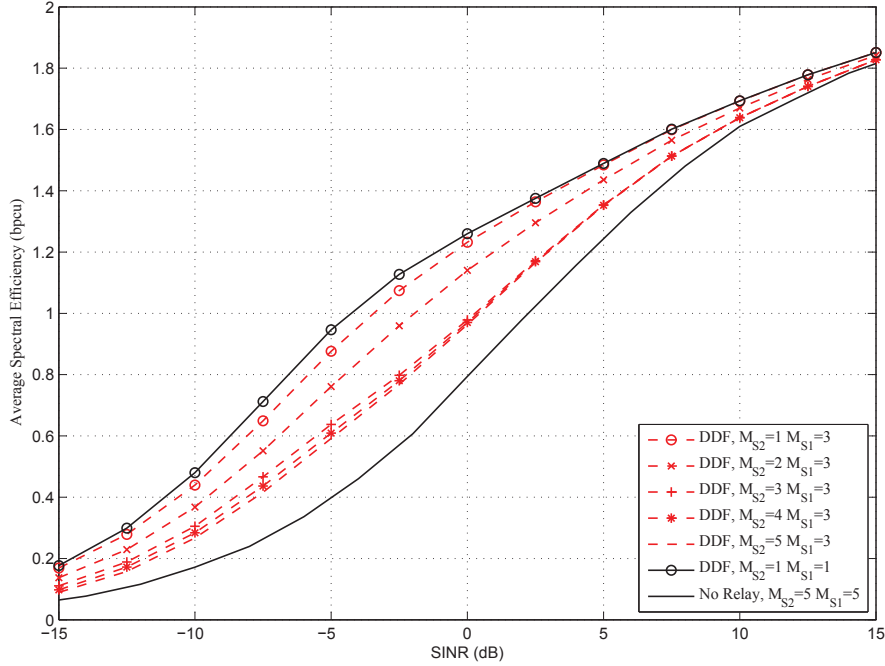


Figure 8: Efficacité spectrale moyenne à D maximisée sur les différents rendements de codage possibles en fonction du SINR, $P_R/P_S = 6dB$, $N_r = 1$ pour $(M_S, M_I) \in \{(1, 1), (5, 5)\}$ et tous les instants M_S lorsque $M_I = 3$. Le relais utilise le protocole DDF avec précodeur optimisé.

de M_S l'instant de décodage du message émis par S_2 au relais, et M_I l'instant de décodage du message émis par S_1 au relais.

Les cas où $M_S = M_I = 1$ et $M_S = M_I = 5$ représentent les meilleurs et pires performances en terme d'efficacité spectrale pour le protocole DDF avec précodeur. Dans le cas où $M_I = 3$ et si $M_S > M_I$ alors les performances sont très similaires. En effet, le relais ayant enlevé une grosse partie de l'interférence, la destination arrive à décoder le message très rapidement. Dans le cas où le SINR est inférieur à 0dB, le relais ne peut pas enlever complètement l'interférence subie à cause de sa limitation en puissance d'émission. Par conséquent, il vaut mieux utiliser cette puissance pour augmenter le niveau de signal utile et l'instant M_S impacte sur les performances.

2 Combinaison du précodage et de la technique de Patching

Les résultats de simulation montrent que plus le nombre de bits affecté par le précodeur utilisé au relais est grand meilleures sont les performances, tant en terme de probabilité de coupure qu'en efficacité spectrale.

Pour cette raison, nous adaptions la technique de Patching au précodage et au canal à interférence et relais.

Nous proposons un algorithme dans le cas du canal à interférence et relais comportant n paires. Il est ensuite explicité pour l'exemple du cas à deux paires.

Similairement à l'utilisation du Patching pour augmenter un ordre de diversité, lorsque cette technique est utilisée pour maximiser le nombre de symboles précodés par le relais, le système utilise une constellation de plus grand cardinal qui a le désavantage d'introduire une perte en gain de codage.

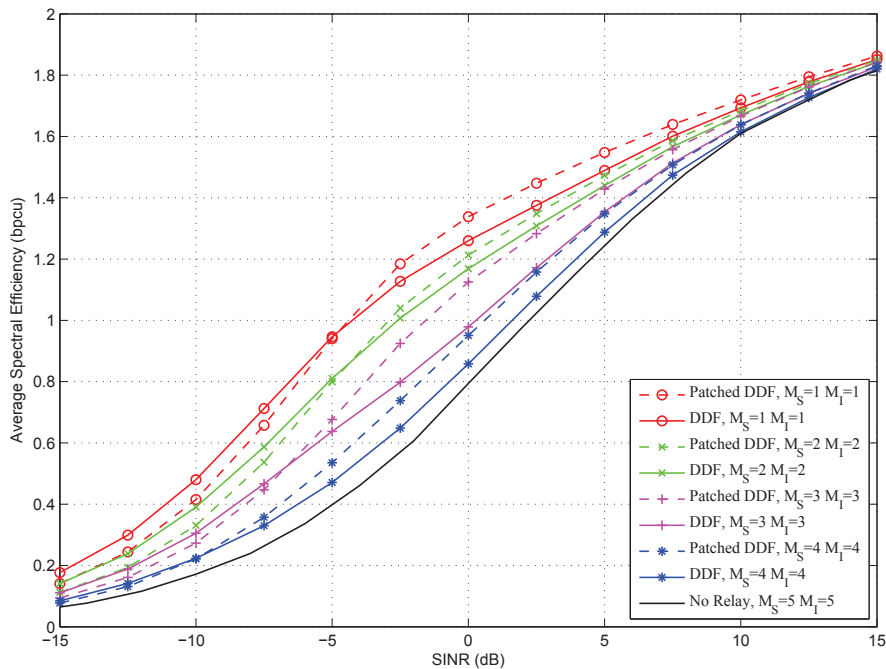


Figure 9: Efficacité spectrale moyenne à D maximisée sur les différents rendements de codage possibles en fonction du SINR, $P_R/P_S = 6dB$, $N_r = 1$ pour $M_S = M_I \in \{1, 2, 3, 4, 5\}$. Le relais utilise le protocole DDF avec précodeur optimisé ou bien le protocole DDF avec Patching et précodeur optimisé.

La Fig. 9, présente l'efficacité spectrale obtenue pour le canal présenté sur Fig. 7 lorsque le relais utilise la technique de Patching combinée au précodage pour $M_S = M_I$. La technique de Patching pour le protocole DDF précodé permet d'améliorer les performances pour un SINR au dessus d'un certain seuil qui dépend du nombre de symboles patchés : plus il y a de symboles patchés, plus cette valeur seuil est élevée. En effet, lorsque $M_S = 1$ et $M_S = 2$, $\frac{3T}{7}$ symboles sont patchés, ce qui donne la même valeur seuil égale à $-5dB$. Pour de plus grandes valeurs de M_S , moins de symboles sont patchés permettant d'avoir une valeur seuil plus petite.

3 Conclusion

Dans ce chapitre, nous avons **adapté le protocole DDF au canal à interférence et relais** lorsque les sources n'ont pas conscience de la présence du relais dans le système. Cette adaptation est intéressante quand elle est **combinée à un précodage au relais permettant de gérer l'interférence**. Nous proposons que cette gestion d'interférence se traduise par une maximisation de la plus petite capacité parmi toute les paires source-destination. Nous avons, de plus, **combiné ce précodage avec la technique de Patching** ce qui permet d'améliorer les performances apportées par le précodage.

Chapitre 5 : Evaluations système des protocoles DDF

Suite à ces conceptions de protocoles, et à leurs bonnes performances au niveau lien, nous proposons dans ce chapitre leur évaluation au niveau système.

1 Transmission Unicast

Lors d'une transmission unicast (par exemple du téléchargement par internet), pour des raisons de sécurité, il est nécessaire d'utiliser des relais dédiés, i.e. qui ne servent qu'à faire du relayage et derrière qui ne se trouve aucun utilisateur.

Dans ce chapitre, et pour cette application, nous considérons un environnement macro cellulaire urbain, et un déploiement indoor où trois femto cellules sont assistées par des relais.

Dans les deux cas, nous comparons les performances du cas sans relais et des protocoles Monostream DDF, DA DDF, DR DDF en terme de fonction de répartition de l'efficacité spectrale sur la zone géographique considérée.

Si l'évaluation lien a montré un gain de codage du DA DDF sur les autres protocoles, il s'avère qu'au niveau système ce gain est bien moins significatif. Aussi, les trois versions du protocole DDF permettent d'obtenir un gain certain en comparaison du cas sans relais, mais ces différentes versions ne se distinguent pas particulièrement les unes des autres.

Ce comportement peut par exemple s'observer sur la Fig. 10. Les couleurs représentent l'efficacité spectrale moyenne atteinte en un point de la carte, toutes les caractéristiques physiques du système sont décrites au chapitre 5.

Par conséquent, dans un souci de simplicité de décodage, et de minimisation de la quantité de signaling nécessaire, nous recommandons l'utilisation du protocole Monostream DDF pour améliorer les performances système.

2 Diffusion

Dans le cadre d'une application de diffusion, par exemple d'une chaîne de télévision, la même information est destinée à tous les utilisateurs. Par conséquent, le souci de sécurité de la transmission unicast disparaît et les relais ne sont plus obligatoirement dédiés.

Nous avons donc cherché dans ce chapitre à utiliser en mode relais grâce au protocole DDF des utilisateurs ayant correctement décodé le message avant les autres pour en améliorer les performances. Il peut donc y avoir simultanément dans le système plusieurs relais actifs.

Cependant, cette méthode introduit une nouvelle contrainte car les relais sont maintenant des utilisateurs qui n'ont pas un accès illimité à une source d'énergie. Les performances du système sont donc nuancées en fonction des performances énergétiques pour atteindre une certaine qualité de service.

Cet aspect énergétique nous a aussi contraint à définir plusieurs modes d'activation aux utilisateurs/relais en fonction des valeurs moyennes des instants de décodage en fonction des SINR long-termes subis:

- un mode *systematique* où dès qu'un utilisateur décode correctement il transmet l'information,
- un mode *early until end* où, si un utilisateur décode correctement avant l'instant moyen de décodage pour sa valeur de SINR long-terme, il transmet jusqu'à la fin du mot de code,

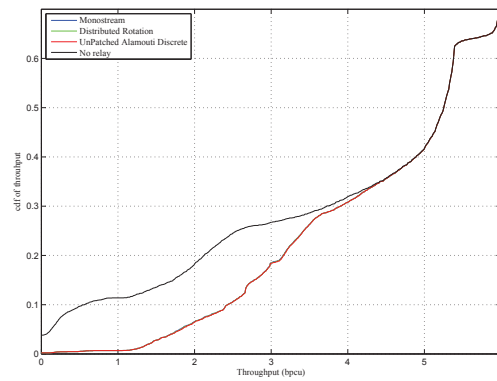
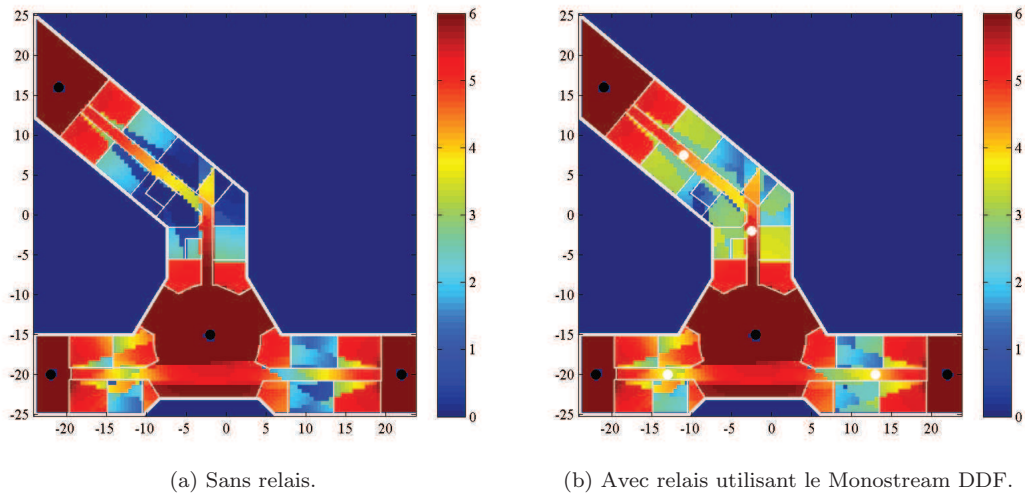


Figure 10: Efficacité spectrale (bpcu) lorsque des femto cellules dans les bâtiments de Mitsubishi Electric R&D Center Europe (points noirs) sont assistées par des relais (points blancs).

- un mode *early until average* où, si un utilisateur décode correctement avant l'instant moyen de décodage pour sa valeur de SINR long-terme, il transmet jusqu'à cet instant moyen.

Ces trois modes d'activation sont ensuite combinés au deux schémas de relayage Monostream DDF et DA DDF.

3 Conclusion

Dans ce chapitre, nous avons étudié les performances du Monostream DDF, du DA DDF et du DR DDF au niveau système pour deux applications : une transmission unicast et une diffusion et deux environnements : un milieu urbain, et une transmission dans un bâtiment. Les résultats montrent que les **performances des trois protocoles sont très proches** en terme d'efficacité spectrale. Nous avons montré **l'intérêt du DA DDF en terme de consommation énergétique dans le cas d'une diffusion.**

Cette évaluation au niveau système se doit d'être complétée par les performances des techniques de Patching, et en prenant en compte la différence de signalisation entre les différents schémas de relayage.

Conclusion

Dans cette thèse, nous avons proposé et étudié une implémentation pratique du protocole DDF pour des relais auto-configurables au niveau lien et système.

Cette implémentation pratique, basée sur du codage correcteur d'erreur et une segmentation de la trame émise (comme pour les mécanismes d'HARQ), est combinée avec différents schémas de relayage tels que le Monostream, l'Alamouti Distribué ou encore les Rotations Distribuées.

Nous avons montré que ces trois schémas atteignent les mêmes ordres de macro et micro diversité. L'ordre de micro diversité se réfère au gain qui peut être acquis via les coefficients d'évanouissement court-terme. Nous avons défini l'ordre de macro diversité comme le nombre de sources desquelles toute l'information peut être entièrement décodée sans l'aide des autres sources. De plus, nous avons prouvé que les trois schémas de relayage permettent d'atteindre de meilleures performances que le cas sans relais, leurs performances ne diffèrent qu'en terme de gain de codage: le DA DDF a de meilleure performance que le DR DDF, qui lui-même a de meilleures performances que le Monostream DDF.

Cependant, les évaluations système ont montré que ce gain de codage n'est pas significatif au niveau système. Cela montre que la métrique pertinente à optimiser pour améliorer les performances est l'ordre de macro diversité atteignable par le protocole; c'est à dire que le gain le plus important apporté par le relayage est un gain de rapport signal à bruit long-terme.

Nous avons donc proposé la technique de Patching pour augmenter l'ordre de macro diversité atteignable par une transmission. Cette technique vise à augmenter le nombre de bits transmis par le relais jusqu'au nombre de bits d'information contenus dans le message. Quand cette technique de Patching est combinée aux codes spatio-temporels, elle permet d'améliorer à la fois l'ordre de macro diversité et l'ordre de micro diversité.

Cette technique de Patching a aussi été utilisée sur le canal à interférence et relais pour lequel nous avons introduit l'usage d'un protocole DDF précodé par un relais partagé par plusieurs paires source/destination. Dans ce cas, le Patching a pour but d'améliorer les performances par rapport au cas avec précodeur uniquement, et ce en maximisant le nombre de symboles précodés par relais.

Les gains résultants de ces nombreuses variations de notre implémentation pratique du protocole DDF sont finalement décrits au niveau système pour un déploiement macro-cellulaire en zone urbaine, et pour un déploiement indoor, en considérant deux applications : une transmission unicast, par exemple du téléchargement sur internet, ou encore de la diffusion, de la télévision par exemple. Les résultats montrent que le Monostream DDF permet d'atteindre de bonnes performances tout en garantissant que la source et la destination n'ont pas conscience de la présence du relais dans le système. Par conséquent, ce protocole est un candidat intéressant pour le déploiement massif de relais auto-configurables dans les réseaux sans fil.

L'étape théorique suivante de ces travaux est de prouver que pour le cas multirelais, les rotations distribuées peuvent permettre d'améliorer l'ordre de micro diversité atteignable comparativement au cas Monostream DDF.

Il serait particulièrement intéressant de poursuivre les études système en évaluant les performances des techniques de Patching, et celles de gestion de l'interférence par précodage au relais qui ont montré des gains intéressants au niveau lien.

De plus, les études système ont permis de montrer qu'une économie d'énergie intéressante pouvait être obtenue en utilisant le Monostream DDF combiné avec différents modes d'activation des utilisateurs en tant que relais, pour la diffusion, tout en garantissant la même couverture.

Cette façon originale de présenter les performances des systèmes est typique des *green com-*

munications. Ce concept est apparu pour deux raisons: tout d'abord le fait que les ressources (fréquences, puissance) sont de plus en plus limitées et ensuite parce que les consommateurs sont de plus en plus sensibles à l'impact des champs électromagnétiques sur la santé. C'est pourquoi le but des communications "vertes" est de garantir une qualité de service tout en minimisant les ressources utilisées. Cette nouvelle façon de concevoir les systèmes de communication mène à la description de leurs performances via de nouvelles métriques par exemple exprimées en bits par seconde, par Hertz, et par Joule.

C'est pourquoi, à plus long-terme, nous sommes intéressés par la conception de protocoles DDF qui tiendraient compte de plusieurs optimisations en terme de puissance : la puissance de transmission, la puissance de calcul (par exemple pour coder / décoder), où encore la puissance consommée par le matériel.

Introduction

Due to the broadcast nature of a wireless transmission, any signal transmitted from a source to a destination can be eared by any other nodes in the network. The aim of these nodes can be distinct. Some of them are eavesdroppers, aiming at intercepting the message and/or perturbing the point to point transmission. Other nodes, called relays, help the point to point transmission by providing spatial diversity to combat fading, and by increasing the useful power received by the destination. The relays are nowadays included into standards, for instance in 3GPP LTE release 10, to provide higher data rate and better coverage.

The operations performed by the relay over the received signals and the timing used to transmit data to the destination define a relaying protocol. Among the plurality of known relaying protocols, the Dynamic Decode and Forward (DDF) protocol experiences the best tradeoff between reliability and spectral efficiency in the high Signal to Noise Ratio (SNR) regime. This protocol has only been studied according to information theory metrics assuming that the three wireless links: source-relay, source-destination and relay-destination experience the same long-term SNRs.

We thus propose in this work a *practical implementation of the DDF protocol* satisfying two assumptions.

First, we assume that the source is *relay-unaware*, i.e. not aware of the relay's presence in the system. It enables to design protocols requiring low signalling as no pilots or control signals dedicated to relaying are transmitted over the source-relay and source-destination links. Moreover, this assumption allows the design of completely decentralized relaying protocols, and it allows old equipments to take benefit from the relaying technique without any upgrade, which is called backward compatibility.

Secondly, we impose that the destination does not need any additional decoding abilities than when compared to the case without relay for backward compatibility reasons.

The performance of this practical implementation are described for unbalanced long-term SNRs. This new description of the performance for the DDF protocol leads to the definition of a new metric called *macro diversity order*.

Outline

This thesis report is organized as follows.

Chapter 1 describes the methodology used in this work to characterize the performance of a transmission. This is a two-step evaluation: the first one is a link level evaluation and the second

one is a system level evaluation. Both steps and the associated state-of-the-art figures of merit are described in this chapter.

In Chapter 2, after a review of the DDF protocol, we focus on deriving additional evaluation tools: we define the macro diversity order achieved by a transmission, and we derive macro and micro diversity upper bounds for some channel models. Then, we propose a practical implementation of the DDF protocol with a relay-unaware source. We evaluate two particular relaying schemes for the DDF protocol: the Monostream DDF protocol and the Distributed Alamouti (DA) DDF protocol.

In Chapter 3, we proposed a so-called Patching technique in order to increase this achievable macro diversity order still guaranteeing that the source is relay-unaware. This Patching technique is also combined with Space Time Block Codes in order to increase both the macro and micro diversity orders. By relaxing the relay-unaware source constrain, we propose other methods to improve the achievable diversity orders such as the modulation adaptation scheme. Finally, Distributed Rotation (DR) combined with the DDF protocol are used to improve the coding gain of the Monostream DDF protocol.

In Chapter 4, after describing state-of-the-art interference mitigation techniques for the Interference Relay Channel, we introduce the use of a precoded DDF protocol at a relay shared by several source/destination pairs. We combine this protocol with our proposed Patching technique in order to improve the performance achieved by the precoded DDF protocol.

Finally, all these proposed variations of the DDF protocol are studied at the system level in Chapter 5 for two applications: unicast transmission, e.g. web browsing, and broadcast transmission, e.g. video broadcasting, and two particular deployments: a urban macro cellular network, and an indoor deployment.

Chapter 1

Modus operandi for wireless transmissions evaluation

Introduction

Due to the increasing demand in services and quality of service for wireless communication system, new transmission techniques need to be defined and integrated into systems, for instance by a standardization process, or by the definition of proprietary techniques. This integration is done if, for instance, the new transmission technique enables to satisfy the needed quality of service or outperforms previously used schemes. This requires a pertinent evaluation of the considered technique.

This evaluation is composed of two steps when the considered system must achieve a given quality of service over a wide area, or for a high number of users. The first step is called *link level evaluation*, in which the performance of this transmission technique is evaluated on a minimal system called *basic channel*. The performance achieved by this transmission are described using information theory metrics such as capacity, outage probability and spectral efficiency. If the evaluated transmission technique shows interesting gains when compared to the state of the art at the link level, a second step must be done. The second evaluation step is called *system level evaluation*, and aims at studying the performance of the considered transmission technique in a full system which can be seen as multiple replicas of the basic channel. In this context, the performance of all users in the system are taken into account leading to performance described by cumulative distribution function (cdf) of a given metric.

The rest of this chapter describes these evaluation steps and the associated metrics. In Section 1.1, we describe various basic channels for link level evaluation: the point to point channel, the relay channel and some relaying protocols, the Multiple Access Channel (MAC) and the broadcast channel. We also define the associated figures of merit to describe the reliability of a transmission or its efficiency. In Section 1.2, we describe the different stages needed for system level evaluation and the associated figures of merit.

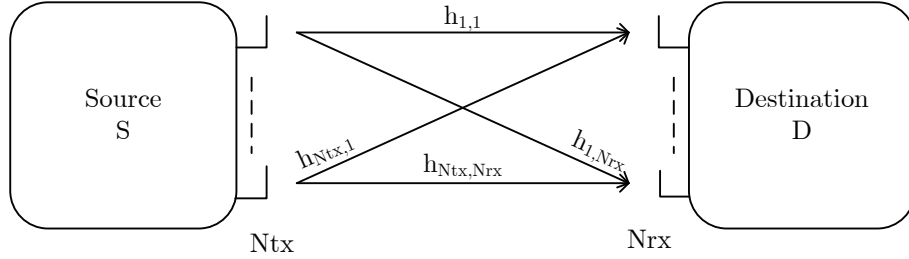


Figure 1.1: Point to point channel, the source carries N_{tx} antennas and the destination carries N_{rx} antennas.

1.1 Link level evaluation : basic channel models and metrics

The link level evaluation consists in evaluating the performance of a single or a small set of point to point transmissions to a single destination without considering any specific geometry of deployment, and under some given assumptions and constraints.

1.1.1 All begins with a point to point transmission

The simplest transmission system is described by the point to point channel. This model describes two nodes among which the source S transmits data to the second node, called the destination and denoted D .

This basic channel is described in Fig. 1.1 where the source carries N_{tx} transmission antennas and the destination has N_{rx} reception antennas.

According to the values N_{tx} and N_{rx} , this channel has distinct names:

- if $(N_{tx}, N_{rx})=(1,1)$, this is a Single Input Single Output (SISO) channel,
- if $N_{tx} = 1$ and $N_{rx}>1$, this is a Single Input Multiple Output (SIMO) channel,
- if $N_{tx}>1$ and $N_{rx}=1$, this is a Multiple Input Single Output (MISO) channel,
- when both N_{tx} and N_{rx} are strictly superior to 1, this is a Multiple Input Multiple Output (MIMO) channel [2].

In this subsection, we first describe a wireless transmission over the basic SISO channel, and then we present the MIMO channel and the associated metrics.

a) SISO case

In this paragraph, we assume that the source and the destination only carry a single antenna.

The source wants to transmit a binary sequence $\mathbf{b} \in \{0, 1\}^n$, called information bits, to the destination. This binary sequence is mapped into a sequence of complex symbols $\mathbf{s} = f(\mathbf{b})$ belonging to a symbol set where f denotes this mapping. This set is called a constellation or a modulation (both terms will be used in the following). We assume that the averaged energy over all symbols in the constellation is equal to one. Two constellation types can be distinguished. The constellation can be a continuous set, for instance when the symbols are complex random variables Gaussian distributed, or the constellation can be finite and consequently discrete set such as a Phase Shift

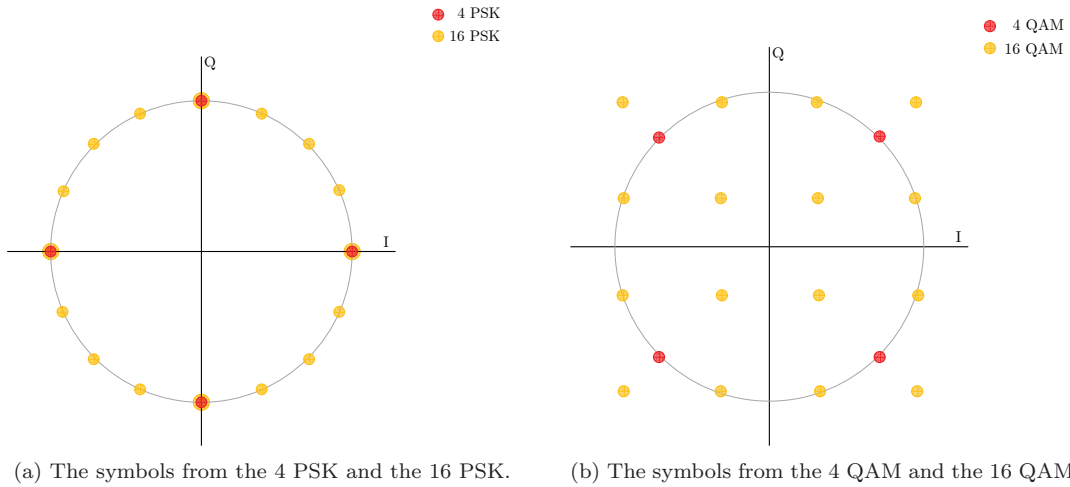


Figure 1.2: Different modulations, the circle represents points of unit energy.

Keying (PSK), or a Quadrature Amplitude Modulation (QAM). For finite constellations, the number of symbols in the set is said to be its cardinality, and its spectral efficiency is the number of bits carried by each symbol. In Fig. 1.2a, the modulation 4PSK of spectral efficiency 2 bits per symbol, and the modulation 16PSK of spectral efficiency 4 bits per symbol are presented. The 4QAM of spectral efficiency 2 bits per symbol and the 16QAM of spectral efficiency 4 bits per symbol are plotted in Fig. 1.2b. The *data rate* of this transmission is defined as the ratio between the number of transmitted information bits and the number of transmitted symbols.

Then, this symbol sequence is transmitted by the source, and is corrupted by its propagation (described in Section 1.2) such that P_S is the average received power from the source at the destination. The transmitted symbol is impacted by a short-term fading coefficient, denoted h representing very small variations in the propagation environment. It is modeled by a complex random variable whose distribution depends on the channel to describe: If a direct link between S and D exists, this variable will be Ricean distributed, but if there is no direct link, the fading coefficient is complex Gaussian distributed of zero mean and unit variance, the signal being only received thanks to several reflexions in the environment surrounding S and D . Thus, in this no line of sight case, the probability density function is:

$$p_h(x) = \frac{1}{2\pi} \exp\left(-\frac{\|x\|^2}{2}\right). \quad (1.1)$$

We assume in all this work that the fading coefficients are quasistatic, i.e., they remain constant during the transmission of a message, and are independent from one transmission to another. Finally, the symbol altered by these fadings is received by the destination, where a thermal noise, generated by the used hardware at D , is added. This noise w is modeled by a complex Gaussian random variable of zero mean and variance $2N_0$. Consequently, if the source sends a symbol denoted s , the destination receives the signal denoted y such that:

$$y = \sqrt{P_S}hs + w \quad (1.2)$$

The destination aims at detecting s from y by knowing the average received power from the source P_S , the fading coefficient h , and the used constellation. The channel coefficients are known thanks to channel estimation. If they are perfectly known, this detection is said to be coherent.

Then, the destination must detect $\sqrt{P_S}hs$ out of the suffered the noise. The higher the received power affected to s is, and the better this detection can be done. Consequently, a first metric characterizing this transmission is its SNR, describing the ratio between the power of the useful signal and the power of the noise b . We define two SNRs.

- The short-term SNR is defined as the ratio of the received useful power $\sqrt{P_S}hs$, averaged over all possible symbols, and the noise power:

$$\frac{P_S \|h\|^2 \mathbb{E}_s [s]}{2N_0} = \frac{P_S \|h\|^2}{2N_0}.$$

- The long-term SNR ρ_{SD} is the expected value of the short-term SNR over all possible values of the fading coefficient h :

$$\rho_{SD} = \mathbb{E}_h \left[\frac{P_S \|h\|^2}{2N_0} \right] = \frac{P_S}{2N_0}.$$

b) MIMO case

We now consider a point to point transmission in which the source carries N_{tx} transmit antennas, and the destination carries N_{rx} reception antennas. When the source uses several antennas, the sent symbols propagating on the same medium (time and frequency) interfere each other, and the destination receives on each reception antenna, a linear combination of the sent symbols. Considering T time-slots during which the source transmits a matrix of symbols $\mathbf{S} = f(\mathbf{b})$ derived from the binary sequence \mathbf{b} :

$$\mathbf{S} = \begin{pmatrix} s_{1,1} & \cdots & s_{1,T} \\ \vdots & \ddots & \vdots \\ s_{N_{tx},1} & \cdots & s_{N_{tx},T} \end{pmatrix}.$$

T is also called the length of the transmitted codeword \mathbf{S} . By denoting $h_{i,j}$ the fading coefficient between the i -th source's antenna and the j -th destination antenna, the transmission is described by the following matrix model:

$$\begin{aligned} \mathbf{Y} &= \sqrt{P_S} \begin{pmatrix} h_{1,1} & \cdots & h_{1,N_{tx}} \\ \vdots & \ddots & \vdots \\ h_{N_{rx},1} & \cdots & h_{N_{rx},N_{tx}} \end{pmatrix} \mathbf{S} + \mathbf{W} \\ \Leftrightarrow \mathbf{Y} &= \mathbf{H}\mathbf{S} + \mathbf{W}. \end{aligned} \tag{1.3}$$

The covariance matrix of the noise \mathbf{W} is equal to $2N_0\mathbf{I}_{N_{rx}}$ and \mathbf{H} is called the equivalent channel matrix. We assume that the antennas on a same node are sufficiently isolated from each other so that the fading coefficients are independent from each other.

The destination aims at recovering \mathbf{b} , from the received signals \mathbf{Y} , knowing the mapping function f , and the fading coefficients (long term and short-term), i.e., knowing \mathbf{H} . To reach this goal, several detectors can be used, leading to distinct performance in term of binary error probability. Optimal detectors are based on the Maximum A Posteriori (MAP) criterion which can be described as: detecting the symbol matrix $f(\hat{\mathbf{b}})$ maximizing the probability that the received signal is \mathbf{Y} knowing that $\mathbf{H}f(\mathbf{b})$ is transmitted. These detectors are equivalent to the Maximum Likelihood (ML) detector if all possible $f(\mathbf{b})$ are equiprobable, see e.g. [3], ch.5. The ML detection criteria is defined as the minimal distance detection criteria:

$$\hat{\mathbf{b}} = \arg \min_{\mathbf{b}} \|\mathbf{Y} - \mathbf{H}f(\mathbf{b})\|. \tag{1.4}$$

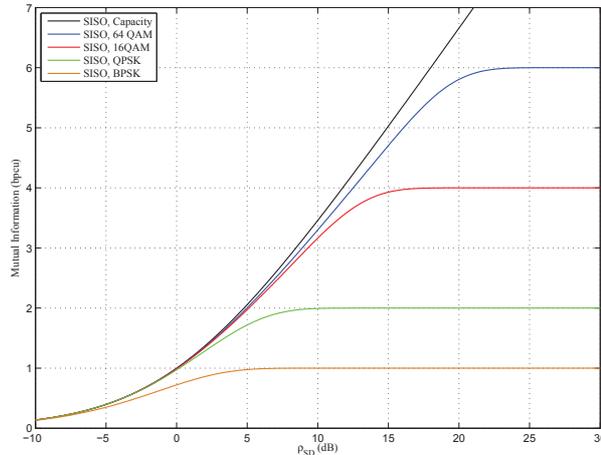


Figure 1.3: Mutual information and capacity of the SISO channel According to ρ_{SD} .

An exhaustive receiver satisfying this rule is optimal, however, it requires high computing abilities. There exist several optimal receivers which require lower computing skills such as the sphere decoder, or the stack decoder.

c) Capacity and mutual information

The channel theoretically allows the error-free transmission of a maximal number of information bits per time-slot called channel capacity. This capacity is expressed in bit per channel use (bpcu).

Telatar proved in [2] that the capacity of a MIMO transmission described by Eq. (1.3), for a fixed \mathbf{H} , is equal to

$$C(\mathbf{H}) = \log_2 \left(\det \left(\mathbf{I}_{N_{\text{rx}}} + \frac{1}{2N_0} \mathbf{H}\mathbf{H}^\dagger \right) \right). \quad (1.5)$$

This capacity is achievable under the assumption that the sent symbols $s_{i,j}$ are complex random variable Gaussian distributed.

However, from a practical point of view, using a continuous symbol alphabet is unfeasible. Consequently, one important research issue is to design the transmitted symbols from discrete and finite sets to reach this capacity.

The quantity measuring how many information bits of the transmitted symbols \mathbf{S} can be extracted out of the received signals \mathbf{Y} for a fixed channel matrix \mathbf{H} is the mutual information $I(\mathbf{S}; \mathbf{Y}|\mathbf{H})$, which is expressed as the expected value of the log likelihood ratio over noise and symbols [4],

$$I(\mathbf{S}; \mathbf{Y}|\mathbf{H}) = \mathbb{E}_{\mathbf{S}, \mathbf{w}} \left[\log_2 \left(\frac{p(\mathbf{Y}|\mathbf{S})}{\sum_{\mathbf{S}'} p(\mathbf{Y}|\mathbf{S}')p(\mathbf{S}')} \right) \right] \quad (1.6)$$

This mutual information is limited by the number of bits that can be simultaneously transmitted: if the sent symbols matrix \mathbf{S} is taken from a set of cardinality M , then the mutual information will be limited by $\log_2(M)/T$ bpcu. The capacity of the channel is equal to the mutual information between \mathbf{S} and \mathbf{Y} , when the symbols are Gaussian distributed (the discrete sum becoming an integral). The mutual information of the SISO channel is presented in Fig. 1.3, for symbols from a Gaussian alphabet (capacity of the channel), and symbols from several modulations: BPSK, QPSK, 16QAM and 64QAM, according to the long term SNR between source and destination.

The figure shows how the achievable mutual information is limited by the constellation size when symbols from a finite symbol alphabet are transmitted.

d) Reliability of the transmission

The capacity of the channel is the maximal quantity of information to be transmitted over a link with an error probability as small as desired. We need to define the reliability notion, which describes the ratio of information correctly recovered at the destination to the quantity of information transmitted by the source. This notion of reliability is important for the transmission system design. Indeed, the transmission must at least achieve a targeted maximal error probability, or outage probability, that we define as a physical layer Quality of Service (QoS). Then, all positions of the destination satisfying this QoS define the coverage area of the source. Achieving this QoS is of particular importance when there is no feedback link between the source and the destination, i.e., in case of an *open loop* transmission. The destination has no possibility to ask for a new transmission of the message.

The reliability of a transmission depends on the set of transmitted matrices \mathbf{S} , on the experienced matrix \mathbf{H} , and on the noise variance. It is described by the error probability $P_{e|\mathbf{H}}$. Averaging over the possible matrix realizations, the reliability of the transmission is described by the error probability $P_e = \mathbb{E}_{\mathbf{H}}[P_{e|\mathbf{H}}]$ which is lower bounded, for very long codewords, by the outage probability. This outage probability represents the fact that the instantaneous channel matrix is so bad that the resulting channel cannot support the data rate transmitted by the source, the channel is said to be in outage.

Error probability The probability that the destination makes a detection error is equal to

$$P_{e|\mathbf{H}} = \sum_{\mathbf{X}} P\{\mathbf{X} = \mathbf{S}\} P\{\hat{\mathbf{S}} \neq \mathbf{S} | \mathbf{X} = \mathbf{S}, \mathbf{H}\} \quad (1.7)$$

where $P\{\mathbf{X} = \mathbf{S}\}$ is the probability that the source transmits \mathbf{S} , $P\{\hat{\mathbf{S}} \neq \mathbf{S} | \mathbf{X} = \mathbf{S}, \mathbf{H}\}$ is the probability that the destination makes a decoding error knowing that the source transmits \mathbf{S} . An upper bound on the error probability, thigh for high SNR values, is usually used. It is derived from the union bound of $P\{\hat{\mathbf{S}} \neq \mathbf{S} | \mathbf{X} = \mathbf{S}, \mathbf{H}\}$:

$$\Pr\{\hat{\mathbf{S}} \neq \mathbf{S} | \mathbf{X} = \mathbf{S}, \mathbf{H}\} \leq \sum_{\mathbf{X}', \mathbf{X}' \neq \mathbf{S}} P_{\mathbf{S} \rightarrow \mathbf{X}' | \mathbf{H}} \quad (1.8)$$

where $P_{\mathbf{S} \rightarrow \mathbf{X}' | \mathbf{H}}$ is the pairwise error probability, i.e., the probability that the destination decodes \mathbf{X}' whereas the source sent \mathbf{S} for fixed a \mathbf{H} , assuming that \mathbf{X}' and \mathbf{S} are the only possible sent codewords.

This pairwise error probability mainly depends on the detection rule used by the destination, i.e., it depends on the used detector. Assuming that a ML detector is used, it comes:

$$P_{\mathbf{S} \rightarrow \mathbf{X}' | \mathbf{H}} = Q \left(\sqrt{\frac{\|\mathbf{H}(\mathbf{X}' - \mathbf{S})\|^2}{4N_0}} \right) \quad (1.9)$$

where $Q(x)$ is the error function of Marcuum such that $Q(x) = \frac{1}{2\pi} \int_x^{+\infty} \exp(-t^2/2) dt$. A closed form expression of this pairwise error probability has been derived in [5], but it can also be upper bounded by $Q(x) \leq \frac{1}{2} \exp(-x^2/2)$.

The expected pairwise error probability over the fading coefficients $h_{i,j}$, which are assumed to be independent, can be approximated at high SNR by:

$$P_{\mathbf{S} \rightarrow \mathbf{X}'} \propto \frac{1}{a(\rho_{SD})^{\hat{d}}} \quad (1.10)$$

and then

$$P_e = \mathbb{E}_{\mathbf{H}} [P_{e|\mathbf{H}}] \propto \frac{1}{\hat{a}(\rho_{SD})^{\hat{d}}} \quad (1.11)$$

where $\sqrt{\hat{a}}$ defines the coding gain of the scheme, and \hat{d} is the diversity order achieved by this transmission scheme, defined as the minimal diversity order d experienced among all possible pairs $(\mathbf{S}, \mathbf{X}')$. This order is an integer which is at least equal to the number of reception antennas N_{rx} [6], and which is upper bounded by $N_{tx}N_{rx}$. It physically represents the minimal number of independent paths experienced by each information symbol. The higher this diversity is, the lower the error probability is in the high SNR regime, which is also true for the coding gain: if two schemes experience the same diversity order, the scheme achieving the highest coding gain experiences the smallest error probability for high values of SNR.

Different coding schemes have been proposed in order to improve (decrease) the error probability. We are particularly interested in two of them: channel coding and space-time coding.

- Channel coding aims at increasing the distance between codeword matrices to be transmitted by generating from the information bits, a longer bit sequence, also called codeword. The generated sequence has a *coding rate* R_c equal to the ratio of the number of information bits K over the total number of transmitted bits L . Several code families exist among them one can cite the convolutional codes [3], the turbo codes [7], and the rateless codes [8].
- Space-time coding aims at maximizing the recovered spatial diversity (diversity offered by the transmission antennas) by generating N_{tx} independent linear combinations of all symbols from \mathbf{S} over several time-slots. Construction criteria of the codeword matrices \mathbf{S} have been derived in [6] so that the resulting diversity and the coding gain are maximized. The first proposed block space time code, and the most famous one, has been derived by Alamouti in [9] for a system with $N_{tx}=2$ and $N_{rx}=1$. This space time code achieves the maximal diversity of 2 and the maximal data rate of 1 symbol per channel use. For a $N_{rx} \times N_{tx}$ MIMO system, the perfect codes provide the maximal diversity order and full data rate, such as the Golden Code [10] for a 2×2 MIMO system.

Outage probability We just show that the error probability of a transmission is a metric derived for a particular encoding scheme (channel encoding and space-time encoding). To get rid of this code consideration, another reliability metric for a transmission over a channel \mathbf{H} is its outage probability.

If no channel state information is known at the source, the instantaneous mutual information can be lower than the data rate R used by the source. The occurrence probability of this event defines the outage probability P_{out} of the transmission:

$$P_{out} = P_{\mathbf{H}} \{I(\mathbf{S}; \mathbf{Y}|\mathbf{H}) < R\} \quad (1.12)$$

The outage probability can be derived either for symbols from Gaussian alphabet using the fact that $I(\mathbf{S}; \mathbf{Y}|\mathbf{H}) = C(\mathbf{H})$, or for symbols from a finite alphabet using Eq. (1.6).

For very long codewords, the outage probability is a lower bound on the error probability, which, for asymptotically large values of SNR, becomes proportional to

$$P_{out} \propto \frac{\xi}{(\rho_{SD})^{\hat{d}}} \quad (1.13)$$

where \hat{d} is an upper bound on the diversity order achieved by the transmission, and ξ is called the outage gain [11, 12]. Thus, the higher the diversity order, the lower the outage probability, and the lower the outage gain, the better the performance.

e) Spectral efficiency and throughput

The second figure of merit to characterize a transmission is the spectral efficiency expressed in bpcu. It represents the average number of information bits correctly recovered at the destination using a unit amount of time and frequency. When the bandwidth used for transmission is known, the performance can be expressed in terms of throughput which is expressed in bits per second.

The aim of any transmission is to achieve a spectral efficiency as close as possible of the channel capacity, i.e, to maximize the number of transmitted bits without error per channel use. This metric is particularly relevant for *closed-loop* transmission in which a feedback link between the source and the destination exists. Using this link, the destination can ask for retransmission if it fails to correctly decode the message. In a practical system, Cyclic Redundancy Check (CRC) codes are used by the destination to ensure the correctness of the decoded bits, [13].

In the literature, several techniques have been proposed to increase the spectral efficiency of a transmission and minimize the mis-reception of a whole codeword.

Automatic Repeat reQuest A first simple way of increasing the spectral efficiency is to repeat the whole codeword in case of a first mis-decoding. Let's imagine that the channel is in outage during the first transmission of the codeword \mathbf{S} spreading over T channel uses. Decoding cannot be done without error. It results a spectral efficiency of 0 bpcu. However, if the destination could be aware of its misdecoding and could warn the source, \mathbf{S} could be repeated over a channel experiencing a distinct fading coefficient, leading to a smaller outage probability. Assuming that the second transmission of \mathbf{S} is correctly decoded by the destination, the transmission would achieve a spectral efficiency of $K/(2T)$ bpcu which is much better than a null spectral efficiency. This technique is called Automatic Repeat reQuest (ARQ) and has been proposed in [14]. Using ARQ the destination flushes its memory between the two transmissions, deleting the information carried by the previously received signals. The retransmissions occur until the destination correctly decodes the message or until a maximal number of retransmissions is reached.

Hybrid ARQ A second method to improve spectral efficiency is called Hybrid Automatic Repeat reQuest (HARQ) taking benefit from a new transmission of data from the source and the previously received signals. It is called HARQ and has been described in [15, 16, 17].

Two types of HARQ exist. The first one is the Hybrid Automatic Repeat reQuest with Chase Combining (HARQ-CC). Using this HARQ technique, the source always transmits \mathbf{S} until the destination correctly decodes the message or until a maximal number of retransmission is achieved as for ARQ, but the destination stores all received versions of the data and uses a Maximum Ratio Combining (MRC) detector to coherently combine the signals.

The second type of HARQ is the Hybrid Automatic Repeat reQuest with Incremental Redundancy (HARQ-IR): The source uses a channel encoder such as a rateless code, or a punctured turbo-code

to encode the data. If the destination fails in decoding the message, the source does not send the same symbols but additional redundancy. The concatenation of the received signals at the destination represents the same message encoded with a lower coding rate, making decoding easier. These steps are repeated until the destination correctly decodes the message or until a maximal retransmissions number from the source. This method is particularly interesting as the source dynamically adapts the transmitted data rate to the quality of the source-destination link thank to the feedback link.

In the rest of this thesis, in case of a closed-loop transmission, we assume that the existing feedback link between the source and the destination is error free and does not introduce any delay.

f) Trade off between reliability and efficiency

Channel coding is an efficient way of improving the transmission reliability. However, it requires the source to transmit redundancy bits leading to the use of a higher number of resources (by keeping constant the modulation used by the source, and N_{tx}). Consequently, the higher the transmission duration, the higher the transmission reliability but it lowers the resulting spectral efficiency. Consequently, there is a trade off between reliability and efficiency which is described, for asymptotically large values of SNR, by the Diversity Multiplexing Trade off (DMT) of a transmission. This metric, proposed by Zheng and Tsé in [18], describes the achievable diversity according to the multiplexing gain $r = \lim_{\rho \rightarrow \infty} \frac{R}{\log \rho}$ by deriving the outage events for asymptotically large values of SNR.

The authors derive the DMT close-form expressions for the point to point channels:

$$\begin{aligned} d_{SISO} &= 1 - r \\ d_{MISO} &= N_{tx}(1 - r) \end{aligned}$$

and the DMT of a MIMO transmission is the piecewise linear function passing through the points $(k, (N_{tx} - k)(N_{rx} - k))$ with $k \in \{0, \dots, \min(N_{rx}, N_{tx})\}$. These DMTs are represented in Fig. 1.4.

1.1.2 Relay channel

In the previous section, we introduced the MIMO point to point channel, and defined several metrics to characterize the reliability and the efficiency of such a transmission. In this section, we describe another basic channel usually used for link level evaluation called relay channel.

Due to the broadcast nature of the wireless medium, any signal transmitted during a point to point transmission can be eared by any other nodes in the network.

The aim of these nodes can be distinct. Some of them, such as eavesdroppers, aim at intercepting the message and keep it for itself or perturbing the point to point transmission, see for instance [19] and references there in. A second category of nodes can help the point to point transmission, they are called relays.

The combination of a source S , a relay denoted R and a destination D forms a basic channel called the relay channel presented in Fig. 1.5, and introduced by Van Der Meulen in 1971 [1]. The fading coefficients between the source and the relay, between the source and the destination, and between the relay and the destination are denoted h_{SR} , \mathbf{h}_{SD} and \mathbf{h}_{RD} respectively.

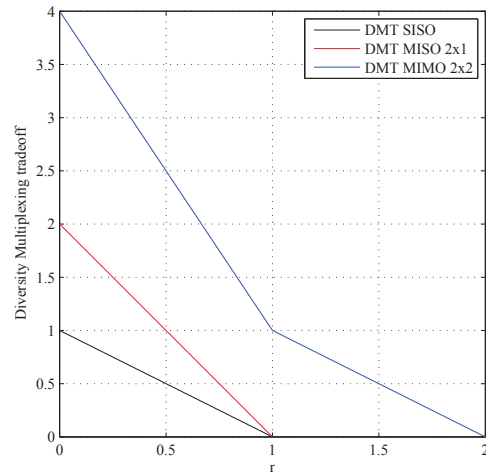


Figure 1.4: DMT of different MIMO schemes.

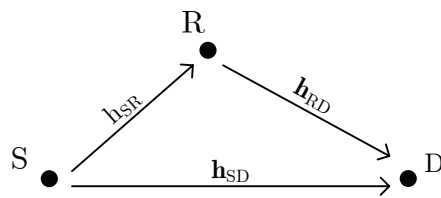


Figure 1.5: The relay channel.

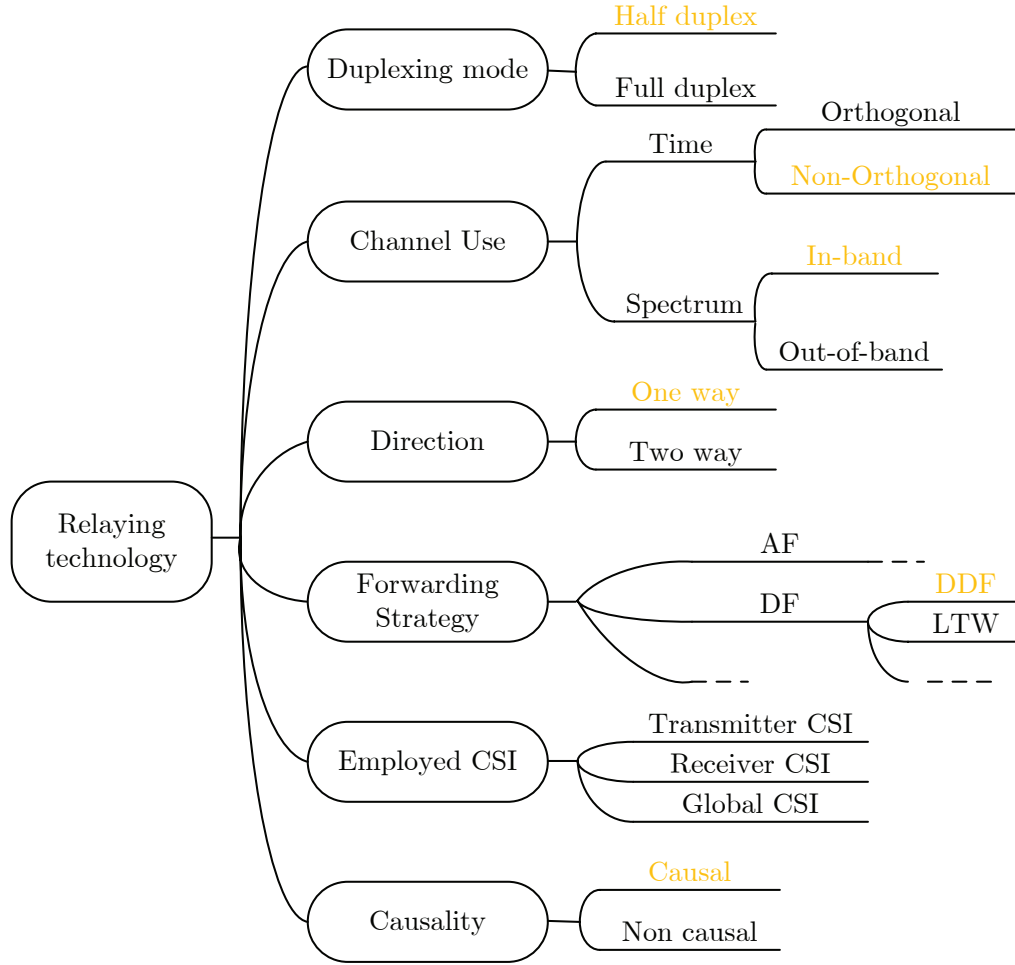


Figure 1.6: A taxonomy of current technologies for Type 2 layer 2 relays.

From the destination point of view, this channel forms a distributed MIMO scheme as it receives data representing the same information from two independently faded links, [20].

The relay channel has been introduced for two reasons. On one hand, it enables to improve the reliability of the transmission by providing spatial diversity. Several studies have been proposed such as [21, 22] where the authors exploit the available spatial diversity using repetition coding or distributed space-time coding.

On another hand, the relay channel has been introduced to increase the spectral efficiency at the destination leading to define the achievable capacity over such a channel, and coding schemes enabling to reach this capacity. This is for instance the case in [23] where the authors aim at deriving the capacity region of this channel.

a) Characterization of a relay

We can distinguish several relays categories according to their abilities.

In this work, we consider static relays, they can be opposed to moving relays that would, for instance, be deployed in a train.

The relays operating at the network layer of the OSI model, are called *type 1* relays in 3GPP Rel.10 in which they appear as base stations for users and are employed to increase spectral

efficiency and improve coverage.

The relays only operating at the physical or data link layers are called *type 2* relays in 3GPP Rel.10. Among these relays, two categories can be distinguished: the *layer 1* relays which are repeaters, and the *layer 2* relays which can access the transmitted symbols.

In this thesis, we only focus on these type 2 layer 2 relays as they might be introduced in future standards and provide a wide research area. These relays present numerous characteristics defined hereafter .

Causality A relay is said to be *causal* when it accesses the information transmitted by the source through the wireless channel between the source and the relay. This acquisition step requires resources that must be taken into account in order to characterize the performance of the relaying scheme. On the contrary, the relay is said to be non causal when it knows the information to be transmitted by the source prior to any transmission. This is an ideal set up, also called *genie aided*. This feature is used to derived upper bounds on the performance.

Duplexing mode A relay is a *full-duplex* relay if it can transmit and receive at the same time. The difficulty resulting from this property is that the power of the received signal might be much smaller than the transmitted signal leading to the generation of strong self-interference. On the contrary, the relay is said to be *half-duplex* when it cannot transmit and receive at the same time.

Used Resource A resource block is composed of time-slots and frequency slots. Consequently, 2 characteristics of the relay are defined according to the resources it uses. If the relay transmits using the same frequency slots as the source, the relay is an *in-band* relay; if not, the relay is *out-band*. Regarding time resources, if the relay transmits using the same time-slots as the source, the relaying protocol is said to be *non-orthogonal*, if the relay uses different time-slots, the relaying protocol is said to be *orthogonal*.

Direction In a relay channel, the destination is the only node needing the source's information. The relay is present to help the destination to recover this information. Thus, the relay transmits only to the destination. This is a *one-way* relay. However, if in the considered system, both nodes would exchange data, the relay could help both nodes leading to a *two-way* relay channel.

Employed Channel State Information (CSI) The relay accesses a *global CSI* when it perfectly knows the fading coefficients of each link in the system. This is an ideal case requiring a lot of feedback between the nodes. The relay has *receiver CSI*, when it perfectly knows the source to relay fading coefficient only, and it has *transmitter CSI* when it perfectly knows the fading coefficients of the relay to destination link.

Forwarding strategy The process used at the relay before transmitting enables to mainly distinguish 3 general forwarding strategies: if the relay linearly processes the received signal, it results Amplify and Forward (AF) relaying strategies. If it only transmits a quantized version of its received signals, this is a Compress and Forward (CF) relaying strategy, and finally, if the relay processes the received signal up to recovering the transmitted information bits, it leads to Decode and Forward (DF) relaying protocols. In the following, we give more insights on forwarding strategies and the resulting relaying protocols.

All these characteristics are summarized in Fig. 1.6 where we highlighted the considered characteristics of the relays studied in this thesis. We consider a type 2 layer 2 relay with the following characteristics chosen to design practical relaying protocols: causal, half-duplex, in-band, and non-orthogonal. Consequently, there is no increased need in physical resource when compared to the no relay case.

b) Relaying protocols

The combination of a forwarding strategy and the resource scheduling between the source and the relay defines a relaying protocol.

In this section, we briefly review some of the relaying protocols designed for the one-relay case satisfying our previously described characteristics (causal, half-duplex, in-band, one way).

AF protocols A relay using an AF strategy forwards an amplified version of its received signals to the destination in the limit of a predefined power budget. This forwarding strategy, defined in [21, 24], is of particular interest as it only requires a linear processing at the relay. However, the noise sample included into the received signal is also amplified which can mislead the destination. Furthermore, it requires the destination to estimate the fading coefficient between the source and the relay.

Distinct time allocations at the relay lead to different AF protocols.

- **The Orthogonal Amplify and Forward (OAF):** this protocol, defined in [24], is composed of two phases of equal lengths. During the first phase, the source transmits its signal, while both the destination and the relay listen. During the second phase, the relay transmits its received signal affected by a constant, while the source remains silent and the destination listens. The DMT of this protocol is

$$d_{OAF}(r) = 2(1 - 2r)^+.$$

- **The Non-Orthogonal Amplify and Forward (NAF):** This protocol, proposed for the one-relay case in [25], enables the source and the relay to transmit simultaneously during the second phase of the protocol to increase the achievable spectral efficiency. The DMT of this protocol is

$$d_{NAF}(r) = (1 - r)^+ + (1 - 2r)^+.$$

This relaying protocol is the AF protocol providing the best DMT.

DF protocols A relay using the DF strategy detects the symbols sent by the source, possibly re-encodes this information, and forwards the resulting symbols to the destination. This forwarding strategy enables to get rid of the suffered noise at the relay, and only receiver CSI is needed at the destination. However, if the relay erroneously detects the symbols sent by the source, it misleads the destination.

Several time schedules exist, leading to several DF protocols.

- **The Laneman Tse Wornell Decode and Forward (LTW DF):** this DF protocol defined in [24] uses the same time schedule as the OAF protocol, but the forwarding strategy differs: During the first phase of the protocol, the source transmits data to both the relay and the destination. During the second phase, the relay transmits the detected symbols from

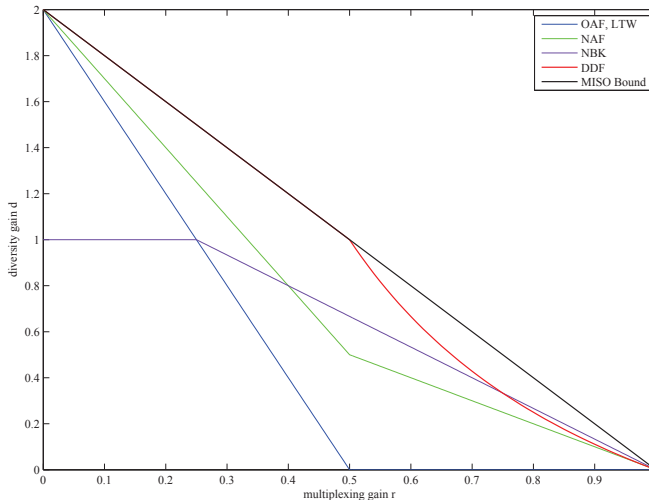


Figure 1.7: DMT of different AF and DF protocols.

its received signals to the destination while the source remains silent. This protocol achieves a DMT equal to

$$d_{LTW}(r) = 2(1 - 2r)^+.$$

Similarly as the OAF protocol, the LTW DF suffers from a low spectral efficiency as the second phase is only used to retransmit information on the relay to destination link.

- **The Nabar Bolcskei Kneubehler Decode and Forward (NBK DF):** This protocol presented in [25] aims at solving this low rate disadvantage of the LTW DF protocol. The source is allowed to transmit new data during the second phase of the protocol while the relay transmits symbols related to those sent during the first phase. This protocol achieves a DMT, derived in [26], equal to

$$d_{NBK}(r) = \begin{cases} 1 & \text{if } 0.25 > r \geq 0 \\ \frac{4}{3}(1 - r)^+ & \text{if } 1 \geq r \geq 0.25 \end{cases}.$$

- **The Dynamic Decode and Forward (DDF):** This last version of DF protocols, simultaneously defined in [27], and [28], aims at using the relay only when it can enhance the transmission: the relay begins to transmit only if it has correctly decoded the message. The protocol is said to be dynamic as this instant of correct decoding depends on the source to relay fading coefficient. The authors of [27] prove that the DMT of this protocol is

$$d_{DDF}(r) = \begin{cases} 2(1 - r), & \text{if } 0 < r \leq 0.5 \\ (1 - r)/r, & \text{if } 0.5 < r \leq 1 \end{cases}.$$

In Fig. 1.7, the DMT of all these protocols and maximal performance corresponding to the non causal relay case (also called MISO bound) are presented. The DDF protocol, designed for a causal, half duplex, in band relay is the non-orthogonal protocol leading to the best DMT performance.

Other various forwarding strategies Several other forwarding strategies for the relay channel are proposed in the literature. One can cite for instance the Compress and Forward relaying strategy or the Rotate and Forward protocol.

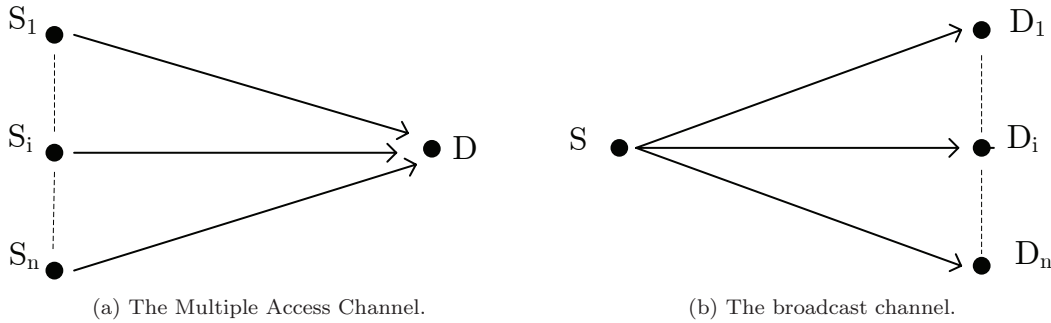


Figure 1.8: Two basic channels.

The Compress and Forward, is also called estimate and forward in [23], or quantize and forward in [29]. The relay using this protocol first quantizes its received signal and then transmits the corresponding quantification level to the destination.

If the relay uses the Rotate and Forward protocol, defined in [30], it transmits its decoded version of the symbols sent by the source affected by a complex constant of unit modulus.

1.1.3 Multiple Access channel

In this section, we still describing basic channel models for link level evaluation, and we particularly focus on the MAC.

The third basic channel is called the MAC, described in Fig. 1.8a, where several sources using the same physical resource transmits independent messages to a single destination. An interesting overview of the known results is done in [31] where the capacity regions of this channel for any number of sources, nodes' antennas and several CSI knowledges are recalled.

Over this channel, the main problem is the generated interference from one source on the others and suffered at the destination, leading to the design of successive interference cancellation receivers.

When this channel is combined with a relay, it forms the Multiple Access Relay Channel, where the relay helps the sources to deliver their messages to the destination by using one of the before mentioned forwarding strategies. This channel was first described in [32] for Additive White Gaussian Noise (AWGN) channels. The capacity region of this channel is unknown.

1.1.4 Broadcast channel

The fourth basic channel is called the broadcast channel, and is described in Fig. 1.8b.

This channel is the perfect mirror of the MAC: a single source transmits independent messages to a several destinations. A lot of work is done in order to derive the capacity region of this channel which still unknown. An interesting overview of the known results is given in [31].

When this channel is combined with a relay, it forms the Broadcast Relay Channel, where the relay helps the source to deliver its messages to the destination.

1.1.5 Interference channel

The last basic channel usually considered in the literature is called the interference channel. In this channel, described in Fig. 1.9, several source/destination pairs use the same resource to transmit

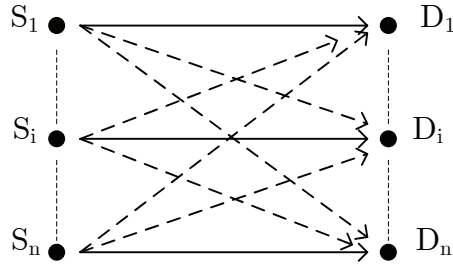


Figure 1.9: The interference channel.

independent messages, thus interfering one on each other. On the figure, the useful links are represented by full arrows while the interfering links are denoted by dashed arrows.

Similar to the MAC or the broadcast channel, if a relay is included in an interference channel, it forms an Interference Channel with Relay (IRC). A detailed review of the known results linked to this basic channel will be given in Chapter 4.

In this section, we thus described 5 basics channels: the point to point channel, the relay channel, the MAC, the broadcast channel and the Interference Channel (IC). We also defined the used metrics at the link level to characterize the performance of transmission schemes on these channels.

1.2 System level evaluation : application, deployment and propagation models

A transmission scheme providing gains for a given metric, for a particular range of SNRs at the link level must be evaluated at the system level. Indeed, in a system, it is possible that the typically experienced ranges of SNRs do not match with those providing gains at the link level.

Consequently, the second step evaluates the performance of a transmission technique at the system level.

These system level evaluations are usually performed through a system level simulator for a given application, describing the considered nodes deployment, and modeling propagation over a particular area.

In this section, we define these notions of applications, deployment and propagation needed for system level evaluation and the associated figures of merit.

1.2.1 Application

The application defines the purpose of the studied transmission scheme. We here give three application examples for wireless systems:

A wireless system can be used for broadcasting information. For a broadcast application, the same message is intended at all users. For instance, radio or TV programs are broadcasted. This application must be differentiated from the previously defined broadcast channel where a single source transmits independent messages to several destinations. For a broadcast application, all users receive on the same physical resource (time and frequency).

When wireless communication is used for multi-cast, the same message is intended at a subset of users. For example, subscribers of the same TV channels generate such a subset. Different access methods can be used to simultaneously transmit to several subsets of users such as Orthogonal Frequency Division Multiplexing (OFDM) for the Digital Video Broadcasting - Terrestrial, where these subsets listen to distinct resource blocks to recover their information.

Another example of application for a wireless system is a unicast transmission, e.g. voice transmission or web browsing. In this case, each user in the network aims at receiving distinct messages. The used access method defines how the whole available resource is shared between users. In standards currently designed, the OFDM is usually chosen. If two users share the same resource, they can hear the information intended at the other user, generating interference which is one of the major difficulties in such a system.

1.2.2 Deployment

After defining the application, the next step is to define the considered deployment, i.e., the environment in which transmission occurs.

The deployment model of a wireless transmission system characterizes 3 aspects of this system: the considered area, the distinct families of nodes (their hierarchical relations and their characteristics), and finally the nodes topology.

The deployment models the considered area over which the different nodes in this system are distributed. Several areas are usually considered: for instance rural, urban or indoor.

Then, the nodes characteristics are defined. Several types of nodes can be considered among them must be cited: the Mobile Station (MS) which are the end users in a wireless systems, the Base Station (BS) belonging to providers and the dedicated Relay Station (RS) which are intermediate nodes assisting the transmission of the intended data at the MSs. A transmission system can also be built from a sensor network where the nodes are sensors.

Each node has several characteristics which differ according to the node types. Among the plurality of characteristics, we can cite their height, their transmit power, and their antenna diagram. This will be described with more details in Chapter 5.

Moreover, two nodes of the same type experience the same hierarchical level, there is no master/slave relation between them. When deployment is done considering nodes from a single type, the resulting network is said to be ad-hoc.

On the contrary, if two nodes of distinct types are considered, there can be a master/slave relation. This is typical of the BS/MS relation, but this is not mandatory for the RS/MS relation or the BS/RS relation. When several nodes from several types are deployed experiencing master/slave relation, the deployment is said to be cellular. These created cells are called macro, micro, femto or pico cells, according to their diameter, from the biggest to the smallest one.

Finally, the deployment defined the topology of the transmission system, i.e. the way of distributing the different nodes over the area according to their types. Usually, the MSs are randomly placed over the area, and the distinct BS locations are modeled by an hexagonal pattern. There are several ways of placing the RSs which will be detailed in Chapter 5.

One has to be careful as certain combinations of these parameters (area, deployment and topology) make no physical sense. For instance, it is irrelevant to consider a macro cellular network for an indoor area.

After deployment definition, the short-term Signal to Interference plus Noise Ratio (SINR) between all nodes in the system must be derived in order to compute their achieved performance.

1.2.3 Propagation models

This short-term SNR derivation is done thanks to propagation models, usually defined combining theoretic and heuristic results [33].

This derivation is composed of two steps. The first step is the derivation of the long-term received power (denoted P_S in Eq. (1.2)) between two nodes from the large-scale propagation model. It mainly depends on the distance between highly separated nodes and the considered area. The second step is the derivation of the small variation of the received power over short distance and time durations (denoted h in Eq. (1.2)) using small scale propagation model.

a) Large scale propagation

The long term received power described by the large scale propagation model depends on 3 main effects: the antenna gains, the pathloss depending on the distance between the nodes, and the considered shadowing.

The antenna gain describes the power repartition into space at the output of the transmission antenna. The antenna gains are known from the antenna diagram representing the power at the output of the antenna according to the considered direction. For instance, the output power of an omnidirectional isotropically spreads power into space.

Then, this energetic wave used to transmit data goes through the area and fades due to the distance separating both nodes. This effect is illustrated on Fig. 1.10a representing the map of the experienced long term SNRs for every MS positions in the considered cell. The BS, placed at the cell center, has an omnidirectional antenna. The system simulator models a transmission occurring in a urban area. The closer from the BS and the better the average SNR.

The last long term fading experienced during this transmission is called shadowing. It models the effect of the different static obstacles that can be encountered during propagation such as trees, or buildings. There exist several shadowing models. For instance, in Fig. 1.10b, the experienced shadowing is a real Gaussian random variable and in Fig. 1.10c, the shadowing keep being a random variable but which is correlated over space. This second model is much closer from reality as deeply faded areas can be interpreted for instance as urban canyon.

b) Small scale propagation

This long term received power is affected by a *fading* representing the rapid fluctuations of the phase and amplitude of the signal through a short time period. This fading is due to the relative speed between the source and the destination and the interference of several versions of the same symbol arriving at a receiver at slightly distinct instants. This phenomenon is called *multipath* and is caused by the multiple reflexions of the sent signal on the environment.

This time dispersion of the signal induces either *flat fading* or *frequency selective fading*.

The suffered fading is said to be flat if the symbol duration is very long when compared to the delay spread of the signal and when the frequency impulse response of the channel is constant over the signal bandwidth, i.e., the coherence bandwidth of the channel is much higher than the transmission bandwidth. This channel is also said to be a narrow band channel. The signal amplitude observed when transmitted over a flat fading channel follows a Rayleigh distribution.

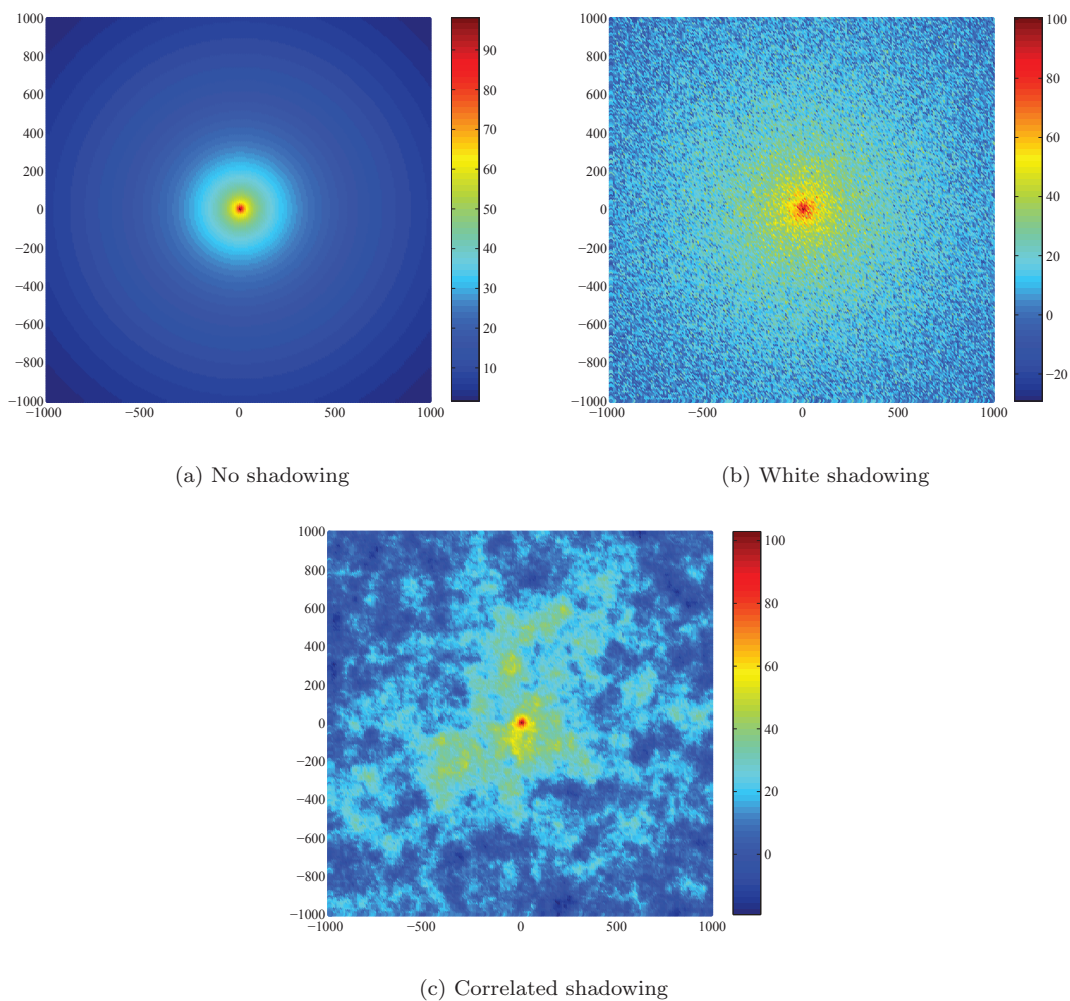


Figure 1.10: Map of SNR in dB between the BS and the UEs in an isolated cell according to the shadowing model. The axes values represent the distance in meter from the base station.

This justifies the fact that we model the channel coefficients by complex Gaussian random variables in Eq. (1.2) and Eq. (1.3).

A signal undergoes frequency selective fading if the coherence bandwidth of the channel is much smaller than the signal bandwidth, equivalently, if the time delay spread is much higher than the symbol duration. Consequently, transmission over frequency selective channels generates Inter Symbol Interference (ISI). These channels are modeled according to wideband multipath measurements. Two examples are described in Chapter 5 for a urban environment, and an indoor environment.

Moreover, according to the speed of the channel response fluctuation, the channel experiences either a *fast fading* or a *slow fading*. In this thesis, we only consider slow fading, i.e., the channel response is constant over time during several time-slots.

1.2.4 Metrics of interest for system level evaluation

After the nodes deployment over the considered area for system level evaluation and derivation of the short term SNR of each source to destination links (useful and interfering links), the metric of interest must be derived.

The aim of this section is to describe the figures of merit usually used according to the considered application.

In a system used for TV broadcasting, each user intends the same message satisfying a given QoS. The providers are interested in covering a maximal number of users for a given transmit power. Thus, the interesting metric is the coverage: i.e. the percentage of the area over which this minimal QoS is reached.

However, in a system used for voice transmission, the users are interested in receiving their data in a minimal delay with high reliability. This is precisely described by the spectral efficiency of their transmission. At the system level, providers are not interested by the performance of a single user, but by the performance of all users. This is described by the cumulative density function of spectral efficiency. It represents the pourcentage of users achieving at most a given spectral efficiency.

This metrics presentation for system level evaluation is clearly not exhaustive, there are many other ways of presenting performance according to the effect and parameters one wants to deal with.

1.3 Examples

In this section, we describe concrete system situations modeled by the previously described basic channels.

We consider the cellular system presented in Fig. 1.11, where each hexagon represents 3 cells, each black point represents three collocated base stations, and the distinct used resources are modeled by arrows of distinct colors.

Let's consider a single cell from a cellular system and two users, for instance users a and b . These users are scheduled on two distinct resources, they do not interfere each other, and the situation can be described by two basic point to point channels. However, if these users are scheduled on the same resource, they generate interference on each other. In the *downlink*, i.e. from the base station to the users, the situation generates a broadcast channel (users c and d), and in the *uplink* (users e and f), i.e. from the users to the base station, a MAC is created.

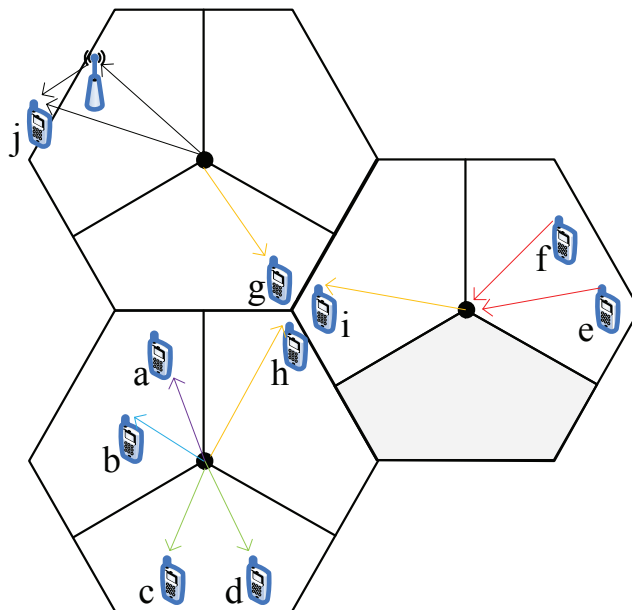


Figure 1.11: Basic channels in a cellular system.

By now considering neighboring cells, and a user from each cell scheduled on the same resource, an 3-pair interference channel is generated (users g , h and i). If more cells and users are considered, it increases the number of pairs to be integrated in the model.

By introducing relays in these cells, the point to point channel can become a relay channel users j , and similarly, it generates IRC, Multiple Access Channel with Relay (MARC) and Broadcast Relay Channel (BRC).

In an ad hoc network, the distinct hops used to transmitted data can lead to the generation of these basic channels.

Conclusion

In this chapter, we reviewed the link and system level evaluations of a transmission protocol, and we presented the classic metrics usually derived to quantify its performance according to the considered step.

Focusing on relaying technologies which are nowadays included in standard as a promising technique to increase data rate and coverage, we showed that the DDF protocol provides the better DMT over all known relaying protocols.

In the following we thus focus on this particular protocol considering that:

- the nodes are perfectly synchronized,
- all considered sources are relay-unaware, i.e. they are not aware of the relay's presence in the system,
- the designed relaying schemes do not impose additional decoding abilities at the destination when compared to the no relay case.

These assumptions enable the introduction of relays in an already set up network without any upgrade, i.e. it guarantees backward compatibility. Moreover, it enables to define completely decentralized relaying protocols as it forbids signaling dedicated to relaying over the source to relay link.

Chapter 2

Achievable macro diversity order using the DDF protocol

Introduction

In this chapter, after a bibliographical study of the DDF protocol, we focus on designing and evaluating a practical implementation of this protocol.

The implementation satisfies two particular assumptions: the source is relay-unaware, and the destination has low complexity decoding abilities. We previously showed the interest of these constraints for the design of distributed protocols and for backward compatibility. The evaluation is done at the link level, i.e., by only considering this implementation for the relay channel composed of a source, a relay and a destination.

The rest of this chapter is organized as follows: We first give a more detailed view of various results on the DDF protocol and we describe some useful practical implementations of DF protocols in Section 2.1. We then introduce the needed macro and micro diversity toolbox in Section 2.2 where diversity upper bounds are derived for several channel models. In Section 2.3, the proposed practical implementation of the DDF protocol is described and the associated figures of merit are defined. In Section 2.4 and Section 2.5, two relaying schemes for this practical implementation of the DDF protocol, the Monostream DDF and the DA DDF, are studied according to the macro and micro diversity orders. The analytical performance are then confirmed through simulation results in Section 2.6.

2.1 The DDF protocol

2.1.1 Original protocol

In 2005, the DDF protocol was simultaneously proposed in two papers [27] and [28] for the relay channel with half duplex relays.

In [27], the authors propose and derive the performance of the DDF protocol for several channels: the relay channel, the cooperative broadcast channel in which a source transmits data to a plurality of destinations allowed to cooperate between each other, and the cooperative multiple access channel in which several sources are allowed to cooperate in order to transmit data to a single destination. For the relay channel, the authors show that the DMT of the DDF protocol

reaches the MISO bound (maximal value of diversity) for all rates between 0 and 0.5 for the one relay-case, and outperforms all AF protocols for all rates.

Simultaneously, Mitran et al. in [28] proposed a similar behavior at the relay. Their study shows that there exists a coding scheme achieving a communication rate R_{bpcu} whatever the channel conditions between the three nodes.

a) Description of the protocol

We describe in the following the DDF protocol for the relay channel. Consequently, we only describe the proposed protocol for this basic channel.

Due to the broadcast nature of the wireless medium, as the source transmits the codeword to the destination, the relay can listen to this message. This is the listening phase, or the first phase, of the DDF protocol. It ends as soon as the decision rule, a predefined criteria, is satisfied at the relay. In the original DDF protocol, this decision rule is the following: The relay listens to the message transmitted by the source until the resulting mutual information between the message and the received signal becomes equal to the number of information bits contained in the message. This test is realized at each time-slot of the transmission. Thanks to the assumption of Gaussian alphabet and long codeword, this decision rule is equivalent to the beginning of the relay's transmission after having correctly decoded the message.

This protocol is said to be dynamic as, for a fixed data rate, the duration of the listening phase depends on the fading coefficient, and thus on the short-term SNR, between the source and the relay which varies through time.

After this correct decoding of the message, the relay perfectly knows the information bits contained in the message. Thus, it re-encodes the message by using an independent codebook and transmits the resulting codeword on the same physical resource as the one used by the source. This is the transmission phase, also called the collaboration phase in [28], or second phase, of the DDF protocol.

Consequently, during the first phase of the DDF protocol, the destination receives data from the source, and during the second phase of the DDF protocol, the destination receives the sum of the signals from the relay and from the source.

b) DMT performance

In [27], after an outage analysis for the one relay case, this protocol is shown to achieve a DMT equals to $d_{DDF,1}(r)$, such that:

$$d_{DDF,1}(r) = \begin{cases} 2(1-r), & \text{if } 0 < r \leq 0.5 \\ (1-r)/r, & \text{if } 0.5 < r \leq 1 \end{cases} . \quad (2.1)$$

The DMT achieves the maximal performance for all rates between 0 and 0.5 and outperforms all known schemes for these rates.

The DMT of the DDF protocol in a system comprising N relays is derived in [27], and is equal to:

$$d_{DDF,N}(r) = \begin{cases} (N+1)(1-r), & \text{if } 0 < r \leq \frac{1}{N+1} \\ 1 + \frac{N(1-2r)}{1-r}, & \text{if } \frac{1}{N+1} < r \leq 0.5 \\ (1-r)/r, & \text{if } 0.5 < r \leq 1 \end{cases} . \quad (2.2)$$

This DMT achieves the MISO bound for rates between 0 and $1/N + 1$. These DMT are illustrated in Fig. 2.1 according to the asymptotic data rate r for distinct numbers of relays in $\{1, 2, 4\}$.

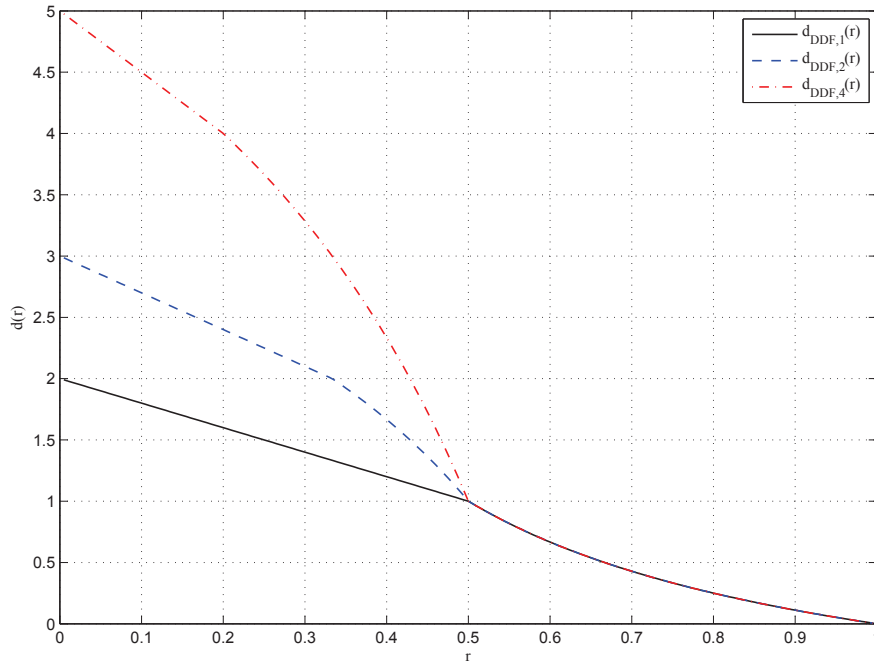


Figure 2.1: DMT of the DDF protocol with 1, 2 or 4 relays.

c) Limits of this DDF protocol

The proposed DDF protocol by Azarian experiences good DMT performance but is not designed for practical implementation. Indeed, most of the considered assumptions are unpractical:

- The source and the relay transmits codewords from a Gaussian alphabet,
- The codewords are of infinite length in order to guaranty that a non outage event is equivalent to a correct decoding of the message,
- The protocol requires high complexity and very fast computation abilities at the relay so that it is able to check the decision rule after each time-slot,
- The protocol requires multi-stream advance receiver at the destination so that it can decode a signal containing multiple independent streams coding for the same information.

2.1.2 Derived versions of the DDF protocol

Since 2005, several studies of the DDF protocol have been proposed trying to deal with the aforementioned limitations. Three main research axes can be distinguished: code construction for the DDF protocol in order to reach its DMT, design of decision rule used at the relay, and combination of channel coding and cooperation for the design of practical protocols.

In [34, 35, 36], the authors present an implementation of the DDF protocol reaching the DMT performance for any number of relays, any fading statistics and any number of antennas at the nodes. These codes are based on algebraic constructions. A particular example is based on the Alamouti code construction for the one relay case. In [36, 37], the authors propose that the relay

transmits symbols so that the combination of the source and relay streams generate an Alamouti codeword. Another space-time encoding for the DDF protocol is proposed in [38], where the authors propose to combine the DDF protocol and the Rotate and Forward protocol. They prove that this scheme achieves the DMT of the DDF protocol for the one-relay two-rotation case. These Distributed Rotations are originally used to recover spatial diversity in [30].

The authors of [36] also show that if the relay uses the outage criteria as decision rule, it leads to non monotonic error probability as it introduces events where the relay is not in outage but does not correctly decodes the message. To combat this effect, different decision rules have been studied. Most of them are summarized in [39], where C. Hucher and P. Sadeghi propose an overview of several DDF studies. For instance, in [36], the relay uses an additional received signal after its no outage event to decode the message. This results in a longer listening phase. Among other decision rules, we can cite [37] in which the relay must at least wait for receiving half of the codeword and for a non outage event before transmitting data. This decision rule is shown to conserve the DMT of the protocol. In [40], Prasad and Varanasi describe a new decision method depending on a parameter β such that the relay must reach a mutual information equal to β times the number of information bits to switch to the transmission phase. This new version is shown to achieve the DMT of the DDF protocol.

Still deriving performance in terms of DMT, the authors in [41] propose the combination of ARQ and the DDF protocol for the relay channel. This combination is then used for the MARC and for a MAC where the two users are used as relay by the other one. In all cases, this combination is shown to reach good DMT performance.

This combination of relaying and ARQ and/or HARQ for DF protocols has been studied in many articles. We particularly focus on those describing a relaying protocol close to the DDF, i.e. assuming that the relay only transmits if it correctly decodes the message at a predefined instant known by the destination (e.g. relaxing the dynamic constraint).

In 2004, prior to the definition of the DDF protocol, a protocol called Cooperative HARQ Type II was described in [42]. A first interesting feature of this orthogonal protocol is that it assumes a slotted version of the transmission: The source generates a codeword from an encoder of coding rate $1/2$. In the first part of the transmission, the source transmits half the codeword. In the second part, if the relay succeeds in correctly decoding the message, it transmits the other symbols of the codeword. Even if this protocol is not as flexible as the DDF protocol, it has two interesting properties: the relay is used only when not misleading the destination with corrupted data, and the relay transmits additional redundancy bits.

In [43], B.Zhao and C.Valenti describe a relaying protocol for a system comprising a source, a destination and a plurality of relays. The source transmits an HARQ codeword thus divided into blocks. After each received block, one relay among those having correctly decoded the message, transmits data. This relay could be the one experiencing the best short-term SNR (instantaneous relaying) with the destination, or the best long-term SNR (HARBINGER technique). This chosen relay transmits the following HARQ block until a relay with better SNR correctly decodes the message or until the destination correctly decodes the message. The performance is described in terms of throughput, delay and outage probability.

In [44], the authors propose a relaying protocol for the relay channel in which the source transmits a codeword from a rateless code. When the relay correctly decodes the message, it

transmits a codeword from an other rateless code. Using this relaying scheme, the authors aim at deriving the achievable rates with such a system. For simulation results, the authors propose a practical implementation in which, during the second phase of the protocol, the source and the relay transmits symbols of the same raptor code so that an Alamouti codeword is seen at the destination side. This implementation enables a low complexity decoding at the destination. This relaying scheme thus combines channel coding and space-time coding.

In [45], the authors propose two protocols: the repetition coding and the unconstrained coding for the relay channel in which the relay transmits only if it correctly decodes the message. When the relay uses the repetition coding, the source transmits the whole codeword during the first phase, and during the second one, the source and the relay build an Alamouti codeword using the symbols sent during the first phase. However, if the relay uses the unconstrained coding, it transmits the additional redundancy bits so that the experienced coding rate at the destination decreases. An analytical derivation of the latency and the throughput for Gaussian symbol alphabet is then done for both protocols.

Finally, the authors of [46, 47] describe a Sequential Decode and Forward (SDF) protocol, which has a similar definition as the DDF protocol in [27], for the relay channel considering two particular assumptions. The first one is that the relay is so close from the source that the source-relay link is modeled by an AWGN channel. The second assumption is that the source is not aware of the relay's presence leading to the design of oblivious protocols. This assumption is particularly relevant for the design of distributed schemes or for backward compatibility. However, in this article, no practical implementation of this protocol is proposed. The system is only described thanks to capacity values, and the maximal achievable data rates are derived according to power allocation between source and relay for several versions of the SDF protocol.

Regarding all these works, solutions to some of the before mentioned original DDF protocol limitations can be highlighted. More particularly, a space-time coding scheme using Alamouti codeword during the second phase of the DDF protocol are proposed to reduce the decoding complexity at the destination still guaranteeing a DMT optimal scheme. Furthermore, the slotted transmission generated by the HARQ mechanism for several DF protocols can be used so that the checking of correct decoding is not done on a per time-slot basis and could satisfy the dynamic nature of the DDF protocol.

In this thesis, we propose a practical implementation of the DDF protocol where the sent frames are based on HARQ, i.e. considering channel coding, and satisfying two assumptions: the source is relay-unaware and the destination has low complexity decoding abilities.

In the following section, we derive upper bounds on the achievable diversity order by a transmission scheme with symbols from finite alphabets and channel coding.

2.2 Definitions and bounds for diversity

2.2.1 Macro diversity

When several highly separated sources are used in order to deliver the same message to a single destination, the same signal is transmitted over several links experiencing independent path gains. At the destination, on a long term basis, this multiplicity of path gains leads to an improvement

of the long-term SNR. Particularly, if one of these links experiences very poor channel condition, others are present to maintain the transmission.

This effect is called macro diversity. The prefix *macro* stands for the effect of long term SNR, and the word *diversity* expresses the fact that there is a plurality of independent links participating in the transmission. This concept is described in the late '80s in several papers. In [48], Bernhardt compares the cumulative distribution functions of received power for several BS configurations. He concludes that the more BSs a mobile can receive data from, the better its long-term received power. This effect is also illustrated in [49], where Weiss plotted maps of received power comparing the single base station case with 2 distinct schemes. Using the first scheme, the user is linked to the BS experiencing the best link among 3 BSs, and using the second scheme, data is received from these 3 BSs. The last scheme experiences the best performance in terms of long-term received power. This map representation is also used in [50], where the minimal SNR needed to achieve at least an error probability of 10^{-2} is presented for users connected to 3 sources.

In all these studies, all cooperating nodes are base stations. Thus, they access the information through wired links and transmit the same message on the same physical resources.

The introduction of relays in a network seems to be of interest in order to achieve macro diversity. Indeed their path gains to the users are independent from the path gains between the serving base station and the users.

However, as we consider that the source is relay-unaware, there is a latency between the beginning of the transmission at the source and the beginning of transmission at the relay. Even then, the relay may probably not transmit the whole codeword. In this case, some questions arise: is it possible to experience macro diversity? What are the conditions to fully exploit all independently long-term faded links?

All these interrogations lead us to define the macro diversity order achievable for a certain metric of performance in a transmission from several highly separated nodes to a single destination.

2.2.2 Definition of the macro diversity order

Definition 2.1. *Given a figure of merit U , function of n long-term SNRs (ρ_1, \dots, ρ_n) and increasing according to each variable ρ_i taken separately; given a target value U_t ; the macro diversity order d for the target value U_t is defined by*

$$d = \min_{\Omega \subset \{1:n\}} \left(|\Omega| \left| \lim_{\substack{\forall j \in \Omega, \rho_j \rightarrow 0 \\ \forall i \notin \Omega, \rho_i \rightarrow +\infty}} U(\rho_1, \dots, \rho_n) < U_t \right. \right).$$

The macro diversity order is defined as the minimal number of links to turn off so that the target U_t is no longer asymptotically achievable through the remaining links. The figure of merit U could be, for instance, the spectral efficiency or the probability that the transmission is not in outage.

By definition, the full macro diversity order is achievable if $d = n$. Consequently, the system experiences a full macro diversity order for the target value U_t if and only if

$$\forall j \in \{1, \dots, n\}, \lim_{\rho_j \rightarrow +\infty} U(0, \dots, 0, \rho_j, 0, \dots, 0) \geq U_t$$

which means that every single link asymptotically allows to achieve the target.

In the following, we derive upper bound on the achievable micro and macro diversity orders according to several channel models.

2.2.3 Recovering diversity with channel coding

As previously described, our practical implementation of the DDF protocol will use channel coding and symbols from a finite alphabet. We thus focus on deriving diversity bounds for a transmission scheme using channel coding according to the considered channel model: a block-fading (BF) channel, a BF channel with correlated fading coefficients adding non coherently, and a BF channel with correlated fading coefficients adding coherently (also called Matryoshka channel).

a) Block fading channel with uncorrelated fading coefficients

A codeword transmission is done over a so called BF channel if the equivalent channel matrix of the transmission is block diagonal. This situation occurs for instance when the coherence time of the channel is shorter than the codeword length. **BF channel with equal block lengths** We denote L_{BF} the number of bits transmitted during each block of the channel, and N the number of blocks.

When each block is associated to an independent coefficient, the channel offers N degrees of freedom. A simple way to exploit these degrees of freedom is to transmit a repetition of the same message over each channel block and to use MRC at the destination to coherently combine each version of the message with the others. Thus, full diversity is achieved using a repetition code of coding rate $1/N$ and a specific detector.

More generally, for a transmission scheme of coding rate R_c occurring over a block-fading channel of N blocks, the maximal achievable diversity order is described by the Singleton bound [51, 52]:

$$d_{BF} = \lfloor N(1 - R_c) \rfloor + 1$$

We recall the proof in Appendix A.

This upper bound on the diversity order is valid only for transmission using finite symbol alphabet, it only depends on the coding rate, and on the number of channel blocks. It is independent of the considered code and of the constellation shaping and mapping. However, these characteristics appear to be relevant to reach the bound. Several studies deal with code and interleaver designs to reach this bound, for instance in [53].

In order to model cooperative transmissions, the BF channel model might be slightly modified: the channel blocks might have different lengths, and the fading coefficients can be correlated. Consequently, the diversity upper bound has to be adapted.

BF channel with unequal block lengths In this paragraph, we consider a BF channel of unequal block lengths. For instance, this particular channel model arises when considering an orthogonal DDF transmission. Both parts of the codeword experience an independent short-term fading coefficient, and due to the dynamic nature of the DDF protocol, both parts do not last the same number of time-slots. The maximal achievable diversity order of a transmission over such a channel is described by the following theorem, derived in [54]:

Proposition 2.1. *The diversity obtained after decoding a rate- R_c linear code transmitted over a $\mathcal{B}(\mathcal{L})$ independent block-fading channel, where $\mathcal{L} = (L_1, \dots, L_N)$ is the vector of block lengths and*

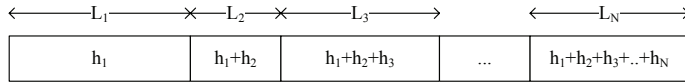


Figure 2.2: BF channel of N blocks with correlated fading coefficients (correlation A).

where the fading coefficient of the blocks are independent one from the others, is upper-bounded by $d_{\mathcal{B}}(\mathcal{L}) = N - i + 1$ where i is given by the following inequality:

$$\sum_{j=1}^{i-1} L_{s(j)} < R_c \sum_{j=1}^N L_j \leq \sum_{j=1}^i L_{s(j)} \quad (2.3)$$

where $s()$ denotes a sorting operation such that $\forall j, L_{s(j)} \leq L_{s(j+1)}$.

Proof. Let $K = R_c \sum_{j=1}^N L_j$ be the number of information bits per codeword. The diversity order of the coded modulation is defined by the lowest diversity order observed among all pairwise error probabilities. Consider permutations Ω of strictly positive integers lower than N . If i is the maximal integer, function of Ω , K , and \mathcal{L} , such that $\sum_{j=1}^{i-1} L_{\Omega(j)} < K$, for any code structure, selecting only the coded bits of the blocks of index in $\{\Omega(1), \dots, \Omega(i)\}$ builds a null-Hamming distance code. Thus, there exists at least one pair of codewords exhibiting a diversity order lower or equal to $N - i + 1$. Furthermore, the configuration Ω maximizing i gives the lowest diversity order $N - i + 1$ among all pairwise error probabilities, which is obtained by choosing $\Omega = s$, sorting the blocks in increasing length order. \square

b) BF channel with non coherent combinations of the fading coefficients

We define another block-fading channel whose blocks are of unequal lengths and whose fading coefficients are *correlated* and *non coherently* combined. The upper bound on the achievable diversity order of such a channel depends on the block lengths but also on the correlation between the fading coefficients. We thus focus on two particular correlations useful for our following study of the DDF protocol.

BF channel with correlation A The first BF channel model with correlated coefficients is the following: we assume that the equivalent fading coefficient of the n -th block is the sum of the fading coefficient associated to the previous block and an independent fading coefficient. This channel is presented on Fig. 2.2. The particular 2 block case has been presented in [55].

In the following of this thesis, we will be interested in the micro diversity order achievable over such a channel.

Proposition 2.2. *The achieved diversity order over a correlated BF channel where the fading coefficient of the n -th block is the sum of the fading coefficient associated to the previous block and an independent fading coefficient, is equal to the number of channel blocks over which each codeword pair of the code are different.*

The maximal diversity order is achieved when the Euclidean distance d_i on each channel block is non null.

Proof. By denoting \mathbf{x} the transmitted codeword, P the average received power at the destination, \mathbf{w} the vector of complex Gaussian noise sample suffered at the destination and \mathbf{H} the equivalent

channel matrix of this correlated BF channel, the received signals at the destination \mathbf{y} are

$$\mathbf{y} = \sqrt{P}\mathbf{H}\mathbf{x} + \mathbf{w} \quad (2.4)$$

where \mathbf{H} is a block diagonal matrix generated from the matrices $h_1\mathbf{I}_{L_1}, (h_1 + h_2)\mathbf{I}_{L_2}, \dots, (h_1 + \dots + h_n)\mathbf{I}_{L_n}$.

The pairwise error probability between two codewords \mathbf{x} and \mathbf{x}' can be described by Eq. (1.9). After averaging over all fading realizations, the pairwise error probability between \mathbf{x} and \mathbf{x}' can be written as

$$P_{\mathbf{x} \rightarrow \mathbf{x}'} \approx \frac{1}{\det(\mathbf{I} + \rho(\mathbf{X} - \mathbf{X}')(\mathbf{X} - \mathbf{X}')^\dagger)} \quad (2.5)$$

where $\rho = \frac{P}{4N_0}$ and

$$\mathbf{X} - \mathbf{X}' = \begin{pmatrix} d_1 & d_2 & \cdots & d_m \\ 0 & d_2 & \cdots & d_m \\ \vdots & \vdots & \ddots & d_m \\ 0 & 0 & \cdots & d_m \end{pmatrix} \quad (2.6)$$

where d_i is the Euclidean distance between \mathbf{x} and \mathbf{x}' over the i -th channel block and $\|\mathbf{x} - \mathbf{x}'\|^2 = \sum_i d_i^2$, mainly depending on the used constellation, and the Hamming distance between the codewords if a binary error correcting code is used.

We focus on deriving the maximal power of ρ^{-1} in Eq. (2.5) which is equal to the achieved diversity order over this correlated BF channel.

$$\begin{aligned} \det(D_m) &= \det(\mathbf{I} + \rho(\mathbf{X} - \mathbf{X}')(\mathbf{X} - \mathbf{X}')^\dagger) \\ &= \det \begin{pmatrix} 1 + u_1 & u_2 & \cdots & u_m \\ u_2 & 1 + u_2 & \cdots & u_m \\ \vdots & \vdots & \ddots & u_m \\ u_m & u_m & \cdots & 1 + u_m \end{pmatrix} \end{aligned}$$

where $u_i = \sum_{k=i}^m \rho d_k^2$. After some elementary operations over lines and columns, this determinant can be written as:

$$\begin{aligned} \det(D_m) &= \det \begin{pmatrix} u'_1 & -1 & 0 & \cdots & 0 \\ -1 & u'_2 & -1 & \ddots & \vdots \\ 0 & -1 & u'_3 & -1 & 0 \\ \vdots & \ddots & \ddots & \ddots & -1 \\ 0 & \cdots & 0 & -1 & 1 + \rho d_m^2 \end{pmatrix} \\ &= (1 + \rho d_m^2) D'_{m-1} - D'_{m-2} \end{aligned}$$

where $u'_i = 2 + \rho d_i^2$, and D'_i is the minor of size $i \times i$ composed of the first i columns and lines of D_m . Deriving a closed form expression is untractable as the coefficients u'_i can be different according to the considered index i . In the high SNR regime, using recursivity one can show that $\det(D_m)$ is equivalent to

$$\prod_{i, d_i \neq 0} \rho d_i^2$$

Consequently, the achieved diversity order is equal to the minimal number of non zero Euclidean distance d_i , among all possible codeword pairs. A maximal micro diversity order of NN_{rx} is achieved if $\forall i \in \{1, N\}, d_i \neq 0$. \square

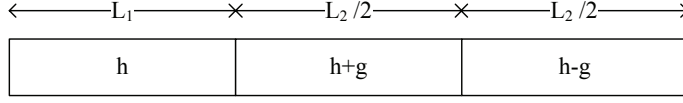


Figure 2.3: Block fading channel of three blocks with correlated fading coefficients (correlation B).

BF channel with correlation B The second BF channel with correlated coefficients is a BF channel composed of 3 blocks. The first one, of length T_1 , is characterized by the random value h_1 , the second channel block, of length $T_2/2$, is associated to the sum of h_1 and another random variable h_2 , and the last block of length $T_2/2$ is characterized by the difference $h_1 - h_2$. This channel is described in Fig. 2.3. Its diversity behavior have been derived in [56].

Proposition 2.3. *The diversity offered by a correlated BF channel of 3 blocks, where the first one, of length T_1 , is characterized by the random value h_1 , the second channel block, of length $T_2/2$, is associated to the sum of h_1 and another random variable h_2 , and the last block of length $T_2/2$ is characterized by the difference $h_1 - h_2$, is recovered if each pair of codewords are distinct over the first channel block and over the rest of the codeword.*

Proof. By denoting \mathbf{x} the transmitted codeword, P the average received power at the destination, \mathbf{w} the vector of complex Gaussian noise sample suffered at the destination and \mathbf{H} the equivalent channel matrix of this correlated BF channel, the received signals at the destination \mathbf{y} are

$$\mathbf{y} = \sqrt{P}\mathbf{H}\mathbf{x} + \mathbf{w}.$$

In order to derive the achieved diversity order when a transmission occurs over this channel, we derive an upper bound on the pairwise error probability. The pairwise error probability for a given channel \mathbf{H} can be upper bounded by:

$$P_{\mathbf{x} \rightarrow \mathbf{x}' | \mathbf{H}} = \mathbf{Q} \left(\sqrt{\frac{P \|\mathbf{H}(\mathbf{x} - \mathbf{x}')\|^2}{4N_0}} \right) \leq e^{-\frac{P \|\mathbf{H}(\mathbf{x} - \mathbf{x}')\|^2}{8N_0}} \quad (2.7)$$

Averaging Eq. (2.7) on the real and imaginary parts of the fading coefficients, and denoting $\rho = \frac{P}{4N_0}$ it comes:

$$P_{\mathbf{x} \rightarrow \mathbf{x}' | T_1} \leq \iint_{u_R, u_I} e^{-\frac{\rho}{2}(u_R^2 + u_I^2)d_1^2} I(u_R) I(u_I) p(u_R) p(u_I) du_R du_I$$

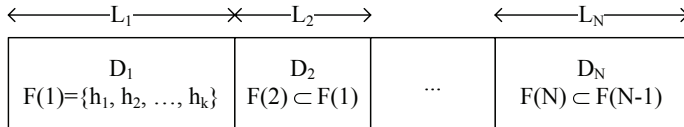
in which:

$$\begin{aligned} I(u) &= \int_{-\infty}^{+\infty} e^{-\frac{\rho}{2}u^2(d_{21}^2 + d_{22}^2) - t\frac{\rho}{2}2u(d_{21}^2 - d_{22}^2) - t^2(\frac{\rho}{2}(d_{21}^2 + d_{22}^2) + \frac{1}{2})} \frac{dt}{\sqrt{2\pi}} \\ &= \frac{1}{\sqrt{1 + \rho d_2^2}} \exp \left(u^2 \frac{\frac{\rho^2}{4}(d_{21}^2 - d_{22}^2)^2 - \frac{\rho}{2}d_2^2(\frac{\rho}{2}d_2^2 + \frac{1}{2})}{\frac{\rho}{2}d_2^2 + \frac{1}{2}} \right). \end{aligned}$$

Inserting this expression in the pairwise error probability bound, it follows that:

$$P_{\mathbf{x} \rightarrow \mathbf{x}' | T_1} = \frac{1}{(1 + \rho d_2^2)} \frac{1}{\left(1 + (d_1^2 + d_2^2)\rho - (d_{21} - d_{22})^2 \frac{\rho^2 d_2^2}{1 + d_2^2 \rho}\right)}$$

in which $d_1^2 = \sum_{i=1}^{T_1} |x_i - x'_i|^2$ ($d_2^2 = \sum_{i=T_1+1}^T |x_i - x'_i|^2$) is the Euclidean distance between the codewords during the first (second) channel block and $d_{21}^2 = \sum_{i=T_1+1}^{T_1+(T-T_1/2)} |x_i - x'_i|^2$, $d_{22}^2 = \sum_{i=T_1+(T-T_1/2)+1}^T |x_i - x'_i|^2$. Consequently, a full diversity scheme is achievable if any pairs of codewords satisfies $d_2 \neq 0$ and $d_1 \neq 0$. \square

Figure 2.4: Matryoshka channel of N blocks.

c) Matryoshka channel

When the channel blocks are associated to *correlated coherent* combinations of coefficients, the channel is called a Matryoshka channel.

It was introduced in [57], to design full diversity coding schemes for the Non-Orthogonal Amplify and Forward protocol. Originally, this channel was defined for coherent combination of short-term fading coefficients. However, the nature of the coefficient is not critical for the diversity bound derivation. Consequently, the result can directly be applied to any coefficients adding coherently such as long-term SNRs which will be of importance in the following of this thesis.

We here recall the upper bound on the achievable diversity order when a rate R_c code and finite symbol alphabet are used.

A $\mathcal{M}(\mathcal{D}, \mathcal{L})$ Matryoshka channel is a block channel whose coefficient associated to the i block is a coherent combination of the coefficients of the block $i + 1$, and an independent coefficient. We denote $\mathcal{L} = (L_1, \dots, L_N)$ the vector of block lengths and $\mathcal{D} = (D_1, \dots, D_N)$ the vector of diversity orders intrinsic to each block. Such a channel is illustrated in Fig. 2.4.

As derived in [57], the diversity observed after decoding a rate R_c linear code transmitted over a $\mathcal{M}(\mathcal{D}, \mathcal{L})$ channel is upper bounded by $d = D_i$, where i is given by the following inequality:

$$\sum_{k=1}^{i-1} L_k < R_c \sum_{k=1}^N L_k \leq \sum_{k=1}^i L_k$$

the proof is given in Appendix A.

As a result, the full diversity order is achieved as soon as $K \geq L_1$, where L_1 is the number of coded bits in the block of highest diversity order. This diversity behavior has been described for a Matryoshka channel of short-term fading, we thus talk about micro diversity.

It is possible to similarly define a Matryoshka channel of long-term fading, and thus a Matryoshka channel of long-term SNR. The same upper bound affects a Matryoshka channel of long-term SNRs, leading to a macro diversity bound.

2.3 Practical implementation of the DDF protocol

In this section, we propose a practical implementation of the DDF protocol for the relay channel based on HARQ, i.e., considering channel coding, and we derive the interesting figures of merit.

We recall that the source is denoted S, the relay R and the destination D. We assume that the source is relay-unaware and that the destination has low complexity decoding capabilities. These assumptions allow backward compatibility and the design of decentralized networks. We also assume a perfect knowledge of the fading coefficients at the receivers (coherent transmission).

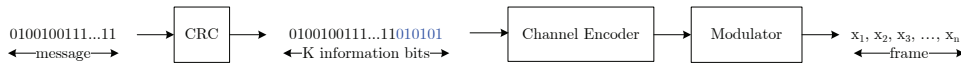


Figure 2.5: Codeword generation.

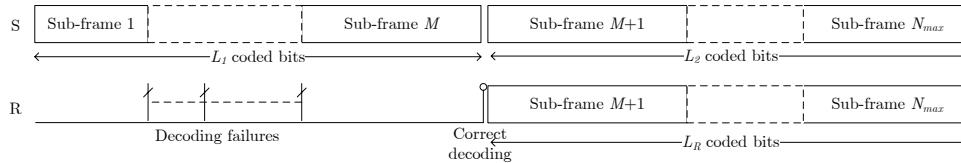


Figure 2.6: Codeword details and details on the DDF transmission.

2.3.1 DDF implementation based on HARQ principles

We propose a practical implementation of the DDF protocol based on HARQ. This choice is motivated by two reasons: the relay accesses an increasing number of redundancy bits through time and it enables a slotted checking of the correct decoding at the relay.

Consequently, before transmission, several processing steps must be done by the source, these steps are presented on Fig. 2.5. First, the source adds CRC bits to the message bits allowing the relay and the destination to check the validity of their decoded messages. These added bits usually represent a very small fraction of the message bits. Thus, we assume that the resulting throughput loss is negligible. We denote K the number of information bits resulting from the concatenation of the message bits and the CRC bits.

These K bits are then encoded by a channel encoder such as the turbo-code of the LTE combined with a rate matching algorithm. The generated codeword can be described as the concatenation of the information bits with several sub-frames of redundancy bits, each new concatenation leading to a decreasing coding rate R_{c_j} such that $1 \geq R_{c_j} > R_{c_i} \geq R_c$, where $j < i$ and R_c is the minimal considered coding rate.

The resulting codeword is modulated with a finite symbol alphabet of 2^{m_s} symbols, such as a QPSK, to form a frame of T symbols, divided into N_{max} sub-frames. We denote t_i the number of symbols contained in the i -th sub-frame. These details are presented in Fig. 2.6. The resulting symbols are then sent to the destination.

Due to the broadcast nature of the wireless medium, the relay receives the signals intended at the destination. Each received signal is memorized and concatenated with the others previously memorized. The relay tries to decode these combinations resulting in a set of codewords of decreasing coding rate as if a transmission with HARQ-IR were used. The latency due to the decoding process at the relay is totally absorbed by the inter sub-frames intervals required by the HARQ scheme. Decoding errors can be detected thanks to the included CRC bits. We assume that the probability of undetected error using CRC is so small that it can be considered as null. All these steps occur during the listening phase of the DDF protocol. We denote T_1 the number of symbols transmitted during this listening phase, which corresponds to $L_1 = m_s T_1$ coded bits, these details are illustrated in Fig. 2.6.

After correctly decoding the message, the relay perfectly knows the information bits, the encoding algorithm and the modulation used by the source. It can thus perfectly build the symbols previously sent by the source and the symbols the source is going to send. Then the relay switches into a transmission mode. This is the beginning of the second phase of the DDF protocol.

The second phase of the DDF protocol is composed of T_2 time-slots, thus the source transmits $L_2 = m_S T_2$ coded bits and the relay, using a 2^{m_R} -QAM, transmits $L_R = m_R T_2$ coded bits. We assume that the relay transmits symbols according to a relaying scheme chosen autonomously by the relay. In this chapter, these relaying schemes are the Monostream scheme and the Distributed Alamouti (DA) scheme, respectively described in Section 2.4 and Section 2.5.

The destination receives the signals from the source during the listening phase, and receives the combination of the source and the relay signals during the transmission phase of the DDF protocol. We assume that the channel is estimated by the destination at the beginning of each sub-frame. According to the chosen relaying scheme, the destination needs to receive distinct additional informations from the relay. This will be further detailed in Section 2.4 and Section 2.5.

The destination realizes MRC over its reception antennas to coherently combine the simultaneously received signals and apply a ML detection unless stated otherwise in the following. This detection step at the destination consists in decoding a single stream of data leading to low complexity decoding.

The phases durations (T_1 and T_2) are conditioned by the existence of a feedback link between the source and the destination :

- In case of an open-loop transmission, i.e. no feedback link available, the source transmits the whole codeword and $L_1 + L_2 = L$. There are two possible decoding strategies at the destination side: either the destination waits for receiving the whole codeword before trying to decode, or the destination tries to decode the message after each received sub-frame (as the relay). Using the second strategy, the destination turns to an idle mode after correctly decoding the message, i.e. stop listening to the source from its correct decoding until the transmission's end, which enables saving power. If the destination cannot correctly decode the message before the codeword's end, no retransmission from the source is allowed, i.e. the whole codeword is lost.
- In case of a closed-loop transmission, as soon as the destination correctly decodes the message, the transmission stops, and $L_1 + L_2 \leq L$. Eventually, if the destination correctly decodes the message before the relay, or if the relay does not correctly decode the message before the transmission's end, the second phase of the DDF protocol is non existent and $L_2 = 0$.

In the following Section, all figures of merit described in Chapter 1 are adapted to this practical implementation of the DDF protocol. All needed notations were described in Section 1.1.2.

2.3.2 Metrics of performance

Due to the proposed codeword segmentation, the figures of merits described in Chapter 1 need to be adapted. Thus, in this Section, we define the figures of merit for open-loop and closed-loop transmissions.

a) Mutual information

Using the previously detailed practical implementation of the DDF protocol, the mutual information observed after the n -th sub-frame by assuming that the relay transmits from the beginning of the M -th sub-frame, with $1 \leq M < n$, is defined by

$$I_D^{(n,M)} = I_{S \rightarrow D}^{(n,M)} + I_{\{S,R\} \rightarrow D}^{(n,M)} \quad \text{with } 1 \leq n \leq N_{max} \quad (2.8)$$

where $I_{S \rightarrow D}^{(n,M)} = \frac{I_{S \rightarrow D} \sum_{i=1}^{M-1} t_i}{\sum_{i=1}^n t_i}$ is the mutual information $I_{S \rightarrow D}$ observed when only the source transmits, weighted by the ratio between the length of the first phase and the total codeword length. It depends on the spectral efficiency m_S of the QAM modulation used by the source, the long-term SNR ρ_{SD} and the fading coefficient \mathbf{h}_{SD} between the source and the destination. The mutual information $I_{\{S,R\} \rightarrow D}^{(n,M)} = \frac{I_{\{S,R\} \rightarrow D} \sum_{i=M}^n t_i}{\sum_{i=1}^n t_i}$ is observed during the second phase of the DDF protocol and depends on m_S , ρ_{SD} , \mathbf{h}_{SD} but also on the relay-destination link ρ_{RD} , m_R , \mathbf{h}_{RD} and on the relaying scheme. We denote the fact that the relay does not transmit during the n sub-frames, i.e., when no correct decoding occurred at the relay before the codeword's end, by $M = \emptyset$. Thus,

$$I_D^{(n,\emptyset)} = I_{S \rightarrow D}.$$

Similarly, $I_{S \rightarrow R}$ is the mutual information observed between the source and the relay and depends on the spectral efficiency m_S of the QAM modulation used by the source, the ρ_{SR} and the fading coefficient between the source and the relay \mathbf{h}_{SR} .

b) Outage probability

As described in the previous chapter, the outage probability is a relevant metric for open-loop transmissions. There is a failure in the transmission only if the destination cannot correctly decode the message after receiving the N_{max} sub-frames. An outage event thus always refers to the reception of the whole codeword and is denoted $P_{out,D}$.

The destination D is in outage knowing that the relay begins to transmit during sub-frame M , if the mutual information $I_D^{(N_{max},M)}$ is lower than the data rate $R_{N_{max}}$ used by the source. Because the number of CRC bits is neglected when compared to the number of bits in the message, we define the data rate at the end of the n^{th} sub-frame as the ratio of the number of information bits and the number of channel uses:

$$R_n = \frac{K}{\sum_{i=1}^n t_i}.$$

Thus, the outage probability observed at D, knowing that the relay begins to transmit during the M -th sub-frame, is defined as:

$$\begin{aligned} P_{out,D}^{(M)} &= \text{Prob} (I_D^{(N_{max},M)} < R_{N_{max}}) \\ &= \text{Prob} (I_D^{(N_{max},M)} < \frac{K}{T}). \end{aligned}$$

After averaging on the instant of correct decoding at the relay, the outage probability observed at D is

$$P_{out,D} = \sum_{M=2}^{N_{max}} P_{out,D}^{(M)} P_{1^{st},R}^{(M-1)} + P_{out,D}^{(\emptyset)} P_{out,R}^{N_{max}-1} \quad (2.9)$$

where $P_{out,D}^{(\emptyset)}$ is the probability that the relay does not transmit and the destination is in outage, where $P_{out,R}^n$ is the probability that the relay is in outage after receiving n sub-frames defined as

$$P_{out,R}^n = \text{Prob}(I_{S \rightarrow R} < R_n) = 1 - \sum_{i=1}^n P_{1^{st},R}^{(i)},$$

and where $P_{1^{st},R}^{(M-1)}$ is the probability that the relay is in outage after receiving the $M - 2$ -th

sub-frame, but is no longer in outage after receiving the $M - 1$ -th sub-frame, i.e.,

$$\begin{aligned} P_{1^{st},R}^{(M-1)} &= \text{Prob} (R_{M-1} \leq I_{S \rightarrow R} < R_{M-2}) \\ &= \text{Prob} \left(\sum_{i=1}^{M-2} t_i I_{S \rightarrow R} < K \leq \sum_{i=1}^{M-1} t_i I_{S \rightarrow R} \right). \end{aligned}$$

Describing $P_{1^{st},R}^{(M-1)}$ thanks to a non outage event means that we assume that the decision rule based on CRC bits and the no outage state leads to the same performance. The longer the included CRC bits, the better this approximation.

Similarly, $P_{1^{st},D}^{(n,M)}$ is the probability that the destination correctly decodes the message after receiving the n -th sub-frame and not before, knowing that the relay begins to transmit during the M -th sub-frame, and is defined by

$$P_{1^{st},D}^{(n,M)} = \text{Prob} (R_n \leq I_D^{(n,M)} < R_{n-1}).$$

c) Spectral efficiency

When HARQ with incremental redundancy is considered, the overall spectral efficiency is improved by allowing the destination to acknowledge the correct decoding of the message after each received sub-frame (closed-loop transmission), leading to the transmission of another codeword by the source. The spectral efficiency \mathcal{S} of our practical DDF scheme can be expressed as

$$\mathcal{S} = \sum_{n=1}^{N_{max}} R_n \left[P_{out,R}^{(n-1)} P_{1^{st},D}^{(n,\emptyset)} + \sum_{m=1}^{n-1} P_{1^{st},R}^{(m)} P_{1^{st},D}^{(n,m)} \right]. \quad (2.10)$$

All these figures of merits are derived for the proposed practical implementation of the DDF protocol, and a particularly adapted to the sub-frame decomposition of the codeword.

In the rest of this thesis, we use these metrics in order to characterize several relaying schemes. More particularly, in this chapter, we focus on the Monostream relaying scheme and the Distributed Alamouti relaying scheme.

2.4 Monostream DDF protocol

2.4.1 Monostream scheme

As previously described, the relay involved in the DDF protocol has the ability to build exactly the same codeword as the one transmitted by the source. Indeed, its perfect knowledge of the message bits and of the rate matching algorithm used by the source enables a perfect matching of the generated codewords.

Because we are interested in keeping the decoding complexity very low at the destination, we study the most simple relaying scheme for the DDF protocol: the Monostream DDF.

Definition 2.2. *The relay using the Monostream scheme transmits exactly the same T_2 symbols as those transmitted by the source on the same physical resource (time and frequency) during the transmission phase of the DDF protocol.*

Thus, when the relay uses this relaying scheme $m_R = m_S$ and the received signals at the destination during time slot i are the following:

$$\mathbf{y}_i = \begin{cases} \sqrt{P_S} \mathbf{h}_{SD} x_i + \mathbf{w}_i & \text{if } 1 \leq i \leq T_1 \\ (\sqrt{P_S} \mathbf{h}_{SD} + \sqrt{P_R} \mathbf{h}_{RD}) x_i + \mathbf{w}_i & \text{if } T_1 + 1 \leq i \leq T_2 \end{cases}$$

in which \mathbf{w}_i is the vector of noise samples experienced at the reception antennas, Gaussian distributed of zero mean and variance N_0 per real dimension.

Moreover, the relay transmits the same pilot signal as the one used by the source on the same physical resource with the same power ratio between pilot signal and data as the source so that the destination estimates the resulting fading coefficient $\sqrt{P_S}\mathbf{h}_{SD} + \sqrt{P_R}\mathbf{h}_{RD}$ during the second phase of the DDF protocol. Doing so, the destination does not need to be informed by the relay neither of the beginning of the second phase, nor of the used relaying scheme. Consequently, this relaying scheme does not need any additional overhead when compared to the point to point transmission.

Thus, the Monostream DDF protocol can be used if the destination is relay-unaware.

2.4.2 Equivalent channels analysis

The vector $\mathbf{y} = (\mathbf{y}_1^t, \dots, \mathbf{y}_{T_2}^t)^t$ of all received signals during the transmission of the codeword for a fixed instant of correct decoding at the relay, can be described under the following matrix form:

$$\mathbf{y} = \begin{pmatrix} \mathbf{A} & \mathbf{0} \\ \mathbf{0} & \mathbf{B}_M \end{pmatrix} \mathbf{x} + \mathbf{w}$$

in which $\mathbf{A} = \sqrt{P_S}\mathbf{h}_{SD}\mathbf{I}_{T_1}$, and $\mathbf{B}_M = (\sqrt{P_S}\mathbf{h}_{SD} + \sqrt{P_R}\mathbf{h}_{RD})\mathbf{I}_{T_2}$. In the following of this section, we'll use the following notation to denote the equivalent channel matrix of the Monostream scheme:

$$\mathbf{y} = \mathbf{H}_{T_1, T_2, M} \mathbf{x} + \mathbf{w}.$$

Under this form, the channel matrix $\mathbf{H}_{T_1, T_2, M}$ is a block diagonal matrix, composed of two diagonal matrices. The upper one is of size T_1 and carries the fading coefficient $\sqrt{P_S}\mathbf{h}_{SD}$, and the second one, of size T_2 carries the fading coefficient $\sqrt{P_S}\mathbf{h}_{SD} + \sqrt{P_R}\mathbf{h}_{RD}$.

a) Macro diversity

For a fixed (T_1, T_2) , the transmission of a codeword is done on a block channel of long-term SNRs composed of two blocks characterized by ρ_{SD} and $\rho_{SD} + \rho_{RD}$. The second block is associated to the coherent combination of the long-term SNR characterizing the first block, and another long-term SNR. This channel is thus a Matryoshka channel of long-term SNR whose diversity behavior has been derived in Section 2.2.3b, leading to the following proposition:

Result 2.1. *For a fixed instant of correct decoding at the relay T_1 , and a transmission phase of L_2 bits, a macro diversity order of 2 is achievable for the Monostream DDF if $L_2 \geq K$.*

b) Micro diversity

For a fixed T_1 , the transmission of a codeword occurs on a block-fading channel composed of two blocks whose associated fading coefficients are $\sqrt{P_S}\mathbf{h}_{SD}$ and $\sqrt{P_S}\mathbf{h}_{SD} + \sqrt{P_R}\mathbf{h}_{RD}$. The second block is associated to the sum of the fading coefficient characterizing the first block, and another random variable. This channel is thus a block fading channel composed of two blocks whose associated random variables are correlated (correlation A in Section 2.2.3a). Its diversity behavior have been previously described, leading to the following proposition:

Result 2.2. *For a fixed instant of correct decoding at the relay T_1 , and a transmission phase of L_2 bits, full micro diversity is achievable for the Monostream DDF transmission if $\min\{L_1, L_2\} \geq K$ which reduces to $L_2 \geq K$ as the correct decoding condition at the relay ensures that $L_1 \geq K$.*

c) Averaging on the instants of correct decoding at the relay

These previous analyses enable to upper bound the achievable macro and micro diversity orders for a fixed T_1 and a codeword length of $T_1 + T_2$ time-slots. For a given coding rate, these bounds only depends on the instants of correct decoding at the relay and at the destination: the sooner the relay correctly decodes the message and the later the source stops transmitting, the higher the probability of reaching a maximal diversity order.

However, as the average performance (outage probability Eq. (2.9) or spectral efficiency Eq. (2.10)) takes into account the non null probability that the relay does not correctly decode the message, in average, the diversity orders are always equal to 1, for the macro diversity, and N_{rx} for the micro diversity. But this effect usually appears for very high values of SNR, whereas for usual values of SNR, a maximal diversity behavior can be observed. This will be described with more details in the simulation results (see Section 2.6).

2.4.3 Analytic analysis

The observation of the equivalent channel models and the knowledge of bounds on the diversity enable to understand the macro and micro diversity behaviors of the Monostream DDF.

However, analytic derivations need to be done especially in order to compare several protocols achieving a same diversity order (coding gain and outage gain derivation), and to describe the resulting tradeoff between reliability and efficiency in the high SNR regime (DMT derivation).

We assume in this section that each node carries a single antenna.

a) Coding gain

The coding gain of the Monostream DDF is derived considering the pair of codewords, among all possibilities, leading to the worst pairwise error probability. The resulting fading channel of the Monostream DDF protocol for a fixed instant of correct decoding at the relay is a BF channel composed of 2 blocks whose fading coefficients are correlated (correlation A). For this particular number of blocks, a closed form expression of the pairwise error probability derived in Section 2.2.3 can be obtained:

We assume that the worst pairwise error probability is the probability to decode \mathbf{x}' whereas \mathbf{x} was sent. This pairwise error probability for a given channel $\mathbf{H}_{T_1, T_2, M}$, can be upper bounded by:

$$P_{\mathbf{x} \rightarrow \mathbf{x}' | T_1, T_2, \mathbf{H}_{T_1, T_2, M}} = \mathbf{Q} \left(\frac{\|\mathbf{H}_{T_1, T_2, M}(\mathbf{x} - \mathbf{x}')\|}{\sqrt{4N_0}} \right) \leq e^{-\frac{\|\mathbf{H}_{T_1, T_2, M}(\mathbf{x} - \mathbf{x}')\|^2}{8N_0}} \quad (2.11)$$

Averaging on the channels coefficients, and denoting $h_{SD} = u_R + iu_I$ and $h_{RD} = v_R + iv_I$, it comes:

$$\begin{aligned} P_{\mathbf{x} \rightarrow \mathbf{x}' | T_1} &\leq \int_{\mathbb{R}^{4+}} e^{\left(-\frac{(u_R^2 + u_I^2)P_S \sum_{i=1}^{T_1} |x_i - x'_i|^2}{8N_0} - \frac{((\sqrt{P_S}u_R + \sqrt{P_R}v_R)^2 + (\sqrt{P_S}u_I + \sqrt{P_R}v_I)^2) \sum_{i=T_1+1}^T |x_i - x'_i|^2}{8N_0} \right)} \\ &\quad p(v_R)p(v_I)p(u_R)p(u_I)dv_I dv_R du_I du_R \\ &= \iint_{u_R, u_I} \exp \left(-\frac{P_S(u_R^2 + u_I^2)d_1^2}{8N_0} \right) I(u_R)I(u_I)p(u_R)p(u_I)du_R du_I \end{aligned} \quad (2.12)$$

where $d_1^2 = \sum_{i=1}^{T_1} |x_i - x'_i|^2$ and $d_2^2 = \sum_{i=T_1+1}^T |x_i - x'_i|^2$ are the distances over the two channel blocks between \mathbf{x} and \mathbf{x}' .

We thus first focus on deriving $I(u)$:

$$I(u) = \frac{1}{\sqrt{2\pi\sigma^2}} \int_{-\infty}^{+\infty} \exp\left(-\frac{P_S u^2 d_2^2}{8N_0} - t \frac{u\sqrt{P_S P_R} d_2^2}{4N_0} - t^2 \left(\frac{P_S d_2^2}{8N_0} + \frac{1}{2\sigma^2}\right)\right) dt$$

We recall that the fading coefficients are complex Gaussian distributed of zero mean and unit variance. Thus, $\sigma^2 = 1$, and will be omitted in the following.

Using the following results: $\int_{-\infty}^{+\infty} \exp(-ax^2 + bx + c) dx = \sqrt{\frac{\pi}{a}} \exp\left(\frac{b^2 - 4ac}{4a}\right)$, the expression of $I(u)$ becomes:

$$I(u) = \frac{1}{\sqrt{1 + \frac{P_R d_2^2}{4N_0}}} \exp\left(-u^2 d_2^2 P_S \left(\frac{1}{8N_0} - \frac{d_2^2 P_R 8N_0 2}{(8N_0)^2 (2P_R d_2^2 + 8N_0)}\right)\right)$$

Including this result into Eq. (2.12), it comes:

$$P_{\mathbf{x} \rightarrow \mathbf{x}' | T_1} \leq \frac{1}{1 + \frac{P_R d_2^2}{4N_0}} \frac{1}{2\pi} \left(\int_{-\infty}^{+\infty} \exp\left(-u^2 \left(\frac{P_S (d_1^2 + d_2^2)}{8N_0} + \frac{1}{2} - \frac{d_2^2 P_R 8N_0 2}{(8N_0)^2 (2P_R d_2^2 + 8N_0)}\right)\right) du \right)^2$$

Using the fact that $\int_{-\infty}^{+\infty} e^{-ax^2} dx = \sqrt{\frac{\pi}{a}}$, it comes that the upper bound of the pairwise error probability can be written as:

$$P_{\mathbf{x} \rightarrow \mathbf{x}' | T_1} \leq \frac{1}{\left(1 + d_2^2 \rho_{RD}\right) \left(1 + (d_1^2 + d_2^2) \rho_{SD} - \frac{d_2^4 \rho_{SD} \rho_{RD}}{(1 + d_2^2 \rho_{RD})}\right)} \quad (2.13)$$

where $\rho_{SD} = \frac{P_S}{4N_0}$ and $\rho_{RD} = \frac{P_R}{4N_0}$. The coding gain on this upper bound of the pairwise error probability is observed in the high SNR regime (i.e. for ρ_{SD} and ρ_{RD} going toward infinity).

From this upper bound, we can derive a construction criteria for a full diversity scheme: both d_1 and d_2 might be non null. Practically, this condition can be expressed as “the closest words of the code must be separable over the two transmission phases of the DDF protocol”. This is exactly described by the Singleton bounds previously presented in this thesis: a channel block offered diversity if it contains at least K bits.

When $d_1 \neq 0$ and $d_2 \neq 0$, i.e. when full diversity is achieved, the coding gain is equal to $\zeta_M(T_1) = d_1 d_2$.

Result 2.3. *The coding gain of a Monostream scheme achieving a diversity order of 2, for a fixed instant of correct decoding at the relay T_1 , is equal to:*

$$\zeta_M(T_1) = d_1 d_2 \quad (2.14)$$

in which d_1 (d_2) is the distance between \mathbf{x} and \mathbf{x}' , the pair of codewords leading to the worst error probability, during the listening (transmission) phase of the Monostream DDF protocol.

b) Outage Gain

Using the notations defined in 2.3.2, we study the outage probability of the Monostream DDF protocol for Gaussian symbol alphabet leading to the maximal performance one can achieve with such a scheme. In this paragraph we focus on the outage gain derivation.

The outage probability at the destination for a fixed instant of correct decoding at the relay is

$$P_{out,D}^{(T_1)} = \Pr \left\{ T_1 \log(1 + \rho_{SD}|h_{SD}|^2) + (T - T_1) \log(1 + |\sqrt{\rho_{SD}}h_{SD} + \sqrt{\rho_{SD}}h_{RD}|^2) < TR_{N_{max}} \right\}. \quad (2.15)$$

From this outage expression, it is possible to derive the outage gain. As previously described, this metric enables to compare two transmissions achieving a same diversity order.

Result 2.4. *The outage gain of the Monostream DDF protocol for a fixed instant of correct decoding at the relay, assuming that $\sqrt{\rho_{RD}} = \kappa\sqrt{\rho_{SD}}, \kappa \in \mathbb{R}^{+*}$, is:*

$$\xi_M(T_1) = c \left(1 - 2^{TR_{N_{max}}/T_1} + \frac{T - T_1}{T - 2T_1} \left(2^{TR_{N_{max}}/T_1} - 2^{TR_{N_{max}}/(T-T_1)} \right) \right)$$

in which $c = \kappa c_{h_{SD}} c_{h_{SD}}$ is a constant depending on the probability density functions of the fading coefficients.

One can easily verify that $\xi_M(T_1) = \xi_M(T - T_1)$ which can be explained by the symmetry of the resulting channel when the relay correctly decodes at T_1 or at $T - T_1$. This equality of the coding gain is validated by simulation, see Section 2.6 (Fig. 2.9).

Proof. The outage gain ξ of a diversity d scheme is defined as : $\xi = \lim_{\rho \rightarrow \infty} \rho^d P_{out}$. The outage probability $P_{out,D}^{(T_1)}$ can be written as

$$\begin{aligned} P_{out,D}^{(T_1)} &= \int_{(a,b) \in \mathbb{C}^2} \mathbf{1} \left\{ T_1 \ln(1 + \rho_{SD}|a|^2) \right. \\ &\quad \left. + (T - T_1) \ln(1 + |\sqrt{\rho_{SD}}a + \sqrt{\rho_{RD}}b|^2) < \ln(2^{TR_{N_{max}}}) \right\} p_{h_{SD},h_{RD}}(a,b) da db \\ &= \int_{(a,b) \in \mathbb{C}^2} \mathbf{1} \left\{ T_1 \ln(1 + \rho_{SD}|a|^2) \right. \\ &\quad \left. + (T - T_1) \ln(1 + \rho_{SD}|a + \kappa b|^2) < \ln(2^{TR_{N_{max}}}) \right\} p_{h_{SD},h_{RD}}(a,b) da db \end{aligned} \quad (2.16)$$

in which $\mathbf{1}\{C\}$ is the indicator function, equal to 1 when the condition C is true, and 0 everywhere else.

Because it is more convenient to work with the modulus variables, Eq. (2.16) can be written as:

$$\begin{aligned} P_{out,D}^{(T_1)} &= \int_{(u,v) \in \mathbb{R}^{+2}} \mathbf{1} \left\{ T_1 \ln(1 + u) + \right. \\ &\quad \left. (T - T_1) \ln(1 + v) < \ln(2^{TR_{N_{max}}}) \right\} \\ &\quad p_{|h_{SD}|^2} \left(\frac{u}{\rho_{SD}} \right) p_{|h_{SD} + \kappa h_{RD}|^2} \left(\frac{v}{\rho_{SD}} \mid |h_{SD}|^2 = \frac{u}{\rho_{SD}} \right) \frac{du dv}{\rho_{SD}^2} \end{aligned}$$

We denote c_h and c_g the limits of the probability density functions of $|h_{SD}|^2$ and $|h_{RD}|^2$ right continuous in zero. Since the ensemble in which the indicator function equals one is compact, it is possible to apply Lebesgue's Dominated Convergence Theorem to obtain the outage gain $\xi_M(T_1)$

of a Monostream DDF transmission:

$$\begin{aligned}
\xi_M(T_1) &= \lim_{\substack{\rho_{SD} \rightarrow \infty \\ \rho_{RD} \rightarrow \infty}} \rho_{SD} \rho_{RD} P_{out,D}^{(T_1)} \\
&= \kappa \lim_{\substack{\rho_{SD} \rightarrow \infty \\ \rho_{RD} \rightarrow \infty}} \int_{(u,v) \in \mathbb{R}^{+2}} \mathbf{1}\{T_1 \ln(1+u) + (T-T_1) \ln(1+v) < \ln 2^{TR_{Nmax}}\} \\
&\quad p(|h_{SD}|^2 = \frac{u}{\rho_{SD}}) p\left(|h_{SD} + h_{RD}|^2 = \frac{v}{\rho_{SD}} \mid |h_{SD}|^2 = \frac{u}{\rho_{SD}}\right) dudv \\
&= \kappa \int_{(u,v) \in \mathbb{R}^{+2}} \mathbf{1}\{T_1 \ln(1+u) + (T-T_1) \ln(1+v) < \ln 2^{TR_{Nmax}}\} c_{h_{SD}} c_{h_{SD}} dudv \\
&= \kappa c_{h_{SD}} c_{h_{SD}} \int_{(u,v) \in \mathbb{R}^{+2}} \mathbf{1}\{T_1 \ln(1+u) + (T-T_1) \ln(1+v) < \ln 2^{TR_{Nmax}}\} dudv \\
&= \kappa c_{h_{SD}} c_{h_{SD}} \int_{x=0}^{\ln 2^{TR_{Nmax}}} \frac{e^{x/T_1}}{T_1} \int_{y=0}^{\ln 2^{TR_{Nmax}}-x} \frac{e^{y/(T-T_1)}}{T-T_1} dx dy
\end{aligned}$$

After a simple integration and an integration by parts, it comes:

$$\xi_M(T_1) = c \left(1 - 2^{TR_{Nmax}/T_1} + \frac{T-T_1}{T-2T_1} \left(2^{TR_{Nmax}/T_1} - 2^{TR_{Nmax}/(T-T_1)} \right) \right)$$

in which $c = \kappa c_{h_{SD}} c_{h_{SD}}$ is a constant depending on the probability density functions of the fading coefficients and the constant $\kappa = \sqrt{\rho_{RD}/\rho_{SD}}$. \square

c) DMT analysis

From this outage derivation can be derived the DMT of the Monostream DDF protocol. This derivation is classically done assuming equal SNR values on each link : $\rho_{SD} = \rho_{SR} = \rho_{RD} = \rho$.

Moreover, we use the notation $f \doteq g$ (similarly \doteq and \lesssim) when $\lim_{\rho \rightarrow \infty} \frac{\log(f)}{\log(\rho)} = \lim_{\rho \rightarrow \infty} \frac{\log(g)}{\log(\rho)}$. We assume that $|h_{SD}|^2 \doteq \rho^{-u}$, $|h_{RD}|^2 \doteq \rho^{-v}$ and $|h_{SR}|^2 \doteq \rho^{-w}$.

The DMT of the Monostream DDF protocol, denoted $d_M(r)$, is derived from the outage probability of this protocol Eq. (2.9) which is a sum of a two-term product. More precisely,

$$d_M(r) = \min_{T_1} (d_1(r) + d_2(r))$$

where $d_1(r)$ is the exponent of $P_{1st,R}^{(T_1-1)}$ in the high SNR regime, consequently depending on the source to relay link only, and $d_2(r)$ is the exponent of $P_{out,D}^{(T_1)}$ in the high SNR regime depending on both the source to destination link and the relay to destination link.

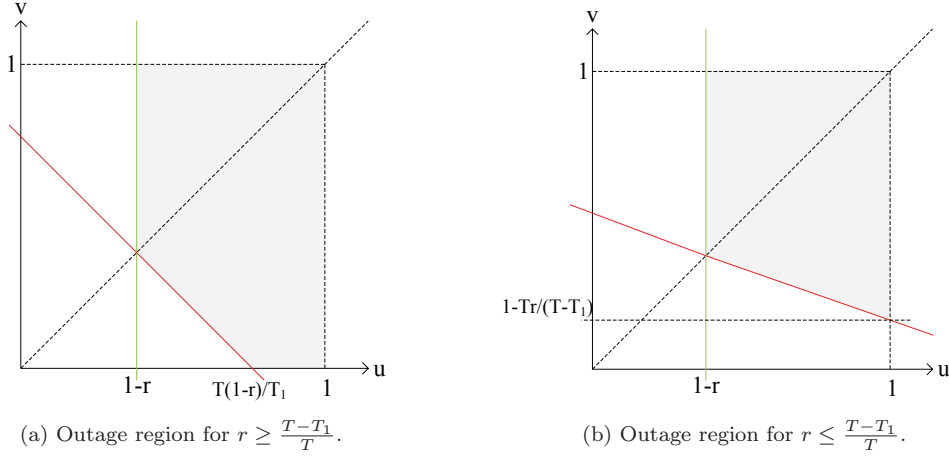
The asymptotic behavior of $P_{1st,R}^{(T_1)}$ described by $d_1(r)$ has been derived in [36]:

$$d_1(r) = \begin{cases} 1 - \frac{Tr}{T_1-1}, & 0 \leq r \leq \frac{T_1-1}{T} \\ 0 & \frac{T_1-1}{T} < r \leq \frac{T_1}{T} \\ \infty & \frac{T_1}{T} < r \leq 1 \end{cases}$$

where the notation $P \doteq \rho^{-\infty}$ indicates that P decreases faster than any polynomial function of ρ .

We now derive an upper bound on $d_2 = \inf\{u+v\}$ on the outage region defined by $P_{out,D}^{(T_1)}$, Eq. (2.15). Because $(|h_{SD}| - |h_{RD}|)^2 \leq |h_{SD} + h_{RD}|^2$, the following inequality holds:

$$\begin{aligned}
P_{out,D}^{(T_1)} &\leq \Pr \{T_1 \log(1 + \rho|h_{SD}|^2) + \\
&\quad (T-T_1) \log(1 + \rho|h_{SD}|^2 + \rho|h_{RD}|^2 - 2\rho|h_{SD}||h_{RD}|) < TR_{Nmax}\} \quad (2.17)
\end{aligned}$$

Figure 2.7: Outage regions according to r values.

And thus, if the right hand term of Eq. (2.17), achieves a diversity d , then $P_{out,D}^{(T_1)}$ achieves at least a diversity d .

$$P_{out,D}^{(T_1)} \leq \Pr \{ T_1(1-u)^+ + (T-T_1) \max(0, 1-u, 1-v) < Tr \}.$$

In order to determine the outage region, we need to distinguish two cases:

- When $u < v$, then $\max(0, 1-v, 1-u) = 1-u$ and the outage region becomes

$$u > 1-r$$

- When $v < u$, then $\max(0, 1-v, 1-u) = 1-v$ and the outage region becomes

$$T_1(1-u)^+ + (T-T_1)(1-v)^+ < Tr$$

Thus, representing these outage regions on Fig. 2.7 according to r , we obtain:

- For $r \geq \frac{T-T_1}{T}$, $d_2 \leq \begin{cases} 2(1-r)^+ & T_1 \leq T/2 \\ \frac{T(1-r)^+}{T_1} & T_1 \geq T/2 \end{cases}$
- For $r \leq \frac{T-T_1}{T}$, $d_2 \leq \begin{cases} 2(1-r)^+ & T_1 \leq T/2 \\ \left(2 - \frac{Tr}{T-T_1}\right)^+ & T_1 \geq T/2 \end{cases}$

Representing this DMT on Fig. 2.8, it comes that the lower bound on $P_{out,D}$ achieves for large T the DMT of the DDF protocol defined by Azarian and thus, the DMT of the Monostream DDF protocol is the DMT of the original DDF protocol.

Remark, that using the fact $|h_{SD} + h_{RD}|^2 \leq (|h_{SD}| + |h_{RD}|)^2$, one can obtain an upper bound on $d_2(r)$ leading to the same DMT. Consequently, the lower and upper bound leading to the same expression, this is the DMT of the Monostream DDF protocol.

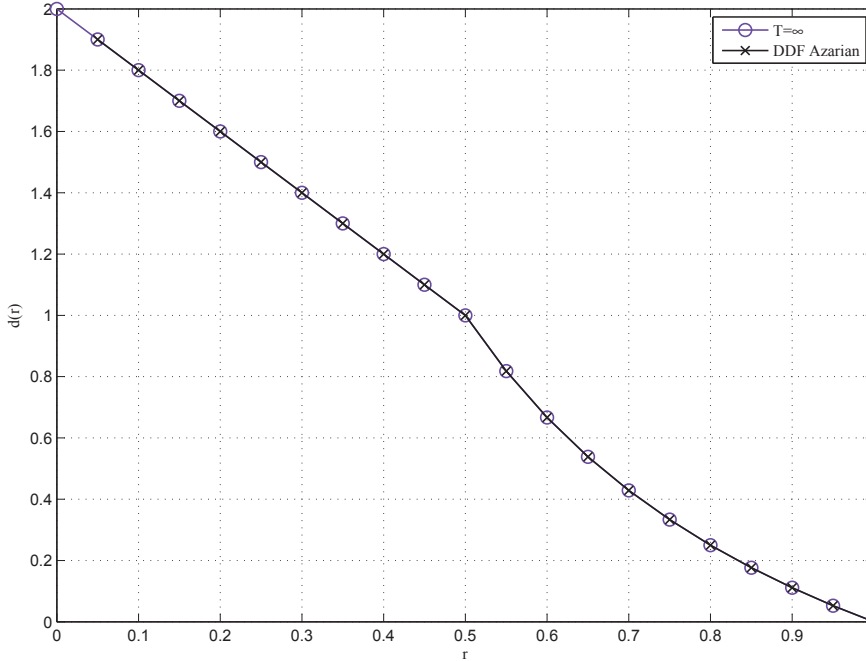


Figure 2.8: DMT of the Monostream DDF protocol matching the DMT of the DDF protocol proposed by Azarian.

2.5 Distributed Alamouti DDF protocol

It has been proposed in [37, 58] to use Distributed Space-Time Block Codes (DSTBC) in order to recover the spatial micro diversity offered by the virtual MIMO scheme formed by the relay channel.

In this section, we propose to study the combination of the DDF protocol and an Alamouti transmission and to compare its performance to those of the Monostream DDF protocol.

2.5.1 DA relaying scheme

This combination of the DDF protocol and the Alamouti code has been proposed in [37] for two reasons: this scheme conserves the DMT of the protocol, and it does not require any additional decoding abilities at the destination side. After its correct decoding, the relay first builds all symbols, $\{x_{T_1+1}, x_{T_1+2}, \dots\}$ concurrently sent by the source. Thus, this scheme can be realized under our relay-unaware source constraint.

Then, the relay transmits:

$$\begin{cases} -x_{T_1+i+1}^* & \text{if } i \text{ is odd} \\ x_{T_1+i-1}^* & \text{if } i \text{ is even} \end{cases} \quad (2.18)$$

where $1 \leq i \leq T_2$ denotes the time-slot index of the second phase of the DDF protocol. Consequently, during the transmission phase of the DDF protocol, the signals received at the destination generate Alamouti codewords.

2.5.2 Equivalent channels analysis

After the classical Alamouti receiver during the transmission phase of the DDF protocol, the resulting fading coefficient is $|\mathbf{h}_{SD}|^2 P_S + |\mathbf{h}_{RD}|^2 P_R$. Consequently, the resulting equivalent matrix model for this transmission is the following:

$$\mathbf{y} = \begin{pmatrix} \mathbf{A} & \mathbf{0} \\ \mathbf{0} & \mathbf{B}_{DA} \end{pmatrix} \mathbf{x} + \mathbf{w}$$

in which $\mathbf{A} = P_S |\mathbf{h}_{SD}|^2 \mathbf{I}_{T_1}$, and $\mathbf{B}_{DA} = (P_S |\mathbf{h}_{SD}|^2 + P_R |\mathbf{h}_{RD}|^2) \mathbf{I}_{T_2}$. In the following of this section, we'll use the following notation to denote the equivalent channel matrix of the Distributed Alamouti scheme:

$$\mathbf{y} = \mathbf{H}_{T_1, T_2, DA} \mathbf{x} + \mathbf{w}.$$

Under this form, the channel matrix $\mathbf{H}_{T_1, T_2, DA}$ is a block diagonal matrix, composed of two diagonal blocks. The upper one is of size T_1 and carries the fading coefficient $P_S |\mathbf{h}_{SD}|^2$, and the second one, of size T_2 carries the fading coefficient $P_S |\mathbf{h}_{SD}|^2 + P_R |\mathbf{h}_{RD}|^2$.

a) Macro diversity

For a fixed instant of correct decoding at the relay T_1 , the transmission of a codeword is done on a channel composed of two blocks whose long-term SNRs are ρ_{SD} and $\rho_{SD} + \rho_{RD}$. The second block is associated to the coherent combination of the long-term SNR characterizing the first block, and another long-term SNR. This long-term SNR channel is thus a Matryoshka channel whose diversity has been derived in Section 2.2.3b.

Result 2.5. *For a fixed instant of correct decoding at the relay T_1 , and a transmission phase of L_2 bits, a macro diversity order equal to 2 is achievable for a Distributed Alamouti transmission if $L_2 \geq K$.*

This condition is the same as the one obtained for the Monostream DDF protocol. Thus, from a complexity point of view, it is better to use the Monostream DDF protocol to reach the same macro diversity order.

b) Micro diversity behavior

For a fixed T_1 , the transmission of a codeword is done on a fading channel composed of two blocks whose associated fading coefficients are $P_S |\mathbf{h}_{SD}|^2$ and $P_S |\mathbf{h}_{SD}|^2 + P_R |\mathbf{h}_{RD}|^2$. The second block is associated to the coherent combination of the fading coefficient characterizing the first block, and another random variable. This channel is thus a Matryoshka channel composed of two blocks.

Result 2.6. *For a fixed instant of correct decoding at the relay T_1 , and a transmission phase of T_2 symbols, a micro diversity order of $2Nrx$ is achievable for a Distributed Alamouti transmission if $L_2 \geq K$.*

c) Averaging on the instants of correct decoding at the relay

These previous analyses enable to upper bound the achievable macro and micro diversity orders. These bounds are only conditioned by the instants of correct decoding by the relay and the destination: the sooner the relay correctly decodes the message and the later the source stops transmitting, the higher the probability of reaching a maximal diversity order.

However, as for the Monostream DDF scheme, after averaging the figure of merits over the instant of correct decoding at the relay, the diversity orders are always equal to 1, for the macro diversity, and N_{rx} for the micro diversity.

2.5.3 Analytic analysis

As for the Monostream DDF protocol, the observation of the equivalent channel models and the knowledge of bounds on the diversity enables to understand the diversity behaviors of the DA DDF.

And similarly, the coding gain and the outage gain must be derived to compare several protocols achieving a same diversity order.

We assume in this section that each node carries a single antenna.

a) Coding gain

The coding gain derivation is usually realized on an upper bound of the pairwise error probability $P_{\mathbf{x} \rightarrow \mathbf{x}' | T_1, T_2, DA}$ which is tight for high values of SNR. The pairwise error probability for a given channel $\mathbf{H}_{T_1, T_2, DA}$, can be upper bounded by:

$$P_{\mathbf{x} \rightarrow \mathbf{x}' | T_1, T_2, \mathbf{H}_{T_1, T_2, DA}} = \mathbf{Q} \left(\frac{\|\mathbf{H}_{T_1, T_2, DA}(\mathbf{x} - \mathbf{x}')\|}{\sqrt{4N_0}} \right) \leq e^{-\frac{\|\mathbf{H}_{T_1, T_2, DA}(\mathbf{x} - \mathbf{x}')\|^2}{8N_0}} \quad (2.19)$$

Averaging Eq. (2.19) on the channels coefficients, it comes:

$$P_{\mathbf{x} \rightarrow \mathbf{x}' | T_1} \leq \iint \exp \left(-\frac{P_S a \sum_{i=1}^{T_1} |x_i - x'_i|^2}{8N_0} - \frac{(P_S a + P_R b) \sum_{i=T_1+1}^T |x_i - x'_i|^2}{8N_0} \right) p_{|h_{SD}|^2}(a) p_{|h_{RD}|^2}(b) da db$$

As $|h_{SD}|^2$ and $|h_{RD}|^2$ are exponentially distributed, the following expressions of the upper bound hold:

$$\begin{aligned} P_{\mathbf{x} \rightarrow \mathbf{x}' | T_1} &\leq \int_0^\infty \frac{1}{\frac{P_R d_2^2}{4N_0} + 1} \exp \left(-a \left(\frac{P_S}{4N_0} (d_1^2 + d_2^2) + 1 \right) \right) da \\ &= \frac{1}{\left(1 + \frac{P_R d_2^2}{4N_0} \right)} \frac{1}{\left(1 + (d_1^2 + d_2^2) \frac{P_S}{4N_0} \right)} \end{aligned}$$

Consequently, regarding this expression for high values of $\rho_{SD} = \frac{P_S}{4N_0}$ and $\rho_{RD} = \frac{P_R}{4N_0}$, we obtain: $\zeta_{DA}(T_1) = \sqrt{d_2^2(d_1^2 + d_2^2)}$.

Result 2.7. *The coding gain of the Distributed Alamouti scheme when the relay correctly decodes the message after receiving T_1 symbols is*

$$\zeta_{DA}(T_1) = \sqrt{d_2^2(d_1^2 + d_2^2)} \quad (2.20)$$

in which d_1 (d_2) is the distance between the closest codewords of the code during the listening (transmission) phase of the DDF transmission.

b) Outage Gain

Using the notations defined in 2.3.2, we study the outage probability of the DA DDF protocol. In this section we focus on the outage gain derivation, and in the following, we derive the DMT of this protocol.

For a given instant of correct decoding at the relay, the outage probability of the Distributed Alamouti scheme equals:

$$P_{out,D}^{(T_1)} = \Pr \left\{ \log(1 + \rho_{SD}|h_{SD}|^2)^{T_1} + \log(1 + \rho_{SD}|h_{SD}|^2 + \rho_{RD}|h_{RD}|^2)^{(T-T_1)} < TR_{N_{max}} \right\}. \quad (2.21)$$

Result 2.8. *The outage gain of the Distributed Alamouti scheme for a fixed instant T_1 of correct decoding at the relay is*

$$\xi_{T_1,DA} = c_{h_{SD}} c_{h_{SD}} \left(\frac{T - T_1}{T - 2T_1} 2^{\frac{TR_{N_{max}}}{T-T_1}} \left(2^{\frac{TR_{N_{max}}(T-2T_1)}{T_1(T-T_1)}} - 1 \right) - \left(2^{\frac{TR_{N_{max}}}{T_1}} - 1 \right) \right)$$

We make the following change of variables $u = \rho_{SD}|h_{SD}|^2$ and $v = \rho_{RD}|h_{RD}|^2$. It comes that the outage gain of the Distributed Alamouti for a fixed T_1 is:

$$\begin{aligned} \xi_{T_1,DA} &= \lim_{\substack{\rho_{SD} \rightarrow \infty \\ \rho_{RD} \rightarrow \infty}} \rho_{SD} \rho_{RD} P_{out,D}^{(T_1)} \\ &= c_{h_{SD}} c_{h_{RD}} \iint_0^\infty \mathbf{1} \{ T_1 \log(1 + u) + (T - T_1) \log(1 + u + v) \leq TR_{N_{max}} \} dudv \end{aligned}$$

Remark that a method to derive this integral has been presented in [11]. We apply it to obtain a closed-form of $\xi_{T_1,DA}$

Using the change of variables $a = T_1 \log(1 + u)$ and $b = (T - T_1) \log(1 + u + v)$, $\xi_{T_1,DA}$ can be expressed as:

$$\begin{aligned} \xi_{T_1,DA} &= c_{h_{SD}} c_{h_{RD}} \iint_0^\infty \mathbf{1} \{ a + b \leq TR_{N_{max}} \} \frac{(\ln 2)^2}{T_1(T - T_1)} 2^{a/T_1} 2^{b/(T-T_1)} da db \\ &= c_{h_{SD}} c_{h_{RD}} \int_{a=0}^{TR_{N_{max}}} \int_{b=0}^{TR_{N_{max}}-a} \frac{(\ln 2)^2}{T_1(T - T_1)} 2^{a/T_1} 2^{b/(T-T_1)} da db \end{aligned}$$

which leads to:

$$\xi_{T_1,DA} = c_{h_{SD}} c_{h_{SD}} \left(\frac{T - T_1}{T - 2T_1} 2^{\frac{TR_{N_{max}}}{T-T_1}} \left(2^{\frac{TR_{N_{max}}(T-2T_1)}{T_1(T-T_1)}} - 1 \right) - \left(2^{\frac{TR_{N_{max}}}{T_1}} - 1 \right) \right).$$

c) DMT analysis

The DMT of this DDF protocol is studied in [37], the authors show that the Distributed Alamouti DDF reaches the optimal DMT of the DDF protocol as defined by Azarian.

d) Comparison with the Monostream DDF

We previously showed that for a fixed instant of correct decoding T_1 , the Monostream DDF and the Alamouti DDF experiences the same macro diversity orders (both schemes must satisfy $L_2 \geq K$).

Moreover, because of the different natures of the equivalent fading channels of the DA DDF and the Monostream DDF, the conditions for full micro diversity achievability are expressed differently

($L_2 \geq K$ and $\min(L_1, L_2) \geq K$ respectively). However, the DDF transmission ensures that $L_1 \geq K$ so that the relay can perfectly decode the message, the two bounds reduce to $L_2 \geq K$. Consequently, the two schemes experience the same micro diversity order under the same condition thanks to channel coding.

Their coding gains must be compared to understand which scheme experience the best performance. From Eq. (2.14) and Eq. (2.20), it comes:

$$\zeta_{DA}(T_1)^2 = \zeta_M(T_1)^2 + d_2^4. \quad (2.22)$$

As $d_2 \neq 0$ is a necessary condition to reach a full diversity order, $\zeta_{DA} > \zeta_M$. Consequently, the Monostream DDF protocol and the DA DDF protocol experience the same macro and micro diversity orders, and the DA DDF provides a coding gain improvement.

2.6 Simulation results

In this section, the previously derived diversity bounds and coding gains are validated through simulation for our proposed practical implementation of the DDF protocol.

The relay uses either the Monostream DDF protocol or the DA DDF protocol. The performance are also compared to the point to point transmission (case without relay).

Furthermore, we consider two transmission types: an open-loop transmission, whose performance are described in terms of outage probability, and a closed-loop transmission without ARQ, whose performance are described in terms of spectral efficiency.

2.6.1 Outage probability

Considering an open-loop transmission, we first validates the outage gain behavior of the Monostream DDF protocol. We then observe the achieved macro and micro diversity orders for fixed instants of correct decoding at the relay using the Monostream DDF and the DA DDF according to ρ_{SD} and ρ_{RD} . Finally, the outage probability of these two schemes averaging on the instants of correct decoding at the relay for fixed values of ρ_{SR} are presented.

a) Performance for fixed instant of correct decoding at the relay

We first focus on the performance achieved by the Monostream DDF protocol.

The derivation of the outage gain $\xi_M(T_1)$ of a Monostream DDF transmission in which the relay correctly decodes the message after receiving T_1 time-slots has been shown to be equal to $\xi_M(T - T_1)$.

This is illustrated in Fig. 2.9. This figure represents the outage probability of the Monostream DDF protocol for fixed instant of correct decoding at the relay when symbols from a Gaussian alphabet are sent according to $\rho_{SD} = \rho_{RD}$. The codeword is composed of 10 time-slots, and $T_1 \in \{1, \dots, 9\}$. The destination carries a single antenna. For all values of $T_1 < T$, the outage probability curves experience a slope of -2 , i.e. full diversity is achieved, and all curves for T_1 and $T'_1 = T - T_1$, i.e the pairs $(T_1, T'_1) \in \{(1, 9), (2, 8), (3, 7), (4, 6)\}$, match at very high SNRs which confirms the outage gains equality.

We now focus on the performance of the practical implementation of the DDF protocol for a particular codeword segmentation presented in Fig. 2.10. We assume that the codeword is composed

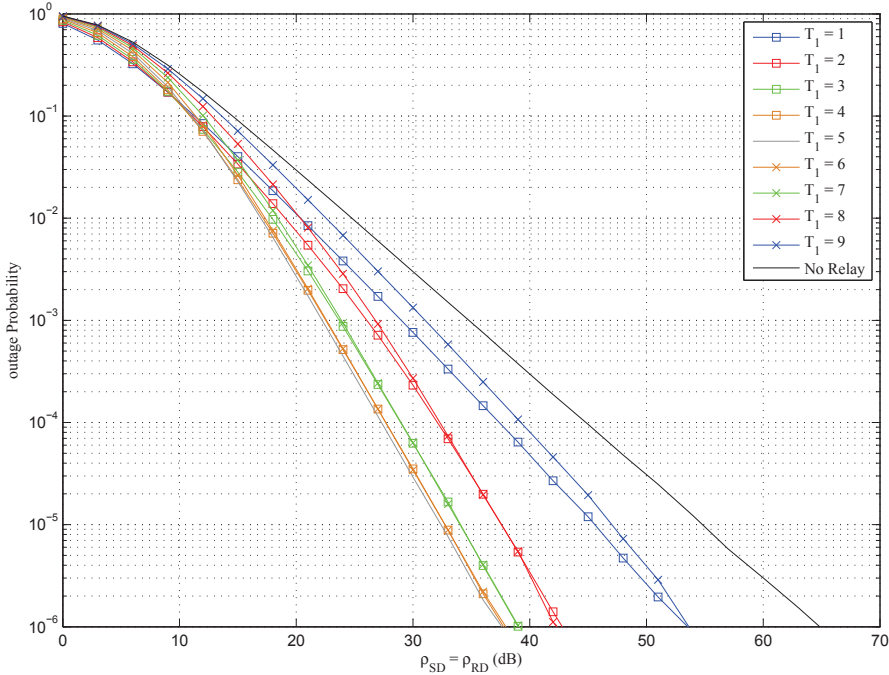


Figure 2.9: Outage probability of the Monostream DDF protocol, for fixed instants of correct decoding at the relay and Gaussian symbol alphabet according to $\rho_{SD} = \rho_{RD}$.

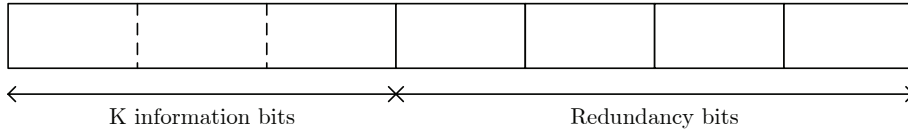


Figure 2.10: Codeword composed of 5 sub-frames, the first one being three time longer than the others and containing only information bits.

of 5 sub-frames, the first one being 3 times longer than the others, and only contains information bits. The source transmits QPSK symbols.

The outage probabilities of the Monostream DDF protocol for fixed instants of correct decoding at the relay according to $\rho_{SD} = \rho_{RD}$ are presented in Fig. 2.11 for $N_{rx} = 1$ or $N_{rx} = 2$. These instants are denoted according to M the sub-frame index after which the relay correctly decodes the message. Recalling that the whole codeword spans over T time-slots, the following notations denote the same instants: $T_1 \in \{\frac{3T}{7}, \frac{4T}{7}, \frac{5T}{7}, \frac{6T}{7}, T\}$ and $M \in \{1, 2, 3, 4, 5\}$. Whatever the instant of correct decoding at the relay, and whatever the considered SNR, the performance using the DDF protocol are better than the performance achieved without the relay. We observe that for $M \in \{3, 4\}$, the slopes of the curves are equal to 1 for the $N_{rx} = 1$ case and 2 for the $N_{rx} = 2$ case. Thus, the achieved micro diversity order is equal to N_{rx} . Indeed, the respective correlated fading channels are $\mathcal{B}(5K/3, 2K/3)$ and $\mathcal{B}(2K, K/3)$ do not satisfy the property $\min(L_1, L_2) \geq K$, whereas for $M \in \{1, 2\}$, the achieved micro diversity order is equal to $2N_{rx}$ as the correlated fading channels satisfy the property $\min(L_1, L_2) \geq K$.

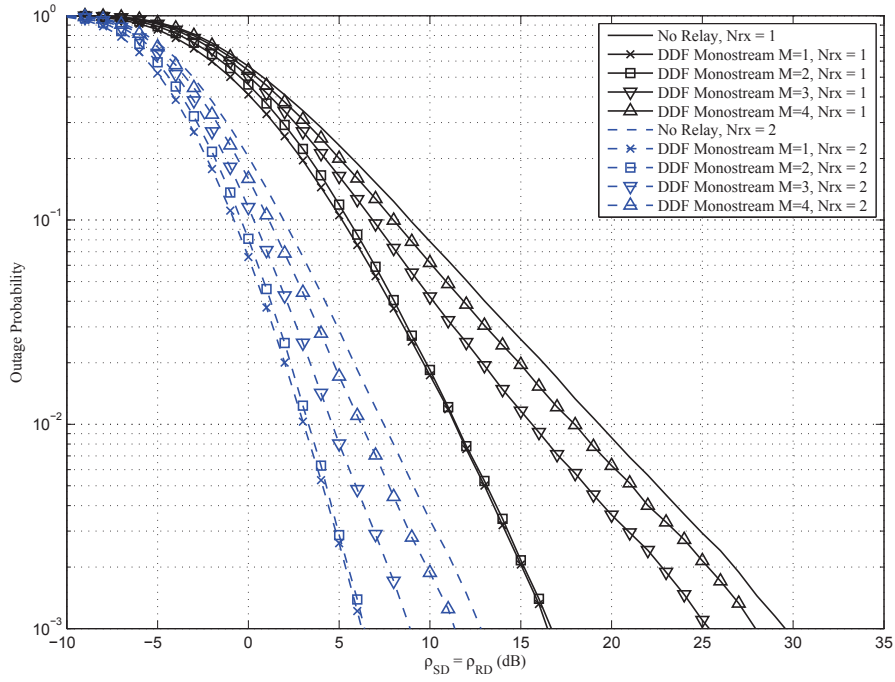


Figure 2.11: Outage probability of the Monostream DDF according to ρ_{SD} and the instant of correct decoding at the relay. $R_{c1} = 1$, $m_S = 2$.

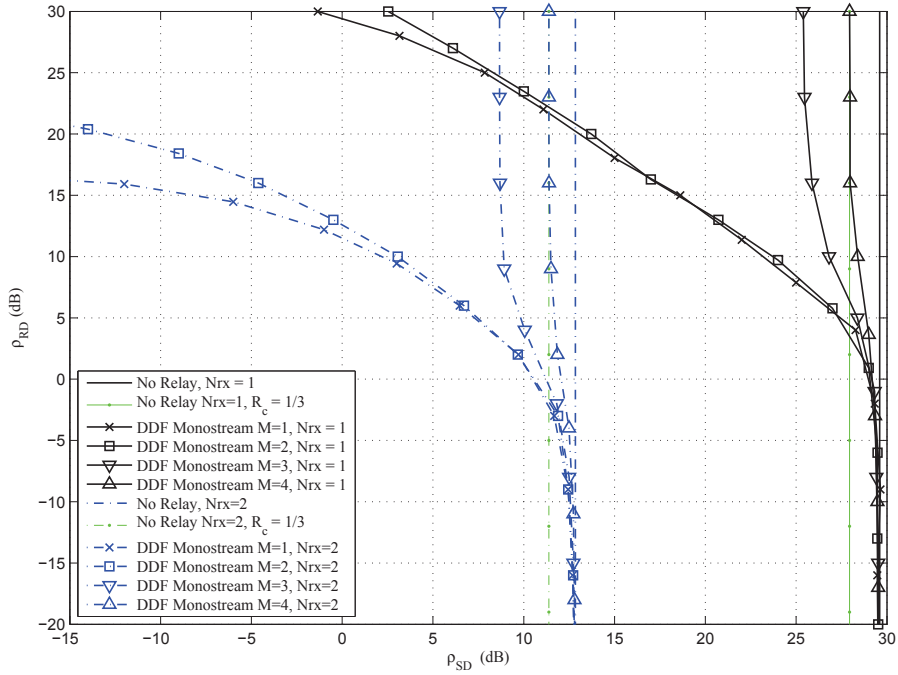


Figure 2.12: Pairs of SNR (ρ_{SD}, ρ_{RD}) achieving the target outage probability of 10^{-3} according to the instant of correct decoding at the relay for the Monostream DDF. $R_{c1} = 1$.

In Fig. 2.12, performance are presented in a unusual way in order to reflect the macro diversity behavior of a transmission scheme for a target value of the considered figure of merit. This figure presents the pairs (ρ_{SD}, ρ_{RD}) , achieving the target outage probability of 10^{-3} according to the instant of correct decoding at the relay M , and the number of reception antennas at the destination N_{rx} . For the point to point transmission, a minimal ρ_{SD} of 29dB (12dB) is needed to reach the target outage probability for the $N_{rx} = 1$ ($N_{rx}=2$) case. Using the DDF protocol, this minimal value is required for very low ρ_{RD} . But, as this SNR increases, this minimal value ρ_{SD} decreases depending on the considered instant of correct decoding. There are two distinct behaviors: either this minimal value is a finite ρ_{SD} ($M \in \{3, 4\}$) or this minimal value is going toward $-\infty$ ($M \in \{1, 2\}$).

Going back to the definition of the achievable macro diversity order, given in Section 2.2.2, the cases $M \in \{3, 4\}$ do not achieve a macro diversity order equal to 2: indeed, when the SNR between the source and the destination is null, the target probability not to be in outage of 0.999 is not achievable through the relay-destination link. This is explained by the fact that the resulting Matryoshka channel of long term SNRs are $\mathcal{M}((1, 2), ((5K/3, 2K/3)))$, and $\mathcal{M}((1, 2), ((2K, K/3)))$ respectively. None of these channel satisfying the condition $L_2 \geq K$, it results a macro diversity order of 1. Consequently, under such representation of the performance, the vertical asymptotes represent a macro diversity order of 1. Furthermore, this minimal value of ρ_{SD} needed to reach the target performance corresponds to the minimal ρ_{SD} needed to reach the target in the no relay case with a coding rate equal to $\frac{K-L_2}{L_1}$. Indeed, it corresponds to the fact that L_2 bits out of K bits are perfectly received from the relay (because $\rho_{RD} \rightarrow +\infty$), and the $K - L_2$ bits left must be decoded within L_1 bits. This is illustrated for the $M = 4$ case by the green curves representing the performance achievable without relay with a coding rate of $\frac{K-L_2}{L_1} = 1/3$.

However, when $M \in \{1, 2\}$, a minimal ρ_{RD} equal to 21dB and 16dB, for the $N_{rx}=1$ case and the $N_{rx} = 2$ respectively, is needed to reach the target probability not to be in outage when ρ_{SD} is going toward $-\infty$. Thus, full macro diversity is achievable. Indeed, the equivalent Matryoshka channels of SNR satisfy the condition $L_2 \geq K$.

These figures validate the derived bounds for the macro and micro diversity orders achievable by a Monostream DDF protocol. We then compare the performance of this relaying scheme to the performance of the DA DDF.

In Fig. 2.13 are presented the pairs (ρ_{SD}, ρ_{RD}) , achieving the target outage probability of 10^{-3} according to the instant of correct decoding at the relay M , for the Monostream DDF protocol and the DA DDF protocol, the destination carrying two reception antennas.

These relaying schemes experience the same macro diversity order as their resulting long term SNR channels for a fixed instant of correct decoding at the relay are the same. Thus, when $M \in \{1, 2\}$, the target outage probability can be reach whatever the ρ_{SD} value, and $M \in \{3, 4\}$, a minimal SNR between the source and the destination is needed to reach this target. Moreover, these two relaying schemes experience the same micro diversity behavior whatever the considered M . Consequently, the gain provided by the DA DDF scheme is not due to a micro diversity gain but is only due to a coding gain improvement which has been derived in Section 2.5.3. This coding gain is only observed for similar values of ρ_{SD} and ρ_{RD} as when one of the two becomes very low, both relaying schemes become equivalent thus leading to the same performance.

The performance achieved for a fixed instant of correct decoding at the relay are useful to vali-

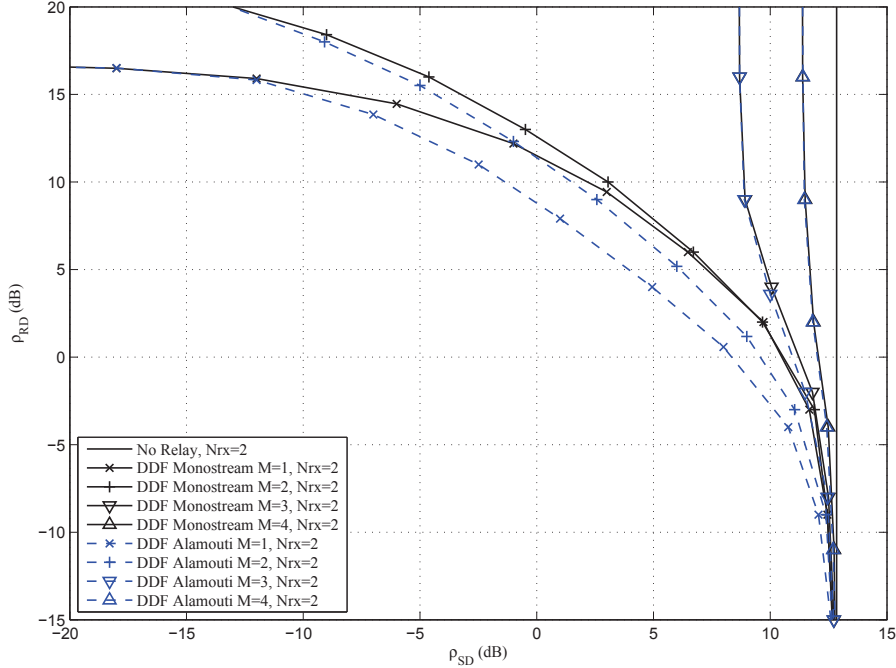


Figure 2.13: Couples of SNR (ρ_{SD}, ρ_{RD}) achieving the target outage probability of 10^{-3} according to the instant of correct decoding at the relay for the Monostream DDF and the DA DDF. $N_{rx} = 2$, $R_{c1} = 1$.

date the derived diversity upper bounds, but they are insufficient to characterize the transmission performance.

b) Averaged performance for fixed ρ_{SR} .

We thus focus on the performance achieved for a particular ρ_{SR} value using Eq. (2.9).

The averaged outage probability of a Monostream DDF transmission when ρ_{SR} takes values in $\{0, 10, 20\}$ dB are presented in Fig. 2.14 according to $\rho_{SD} = \rho_{RD}$. The higher the ρ_{SR} value and the better the performance. Indeed, a high ρ_{SR} value enables a quick decoding of the message at the relay. However, even in that case, the relay may not assist the transmission as deep fading event on the source to relay link can lead to an outage event. Let's consider the $\rho_{SR} = 10$ dB case. For $\rho_{SD} \leq 16$ dB, most of the outage events come from an outage at the destination when both the source and the relay transmit, leading to a $2N_{rx}$ micro diversity order (the slope of the curve is merely equal to 2 for this range of SNR). However, for higher ρ_{SD} values, the more probable outage event comes from the outage of the SR link and the SD link, leading to a micro diversity order of N_{rx} . Thus, the slope of the curve is equal to N_{rx} at high SNR values which is the achieved diversity order for this transmission with a fixed ρ_{SR} value.

The couples (ρ_{SD}, ρ_{RD}) achieving the target average outage probability of 10^{-3} for a transmission without relay (green curve), with a relay using the Monostream DDF (black curves), and a relay using the DA DDF (blue curves) are presented in Fig. 2.15 for several ρ_{SR} values $\rho_{SR} \in \{-8, -6, -5, -4, -3, 0\}$ dB.

The higher the ρ_{SR} value, the sooner the relay correctly decodes the message. Consequently, the higher the number of DDF transmissions experiencing a full macro diversity order. This is

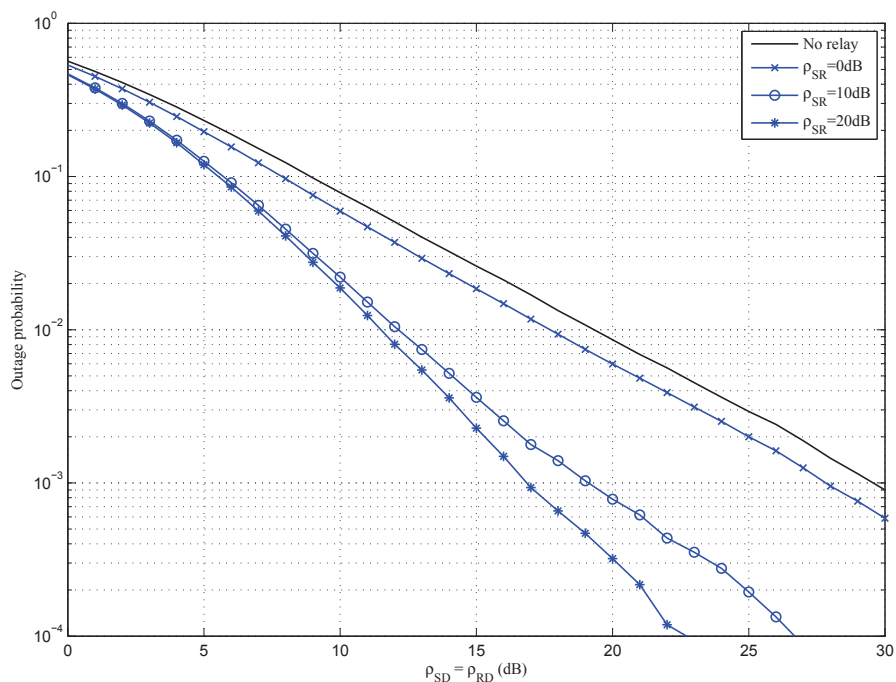


Figure 2.14: Outage probability of the Monostream DDF when $\rho_{SD} = \rho_{RD}$ for several ρ_{SR} values.

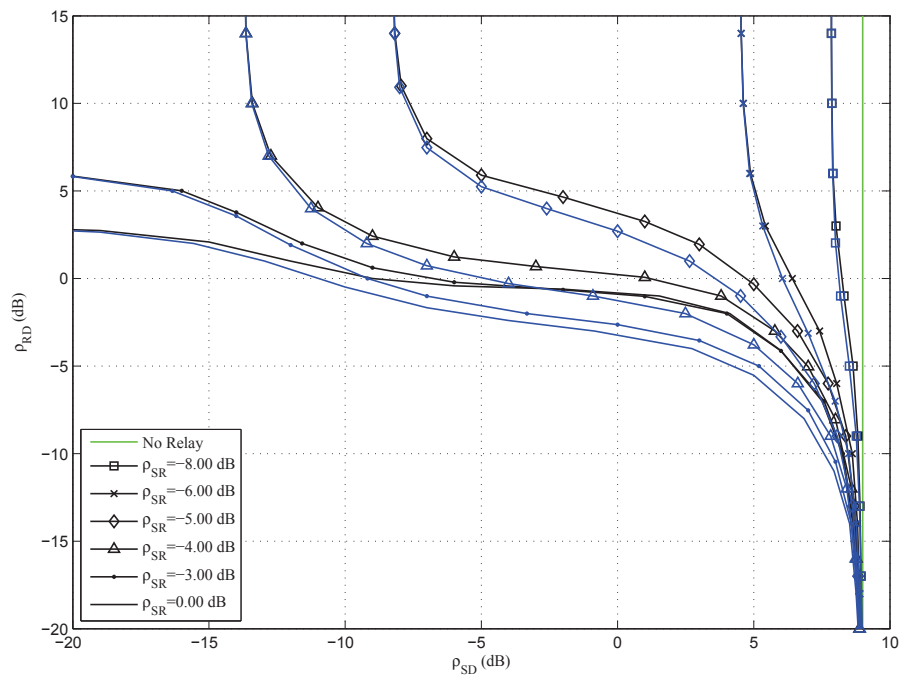


Figure 2.15: Couples (ρ_{SD}, ρ_{RD}) achieving the target outage probability of 10^{-3} for the Monostream DDF (black line) and the DA DDF (blue line).

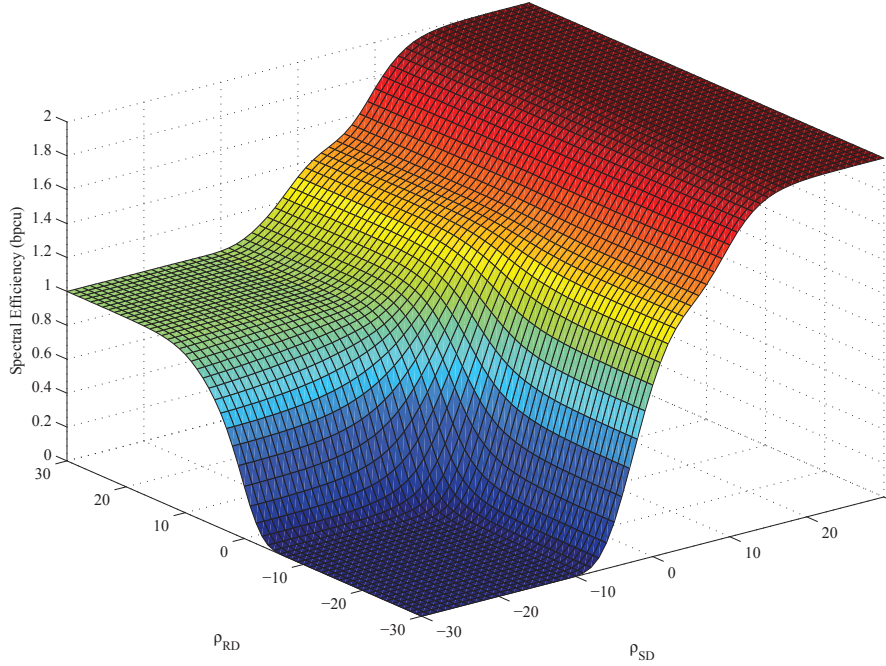


Figure 2.16: Spectral efficiency of the Monostream DDF protocol according to ρ_{SD} and ρ_{RD} when $\rho_{SR} = 30\text{dB}$.

illustrated on the figure as all schemes where $\rho_{SR} \geq -3\text{ dB}$ show an horizontal asymptote for the considered range of ρ_{SD} .

For each ρ_{SR} value, the DA DDF scheme experiences a coding gain improvement when compared to the Monostream DDF relaying scheme which has been proven in Section 2.5.3.

2.6.2 Spectral Efficiency

In this paragraph, we thus derive and compare the spectral efficiency performance of the Monostream DDF and the DA DDF for the previously described codeword segmentation.

We first focus on the Monostream DDF performance when $\rho_{SR} = 30\text{dB}$, i.e. when the relay correctly decodes the message after receiving the first sub-frame almost surely, presented in Fig. 2.16 according to ρ_{SD} and ρ_{RD} . This figure represents the spectral efficiency achieved by the DDF transmission for all couples of SNR in $[-30\text{dB}, 30\text{dB}]^2$ when $\rho_{SR} = 30\text{dB}$. Two macro diversity behaviors can be observed on this figure: Spectral efficiency values higher than 1 bpcu experience a macro diversity behavior equal to 1, and spectral efficiency values lower than 1 bpcu obtain a full macro diversity behavior for these ranges of SNRs. This difference is due to the transmission length at the relay. Indeed, for the destination to achieve a spectral efficiency higher than 1 bpcu , it must correctly decode the message before the end of the 4-th sub-frame, which gives no chance to the relay to transmit the minimal K bits needed to bring its macro diversity order. However, for lower spectral efficiency values, the relay can send at least K bits if it correctly decodes the message after the first sub-frame leading to a full macro diversity behavior.

In Fig. 2.17, the spectral efficiencies of the Monostream DDF and of the DA DDF are compared.

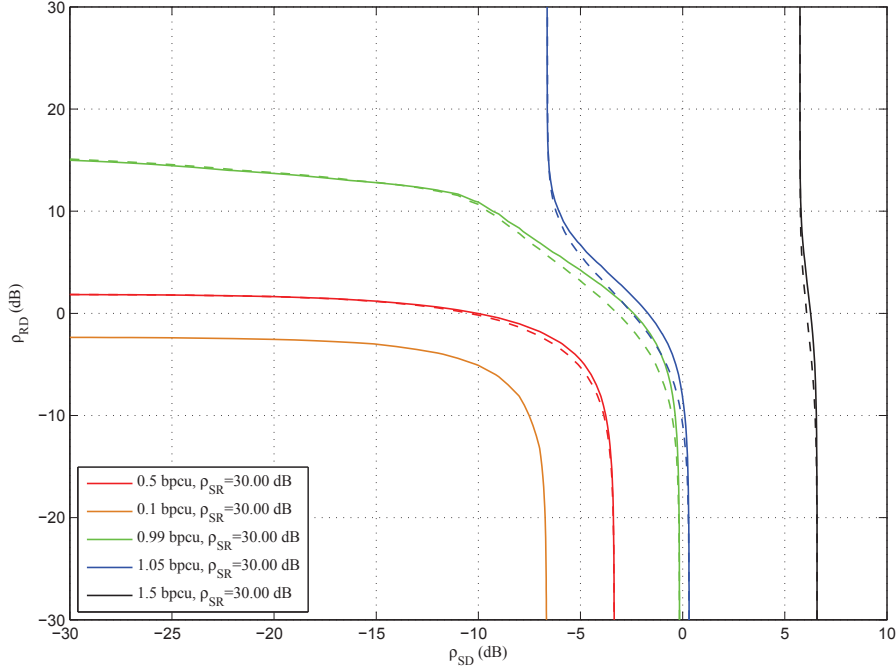


Figure 2.17: Couples of SNRs achieving several target spectral efficiencies for $\rho_{SR} = 30\text{dB}$ when the relay uses the Monostream DDF (full line) or the DA DDF (dotted line).

This figure presents the couples (ρ_{SD}, ρ_{RD}) achieving target spectral efficiencies in $\{1.5, 1, 0.99, 0.5, 0.1\}$ bpcu for $\rho_{SR} = 30\text{dB}$. We previously understood that the Monostream DDF and the DA DDF have the same macro diversity order. Consequently, whatever the target spectral efficiency value, the achieved performance confirms that the two relaying schemes experience the same diversity behavior. Moreover, the DA DDF enables to slightly increase the performance when compared to the Monostream DDF protocol which might be due to the coding gain provided by the DA scheme. For a spectral efficiency equal to 0.5 bpcu, this improvement is so small that the curves seem to be similar.

Conclusion

In this chapter, after defining a macro diversity order and deriving diversity upper bounds for several channel models, we proposed a practical implementation of the DDF protocol. This implementation based on channel coding and codeword segmentation fulfill the assumption of relay-unaware source and the low complexity decoding abilities at the destination constraint.

We characterized the performance of the Monostream DDF and the DA DDF according to their macro diversity and micro diversity using the previously derived upper bounds. The study points out that both relaying schemes experience the same diversities orders, the DA DDF only providing a coding gain improvement when compared to the Monostream DDF protocol.

These results are illustrated by simulation results showing that the performance mainly depends on the instant of correct decoding at the relay: the sooner the relay begins to transmit, the better the performance is.

However, as the source is relay-unaware, the transmission rate cannot be adapted to the source-

relay link to make the listening phase very short. Thus, techniques increasing performance must be designed still satisfying the relay-unaware source constraint and the assumption of low complexity decoding at abilities at the destination.

Chapter 3

Patching technique and Distributed Rotations for the relay channel

Introduction

In the previous chapter, we proved that the performance of the Monostream DDF and the DA DDF only depend on the instant of correct decoding at the relay: the sooner the relay correctly decodes the message, the better the performance.

However, as we are interested in protocols guaranteeing that the source is relay-unaware, the source cannot adapt its modulation and coding scheme to the quality of the source-relay link enabling a quick decoding at the relay. Thus, we introduce a new technique called Patching technique to improve the achievable diversity orders.

In this chapter, the proposed Patching technique is described in Section 3.1, in order to increase the achievable macro and micro diversity orders still satisfying the relay-unaware source assumption. We give four Patching examples: the Patched Monostream, the Patched Distributed Alamouti, the Patched Golden Code and the Patched Silver Code. In Section 3.2, the Distributed Rotation (DR) DDF is introduced. This relaying scheme is shown to experience the same diversity orders than the Monostream DDF, and enables to improve the coding gain still guaranteeing the same constraints. When both constraints are relaxed, we propose to use Spatial Division Multiplexing (SDM) DDF and DDF with adaptation of modulation, to improve the achievable diversity orders. These techniques are described in Section 3.3.

3.1 Patching technique

3.1.1 Definition of the Patching technique

The Patching technique, originally defined in [59], consists in transferring symbols from the first phase of the DDF protocol into the second phase of the DDF protocol. It generates an equivalent transmission in which the relay virtually correctly decodes the message sooner than it really does.

The use of the Patching technique requires that the destination is aware of the relay's presence.



Figure 3.1: Patching principle.

Thus, after its correct decoding of the message, the relay notifies the destination that the Patching technique is used thank to a dedicated signalling or pilot.

This Patching technique is composed of two steps.

The first one is done by the relay. It sends a linear combination of symbols already sent by the source in the first phase of the DDF protocol, and symbols the source is going to send in the second phase of the DDF protocol. This resulting symbol is called an hypersymbol. These combinations are bijections so that decoding the resulting hypersymbol becomes equivalent to decoding multiple symbols. The number of combined symbols per time-slot is optimized so that the maximal diversity becomes reachable in the limit of a maximal spectral efficiency available at the relay. For instance, in LTE systems, a relay can transmit symbols from a 2^{m_S} QAM up to a 64QAM. A particular example is described in Fig. 3.1 where the relay combines the symbol x_i with x_{T1+i} using a linear function denoted f .

The second step of the Patching technique is done at the destination. The destination applies a *patch* over its received signals. This patch consists in using the same linear combination than the relay on the signals received by the destination during the first and the second phase of the DDF protocol. This guarantee a low complexity decoding at the destination side by generating an equivalent codeword transmission composed of a shorter first phase and a second phase containing symbols of a 2^{m_S} QAM and symbols of a 2^{m_R} QAM. Still considering the particular example of Fig. 3.1, the destination generates $f(y_i, y_{T1+i})$.

In the following, we first present the method of combining symbols in order to generate easily decodable hypersymbols. We then apply this Patching technique for the Monostream DDF protocol to increase the achievable macro diversity, and finally, we use the Patching technique to increase the achievable macro and micro diversities by generating Distributed Space-Time Block Codes during the second phase of the equivalent DDF protocol after Patching (Patched DA, Patched Golden and Patched Silver).

3.1.2 Generating hypersymbols of QAM from the combination of QPSK symbols

We focus on generating constellations from the combination of lower cardinality constellations. We are particularly interested in generating a 2^{2n} QAM from the combination of n QPSKs.

Proposition 3.1. *The set of symbols \mathbb{S}_{2n} from a 2^{2n} QAM can be generated from the linear com-*

bination of n QPSK symbols according to:

$$\mathbb{S}_{2n} = \left\{ \sqrt{\frac{3}{4^n - 1}} \sum_{i=1}^n 2^{i-1} s_2(i), \quad (s_2(i))_{1 \leq i \leq n} \in (\mathbb{S}_2)^n \right\}. \quad (3.1)$$

where \mathbb{S}_2 is the set of QPSK symbols.

Proof. Proposition 3.1 is demonstrated using recursivity.

(i) $n = 1$: The QPSK symbols \mathbb{S}_2 are the following :

$$\mathbb{S}_2 = \left\{ \sqrt{\frac{3}{4-1}} s_2, \quad s_2 \in \mathbb{S}_2 \right\}. \quad (3.2)$$

(ii) For a fixed $n \in \mathbb{N}^*$, we assume that the symbols from the 2^{2n} QAM are:

$$\mathbb{S}_{2n} = \left\{ \sqrt{\frac{3}{4^n - 1}} \sum_{i=1}^n 2^{i-1} s_2(i), \quad (s_2(i))_{1 \leq i \leq n} \in (\mathbb{S}_2)^n \right\} \quad (3.3)$$

whose minimal Euclidean distance denoted $d_{min,2n}$ is

$$d_{min,2n} = \sqrt{\frac{6}{4^n - 1}} \quad (3.4)$$

Symbols from a constellation of cardinality $2^{2(n+1)}$ are built linearly combining QPSK symbols and symbols of the 2^{2n} QAM:

$$\mathbb{S}'_{2(n+1)}(\alpha) = \left\{ \frac{1}{\sqrt{1+\alpha^2}} (s_2 + \alpha s_{2n}), \quad s_2 \in \mathbb{S}_2 \text{ and } s_{2n} \in \mathbb{S}_{2n} \right\} \quad (3.5)$$

where $\alpha \in \mathbb{R}^+$. We denote d_2 the minimal Euclidean distance of symbols of the scaled QPSK $\frac{1}{\sqrt{1+\alpha^2}} \mathbb{S}_2$, and d_{2n} the minimal Euclidean distance of symbols of $\frac{\alpha}{\sqrt{1+\alpha^2}} \mathbb{S}_{2n}$. We also denote d the minimal Euclidean distance between the point $(0,0)$ and the projections of the symbols from $\mathbb{S}'_{2(n+1)}(\alpha)$ on the x axis. A particular example illustrating these notations is presented in Fig. 3.2 where two QPSKs are combined with $\alpha = 0.2143$. The resulting symbols of \mathbb{S}'_{16} are the blue stars, and the QPSK symbols resulting from the scaling by $\frac{1}{\sqrt{1+\alpha^2}}$ are represented by red crosses.

Thus, we have :

$$d_2 = \frac{1}{\sqrt{1+\alpha^2}} \sqrt{2} \quad (3.6)$$

$$d_{2n} = \frac{\alpha}{\sqrt{1+\alpha^2}} \sqrt{\frac{6}{4^n - 1}} \quad (3.7)$$

$$d = \frac{1}{2} (d_2 - d_{2n}(2^n - 1)) \quad (3.8)$$

To generate a regular QAM, the minimal distance between points of the resulting constellation must be equal to $2d$. Consequently, α must satisfied $\frac{d_{2n}}{2} = d$ leading to:

$$\alpha = \frac{1}{2^n} \sqrt{\frac{4^n - 1}{3}} \quad (3.9)$$

And finally,

$$\mathbb{S}_{2(n+1)} = \left\{ 2^n \sqrt{\frac{3}{4^{n+1} - 1}} s_2 + \sqrt{\frac{4^n - 1}{4^{n+1} - 1}} s_{2n}, \quad s_2 \in \mathbb{S}_2 \text{ and } s_{2n} \in \mathbb{S}_{2n} \right\} \quad (3.10)$$

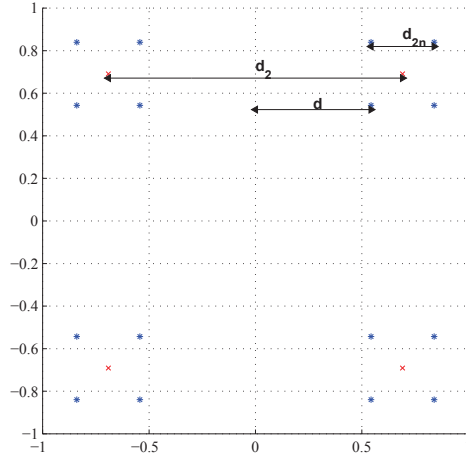


Figure 3.2: Linear combination of two QPSK, $\alpha = 0.2143$.

- (iii) Thus, whatever the natural non zero integer n , the symbols from the 2^{2n} QAM can be generated by a linear combination of QPSK symbols given by:

$$\mathbb{S}_{2n} = \left\{ \sqrt{\frac{3}{4^n - 1}} \sum_{i=1}^n 2^{i-1} s_2(i), \quad (s_2(i))_{1 \leq i \leq n} \in (\mathbb{S}_2)^n \right\} \quad (3.11)$$

□

As an example, we consider the generation of a 16QAM from two QPSKs.

For this generation of hypersymbols, the coefficient α is equal to 0.5. Fig. 3.3a presents the associated mapping, and Fig. 3.3b illustrates the resulting constellation of hypersymbols and the associated mapping. Each 16QAM symbol is labeled by the concatenation of the bits coding for the symbol from $\frac{2}{\sqrt{5}}\mathbb{S}_2$ and the bits coding for the symbol from $\frac{1}{\sqrt{5}}\mathbb{S}_2$. From this knowledge, decoding the hypersymbol at the destination side is equivalent to decode 2 QPSK symbols.

However, over a bi dimensional space, transmitting points from the \mathbb{Z}^2 lattice (i.e. symbols from QAM) is suboptimal in terms of shaping gain. The best lattice to be used over the complex plan is the hexagonal lattice, denoted A_2 . Thus, it would be of interest to build symbols from the A_2 lattice combining QAM symbols. This mathematical construction generates highly energetic points which cannot be used in practice.

For instance, a point $z \in A_2$ can be generated from two QPSK symbols: the first step is to generate a symbol x from a 16QAM using Eq. (3.1), and the second step is combine the real and imaginary parts of x :

$$z = \begin{pmatrix} \mathcal{R}(x) & \mathcal{I}(x) \end{pmatrix} \begin{pmatrix} 1 & 0 \\ 1/2 & \sqrt{3}/2 \end{pmatrix} \begin{pmatrix} 1 \\ i \end{pmatrix}.$$

The Fig. 3.4 presents the symbols resulting from this mathematical generation of symbols from the A_2 lattice. This mathematic combination leads to the generation of highly energetic symbols (particularly those labeled with 0000 and 1111) which does not provide the best shaping gain. Consequently, we only consider QAM generation from QPSK symbols in the following.

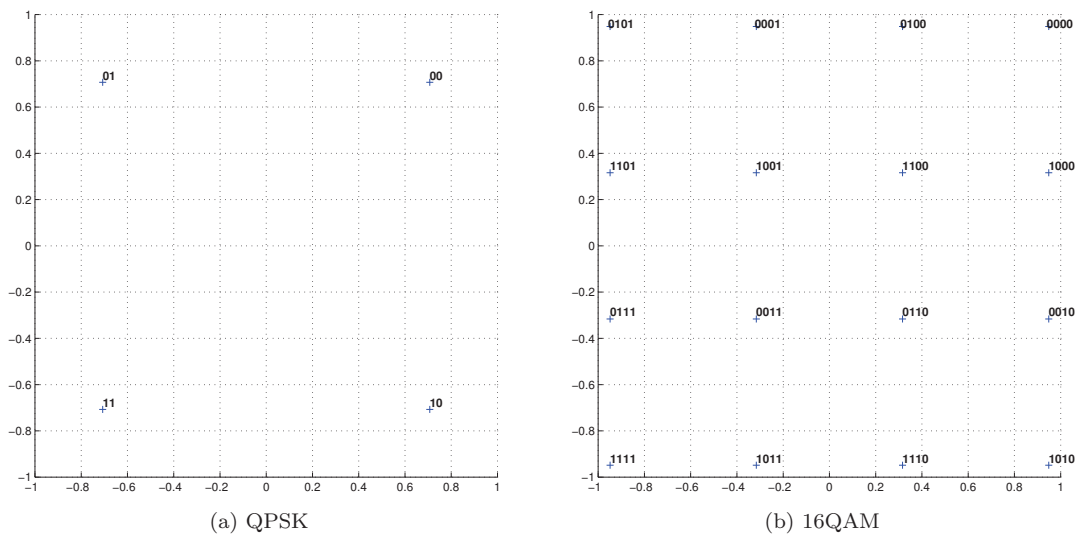


Figure 3.3: The QPSK mapping, and the mapping of the 16 QAM resulting from the linear combination of the two QPSKs with $\alpha = 0.5$

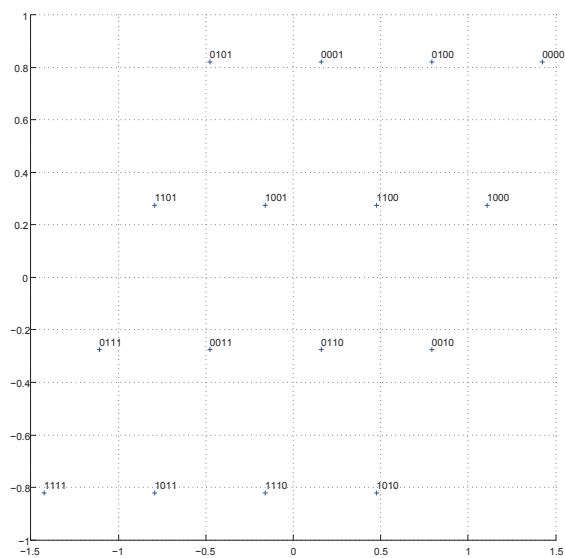


Figure 3.4: A_2 symbols resulting from the combination of 2 QPSKs.

3.1.3 Patched Monostream DDF protocol

a) The Patching step for the Monostream DDF

Let's consider a DDF transmission in which the relay uses the Patching technique only during the first time slot of the second phase. Consequently, during this time-slot, the relay transmits the symbol x_{R,T_1+1} resulting from the linear combination of p symbols already sent by the source: $\{x_1, \dots, x_p\}$, and the symbol x_{T_1+1} sent by the source during this time-slot:

$$x_{R,T_1+1} = \sqrt{\frac{3}{4^{p+1}-1}} \left(\sum_{i=1}^p 2^i x_{p-i+1} + x_{T_1+1} \right). \quad (3.12)$$

According to Eq. (3.1), x_{R,T_1+1} belongs to a $2^{2(p+1)}$ QAM of average energy equal to one. Thus, the relay transmits using its whole power budget.

At the destination side, the second step of the Patching technique is done: it builds the same combination over the received signals $\{\mathbf{y}_1, \dots, \mathbf{y}_p\}$, and \mathbf{y}_{T_1+1} :

$$\tilde{\mathbf{y}}_{T_1+1} = \sqrt{\frac{3}{4^{p+1}-1}} \left(\sum_{i=1}^p 2^i \mathbf{y}_{p-i+1} + \mathbf{y}_{T_1+1} \right) \quad (3.13)$$

$$= \begin{bmatrix} \mathbf{h}_{SD} \sqrt{P_S} & \sqrt{\frac{3}{4^{p+1}-1}} \mathbf{h}_{RD} \sqrt{P_R} \end{bmatrix} \begin{bmatrix} x_{R,T_1+1} \\ x_{R,T_1+1} \end{bmatrix} + \mathbf{w}' \quad (3.14)$$

where \mathbf{w}' is the resulting vector of noise whose samples are Gaussian distributed of zero mean and variance N_0 per real dimension.

b) The resulting channels

At the transmission end, after the second Patching step, the destination uses the signals $\mathbf{y}_{PM} = \{\mathbf{y}_{p+1}, \dots, \mathbf{y}_{T_1}, \tilde{\mathbf{y}}_{T_1+1}, \mathbf{y}_{T_1+2}, \dots, \mathbf{y}_T\}^t$ to decode the message.

$$\mathbf{y}_{PM} = \begin{pmatrix} \mathbf{A} & \mathbf{0} & \mathbf{0} \\ \mathbf{0} & b & \mathbf{0} \\ \mathbf{0} & \mathbf{0} & \mathbf{C} \end{pmatrix} \mathbf{x}_{PM} + \mathbf{w}_{PM}$$

in which $\mathbf{A} = \sqrt{P_S} \mathbf{h}_{SD} \mathbf{I}_{T_1-p}$, $b = \sqrt{P_S} \mathbf{h}_{SD} + \sqrt{\frac{3}{4^{p+1}-1}} \sqrt{P_R} \mathbf{h}_{RD}$, $\mathbf{C} = (\sqrt{P_S} \mathbf{h}_{SD} + \sqrt{P_R} \mathbf{h}_{RD}) \mathbf{I}_{T_2-1}$, $\mathbf{x}_{PM} = \{x_{p+1}, \dots, x_{T_1}, x_{R,T_1+1}, x_{T_1+2}, \dots, x_T\}^t$ and \mathbf{w}_{PM} is the Gaussian distributed vector of noise samples of zero mean and variance N_0 per real dimension.

The loss induced by the Patching technique is twofold: the first loss is a coding gain loss due to the use of a constellation of higher cardinality during a time-slot, and secondly, there is a SNR loss on the relay to destination link during this time-slot. This SNR loss cannot be mitigated by using power control at the relay as it already uses its whole power budget.

Equivalent channel of long term SNRs The channel of long term SNR resulting from the Patching of p symbols from the first phase in one symbol of the second one combined with the Monostream DDF protocol is composed of 3 blocks characterized by ρ_{SD} , $\rho_{SD} + \sqrt{\frac{3}{4^{p+1}-1}} \rho_{RD}$, and $\rho_{SD} + \rho_{RD}$ respectively. The two last blocks are associated to 2 linear combinations of the same long term SNRs. Thus, they are part of the same Matryoshka block in the long-term SNR channel model.

Consequently, the Matryoshka channel of long-term SNRs resulting from the Patched Monostream protocol is described by $\mathcal{M}(\mathcal{D}, \mathcal{L})$ where $\mathcal{D} = (1, 2)$ and $\mathcal{L} = (L_1 - pm_S, L_2 + pm_S)$. Full macro diversity for this Patched Monostream is achievable if $L_2 + pm_S \geq K$ which is less constraining than without Patching where the condition to reach full macro diversity is $L_2 \geq K$.

Thus, the Patching technique enables to obtain a less restrictive condition for the full macro diversity to be achievable when compared to the DDF transmission without Patching. This condition reveals that the higher the number of combined symbols by the relay, the higher the number of bits in the second block of the channel resulting from Patching, and the easier full macro diversity is achievable.

Equivalent fading channel The equivalent fading channel is the correlated block-fading channel $\mathcal{B}(\mathcal{L})$ composed of two blocks resulting from a Monostream DDF transmission where $\mathcal{L} = (L_1 - pm_S, L_2 + pm_S)$.

The condition to reach full micro diversity is $\min\{L_1 - pm_S, L_2 + pm_S\} \geq K$. Thus even if the second channel block is longer than without Patching, the first one is shorter. I.e. even if the Patching technique recovers the diversity of the second channel block, it can lose the diversity offered by the first block. Consequently, the Patched Monostream DDF protocol does not guarantee to improve the achievable micro diversity order.

c) Maximization of the achievable macro diversity order

For a fixed instant of correct decoding at the relay, the Patching technique modifies the conditions to fulfill for the full macro and micro diversity to be achievable.

Thus the relay can adapt the number of combined symbols per time-slots (i.e. adapt m_R), and the number of time-slots P in which it uses the Patching technique, so that the achievable diversity orders increase. Particularly, the Patched Monostream DDF protocol is designed so that the maximal macro diversity order is achievable. However, this patching technique is done at the price of an increased constellation size and a SNR loss on the relay-destination link during some time-slots.

Thus the relay must optimize m_R , in the limit of a maximal spectral efficiency $m_{R,max}$, and P , limited by T_2 , to maximize the achievable macro diversity order at the end of the transmission and to minimize the resulting coding gain loss.

Because this optimization is untractable in practice (similar to the theoretic optimization that should be done to optimize the choice of MCS in the LTE system), several strategies can be considered to reach full macro diversity. We here describe three of them:

- Patching with Maximal Use (MaxU):

The relay transmits symbols from a $2^{m_{R,max}}$ QAM as soon as it correctly decodes the message until the second channel block contains at least K bits. Consequently, the relay transmits during at least $\left\lceil \frac{K}{m_{R,max}} \right\rceil$ time-slots using a $2^{m_{R,max}}$ QAM.

Using the Patching with MaxU, the generated Matryoshka channel of long-term SNRs is

$$\mathcal{L} = \begin{cases} (L_1 - \frac{m_{R,max}}{m_S} T_2, T_2 m_{R,max}) & \text{if } \left\lceil \frac{K}{m_{R,max}} \right\rceil \geq T_2 \\ (L_1 - \frac{m_{R,max}}{m_S} \left\lceil \frac{K}{m_{R,max}} \right\rceil, L_2 + \left\lceil \frac{K}{m_{R,max}} \right\rceil (m_{R,max} - m_S)) & \text{if } \left\lceil \frac{K}{m_{R,max}} \right\rceil < T_2 \end{cases} \quad (3.15)$$

Using the Patching with MaxU leads to equivalent channel models containing an increased number of bits whatever the instant of correct decoding at the relay. More particularly, this Patching technique is used even if the relay correctly decodes the message after receiving few sub-frames, and the destination correctly decodes at the codeword's end, which generally leads to cases where full macro diversity is achievable without Patching. Consequently, the Patching with MaxU is suboptimal as the Patching technique is used even if the full macro diversity is already achievable by the Monostream DDF protocol.

- Patching with Medium Use (MedU):

The relay uses the Patching technique only if the maximal macro diversity order is not achievable at the codeword's end due to its late decoding of the message. Moreover, the same constellation size is used during the whole second phase of the DDF protocol. Thus, the relay chooses m_R as:

$$m_R = \min\{\lceil K/T_2 \rceil, m_{R,max}\} \quad (3.16)$$

i.e. the relay choose the minimal constellation cardinality to reach full macro diversity combining symbols during the whole second phase of the DDF protocol. Thus the resulting channel of long-term SNR is a Matryoshka channel in which

$$\mathcal{L} = \left(\max \left\{ L_1 - \frac{m_R}{m_S} T_2, 0 \right\}, \min \left\{ L_2 + \frac{m_R}{m_S} T_2, L_1 + L_2 \right\} \right). \quad (3.17)$$

- Patching with Minimal Use (MinU):

As for the Patching with MedU, the relay uses the Patching technique only if the maximal macro diversity order is not achievable at the codeword's end due to its late decoding of the message. But the relay stops using the Patching technique as soon as enough bits, i.e. $K - L_2$ bits, have been transferred from the first channel block into the second one. Thus, the relay can use several modulations during the second phase of the DDF protocol. This strategy is called Patching with Minimal use.

However, some combinations of $(T_1, T_2, m_S, m_{R,max})$ may lead to the same Patching behavior at the relay whatever the considered strategy.

Several diversity configurations can arise at the codeword's end according to the combination of (T_1, T_2) and the chosen Patching strategy: First configuration where both the full macro and the full micro diversities are obtained by the Patching technique at the codeword's end (case A). The second configuration where the maximal macro diversity order is obtained by the Patching technique but not the maximal micro diversity order at the codeword's end (case B). The third one where the full macro diversity is not achievable even using the Patching technique at the codeword's end (case C). Some practical transmissions leading to these 3 cases are described in Tab. 3.1 for the Patching with minimal use under the limit of $m_{R,max} = 3m_S$.

3.1.4 Patched Space-Time Blocks Codes for the DDF protocol

Because for the Monostream DDF, the condition to achieve full macro and full micro diversities are different, the Patching strategies are designed so that full macro diversity is achievable at the codeword's end. Thus, in some cases, the Patching enables to bring full macro diversity but not full micro diversity.

	(T, T_1, T_2)	K	SNR channel	macro	Fading channel	micro
case A	(4,3,1)	$2m_S$	$\mathcal{M}((1, 2), (2m_S, 2m_S))$	2	$\mathcal{B}(2m_S, 2m_S)$	2Nrx
case B	(3,2,1)	$2m_S$	$\mathcal{M}((1, 2), (m_S, 2m_S))$	2	$\mathcal{B}(m_S, 2m_S)$	Nrx
case C	(5,4,1)	$4m_S$	$\mathcal{M}((1, 2), (2m_S, 3m_S))$	1	$\mathcal{B}(2m_S, 3m_S)$	Nrx

Table 3.1: Three practical examples leading the 3 possibles configurations after Patching with minimal use. The resulting channels are indicated after the Patching step at the destination side.

	x_{R,T_1+1}	x_{R,T_1+2}
Patched DA	$-\sqrt{\frac{3}{4^{p+1}-1}}(x_{T_1+2}^* + 2\sqrt{\frac{4^p-1}{3}}z_2^*)$	$\sqrt{\frac{3}{4^{p+1}-1}}(x_{T_1+1}^* + 2\sqrt{\frac{4^p-1}{3}}z_1^*)$
Patched Golden	$i\frac{\bar{\phi}(x_{T_1+2} + \bar{\alpha}z_2)}{\sqrt{\bar{\phi}^2(1+\bar{\alpha}^2)}}, \begin{cases} \alpha = \frac{1+\sqrt{5}}{2} \\ \bar{\alpha} = \frac{1-\sqrt{5}}{2} \\ \phi = 1+i-i\alpha \\ \bar{\phi} = 1+i-i\bar{\alpha} \\ i^2 = -1 \end{cases}$	$\frac{\bar{\phi}(x_{T_1+1} + \bar{\alpha}z_1)}{\sqrt{\bar{\phi}^2(1+\bar{\alpha}^2)}}, \begin{cases} \alpha = \frac{1+\sqrt{5}}{2} \\ \bar{\alpha} = \frac{1-\sqrt{5}}{2} \\ \phi = 1+i-i\alpha \\ \bar{\phi} = 1+i-i\bar{\alpha} \\ i^2 = -1 \end{cases}$
Patched Silver	$-\frac{x_{T_1+2}^*}{\sqrt{2}} - \frac{(1-2i)z_1^* + (1+i)z_2^*}{\sqrt{2}\sqrt{7}}, i^2 = -1$	$\frac{x_{T_1+1}^*}{\sqrt{2}} + \frac{(-1+i)z_1^* + (1+2i)z_2^*}{\sqrt{2}\sqrt{7}}, i^2 = -1$

Table 3.2: Generation of x_{R,T_1+1} and x_{R,T_1+2} to be transmitted by the relay according to the considered Patched DSTBC.

We showed in the previous chapter that the conditions for full macro and micro diversity to be achievable using the DA DDF are the same. The idea is now to combine the Patching technique and the Distributed Space-Time Block Codes (DSTBC) to improve both the macro and the micro diversity orders still satisfying the relay-unaware source constraint.

a) The Patching step for the DDF with DSTBCs

The Patching technique with DSTBC aims at generating an equivalent channel model in which the patched symbols form space-time codewords. We derive this technique for 3 space-time codes: the Alamouti code, and the Golden Code and the Silver Code.

This technique with space-time codes of size 2x2 requires two time-slots of the second phase of the DDF protocol to use the Patching technique.

Let's consider that the relay uses the Patching technique during the first 2 time-slots of the second phase transmitting x_{R,T_1+1} and x_{R,T_1+2} , resulting from the combination of (x_1, \dots, x_{2p}) and (x_{T_1+1}, x_{T_1+2}) . And, from $T_1 + 3$ to the last time-slot, the relay uses the DA-DDF protocol.

The first step of the Patching technique is an hypersymbol generation: The relay generates z_1 and z_2 such that:

$$\begin{cases} z_1 &= \sqrt{\frac{3}{4^p-1}} \sum_{i=1}^p 2^{i-1} x_i \\ z_2 &= \sqrt{\frac{3}{4^p-1}} \sum_{i=1}^p 2^{i-1} x_{p+i} \end{cases} \quad (3.18)$$

This hypersymbol generation is followed by a combination of $(z_1, z_2, x_{T_1+1}, x_{T_1+2})$ to form x_{R,T_1+1} and x_{R,T_1+2} . These combinations are given in Tab. 3.2 according to the considered Patched DSTBC.

	$\tilde{\mathbf{Y}}$
Patched DA	$\sqrt{\frac{3}{4^{p+1}-1}} \left(2\sqrt{\frac{4^p-1}{3}} \tilde{\mathbf{Y}}_1 + \mathbf{Y}_2 \right)$
Patched Golden	$\frac{\phi(\alpha \tilde{\mathbf{Y}}_1 + \mathbf{Y}_2)}{\sqrt{ \phi^2(1+\alpha^2) }}$
Patched Silver	$\frac{\tilde{\mathbf{Y}}_1}{\sqrt{14}} \begin{bmatrix} 1+i & -1+2i \\ -(1+2i) & (-1+i) \end{bmatrix} + \frac{\mathbf{Y}_2}{\sqrt{2}}$

Table 3.3: Combinations of received signals done at the destination according to the considered Patched DSTBC.

Consequently, during these two time-slots of the second phase of the DDF protocol, the destination receives:

$$\mathbf{Y}_2 = \begin{bmatrix} \mathbf{y}_{T_1+1} & \mathbf{y}_{T_1+2} \end{bmatrix} \quad (3.19)$$

$$= \begin{bmatrix} \mathbf{h}_{SD}\sqrt{P_S} & \mathbf{h}_{RD}\sqrt{P_R} \end{bmatrix} \begin{bmatrix} x_{T_1+1} & x_{T_1+2} \\ x_{R,T_1+1} & x_{R,T_1+2} \end{bmatrix} + \mathbf{W} \quad (3.20)$$

The second step of the Patching technique is a combination of the received signals at the destination in order to generate an equivalent channel model in which codewords from space-time codes appear to be jointly transmitted by the source and the relay. The destination first generates $\tilde{\mathbf{Y}}_1$ which is then combined with \mathbf{Y}_2 . The generation of $\tilde{\mathbf{Y}}_1$ is done according to the following equation:

$$\tilde{\mathbf{Y}}_1 = \left[\sqrt{\frac{3}{4^p-1}} \sum_{i=1}^p 2^{i-1} \mathbf{y}_i \quad \sqrt{\frac{3}{4^p-1}} \sum_{i=1}^p 2^{i-1} \mathbf{y}_{i+p} \right] \quad (3.21)$$

and the combinations of $\tilde{\mathbf{Y}}_1$ and \mathbf{Y}_2 are presented in Tab. 3.3 according to the considered Patched DSTBC.

The equivalent model after this combination of signals is described by

$$\tilde{\mathbf{Y}} = \begin{bmatrix} c_1 \mathbf{h}_{SD}\sqrt{P_S} & c_2 \mathbf{h}_{RD}\sqrt{P_R} \end{bmatrix} \mathbf{X}_{DSTBC} + \tilde{\mathbf{W}} \quad (3.22)$$

where \mathbf{X}_{DSTBC} is the generated codeword of space time code, presented in Tab. 3.4 according to the considered Patched DSTBC, coding $2(p+1)m_S$ bits, and where $\tilde{\mathbf{W}}$ is the resulting noise sample Gaussian distributed of zero mean and variance N_0 per real dimension.

b) The resulting channels

At the end of the transmission, the destination decodes the message thanks to the received and combined signals $(\mathbf{y}_{2p+1}, \dots, \mathbf{y}_{T_1}, \tilde{\mathbf{Y}}, \mathbf{y}_{T_1+3}, \dots, \mathbf{y}_T)$. The losses induced by the Patching technique are twofold: Firstly, the transmission of symbols from a constellation of higher cardinality leads to a coding gain loss. Secondly, the Patching technique leads to a channel model whose long-term SNRs are lowered by constants (c_1, c_2) described in Tab. 3.4 during certain time-slots.

Equivalent channel of long term SNR For each studied Patched DSTBC, the resulting Matryoshka channel of long-term SNRs is of the form $\mathcal{M}(\mathcal{D}, \mathcal{L})$ where $\mathcal{D} = (1, 2)$ and $\mathcal{L} = (L_1 - 2pm_S, L_2 + 2pm_S)$. The second channel block resulting from the Patched DSTBC is longer than without Patching, and the first channel block is shorter.

	\mathbf{X}_{DSTBC}		(c_1, c_2)
Patched DA		$\begin{bmatrix} x_{R,T_1+2}^* & -x_{R,T_1+1}^* \\ x_{R,T_1+1} & x_{R,T_1+2} \end{bmatrix}$	$(1, \sqrt{\frac{3}{4^{p+1}-1}})$
Patched Golden	$\frac{1}{\sqrt{5}}$	$\begin{bmatrix} \phi(x_{T_1+1} + \alpha z_1) & \phi(x_{T_1+2} + \alpha z_2) \\ i\bar{\phi}(x_{T_1+2} + \bar{\alpha} z_2) & \bar{\phi}(x_{T_1+1} + \bar{\alpha} z_1) \end{bmatrix}$	$(1, \frac{1}{\sqrt{ \phi ^2(1+\bar{\alpha}^2)}})$
Patched Silver	$\frac{1}{\sqrt{2}}$	$\begin{bmatrix} x_{T_1+1} + \frac{(1+i)z_1 + (-1+2i)z_2}{\sqrt{7}} & x_{T_1+2} - \frac{(1+2i)z_1 + (1-i)z_2}{\sqrt{7}} \\ -x_{T_1+2}^* - \frac{(1-2i)z_1^* + (1+i)z_2^*}{\sqrt{7}} & x_{T_1+1}^* - \frac{(1-i)z_1^* - (1+2i)z_2^*}{\sqrt{7}} \end{bmatrix}$	$(1, \frac{1}{\sqrt{2}})$

Table 3.4: Resulting ST codewords and constant values deriving from the Patching technique.

Full macro diversity for these Patched DSTBCs is achievable if $L_2 + 2pm_S \geq K$ which is less constraining than without Patching, where the condition to reach full macro diversity is $L_2 \geq K$. Moreover, the higher the number of combined symbols by the relay, the higher the number of bits in the second block of the channel resulting from Patching, and the easier full macro diversity is achievable.

Equivalent channel of fading Similarly, the resulting fading channel is a Matryoshka channel $\mathcal{M}(\mathcal{D}, \mathcal{L})$ where $\mathcal{D} = (n_r, 2n_r)$ and $\mathcal{L} = (L_1 - 2pm_S, L_2 + 2pm_S)$. The maximal micro diversity order is achievable if $L_2 + 2pm_S \geq K$, which is the same condition to reach full macro diversity.

Using the Patched DSTBCs, the full diversity orders are achievable under the same condition.

3.1.5 Strategy to maximize the achievable diversity orders

If the Patched DSTBCs are designed to maximize the achievable macro diversity order, it results that the achievable micro diversity order is maximized.

As for the Patched Monostream DDF protocol, the number of combined symbols and the number of time-slots used to generate the Patched DSTBCs have to be adapted so that the maximal macro and micro diversity orders are achievable.

Similarly to the Patched Monostream, this optimization is untractable, and the 3 Patching strategies can be similarly defined.

3.2 Distributed rotations

After this improvement of diversity still satisfying the relay-unaware source constrain, we propose to use the DDF with Distributed Rotations (DR DDF) in order to improve the coding gain.

The distributed rotations for cooperative protocols were introduced by S.Yang in [30]. In this article, a two-hop multi-relay channel without direct link is studied in which the distributed rotations are introduced for the AF protocol and for the DF protocol. The authors show that for a high number of available rotations and infinitely long codewords the relaying protocols with distributed rotations reach the maximum diversity by changing the available spatial diversity into time diversity creating an artificial fast fading channel.

C.Hucher proposed in [38, 39], an adaptation of this technique for the DDF protocol with a direct link between the source and the destination. The authors show that for the one-relay two-

rotation case, the resulting DR DDF protocol reaches the DMT of the DDF protocol as defined in [27]. This scheme is very close to the Monostream DDF protocol and satisfies the relay-unaware source assumption. Furthermore, this DR DDF allows the destination to be relay-unaware as it does not require a separate estimation of \mathbf{h}_{SD} and \mathbf{h}_{RD} .

In this section, after deriving the achievable diversity orders thank to equivalent channel analysis, we derive the coding gain and outage gain of the DR DDF. The derived values are then compared to the performance of the Monostream DDF and the DA DDF.

3.2.1 Equivalent channels analysis

Using the DR DDF scheme, the relay transmits exactly the same symbols as those transmitted by the source affected by a coefficient $r \in \{e^{i2\pi}, e^{-i\pi}\}$ so that half symbols from the second phase are affected by 1, and the other one is affected by -1 .

Consequently, the vector \mathbf{y} of all received signals during the codeword transmission for a fixed instant of correct decoding at the relay, can be described under the following matrix form:

$$\mathbf{y} = \begin{pmatrix} \mathbf{A} & \mathbf{0} & \mathbf{0} \\ \mathbf{0} & \mathbf{B} & \mathbf{0} \\ \mathbf{0} & \mathbf{0} & \mathbf{C} \end{pmatrix} \mathbf{x} + \mathbf{w}$$

in which $\mathbf{A} = \sqrt{P_S} \mathbf{h}_{SD} \mathbf{I}_{T_1}$, $\mathbf{B} = (\sqrt{P_S} \mathbf{h}_{SD} + \sqrt{P_R} \mathbf{h}_{RD}) \mathbf{I}_{T_2/2}$ and $\mathbf{C} = (\sqrt{P_S} \mathbf{h}_{SD} - \sqrt{P_R} \mathbf{h}_{RD}) \mathbf{I}_{T_2/2}$. We use the following notation of the equivalent channel:

$$\mathbf{y} = \mathbf{H}_{T_1, DR} \mathbf{x} + \mathbf{w}$$

a) Equivalent channel of long-term SNR

The equivalent long-term SNR channel of the DR DDF is composed of two blocks affected by ρ_{SD} and by $\rho_{SD} + \rho_{RD}$. Consequently, this Matryoshka channel is the same as the one obtained for the Monostream DDF scheme, and for the DA DDF scheme in Chapter 2.

Proposition 3.2. *For a fixed instant of correct decoding at the relay T_1 , and a transmission phase of L_2 bits, full macro diversity is achievable for the DR DDF if $L_2 \geq K$.*

Consequently, the DR DDF, the Monostream DDF and the DA DDF must fulfill the same condition in order for the full macro diversity to be achievable.

b) Equivalent fading channel

The equivalent channel of fading generated by the DR DDF protocol is the studied block fading channel with correlation B which has been studied in the previous chapter. This study leads to the following proposition:

Proposition 3.3. *For a fixed instant of correct decoding at the relay T_1 , and a transmission phase of L_2 bits, full micro diversity is achievable by the DR DDF if $\min\{L_1, L_2\} \geq K$.*

Consequently, the DR DDF and the Monostream DDF must fulfill the same condition in order for the full macro diversity to be achievable.

3.2.2 Analytic analysis

For a fixed instant of correct decoding at the relay, as both relaying schemes for the DDF protocol lead to the same diversity behaviors, we are interested in deriving their coding gain and outage gain to analytically compare their performance..

a) Coding gain

The coding gain derivation is usually realized on an upper bound of the pairwise error probability $P_{\mathbf{x} \rightarrow \mathbf{x}' | T_1, DR}$ which is tight for high values of SNR. The pairwise error probability for a given channel $\mathbf{H}_{T_1, DR}$, can be upper bounded by:

$$P_{\mathbf{x} \rightarrow \mathbf{x}' | T_1, \mathbf{H}_{T_1, DR}} = \mathbf{Q} \left(\frac{\|\mathbf{H}_{T_1, DR}(\mathbf{x} - \mathbf{x}')\|}{\sqrt{4N_0}} \right) \leq e^{-\frac{\|\mathbf{H}_{T_1, DR}(\mathbf{x} - \mathbf{x}')\|^2}{8N_0}} \quad (3.23)$$

This bound, after averaging over fading coefficients, can be written as:

$$P_{\mathbf{x} \rightarrow \mathbf{x}' | T_1} \leq \frac{1}{\left(1 + \frac{P_R d_2^2}{4N_0}\right)} \frac{1}{\left(1 + (d_1^2 + d_2^2) \frac{P_S}{4N_0} - d_2^2 (d_{21} - d_{22})^2 \frac{P_S / (4N_0) P_R / (4N_0)}{1 + d_2^2 P_R / (4N_0)}\right)} \quad (3.24)$$

in which $d_1^2 = \sum_{i=1}^{T_1} |x_i - x'_i|^2$ ($d_2^2 = \sum_{i=T_1+1}^T |x_i - x'_i|^2$) is the distance between the codewords during the listening (transmission) phase of the DDF transmission and $d_{21}^2 = \sum_{i=T_1+1}^{T_1+(T-T_1/2)} |x_i - x'_i|^2$, $d_{22}^2 = \sum_{i=T_1+(T-T_1/2)+1}^T |x_i - x'_i|^2$. Consequently, when $d_2 \neq 0$, the achieved diversity order is maximized. We derive the coding gain of this full diversity transmission scheme.

Proposition 3.4. *The coding gain of the DR DDF when the relay correctly decodes the message after receiving T_1 symbols is*

$$\zeta_{DR}(T_1) = d_2 \sqrt{d_1^2 + 4d_{21}d_{22}} \quad (3.25)$$

in which d_1 (d_2) is the distance between the closest codewords of the code during the listening (transmission) phase of the DDF transmission and $d_{21}^2 = \sum_{i=T_1+1}^{T_1+(T-T_1/2)} |x_i - x'_i|^2$, $d_{22}^2 = \sum_{i=T_1+(T-T_1/2)+1}^T |x_i - x'_i|^2$.

Proof. Averaging Eq. (3.23) on the real and imaginary parts of the fading coefficients, it comes:

$$P_{\mathbf{x} \rightarrow \mathbf{x}' | T_1} \leq \iint_{u_R, u_I} e^{-\frac{P_S(u_R^2 + u_I^2)d_1^2}{8N_0}} I(u_R)I(u_I)p(u_R)p(u_I)du_Rdu_I$$

in which:

$$\begin{aligned} I(u) &= \int_{-\infty}^{+\infty} e^{-\frac{u^2(d_{21}^2 + d_{22}^2)P_S}{8N_0} - t \frac{2u(d_{21}^2 - d_{22}^2)\sqrt{P_S P_R}}{8N_0} - t^2 \left(\frac{d_{21}^2 + d_{22}^2}{8N_0} + \frac{1}{2} \right)} \frac{dt}{\sqrt{2\pi}} \\ &= \frac{1}{\sqrt{1 + \frac{d_2^2 P_R}{4N_0}}} \exp \left(u^2 \frac{\frac{P_S P_R}{(8N_0)^2} (d_{21}^2 - d_{22}^2)^2 - \frac{d_2^2 P_S}{8N_0} \left(\frac{d_2^2 P_R}{8N_0} + \frac{1}{2} \right)}{\frac{d_2^2 P_R}{8N_0} + \frac{1}{2}} \right). \end{aligned}$$

Plug-in this expression into the bound on the pairwise error probability, it follows that:

$$\begin{aligned} P_{\mathbf{x} \rightarrow \mathbf{x}' | T_1} &= \frac{1}{\left(1 + \frac{P_R d_2^2}{4N_0}\right)} \frac{1}{\left(1 + (d_1^2 + d_2^2) \frac{P_S}{4N_0} - (d_{21}^2 - d_{22}^2)^2 \frac{P_S / (4N_0) P_R / (4N_0)}{1 + d_2^2 P_R / (4N_0)}\right)} \\ &= \frac{1}{\left(1 + \rho_{RD} d_2^2\right)} \frac{1}{\left(1 + (d_1^2 + d_2^2) \rho_{SD} - (d_{21} - d_{22})^2 \frac{\rho_{SD} d_2^2 \rho_{RD}}{1 + d_2^2 \rho_{RD}}\right)} \end{aligned}$$

in which $d_1^2 = \sum_{i=1}^{T_1} |x_i - x'_i|^2$ ($d_2^2 = \sum_{i=T_1+1}^T |x_i - x'_i|^2$) is the distance between the codewords during the listening (transmission) phase of the DDF transmission and $d_{21}^2 = \sum_{i=T_1+1}^{T_1+(T-T_1/2)} |x_i - x'_i|^2$, $d_{22}^2 = \sum_{i=T_1+(T-T_1/2)+1}^T |x_i - x'_i|^2$.

Consequently, if any pairs of codewords satisfies $d_2 \neq 0$, full diversity is achieved, and regarding this expression for high values of ρ_{SD} and ρ_{RD} , we obtain a coding gain equal to $\zeta_{DR}(T_1) = d_2 \sqrt{d_1^2 + 4d_{21}d_{22}}$. \square

b) Outage Gain

Using the notations defined in 2.3.2, we study the outage probability of the DR DDF protocol.

For a given instant of correct decoding at the relay, the outage probability of the DR DDF equals:

$$P_{out,D}^{(T_1)} = \Pr \left\{ \log(1 + \rho_{SD}|h_{SD}|^2)^{T_1} + \log(1 + |\sqrt{\rho_{SD}}h_{SD} + \sqrt{\rho_{RD}}h_{RD}|^2)^{\frac{T-T_1}{2}} + \log(1 + |\sqrt{\rho_{SD}}h_{SD} - \sqrt{\rho_{RD}}h_{RD}|^2)^{\frac{T-T_1}{2}} < TR_{N_{max}} \right\}. \quad (3.26)$$

Denoting $T_2 = (T - T_1)/2$, the outage probability $P_{out,D}^{(T_1)}$ can be exactly written as

$$P_{out,D}^{(T_1)} = \frac{1}{\rho_{SD}\rho_{RD}} \int_{\mathbb{R}^4} \mathbf{1} \left\{ \begin{array}{l} T_2 \ln(1+(u'_R-v'_R)^2+(u'_I-v'_I)^2) \\ + T_2 \ln(1+(u'_R+v'_R)^2+(u'_I+v'_I)^2) \\ + T_1 \ln(1+(u_R'^2+u_I'^2)) < \ln(2^{TR}) \end{array} \right\} p(h_R = \frac{u'_R}{\sqrt{\rho_{SD}}}, h_I = \frac{u'_I}{\sqrt{\rho_{SD}}}, g_R = \frac{v'_R}{\sqrt{\rho_{RD}}}, g_I = \frac{v'_I}{\sqrt{\rho_{RD}}}) du'_R du'_I dv'_R dv'_I$$

The outage gain $\xi_{DR}(T_1)$ of the DDF with two distributed rotations, for a given T_1 and denoting $T_2 = (T - T_1)/2$, is:

$$\begin{aligned} \xi_{DR}(T_1) &= \lim_{\rho_{SD}, \rho_{RD} \rightarrow \infty} \rho_{SD}\rho_{RD} P_{out,D}^{(T_1)} \\ &= \int_{\mathbb{R}^4} \mathbf{1} \left\{ \begin{array}{l} T_2 \ln(1+(u'_R-v'_R)^2+(u'_I-v'_I)^2) \\ + T_2 \ln(1+(u'_R+v'_R)^2+(u'_I+v'_I)^2) \\ + T_1 \ln(1+(u_R'^2+u_I'^2)) < \ln(2^{TR}) \end{array} \right\} c_{h_{SD}} c_{h_{RD}} du'_R du'_I dv'_R dv'_I. \end{aligned}$$

Deriving a closed form expression of the resulting outage gain seems to be untractable since a closed form expression of the volume defined by the outage region is difficult to derive.

c) DMT analysis

The DMT of this DR DDF is derived in [38] from outage analysis. The authors prove that this DDF schemes reaches the DMT of the DDF protocol as defined by Azarian.

3.2.3 Comparison with the Monostream DDF and the DA DDF

The DR DDF achieves the same macro and micro diversity orders than the Monostream DDF protocol and the DA DDF protocol, whose performance were presented in the previous Chapter. Consequently, we compare their coding gains to determine the relaying scheme for the DDF protocol minimizing the error probability.

We prove that $\zeta_M(T_1) = d_1 d_2$, and that $\zeta_{DR}(T_1) = d_2 \sqrt{d_1^2 + 4d_{21}d_{22}}$. Consequently, $\zeta_{DR}(T_1)$ can be written as $\zeta_{DR}(T_1) = \sqrt{\zeta_M(T_1)^2 + 4d_{21}d_{22}}$. Consequently, the DR DDF provides a coding gain improvement when compared to the Monostream DDF for a fixed value T_1 .

Thus, after averaging on the instants of correct decoding at the destination, the DR DDF enables to reach better performance in term of coding gain, when compared to the Monostream DDF.

Furthermore, we showed in the previous chapter that the coding gain of the DA DDF protocol is $\zeta_{DA} = \sqrt{d_2^2(d_1^2 + d_2^2)}$. Because $d_2^2 = d_{21}^2 + d_{22}^2 + 2d_{21}d_{22}$, and $d_{21}^2 + d_{22}^2 \geq 2d_{21}d_{22}$, it comes that $d_2^2 \geq 4d_{21}d_{22}$. Consequently, the coding gain of the DA DDF scheme is higher or equal to the coding of the DR DDF protocol.

3.3 Other methods to improve the achievable diversity orders

We introduce the Patching technique to improve the achievable macro and micro diversity orders of the Monostream DDF and the DA DDF. We also improve the achievable coding gain of full diversity scheme when compared to the Monostream DDF by using DR DDF, still satisfying the relay-unaware source constrain and requiring no additionnal channel coefficients estimation at the destination.

Relaxing these constrains, we propose two techniques to improve the achievable diversity orders.

3.3.1 Spatial Division Multiplexing DDF

SDM DDF is an affordable solution to increase the achievable macro and micro diversities at the price of an increased decoding complexity at the destination, and satisfying the relay-unaware source constraint. Moreover, this relaying scheme requires that the destination estimates both \mathbf{h}_{SD} and \mathbf{h}_{RD} .

After a correct decoding at the relay, it can perfectly build the whole codeword transmitted by the source. It can even generate additional redundancy bits.

These redundancy bits are transmitted by the relay using the SDM DDF. Thus, during the second phase of the DDF protocol, the source and the relay transmit different symbol streams, and probably from different constellations.

When a Maximum Likelihood receiver is used at the destination side, such transmission is equivalent to a transmission over a block channel of fading and long-term SNR $\mathcal{B}(\mathcal{L})$ with $\mathcal{L} = (L_1 + L_2, T_2 m_R)$ over which full macro and micro diversities are achievable if $\min\{L_1 + L_2, T_2 m_R\} \geq K$ which is equivalent to $T_2 m_R \geq K$ as the source transmits at least K bits. Consequently, the relay adapts the number of generated redundancy bits to reach full macro diversity: at least K bits must be transmitted by the relay during T_2 time-slots in the limit of a maximal spectral efficiency $m_{R,max}$:

$$m_R = \min\{m_{R,max}, \lceil K/T_2 \rceil\}. \quad (3.27)$$

If the modulation cardinality were not limited, full macro and micro diversity would always be achievable.

However, when high complexity cannot be afforded at the destination, a MMSE receiver is used but it does not recover the micro diversity order offered by the relay-destination link. It would be of interest to analytically derive the macro diversity order achieved when the destination uses this receiver.

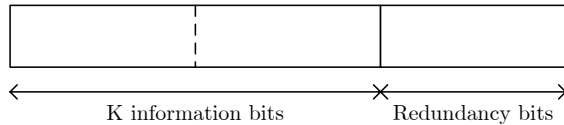


Figure 3.5: Codeword composed of 2 sub-frames, the first one being twice longer than the other and containing only information bits.

3.3.2 Modulation adaptation

The main principle of the SDM DDF is to increase the number of transmitted redundancy bits during the second phase of the DDF protocol only on the relay-destination link to increase the achievable diversity orders but it requires high decoding abilities at the destination. Relaxing the relay-unaware source constraint, both nodes can generate the same increased quantity of redundancy bits and adapt the cardinality of the modulations, so that $T_2 m_S = T_2 m_R \geq K$. This technique is called DDF with modulation adaptation. It can also be described as a Monostream DDF in which the source and the relay adapt their modulation during the second phase of the DDF protocol in the limit of a maximal cardinality. Using this relaying scheme, the destination can be relay-unaware, as it estimates \mathbf{h}_{SD} and $\mathbf{h}_{SD} + \mathbf{h}_{RD}$ only.

Using this technique, the source must know the instant of correct decoding at the relay, thus there must be a feedback link between the source and the relay.

At the destination side, this transmission is very similar to a Monostream transmission in which occurs a change of modulation. Thus, the decoding complexity at the destination is the same as the one needed for a Monostream transmission with a higher constellation size.

3.4 Simulation results

In this section, we illustrate the performance of the proposed relaying schemes for the DDF protocol improving the macro and micro diversity orders, and improving the coding gain.

Similarly as in Section 2.6, we study the performance of open-loop and closed-loop transmissions over a flat fading Rayleigh channel without intersymbol interference. We assume that the source and the relay carry a single transmit antenna and we assume that the destination carries two reception antennas.

3.4.1 Outage probability

We are interested in the performance achieved by the previously described schemes for an open loop transmission whose figure of merit is the outage probability.

a) Performance for fixed instant of correct decoding at the relay.

In Fig. 3.6, we present the outage probability of the previously described schemes achieved for a codeword composed of two sub-frames, the first one being twice longer than the other. The first sub-frame only contains information bits. This structure is presented in Fig. 3.5.

When the relay correctly decodes the message after receiving the first sub-frame, and uses the Monostream scheme, the resulting fading channel is $\mathcal{B}(K, \frac{K}{2})$, and the resulting long-term SNR channel is $\mathcal{M}((1, 2), (K, \frac{K}{2}))$. Consequently, neither the full macro diversity nor the full micro

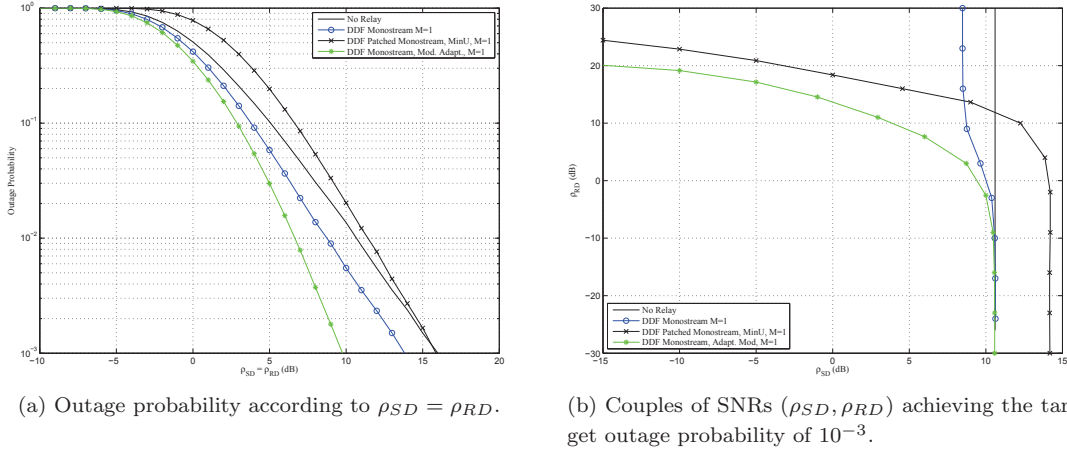


Figure 3.6: Performance of the Monostream DDF, the Patched Monostream DDF and the Monostream with modulation adaptation. $N_{rx} = 2$, $m_s = 2$.

diversity are achievable which is illustrated by the vertical asymptote in Fig. 3.6b and the outage probability slope equal to $N_{rx}=2$ in Fig. 3.6a.

Using the Patched Monostream scheme, the relay combines half symbols from the first sub-frame and all the symbols sent by the source during the second sub-frame to transmit 16QAM symbols. The resulting fading channel is $\mathcal{B}(\frac{K}{2}, K)$, and the resulting long-term SNR channel is $\mathcal{M}((1, 2), (\frac{K}{2}, K))$. Thus, full micro diversity is not achievable using the Patching technique, which is illustrated by the slope of the outage probability curve on Fig. 3.6a still equal to $N_{rx}=2$.

However, full macro diversity becomes achievable using the Patching technique, which is represented by the horizontal asymptote on Fig. 3.6b when ρ_{SD} tends toward $-\infty$ dB. This macro diversity gain is obtained at the price of an increased data rate, and a coding gain loss which can be observed on this Figure for very low values of ρ_{RD} when ρ_{SD} is around 15 dB. Indeed, without Patching, a minimal $\rho_{SD} = 10.5$ dB is needed to achieve the target outage probability whereas using the Patched Monostream, this value is equal to 14 dB. This particular codeword segmentation is a good example to understand that the Patched Monostream DDF primary effect is only to increase the achievable macro diversity order (due to the nature of the resulting channels).

However, relaxing the relay-unaware source constrain, the modulation adaptation scheme can be used. Consequently, during the second phase of the DDF protocol, both the source and the relay transmit 16QAM symbols which leads to a $\mathcal{B}(K, K)$ fading channel, and a $\mathcal{M}((1, 2), (K, K))$ long-term SNR channel, i.e. both full macro and full micro diversities are achievable. This is illustrated on Fig. 3.6a by the slope of $2N_{rx}$, and by the horizontal asymptote for low ρ_{SD} values on Fig. 3.6b. Moreover, there is no coding gain loss using this scheme as the data rate is similar for the Monostream DDF protocol and the DDF with adaptation of modulation.

We now consider the same codeword structure as described in Section 2.6 and presented in Fig. 3.7: the frame is divided into 5 sub-frames, the first one being 3 times longer than the other. And the considered coding rate at the end of the first sub-frame is equal to one.

The couples of SNR achieving the target outage performance of 10^{-3} are presented in Fig. 3.8 for the Monostream DDF, the Patched Monostream DDF with minimal use, and medium use, the

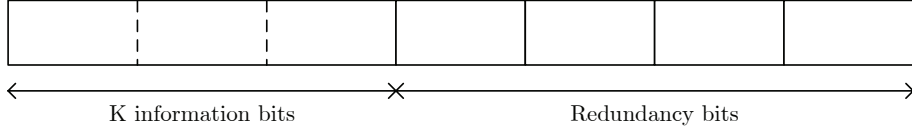


Figure 3.7: Codeword composed of 5 sub-frames, the first one being three time longer than the others and containing only information bits.

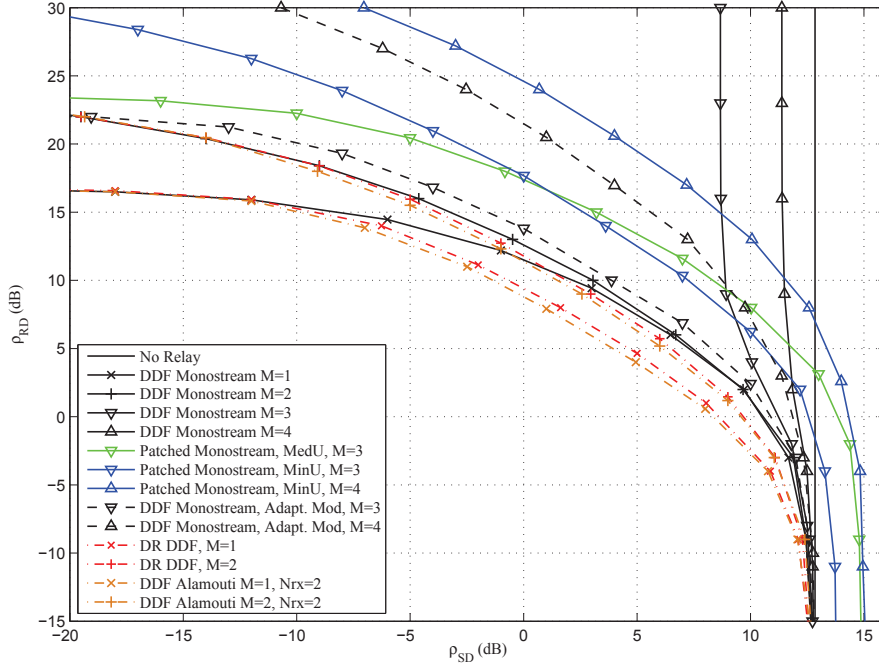


Figure 3.8: Couples of SNR (ρ_{SD}, ρ_{RD}) achieving the target outage probability of 10^{-3} according to the instant of correct decoding at the relay for the Monostream DDF, the Patched Monostream DDF with minimal use and medium use, the Monostream with adapted modulation. $N_{rx} = 2$, $R_{c1} = 1$.

Monostream with modulation adaptation according to distinct instants of correct decoding at the relay.

For $M \in \{1, 2\}$, all schemes achieve the same macro diversity order than the Monostream DDF which is explained by the previous analysis of their equivalent fading channels. We compare the coding gain of the Monostream DDF, the DR DDF and the DA DDF for $\rho_{SD} = \rho_{RD}$. The worst performance is achieved using the Monostream DDF scheme. The DR DDF performs a bit better: its coding gain ζ_{DR} is superior to the coding gain of the Monostream DDF ζ_M . The best performance is achieved using the DA DDF protocol whose coding gain is higher than ζ_{DR} . This confirms the analytical derivation and comparison of Section 3.2.3.

For $M \in \{3, 4\}$, we observe that the Patched DDF and the DDF with modulation adaptation achieve a full macro diversity order. More particularly, when $M = 3$, we observe the performance gain resulting from the Patched Monostream with MinU when compared to the Patched Monostream with MedU: Indeed, by using the Patched Monostream with medium use, the relay transmits 16QAM symbols during the last 2 sub-frames of the codeword resulting in an increased data rate

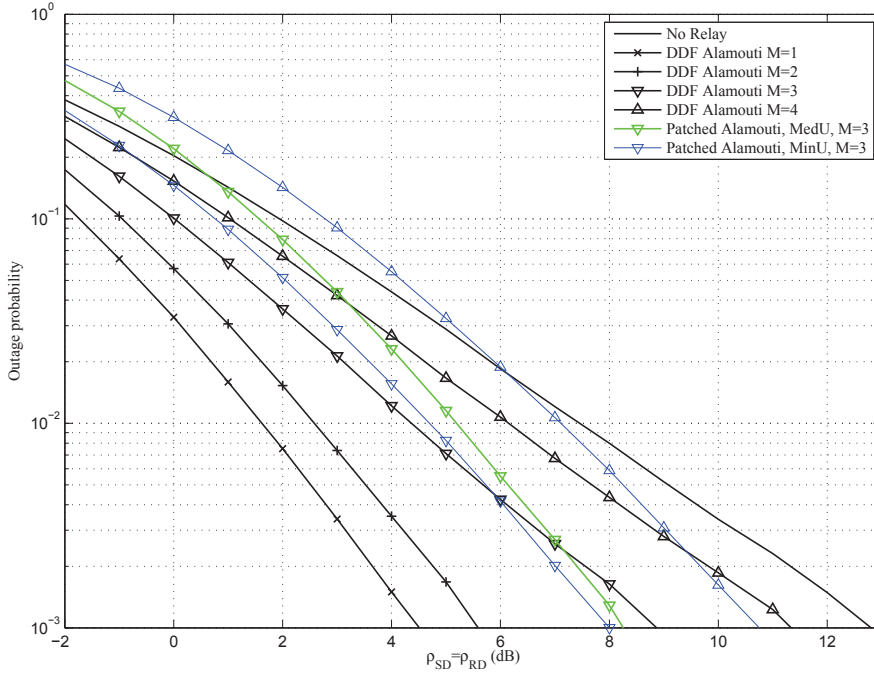


Figure 3.9: Outage probability of distinct DDF protocol using the Alamouti relaying scheme.

equal to $K/5$ bpcu (loss of 2.5dB for low ρ_{RD} values). This strategy generates an equivalent long term SNR channel $\mathcal{M}((1, 2), (K, \frac{4K}{3}))$. But, by using the Patched Monostream with minimal use, the relay transmits 16QAM symbols only during the 4-th subframe, i.e. twice shorter than with the Patching technique with medium use, leading to an equivalent long term SNR channel $\mathcal{M}((1, 2), (\frac{4K}{3}, K))$ and resulting in an increased data rate equal to $K/6$ bpcu (loss of 1.25dB for low ρ_{RD} values). When $M = 4$, there is no difference between the two strategies as both require the relay to transmit 64QAM symbols during the whole last sub-frame leading to the same data rate, the same coding gain loss and the same SNR loss on the relay-destination link.

These examples illustrate the effect of the Patching techniques over the achievable macro diversity behavior.

We now consider the outage performance, of distinct Distributed Alamouti schemes (the DA DDF, the Patched DA DDF with MedU, the Patched DA DDF with MinU) according to the instant of correct decoding at the relay to confirm their micro diversity behaviors.

In Fig. 3.9 are presented the outage probability of these relaying schemes according to $\rho_{SD} = \rho_{RD}$ for several instants of correct decoding at the relay. When $M \in \{1, 2\}$, all schemes achieve the same performance as they all lead to the same transmission, consequently, we only presents the DA DDF performance which achieve full micro diversity: the slope are equal to $-2N_{rx}$. The Patching technique increases the micro diversity order for $M \in \{3, 4\}$. More particularly, for $M = 3$, we observe 0.5dB coding gain loss of the Patched Alamouti with medium use, compared to the Patched Alamouti with minimal use.

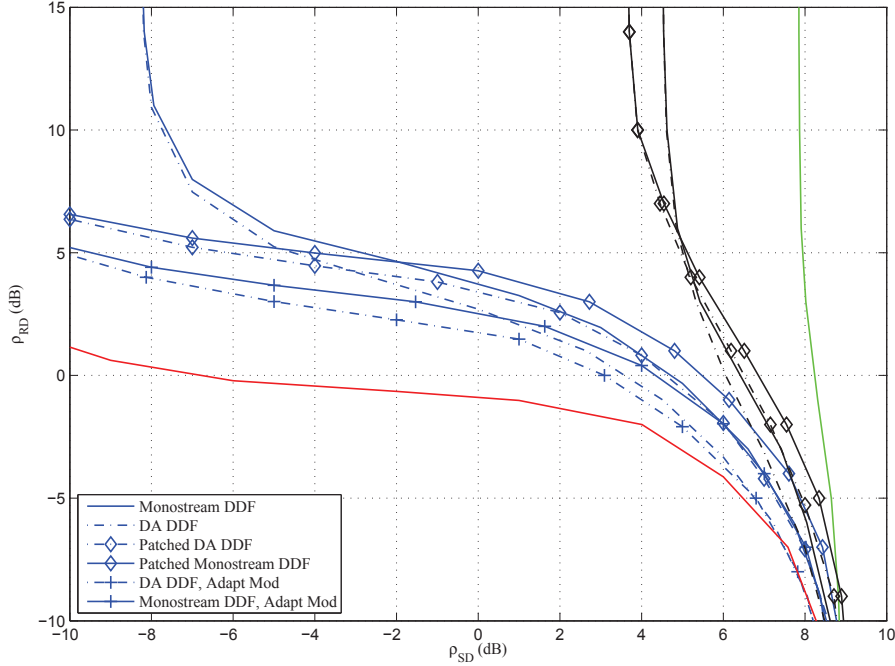


Figure 3.10: Couples (ρ_{SD}, ρ_{RD}) achieving an outage probability of 10^{-3} for several ρ_{SR} . The green curves represents $\rho_{SR} = -8\text{dB}$, the black ones $\rho_{SR} = -6\text{dB}$, the blues ones $\rho_{SR} = -5\text{dB}$ and the purple one represents $\rho_{SR} = -3\text{dB}$.

b) Averaged performance for fixed ρ_{SR} .

In Fig. 3.10 are presented the couples (ρ_{SD}, ρ_{RD}) achieving an outage probability of 10^{-3} for several ρ_{SR} , the green curves represents $\rho_{SR} = -8\text{dB}$, the black ones $\rho_{SR} = -6\text{dB}$, the blue ones $\rho_{SR} = -5\text{dB}$ and the purple one represents $\rho_{SR} = -3\text{dB}$, and several relaying schemes : Monostream DDF, DA DDF, Patched Monostream DDF, Patched DA DDF, and schemes with adaptation of modulation. We observe that, for ρ_{SR} lower than -4dB , a minimal value ρ_{SD} superior to -10dB is required to achieve the target outage probability using the Monostream DDF protocol. For ρ_{SR} values higher or equal to -3dB , this minimal value is much lower than -30dB thus, the Monostream DDF protocol reaches a full macro diversity behavior for these ranges of SNRs. The Patching technique and the DDF with Adaptation of modulation enable to consider lower ρ_{SR} values to observe this full macro diversity behavior: this gain is mainly observed for $\rho_{SR} = -5\text{dB}$. Moreover, whatever the achieved macro diversity order, the Distributed Alamouti relaying scheme outperforms the Monostream relaying scheme, which is justified by its higher coding gain.

3.4.2 Spectral Efficiency

For the closed loop transmission mode, we consider a transmission using HARQ and slow link adaptation: the spectral efficiency is maximized over the available coding rates (0.5, 0.6, 0.7, 0.8, 0.9 or 1 at the end of the first sub-frame) The considered codeword is composed of maximum 3 sub-frames, the first one being 4 time longer than the others. The source transmits QPSK symbols, the destination carries 2 reception antennas and $SNR_{SR} = 10\text{dB}$.

In Fig. 3.11, the couples of SNR_{SD} and SNR_{RD} achieving distinct target values of spectral

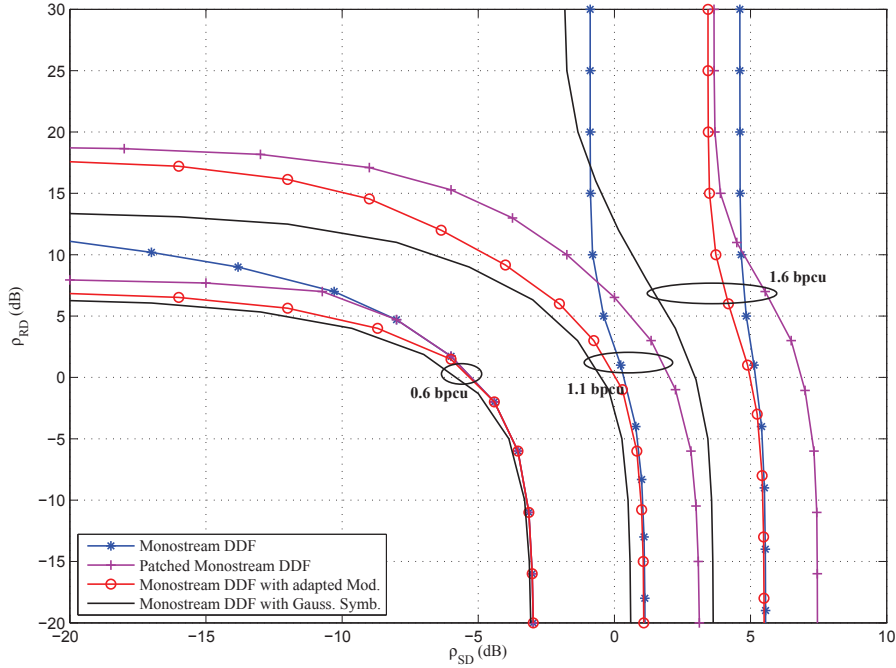


Figure 3.11: Couples (ρ_{SD}, ρ_{RD}) achieving distinct target spectral efficiencies for a $\rho_{SR} = 10dB$, and several Monostream schemes.

efficiency (0.6, 1.1 and 1.6 bpcu) are plotted for the Monostream DDF, the Patched Monostream DDF with MinU, the Monostream DDF with adapted modulation and the performance achieved using Monostream DDF with a Gaussian symbol alphabet. The performance achieved with a Gaussian symbol alphabet are the best performance achievable using Monostream scheme. For low ρ_{SD} , the Patched Monostream DDF protocol enables to fill the gap between the performance achieved using Monostream DDF and the best achievable performance. But for low ρ_{RD} , performance using Monostream DDF are better as the Patching technique introduce a coding gain loss due to the generation of higher modulation. A selection of the best scheme can be done according to the observed SNRs, and a slow link adaptation can be done on the coding rate and on the relaying scheme. The performance achieved with Monostream DDF with adapted modulation enables to fill the gap between Patched Monostream DDF and Monostream DDF with Gaussian symbol alphabet. Consequently, if signalling can be afford, as for the downlink of a cellular transmission, the performance are maximized using Monostream DDF with adapted modulation. If signalling between source and relay is costly, as for the uplink of a cellular transmission, the performance are maximized using Patched Monostream DDF.

Note that because HARQ is used in these different figures, the maximal achievable spectral efficiency never can be achieved through the relay-destination link only. Indeed, the maximal spectral efficiency requires the destination to correctly decode the message after receiving the first sub-frame which can not be transmitted by a causal relay.

3.4.3 Transmission strategies for practical systems

Knowing these results, in a practical transmission system, according to the deployment and the considered situation, distinct strategies arise:

- Considering an ad hoc deployment and an open-loop transmission, every nodes in the network are unaware of the relay's presence. In this case, there is no possible estimation of both source-destination and relay-destination links separately, and no possible patching step at the destination. The only way of improving performance when compared to the Monostream DDF is to use the DR DDF only providing coding gain. None of the proposed techniques enables to improve the achievable diversity orders in this particular case.
- However, in the downlink of a cellular system, the source, equivalently the base station, can be aware of the relay's presence. Consequently, the relay-unaware source constrain can be relaxed. For backward compatibility reasons, the decoding complexity must be kept low at the destination. Then, in order to maximize the performance, the DA DDF with adaptation of modulation must be used if the destination can estimate both channels coefficients, but if it is not possible, the Monostream DDF with adaptation of modulation must be used.
- In the uplink, the source, i.e. the user equipment, cannot be aware of the relay's presence for backward compatibility reasons. In this case, to maximize the performance, if a high computation capacity is available, the SDM DDF enables to improve the performance. However, if low complexity decoding is required, the Patching technique with minimal use must be used guaranteeing a minimal coding gain loss. Moreover, in this case the Alamouti relaying scheme can be used (and performs better than the Monostream relaying scheme) because the destination can estimate both links separately. This provides a marginal gain as it occurs for similar SNR values over the source-destination and relay-destination links. Indeed, in a practical system this SNR configuration appears with low probability.
- For a closed loop transmission, the performance in terms of macro diversity mainly depends on the codeword structure. In this case, an optimization of the codeword structure must be considered before any transmission scheme. However, if this optimization is not possible or insufficient, it is of interest to consider the Patching with Maximal Use, or Adaption of modulation, or SDM-DDF adapted so that the relay transmits K bits in a minimal number of time slot as soon as it correctly decodes the message.

Conclusion

In this chapter, we propose the Patching technique to improve the achievable macro and micro diversity orders when compared to the Monostream DDF and the DA DDF still satisfying the relay-unaware source constraint and the low complexity decoding at the destination. We also prove that the DR DDF provides coding gain when compared to the Monostream DDF, and does not improve the achievable diversity orders.

Relaxing these constrains, the achievable diversity order can be increased by using the SDM DDF or the DDF with adaptation of modulation. From these results, regarding the considered deployment and constrains, we propose several strategies in order to maximize the performance when compared to the case without relay.

In order to minimize the coding gain loss induced by the Patching technique, it is of interest to study the combination of the Patched Monostream DDF and the DR DDF.

Moreover, the highest gains offered by a maximal macro diversity order are observed for low values of ρ_{SD} and high values ρ_{RD} , i.e., the highest gains are observed for a user equipments far from the source and close to the relay. This remark reveals the deployment that should be used to take benefit from the relay in a cellular system: they might be placed at the cell edge but it would lead to an increased interference over neighboring cells. It is of interest to design a DDF protocol dealing with this interference still providing gains for the cell edge users.

Chapter 4

Patching technique for the Interference Channel with Relay

Introduction

In the previous chapters, we describe the introduction of a relay in a wireless network to improve the cell coverage or the throughput by a basic channel called the relay channel.

However, relays can also be deployed in order to deal with the interference suffered in some wireless systems. The interference phenomenon appears when several nodes use the same physical resource to transmit distinct messages. For instance, there is interference in cellular systems with reuse 1 of the bandwidth, i.e., systems in which each cell use the same bandwidth as the surrounding cells. In these systems, interference causes throughput limitations at the cell edge where the suffered interference power is similar to the useful signal power. This channel is modeled by the IRC presented in Fig. 4.1, where the relay is shared by all source/destination pairs.

In this chapter, we still consider that all sources are relay-unaware in order to keep on designing backward compatible schemes. Moreover, we assume that there is no possible cooperation between sources, no cooperation between destinations and that the destinations only try to decode their intended message, the suffered interference being considered as noise. This last assumption is justified by security reason.

The main challenge of a relaying strategy designed for the IRC is to find the right balance between improving useful signal and mitigating interference.

In the following, we first make a state of the art review of the known results on the IRC in Section 4.1. We particularly focus on a precoding technique designed to maximize the performance of the worst source/destination pair. In Section 4.2, after introducing the DDF protocol for the IRC, we adapt the precoding technique to this relaying protocol. Finally, in Section 4.3, the Patching technique proposed in the previous chapter to increase the achievable diversity order, is adapted in order to improve the performance of the designed precoded DDF protocol.

4.1 Dealing with interference

In the literature, there are two main study axes concerning the IRC: On one hand, some of the articles deal with the derivation of bounds on the achievable rate regions, the derivation of the

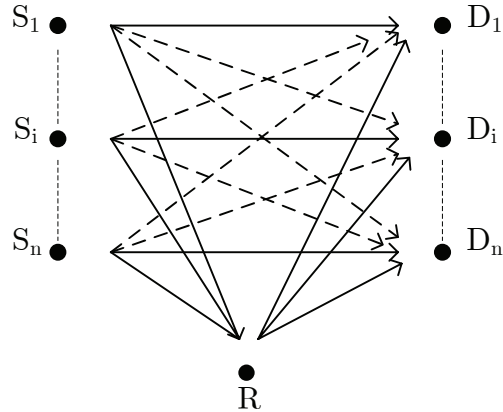


Figure 4.1: The Interference channel with relay.

achievable degrees of freedom, and the code design to reach the maximal rates. On the other hand, some papers deal with relaying strategies for the IRC (signal relaying or interference forwarding, combination of both). Some of these strategies consists in precoding the symbols sent by the relay. Most of these articles consider that the sources are aware of the relay's presence, except [60] on which will particularly focus.

Interference mitigation without precoding at the relay. We first present some interference mitigation techniques not using a precoder at the relay.

In [61], the authors consider a system containing a non-causal relay used to deal with the suffered interference at the destinations. The relay combines several interference management techniques (dirty paper coding as the relay is non-causal, and generalized beamforming) and time division. The authors then derive the achievable rate region using this scheme which is then compared to a time division only scheme, and a scheme only exploiting beamforming.

After recalling some known bounds on the achievable rate region of the IRC, the authors of [62] also describe upper and lower bounds on the achievable rate region of an IRC for a full duplex causal relay using the detect and forward relaying scheme.

In [63], the authors derive the achievable degrees of freedom (pre log factor of the sum capacity) of an IRC with a MIMO relay for distinct power allocations at the sources and the relay. The study reveals that a maximal degree of freedom is achievable when the relay has abundant power budget. However, this study, based on the sum rate, does not take into account fairness criteria between users.

In [64], the authors describe several relaying schemes for distinct uses of resources at the relay when the sources are aware of the relay's presence. We particularly focus on the in band transmission/reception relay corresponding to our study case. The main feature is the use of the Han and Kobayashi scheme by the sources: they both split their messages into a common and a private part. The relay decodes the four resulting messages, and forward them to the destinations using beamforming. At the destinations, the common messages are decoded and removed from the received signal in order to decrease the suffered interference level. The intended private message is then decoded considering the un-removed interference as noise.

In [65], the authors propose an interference forwarding scheme where the relay aims at improving

the performance of a subset of destinations by making their interference strong enough so that it can efficiently be removed. This feature offers the interesting property that if the relay cannot receive the useful signal intended at a destination, but receives the interfering signal, it still can help this destination. The rate regions then achieved by this scheme is studied and compared to the Han-Kobayashi transmission scheme.

Precoding for interference management We now focus on strategies based on precoding at the relay to deal with the suffered interference in an IRC.

In [66], the authors define several relaying schemes in order to deal with interference in a cellular system with several relays types. We particularly focus on the one-way shared relay, which uses an orthogonal DF scheme. The relay first decodes the different messages using a ZF receiver in order to separate the distinct data streams. Then, it broadcasts these messages by using a precoder designed to cancel, i.e., zero-force, the interfering channels to the mobiles. This precoder design requires that the perfectly knows the channel coefficients matrix of the relay/destination links and the source/destination link. Moreover, this relay must have an infinite power budget in order to perfectly zero force these channel.

In [60], the author propose a precoder design for an IRC in which the destinations consider the interference as noise and do not look for decoding the interferers' messages. In this study, the relay non causally knows a subset of the messages and designs the precoder to maximize a minimal figure of merit (capacity with Gaussian alphabet, mutual information with finite symbol alphabet, SINR under MMSE filtering) achieved between all source/destination pairs. This precoder is designed for any number of source/destination pairs, any number of antennas at the nodes, and for several CSI configurations. This precoder design is different from existing precoders mostly derived for AF channels [67][68] or for a joint-source/relay precoding (e.g., [69]), as we assume relay-unaware sources.

As the work of [60] is particularly relevant for our study, we here recall the distinct steps of the precoder design for the capacity metric: maximizing the minimal capacity of the links suffering interference under the constrain of a limited power budget at the relay. The definition of this optimization problem has been done in order to guarantee fairness between users: it guarantees that all source/destination links are alive even if it would be benefic to turn off some of them in order to maximize the sum capacity.

The considered IRC is composed of n source/destination pairs. \mathbf{H}_m is the matrix of fading coefficients between all the sources and the m -th destination, and \mathbf{F}_m is the matrix of fading coefficients between the relay and the m -th destination. The destinations estimate the channel coefficients and forward it to the relay. The relay non-causally knows $k - 1$ messages out of the n (for instance messages of the sources S_1 to S_{k-1}), a linear precoder \mathbf{P}_k of size $N_t \times n$ is applied at the relay in order to improve the capacity obtained at each destination. This precoder is recomputed if the number of known messages varies. When the relay knows k messages, the m -th destination receives the vector $\mathbf{y}_{m,i|k}$ during the i -th time-slot:

$$\mathbf{y}_{m,i|k} = \mathbf{M}_m(\mathbf{P}_k)\mathbf{s}_i + \mathbf{w}_{m,i} \quad (4.1)$$

where

$$\mathbf{M}_m(\mathbf{P}_k) = \mathbf{H}_m + \mathbf{F}_m\mathbf{P}_k\mathbf{\Delta}_k \quad (4.2)$$

and $\mathbf{s}_i = [s_{1,i}, \dots, s_{n,i}]^t$ and $\mathbf{w}_{m,i}$ is the noise vector. We note $\mathbf{\Delta}_k$ as a $n \times n$ matrix whom non-null

entries are the first $k-1$ diagonal coefficients, equal to one. As a result, the $N_t \times n$ precoder matrix \mathbf{P}_k is only applied to the $k-1$ first symbols.

We here recall the derivation of the precoder matrix \mathbf{P}_k according to the channel capacity metrics. We define the capacity at the m -th destination when the relay knows $k-1$ messages as

$$C_{m,k}(\mathbf{P}_k) = \log_2 |\mathbf{M}_m(\mathbf{P}_k)\mathbf{M}_m(\mathbf{P}_k)^\dagger + 2N_0\mathbf{I}| - \log_2 |\mathbf{M}_m(\mathbf{P}_k)\bar{\mathbf{D}}_m\mathbf{M}_m(\mathbf{P}_k)^\dagger + 2N_0\mathbf{I}| \quad (4.3)$$

where \mathbf{D}_m is a $n \times n$ matrix with a single non-null entry at the m -th position on the diagonal, and $\bar{\mathbf{D}}_m = \mathbf{I} - \mathbf{D}_m$. The derivation of $C_{m,k}(\mathbf{P}_k)$ leads to Eq. (4.3), which could be seen as the difference between the capacity of the MIMO scheme formed by all sources and the relay transmitting to the m -th destination and the capacity of the MIMO scheme formed by all interferers (all sources except S_m) and the relay transmitting to the m -th destination. We define $C_k(\mathbf{P}_k)$ as the generalized mean of the capacities $C_{m,k}(\mathbf{P}_k)$

$$C_k(\mathbf{P}_k) = \left(\frac{1}{n} \sum_{m=1}^n C_{m,k}(\mathbf{P}_k)^p \right)^{1/p} \quad (4.4)$$

where p is the parameter of the generalized mean.

As fairness is needed between users the minimal capacity is maximized by considering $p \rightarrow -\infty$, or p negative and sufficiently low.

One can optimize $C_k(\mathbf{P}_k)$ under a total maximal power constraint at the relay $h(\mathbf{P}_k) = \text{Tr}(\mathbf{P}_k \Delta_k \mathbf{P}_k^\dagger) - 1 \leq 0$, which leads to the following Lagrange multipliers system

$$\frac{\partial C_k(\mathbf{P}_k)}{\partial \mathbf{P}_k^*} = \lambda \frac{\partial h(\mathbf{P}_k)}{\partial \mathbf{P}_k^*} \quad \text{and} \quad h(\mathbf{P}_k) \leq 0 \quad (4.5)$$

where

$$\frac{\partial C_k(\mathbf{P}_k)}{\partial \mathbf{P}_k^*} = \frac{C_k(\mathbf{P}_k)^{1-p}}{n} \sum_{m=1}^n C_{m,k}(\mathbf{P}_k)^{p-1} \frac{\partial C_{m,k}(\mathbf{P}_k)}{\partial \mathbf{P}_k^*} \quad (4.6)$$

and which leads, after derivation using the matrix differentiation tools [70] to

$$\begin{aligned} \frac{\partial C_{m,k}(\mathbf{P}_k)}{\partial \mathbf{P}_k^*} = & \frac{1}{\ln(2)} \mathbf{F}_k^\dagger \left[(\mathbf{M}_m(\mathbf{P}_k)\mathbf{M}_m(\mathbf{P}_k)^\dagger + 2N_0\mathbf{I})^{-1} \mathbf{M}_m(\mathbf{P}_k) \right. \\ & \left. - (\mathbf{M}_m(\mathbf{P}_k)\bar{\mathbf{D}}_m\mathbf{M}_m(\mathbf{P}_k)^\dagger + 2N_0\mathbf{I})^{-1} \mathbf{M}_m(\mathbf{P}_k)\bar{\mathbf{D}}_m \right] \Delta_k \end{aligned}$$

No closed form expression can be derived from (4.5), a gradient descent iteratively optimizes the precoder \mathbf{P}_k instead:

$$\mathbf{P}_k \leftarrow \left(\mathbf{P}_k + \mu \frac{\partial C_k(\mathbf{P}_k)}{\partial \mathbf{P}_k^*} \right) / \min \left(\text{Tr} \left(\Delta_k^\dagger \mathbf{P}_k^\dagger \mathbf{P}_k \Delta_k \right), 1 \right) \quad (4.7)$$

where μ is the gradient descent parameter, and the denominator allows for projecting the estimated precoder matrix on the set of solutions satisfying the constraint $h(\mathbf{P}_k)$. It is preferable to choose a moderately high value for the generalized mean parameter such as $p = -5$ in order to find a good trade-off between the approximation of the min function and the good convergence of the system.

We recall the performance achieved by this precoder considering a system comprising two source/destination pairs ($n = 2$) where the wireless links are symmetric, i.e., the long term SNRs and SINRs of the two pairs without relay are equal, and we illustrate the performance achieved by the precoder design of [60]. By assuming that the m -th destination estimates $\mathbf{M}_m(\mathbf{P}_k)$ (full CSI at the receiver) and does not jointly decode the other source symbols for complexity reasons,

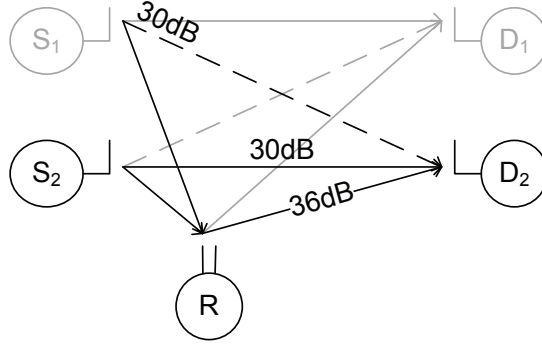


Figure 4.2: The considered 2-pair IRC.

the mutual information $\chi_{m||k}$ when the relay knows k messages out of the n , with a Gaussian approximation of the interference plus noise signal is

$$\chi_{m||k} = E_{s_m, \mathbf{n}} \left[\log_2 \left(\frac{E_{s_{\forall m' \neq m}} [p(\mathbf{y}_{m||k} | \mathbf{s})]}{E_{s'} [p(\mathbf{y}_{m||k} | \mathbf{s}')] } \right) \right] \quad (4.8)$$

where $p(\mathbf{y}_{m||k} | \mathbf{s}) \propto e^{-\|\mathbf{\Lambda}^{-1}(\mathbf{y}_{m||k} - \mathbf{M}_m(\mathbf{P}_k)\mathbf{D}_m\mathbf{s})\|^2}$ and $\mathbf{\Lambda}\mathbf{\Lambda}^\dagger = \mathbf{M}_m(\mathbf{P}_k)\bar{\mathbf{D}}_m\mathbf{M}_m(\mathbf{P}_k)^\dagger + 2N_0\mathbf{I}$.

We focus on the mutual information achieved by one of the two pairs in the system. The transmitting node of this pair is called source S , and the other transmitter is called interferer I . The nodes transmit QPSK symbols. We define as P_R/P_S the ratio of the average power received by the destination from the relay and from the source. We consider that the destination has a single receive antenna $N_r = 1$ and that the relay has two antennas $N_t = 2$. All these considered features are summed up in Fig. 4.2.

Fig. 4.3 illustrates the gain brought by the precoder optimization based on the capacity metric as previously presented. We consider that the relay knows the symbols sent from the source and interferer, and we focus on the improvement of the average QPSK discrete input mutual information observed during the phase in which the relay transmits signal from both sources. When no precoder is used, the relay transmits each symbol of each source from its two transmit antennas. We can observe that for high SINR values, when the interference becomes negligible with respect to the noise level, the relay without precoder introduces interference in the system which drastically degrades the discrete input mutual information. By using the full CSI knowledge at the relay in order to optimize the precoder, we see that the relay transmit power is efficiently used to remove the interference and boost the useful signal. It has to be noted that, since the precoder is not distributed among the sources and relay, the transmit beamforming or zero forcing approach do not show such high performance. When the SINR is close to zero, we see how the relay improves the performance by a factor up to 200%. The performance can be further improved by increasing the number of transmit antennas at the relay N_t .

In this section, after recalling some relaying techniques, we have presented the precoder optimization derived in [60] which is applied at a shared relay in order to reach fairness between the destinations. The relay transmit power is shared between useful signal boosting and interference reduction. The proposed optimization can be applied for any number of sources, transmit antennas at the relay and receive antennas at the destination. In the following, we illustrate how to combine the precoder optimization at the relay with a DDF relaying protocol.

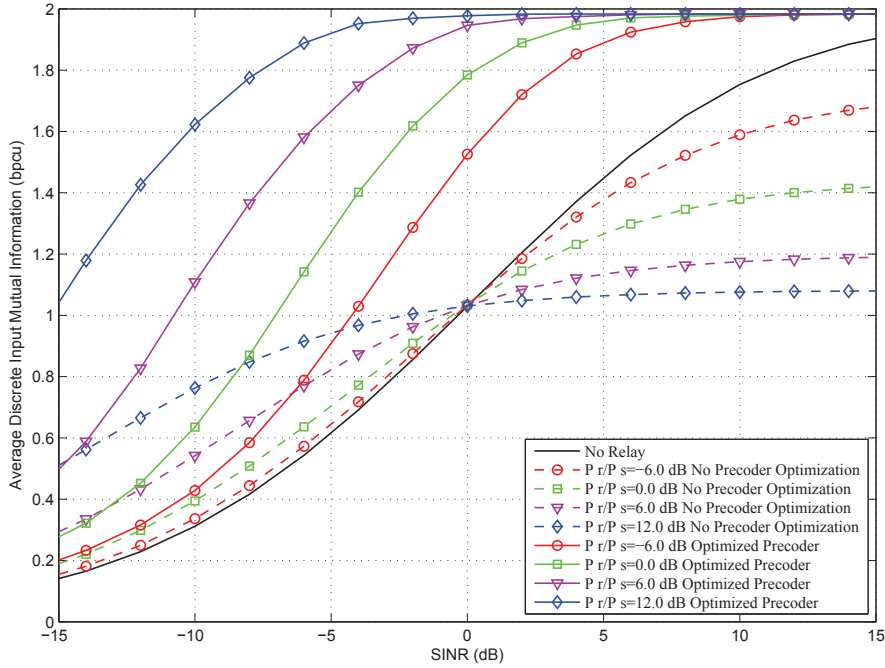


Figure 4.3: Impact of the precoder optimization on the average QSPK input mutual information between the source and destination according to the SINR observed at D , P_R/P_S , for $n = 2$, $N_r = 1$ and $N_t = 2$.

4.2 Precoding for the DDF protocol

In this section, we introduce the DDF protocol for the interference relay channel, which has not been done in the literature.

We first describe the effect resulting from this protocol on a transmission over an interference channel, secondly, we propose to use the previously described precoding technique to deal with interference even when the source are relay-unaware, and finally, we propose to use the Patching technique to improve the performance.

4.2.1 DDF protocol for the IRC

As previously described, independent messages are transmitted by all sources using the same physical resource, and each message is attended at a single destination. We denote n the number of source/destination pairs.

When the full-duplex relay uses the DDF protocol on this channel, it results a maximal phase number of $N + 1$. During the first phase, the relay listen and try to decode the messages. As soon as it correctly decodes a message, this is the beginning of a new phase in which it transmits data related to the correctly decoded messages and still listening to the others sources. Without loss of generality, we denote S_i the source transmitting the i -th message to be correctly decoded by the relay, this correct decoding corresponds to the beginning of the $i + 1$ -th phase. This decoding step can be done using a Minimum Mean Square Error (MMSE) receiver, or any successive interference cancellation method. If the relay does not succeed in correctly decoding one of the message, it remains silent till the transmission ends. Using the DDF protocol, as soon as the relay begins

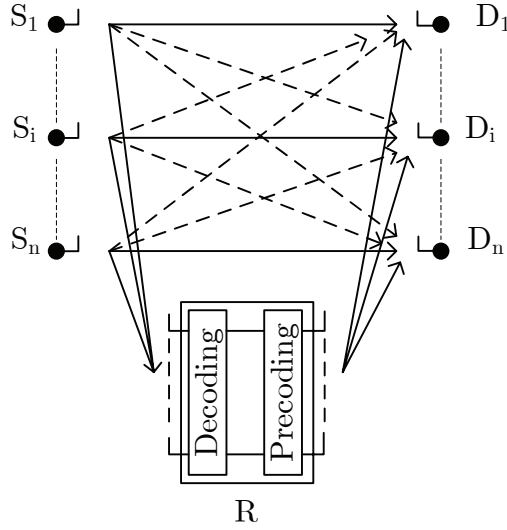


Figure 4.4: IRC with precoding at the relay.

to transmit data, it generates a twofold effect. First, when considering the phase $i + 1$, the relay increases the useful received power at the destinations 1 to i , but it also increases the received power of interfering signals. Thus, there is no possible gains resulting from this transmission, which is illustrated in Fig. 4.3 by the curves obtained without precoder.

For security reasons, the destinations only try to decode their intended message and consider the suffered interference as noise. As previously described for the relay channel, these transmissions can either be open-loop transmissions or closed-loop transmissions. We only assume that all source/destination pairs use the same transmission type.

We find of interest to apply the previously presented precoder optimization technique which can be applied to our DDF protocol dealing with interference by maximizing the minimal capacity among all source/destination pairs.

4.2.2 Precoding DDF for the IRC

In this section, we thus describe the combination of the DDF protocol and the previously reviewed precoding technique of [60].

In each DDF phase, the number of known messages at the relay varies, and it consequently assists distinct numbers of source/destination pairs. Thus, in each phase, the relay must use its power budget efficiently and it must compute a different precoder. This variation of the number of known messages through time is reflected by the variation of Δ_k : in phase k , the relay compute the precoder \mathbf{P}_k considering the channel model $\mathbf{M}_m(\mathbf{P}_k) = \mathbf{H}_m + \mathbf{F}_m \mathbf{P}_k \Delta_k$ where Δ_k is the a $n \times n$ matrix whom non-null entries are the first $k - 1$ diagonal coefficients, equal to one.

4.2.3 Adaptation to a half duplex relay

As explained in Chapter 1, the full duplex relay is an assumption leading to important difficulties for practical implementation. The here proposed DDF protocol for the IRC can be adapted if a half duplex relay is used.

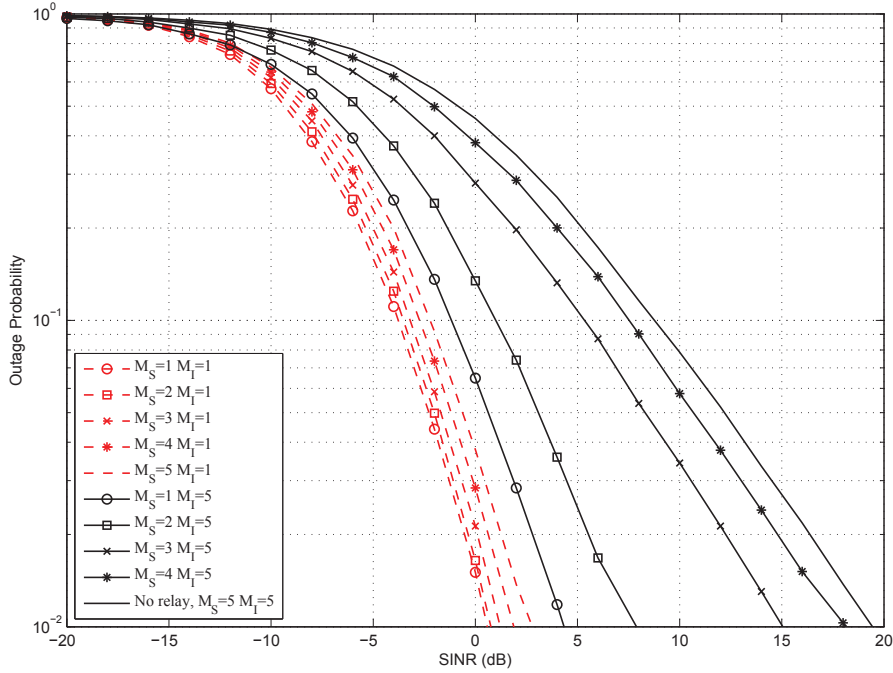


Figure 4.5: Average outage probability at D according to the SINR, $P_R/P_S = 6\text{dB}$, $N_r = 1$. The relay uses DDF protocol with optimized precoder.

The first idea is that the relay only begin to transmit after having correctly decoded all messages. However, this would lead to a situation where the relay is unused most of the transmission time.

Consequently, a second implementation for a half duplex relay would let the relay begin to transmit after having correctly decoded some of the messages and at least at a given frame fraction. For instance, the relay begins to transmit after receiving half the sub-frame.

4.2.4 Simulation results

We still consider the 2-pair IRC described in Fig. 4.2 where the full-duplex relay uses our precoded DDF protocol. Moreover, we consider a particular codeword segmentation, such as for HARQ with Incremental Redundancy (IR) OFDM systems, which restricts the possible instants of correct decoding to the set $\{\frac{3T}{7}, \frac{4T}{7}, \frac{5T}{7}, \frac{6T}{7}, T\}$, where T is the total number of time slots for a given codeword transmission. We denote M_S and M_I the index of the segment after which the relay correctly decodes the source message and the interferer message, respectively. Note that the case with no relay activation corresponds to $M_S = M_I = 5$. All the results are presented according to the SINR observed at D for a SNR between the source and destination of 30dB, for an open-loop transmission in Fig. 4.5, and for a closed-loop transmission in Fig. 4.6.

Outage probability In Fig. 4.5, we consider an open loop transmission whose performance is described by the outage probability. We assume that the first $\frac{3T}{7}$ time-slots only carry information bits. In Fig. 4.5, the averaged outage probability achieved for $M_I \in \{1, 5\}$ and $M_S \in \{1, 2, 3, 4, 5\}$ are presented. The relay uses the DDF protocol with the optimized precoder presented in Section ???. The performance obtained when the relay uses the DDF protocol outperforms the case without relay whatever the considered couples (M_S, M_I) . The sooner the relay correctly decodes the source

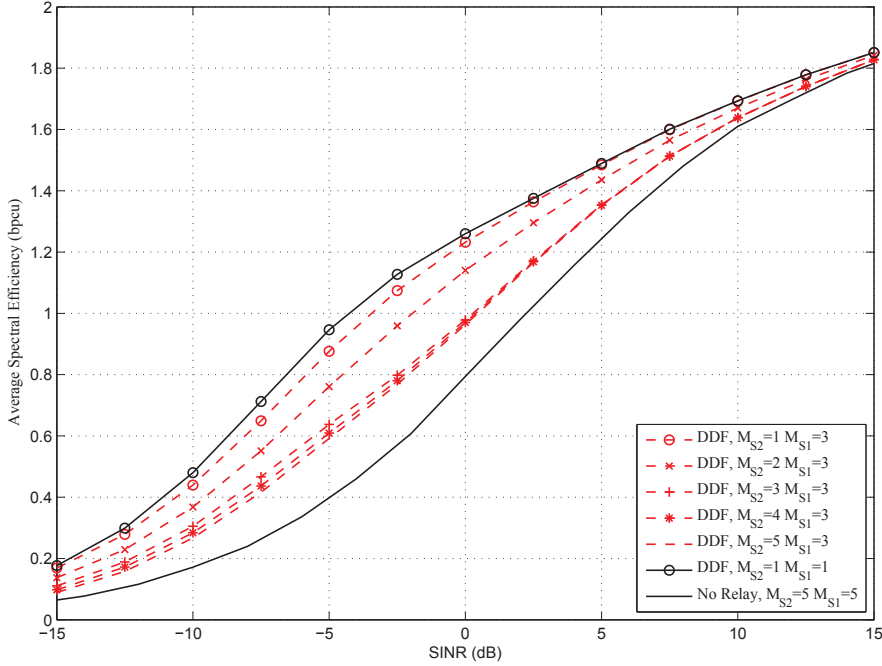


Figure 4.6: Average spectral efficiency at D maximized over the available coding rates, according to the SINR, $P_R/P_S = 6dB$, $N_r = 1$ for $(M_S, M_I) \in \{(1, 1), (5, 5)\}$ and all possible M_S for $M_I = 3$. The relay uses the DDF protocol with an optimized precoder.

message, the higher the performance, which is due to the power boosting by the relay. Furthermore, the sooner the instant of correct decoding of the interferer, the higher the performance, which is due to the interference reduction by the relay.

Spectral efficiency We consider a closed loop transmission in which the destination tries to decode the message after each frame segment, and transmits acknowledgment message when it correctly decodes the message. The figure of merit is the spectral efficiency in bit per channel use (bps/Hz). It is classically computed for the HARQ-IR systems by taking into account the events of correct decoding after each codeword segment. Moreover, the available coding rates at the end of the first $\frac{3T}{7}$ can vary from 0 to 1. Thus, slow link adaptation is realized, i.e. the coding rate is adapted according to the SINR to maximize the averaged spectral efficiency.

In Fig. 4.6, the cases $M_S = M_I = 1$ and $M_S = M_I = 5$ illustrate the best and worst achievable spectral efficiency for the DDF protocol. The case $M_I = 3$ presents the fact that when $M_S > M_I$ performance are quite similar. Indeed as the relay has already removed the suffered interference, it results that the destination correctly decodes the message very quickly. For SINR lower than 0dB, because of its power constraint, the relay cannot totally remove the interference, thus M_S influences the performance.

These simulation results reveal that the higher the number of precoded symbols and the higher the improvement of performance thanks to relaying.

4.3 Combining Patching and precoding

The Patching technique presented in the previous chapter was introduced in order to improve the achievable macro and micro diversity orders by increasing the number of bits experiencing the relay to destination link up to the number of information bits in the message.

Consequently, we introduce this Patching technique over the interference channel with a relay using the precoded DDF protocol in order to increase the number of precoded symbols.

We first describe the proposed Patching technique for the general IRC. Then, this Patching technique is described for a particular example (codeword segmentation and instants of correct decoding at the relay) over a 2-pair IRC. Finally, simulation results are given to illustrate the gains brought by this Patching technique for the precoded DDF.

4.3.1 Generalization to the n-pair case

In this chapter, the Patching technique combines symbols of different phases in order to increase the number of symbols virtually sent through the precoder.

For the sake of clarity, we present the simplest version of the Patching algorithm, where Patching is only applied on the symbols of Phase 1, experiencing and generating interference. We denote L_1 the number of time-slots in the first phase of the DDF protocol. At the beginning of a new transmission, a variable v storing the index of the last patched symbol of Phase 1 is initialized to zero. Then, the relay executes Algorithm 1 for each time slot i of each Phase k ($2 \leq k \leq n+1$), for each source $m \leq k-1$ and for a Patching order q .

Algorithm 1 Generation of m -th symbols $\tilde{s}_{m,k,i}$ to be precoded by the relay for the i -th time slot of Phase k .

- 1: $\tilde{s}_{m,k,i} \leftarrow 0$
 - 2: $j_{k,i} \leftarrow 1$
 - 3: **while** $v + j_{k,i} \leq L_1$ **and** $j_{k,i} < q$ **do**
 - 4: $\tilde{s}_{m,k,i} \leftarrow \tilde{s}_{m,k,i} + 2^{j_{k,i}-1} s_{m,1,v+j_{k,i}}$
 - 5: $j_{k,i} \leftarrow j_{k,i} + 1$
 - 6: **end while**
 - 7: $\tilde{s}_{m,k,i} \leftarrow a(j_{k,i})(\tilde{s}_{m,k,i} + 2^{j_{k,i}-1} s_{m,k,i})$
 - 8: $v \leftarrow v + j_{k,i}$
-

As a remark, as soon as all symbols from Phase 1 have been precoded, the system behaves as the precoded DDF protocol for IRC. The m -th destination receives

$$\mathbf{y}_{m,k,i} = \mathbf{H}_m \mathbf{s}_{k,i} + \mathbf{F}_m \mathbf{P}_k \mathbf{\Delta}_k \times (\tilde{s}_{1,k,i}, \dots, \tilde{s}_{k-1,k,i}, 0, \dots, 0)^t + \mathbf{w}_{k,i}$$

where $s_{m,k,i}$ is the symbol sent by the source S_m and $\mathbf{y}_{m,k,i}$ is the signal received by the destination D_m during the i -th time-slot of the Phase k . By knowing the instant of correct decoding at the relay, each destination m applies Algorithm 1 for combining the received vectors $\mathbf{y}_{m,k,i}$ instead of the symbols $s_{m,k,i}$, which leads to the following equivalent channel model:

$$\tilde{\mathbf{y}}_{m,k,i} = (\mathbf{H}_m + \mathbf{F}_m \mathbf{P}_k \mathbf{\Delta}_k a(j_{k,i}) 2^{j_{k,i}-1}) \tilde{\mathbf{s}}_{k,i} + \mathbf{w}'_{k,i}$$

where $\tilde{\mathbf{s}}_{k,i} = (\tilde{s}_{1,k,i}, \dots, \tilde{s}_{n,k,i})^t$, i.e. the symbol combination described by the Algorithm 1 is realized for all sources symbols, $\mathbf{w}'_{k,i}$ is the resulting complex Gaussian noise, and $a(q) = \sqrt{\frac{3}{4^q - 1}}$.

During the i -th time slot of Phase k , the symbols after patching are $4^{j_{k,i}}$ -QAM symbols sent on the equivalent channel with power boosting and interference reduction thanks to the precoding of the symbols decoded at the relay, i.e. from sources 1 to $k - 1$. If Phase 1 is longer than the cumulated length of the other phases, unprecoded symbols remain. When all sources are decoded at the same time, if Phase 1 is shorter than the last Phase, all symbols are precoded, some of them being patched, the other being transmitted through the relay-destination link using the precoded DDF protocol. An adaptation of this protocol to half-duplex relays implies that the relay waits for all messages to be correctly decoded before switching into the transmission mode.

4.3.2 Two interfering pairs

Let's consider a 2-pair IRC, where the frames transmitted by both sources are composed of 5 QPSK symbols. We assume that the relay correctly decodes the message of S_1 after receiving the second symbol, and that it correctly decodes the message of S_2 after receiving the third symbol. This means that the first phase contains 2 time-slots, the second phase contains one time-slot and the last phase contains 2 time-slots.

The relay transmits using a DDF protocol with precoder optimization and Patching. We define the Patching order $q = 2$, which means that the relay generates 16-QAM symbols. The variable v (see Algorithm 1) is set to zero at the beginning of the transmission.

During the second phase of the DDF protocol with Patching, the relay generates the symbol $\tilde{s}_{1,2,1} = a(2)(2s_{1,2,1} + s_{1,1,1})$ which is precoded by \mathbf{P}_2 . The variable v is now equal to 2. Both destinations realize the combination of received signals:

$$\begin{aligned} \tilde{\mathbf{y}}_{m,2,1} &= a(2)(2\mathbf{y}_{m,2,1} + \mathbf{y}_{m,1,1}) \\ &= \mathbf{H}_m \begin{bmatrix} a(2)(2s_{1,2,1} + s_{1,1,1}) \\ a(2)(2s_{2,2,1} + s_{2,1,1}) \end{bmatrix} + 2a(2)\mathbf{F}_m\mathbf{P}_2 \begin{bmatrix} \tilde{s}_{1,2,1} \\ 0 \end{bmatrix} + \mathbf{w} \\ &= \mathbf{H}_m \begin{bmatrix} \tilde{s}_{1,2,1} \\ \tilde{s}_{2,2,1} \end{bmatrix} + 2a(2)\mathbf{F}_m\mathbf{P}_2 \begin{bmatrix} \tilde{s}_{1,2,1} \\ 0 \end{bmatrix} + \mathbf{w} \end{aligned}$$

with $m = 1, 2$, and where the resulting noise \mathbf{n} is a complex white Gaussian noise of zero mean and variance $2N_0$. Consequently, during this time slot, thanks to the Patching technique, a 16-QAM symbol is precoded by \mathbf{P}_2 with a SNR loss coming from the $2a(2)$ coefficient, whereas without Patching, only a QPSK symbol would have been precoded by \mathbf{P}_2 .

During the first time-slot of the third phase of the DDF protocol with Patching, as the condition $v \leq L_1 = 2$ is satisfied, the relay generates the symbols $\tilde{s}_{m,3,1} = a(2)(2s_{m,3,1} + s_{m,1,2})$, with $m = 1$ and $m = 2$. These symbols are then precoded by \mathbf{P}_3 , and the variable v is now equal to 4. Both destinations realize the combination of received signals:

$$\begin{aligned} \tilde{\mathbf{y}}_{m,3,1} &= a(2)(2\mathbf{y}_{m,3,1} + \mathbf{y}_{m,1,2}) \\ &= \mathbf{H}_m \begin{bmatrix} \tilde{s}_{1,3,1} \\ \tilde{s}_{2,3,1} \end{bmatrix} + 2a(2)\mathbf{F}_m\mathbf{P}_2 \begin{bmatrix} \tilde{s}_{1,3,1} \\ \tilde{s}_{2,3,1} \end{bmatrix} + \mathbf{w} \end{aligned}$$

with $m = 1, 2$, and where the resulting noise \mathbf{w} is a complex white Gaussian noise of zero mean and variance $2N_0$. Consequently, during this time slot, thanks to the Patching technique, two 16-QAM symbols are precoded by \mathbf{P}_3 with a SNR loss coming from the $2a(2)$ coefficient, whereas without Patching, only two QPSK symbols would have been precoded by \mathbf{P}_3 .

During the second time slot of the third phase, the condition $v \leq L_1$ is not satisfied, the relay does not use Patching and transmits the precoded versions of $s_{1,3,2}$ and $s_{2,3,2}$ by \mathbf{P}_3 .

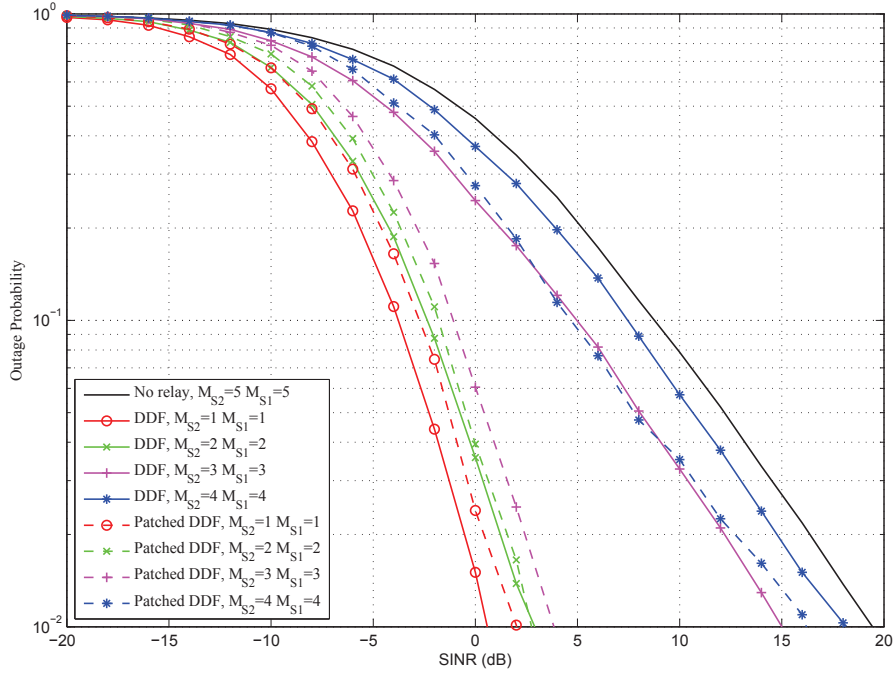


Figure 4.7: Average outage probability at D according to the SINR, $P_R/P_S = 6dB$, $N_r = 1$ for $M_S = M_I \in \{1, 2, 3, 4\}$. The relay uses the optimized precoder for the DDF protocol or the Patched DDF protocol.

4.3.3 Adaptation to a half duplex relay

As previously described, the adaptation of the Patching for precoded DDF protocol for a half duplex relay can easily be done as it only affects the begin of transmission at the relay.

4.3.4 Simulation results

We consider the same set up for simulations as in Section 4.2.2. Moreover, we first consider the performance of an open-loop transmission, and then, the performance of a closed-loop transmission.

Outage probability In Fig. 4.7, the averaged outage probability obtained using the DDF protocol or the Patched DDF protocol, is presented for $M_S = M_I$, which is also the performance obtained for a half duplex relay (beginning to transmit after the correct decoding of both messages). Using the Patched DDF protocol enables to improve the performance for late decoding at the relay ($M_S = M_I = 3$ or 4), whereas for the other cases, performance are lightly decreased due to the coding gain loss resulting from the generation of hyper-symbols and the SNR loss induced by the Patching operation.

Spectral Efficiency In Fig. 4.8, the spectral efficiency achievable with the precoded DDF protocol or the precoded Patched DDF protocol, are presented for $M_S = M_I$. The precoded Patched DDF protocol enables to improve the performance achieved with the precoded DDF protocol for SINR above a threshold depending on the number of patched symbols. The higher the number of patched symbols by the relay, the higher the threshold. Indeed, when $M_S = 1$ and $M_S = 2$,

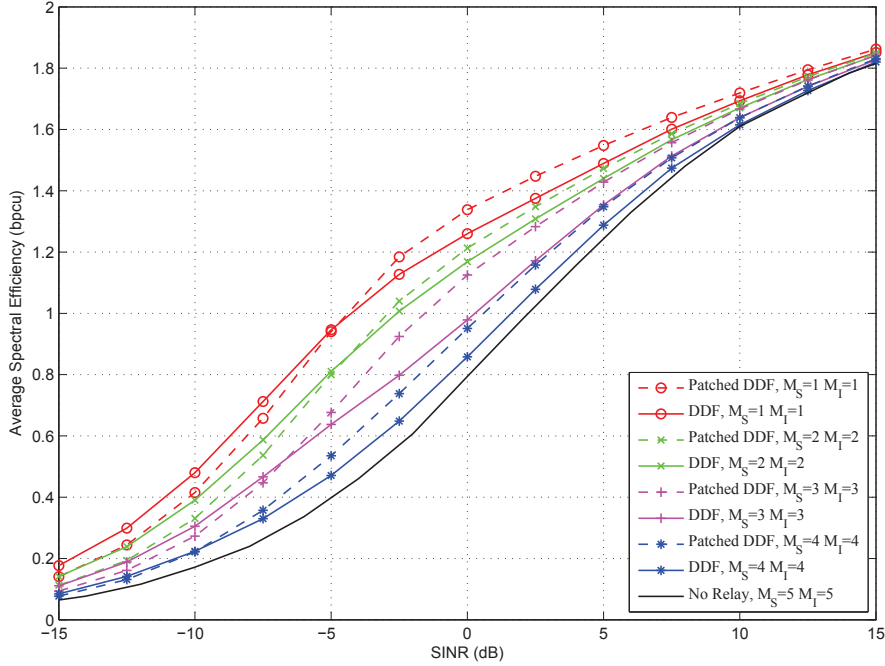


Figure 4.8: Average spectral efficiency maximized over the coding rates, according to the SINR observed at D , $P_R/P_S = 6dB$, $N_r = 1$ for $M_S = M_I \in \{1, 2, 3, 4, 5\}$. The relay uses the optimized precoder for the DDF protocol or the Patched DDF protocol.

$\frac{3T}{7}$ symbols are patched which leads to the same threshold of $-5dB$. For higher values of M_S , less symbols are patched resulting in a lower threshold.

Conclusion

In this chapter, we propose to adapt the DDF protocol for the IRC, where the relay is shared by all source/destination pairs, and where the sources are relay-unaware.

This adaptation of the DDF protocol is pertinent when combined with a precoding technique used at the relay only in order to maximize the minimal capacity between all pairs guaranteeing fairness between users. Simulation results show that the higher the number of precoded symbols by the relay and the better the performance.

We consequently propose to adapt the Patching technique in order to increase the number of precoded symbols and consequently, the achieved performance.

It would be relevant to adapt this scheme to the MARC. Indeed, both channels differ in that the MARC contains a single destination which can consequently performs a joint decoding of the messages. Moreover, over this MARC, the whole power available at the relay is used to convey information toward a single node, and thus experiencing a single pathloss, which leads to a better use of the available power budget.

Chapter 5

System level evaluation of the DDF protocols

Introduction

In the previous chapters, we proposed several DDF relaying schemes for a system comprising relay-unaware sources, and destinations with low complexity decoding abilities.

The performance of these relaying schemes outperforming the no relay case, were derived on a link level basis. However, these transmission schemes need to be evaluated at the system level in order to confirm the provided gains in a full system.

In this chapter, we evaluate the performance of the aforementioned relaying schemes for several scenarios. In Section 5.1, the simulation results concerning unicast are presented for two distinct deployment configurations: the macro cellular system, and an indoor system. Then, in Section 5.2, the performance of these relaying scheme are studied for a broadcast application considering the macro cellular system.

5.1 Unicast transmission

5.1.1 Dedicated relays

In a transmission system dedicated to unicast transmission, e.g. web browsing, each user is attending a different message. For security reasons, a user is not allowed to decode the message intended at another user. Consequently, a user cannot act as a relay for others, and in this system configuration, dedicated relays are needed.

5.1.2 Typical urban macro cellular network

We first consider a unicast transmission in a typical urban macrocellular environment using a 5MHz bandwidth on a frequency carrier of 2GHz. After describing the considered deployment, the propagation models are described so as the nodes association and resource allocation.

		BS	RS	MS
	Height	32m	5m	1.5m
Tx	Ntx	2	2	2
	Ant. type	Omni. (Iso.)/120 pattern (Cell.)	Omni.	Omni.
	Ant. gain	14 dBm	5 dBm	0 dBm
	Ant. downtilt	6	0	0
	Ptmax	43dBm	30dBm	23dBm
	Pt	29.02dBm	16.02dBm	23dBm
Rx	Nrx		2	2
	Ant. type		Direct link to BS	Omni.
	Ant. gain		7dBm	0dBm
	Noise Power		-112.4 dBm	-112.4 dBm

Table 5.1: Nodes characteristics for macro cellular deployment.

a) Deployment

Nodes characteristics In this environment, we consider three types of nodes, the BSs, the MSs, and the RSs which are dedicated relays as described in Chapter 1. We use the nodes characteristics described by the 3GPP TR 36.814 (available online) and some of them are recalled in Tab. 5.1.

Topology These nodes are then differently deployed over the considered area.

We consider two possible deployments for the BSs: we consider a system with an isolated cell, and a system comprising several BSs.

- When the considered system contains a single BS, it is deployed in the middle of the area, and its antenna is omnidirectional. This configuration is described by the long-term SNR map in Fig. 5.1a (considering no shadowing in order to clearly show the BS deployment).
- When there are several BSs in the system, they are deployed such that they generate an hexagonal lattice. Each BS has an antenna diagram of width 120 leading to the formation of three sectors per cell whose antennas are collocated (this is described in 3GPP TR 25.996). In this study, the distance between two sites is equal to 1732m. This deployment is reflected in Fig. 5.1b which shows the achieved long term SINRs at the mobiles over the considered area (considering no shadowing in order to clearly show the BS deployment).

The MSs are uniformly positioned over the area so that the performance reflect all possible MSs positions.

Finally, the relays are placed over the area. We assume that each sector of each cell contains the same number of relays. We consider two deployment models: a circular deployment or a smart deployment.

- When circular deployment is used to place relays in the network. The N relays of a sector are all located at the same distance from the base station and on a regular basis.
- On the contrary, when a smart deployment algorithm is used, the relays are placed in deeply faded areas of the considered cell guaranteeing a minimal distance between them. This relay deployment is presented in Fig. 5.2. On these Figures considering an isolated cell, the distinct

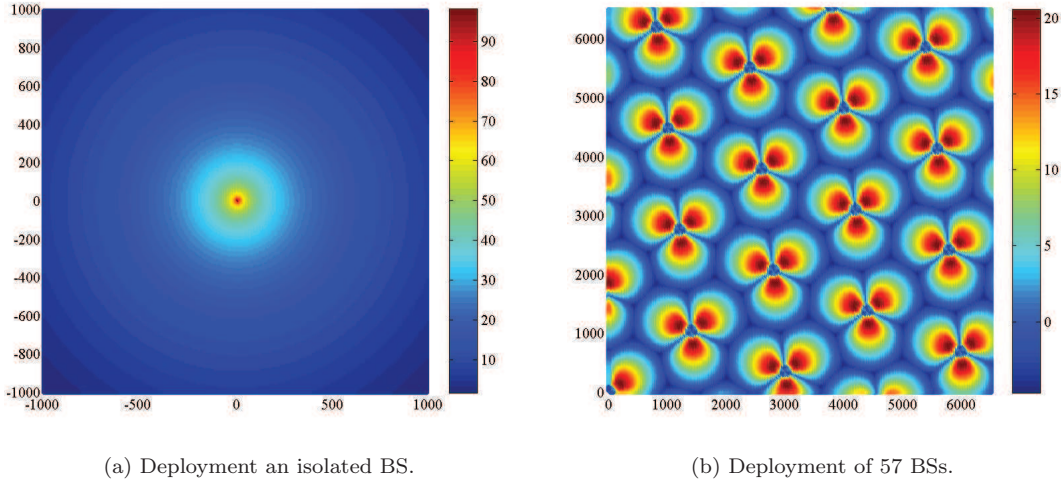


Figure 5.1: Long term SINR at the mobiles over the considered area for two deployment of BSs, considering no shadowing.

colors represent distinct long term SNR levels between the base station and the mobiles. The stars represent the relays' positions. The first two subfigures guarantee a minimal distance of 400m between the relays. However, on the last subfigure, this minimal distance equals 600m for 8 relays which are thus differently placed with respect to Fig. 5.2b.

Propagation model After the deployment of the different nodes in the network, the received power at each node must be computed in order to derive the SINR achieved on each link. This step is done thanks to propagation models used for 3GPP system level simulations described in TR 25.996. As explained in Chapter 1, this derivation is twofold. First, the average received power at the nodes is computed thanks to large scale propagation models. Second, the short-term fading coefficients are generated using multipath propagation models (small scale propagation).

- The pathloss between a BS and a MS is generated by the following expression, coming from the macro cellular LTE propagation model:

$$PL = 40(1 - 4 \cdot 10^{-3}h) \log_{10}(d) - 18 \log_{10}(h) + 21 \log_{10}(f_c) + 80$$

where h is the BS antenna height in meters, f_c is the carrier frequency in MHz, and d is the distance between the BS and MS in kilometers. The shadowing is a correlated random variable of standard deviation 8dB and correlation distance 50m. A penetration loss of 20dB is added.

- The pathloss between a BS and a RS is modeled by

$$PL = 124.5 + 37.6 \log_{10}(d)$$

where d is the distance between the BS and RS in kilometers. These links experience no shadowing, and no penetration loss as the relays are deployed to have a good link with the BS, for instance on the top of buildings.

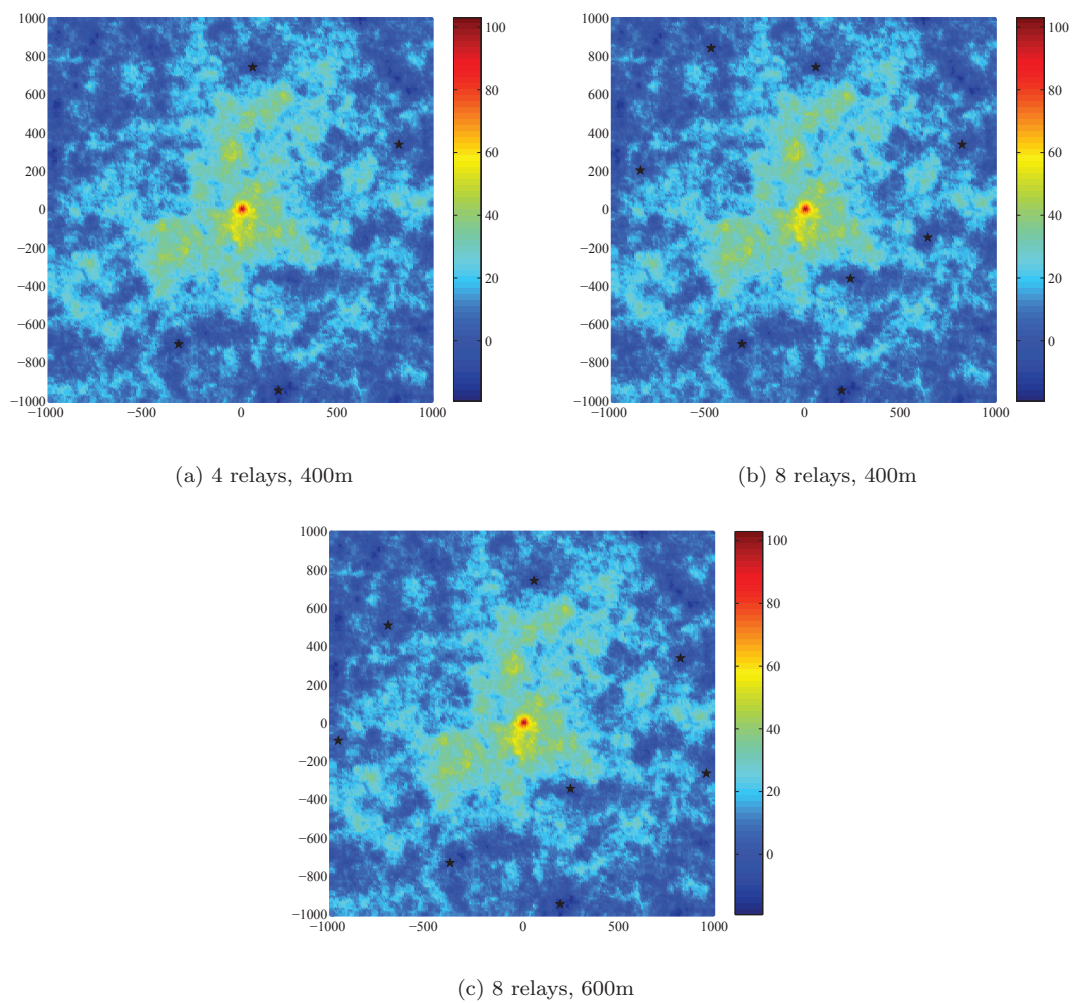


Figure 5.2: Map of SNR between the BS and the UEs in an isolated cell and the relays positions (stars).

- The pathloss between a RS and a RS is modeled by

$$PL = p(103.8 + 20.9 \log_{10}(d)) + (1 - p)(145.4 + 37.5 \log_{10}(d))$$

with

$$p = 0.5 - \min(0.5, 3 \exp(-0.3/d)) + \min(0.5, 3 \exp(-d/0.095))$$

where d is the distance between the RS and the MS in kilometers. These links experience a correlated shadowing of variance 10dB, and a correlation distance of 50m. A penetration loss of 20dB is added.

- The fading coefficients due to the multipath propagation are generated based on a typical urban model whose parameters are described in Tab. 5.4.

b) Nodes association and resource allocation

The mobiles are associated to the BS providing the best path gain, and to the RS in this cell providing the best path gain. Relays belonging to the same cell do not generate any interference between each other as the MSs are perfectly scheduled over the bandwidth. Furthermore, the interference generated by these relays over the users belonging to another cell is neglected.

The MSs are scheduled on the chunk guaranteeing the best short term SNR with the BS over the bandwidth. The proposed relaying schemes are designed so that the BS is relay-unaware, hence, this scheduling is done as if there were no relays in the system.

c) Simulation results

Considering distinct numbers of relays in the cell (between 2 and 16), and several minimal distance for deployment between 200m up to 800m, we obtain the resulting throughput values at each mobile in the cell.

We compare the performance of the case without relay, the Monostream DDF, the DR DDF and the DA DDF when the source transmits a codeword composed of 5 sub-frames. We assume that the first sub-frame is 3 times longer than the other and the coding rate is $R_{c1} \in \{0.5, 0.6, 0.7, 0.8, 0.9, 1\}$. The source can use QPSK, 16QAM or 64QAM. Moreover, we assume that the relay uses modulations up to 64QAM. We modeled the effect of the Modulation and Coding Scheme (MCS)s by choosing at each mobile the coding rate value R_{c1} leading to the maximal throughput value.

We particularly focus on 3 points: the mean throughput in the cell, the 5 percentile throughput in the cell, which is the throughput at least achieved by 5% of the users, and the percentage of users with an improved throughput. Due to computation uncertainties, we consider that a mobile has an improved performance when it is increased of at least 1% when compared to the no relay case. We then study the throughput cdf (defined in Chapter 1) of these users.

Isolated macro cell The cdf of the users throughput are presented in Fig. 5.3, considering the circular and the smart deployments (minimal distance: 400m) of 8 relays, and comparing the performance of the Monostream DDF, the DA DDF and the no relay case. One can observe that both relaying schemes enable to improve the performance when compared to the case without any relay in the cell. Moreover, this improvement through the relay help is possible for all throughput values lower than 4.5bps. Indeed, this value is the maximal spectral efficiency that can be

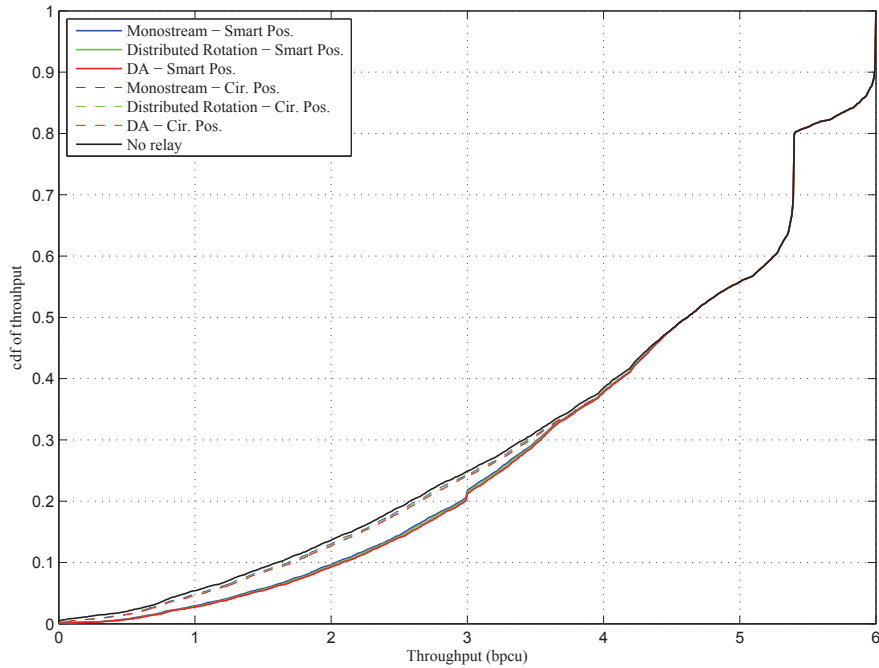


Figure 5.3: Cdf of throughput of the users in an isolated cell containing 8 relays. Comparison of the Monostream relaying scheme and the DA relaying scheme according to the deployment of relays.

obtained with the help of the relay. It corresponds to a correct reception of the message at a MS after receiving the first 2 suf-frames of the codeword using the MCS, $R_{c_1} = 1$ and 64 QAM symbols. The saturations observed at 5.5bpcu and 6bpcu appear as we consider a limited number of available coding rates and modulations. More available MCSs would lead to smoother cdfs.

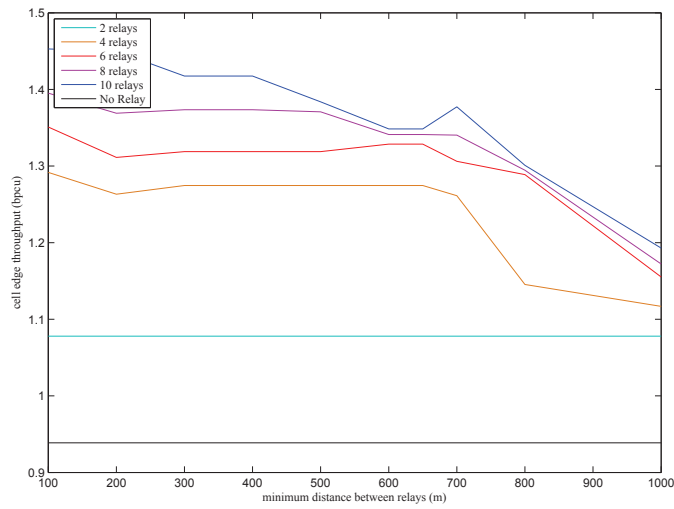
One can observe that the circular deployment for the relay provides very few gains when compared to the case without any relay. The smart deployment achieves better results as relays are deployed in areas where the MSs suffer from deep shadowing.

Finally, whatever the considered deployment methods, both relaying schemes experience quite similar performance as their performance at the link level are already similar for unbalanced SNRs on the BS-MS and RS-MS links. Consequently, the Monostream relaying scheme must be used as it guarantees good performance and requires no additional signaling when compared to the case without relay.

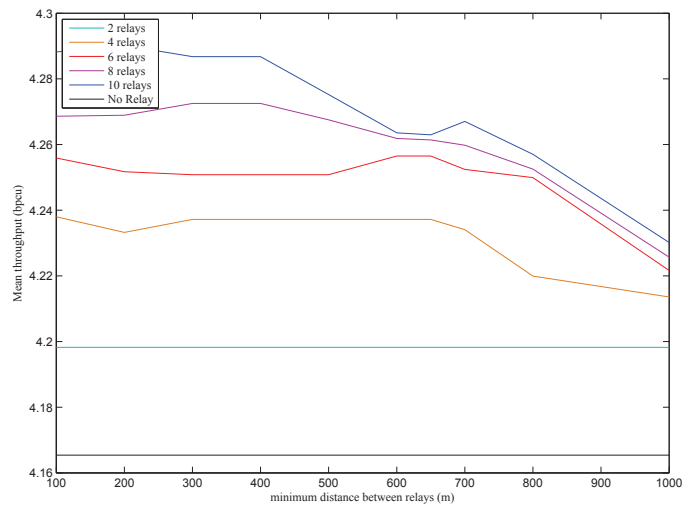
Thus, in the following Figure we consider that the relays are deployed using the smart deployment method, and that they use the Monostream relaying scheme.

The Fig. 5.4 represent the evolution of the cell edge throughput (5 percent-ile), the mean throughput, and the percentage of users whose throughput is improved of at least 1 percent, according to the number of relays in the cell and the minimal distance guaranteed between them.

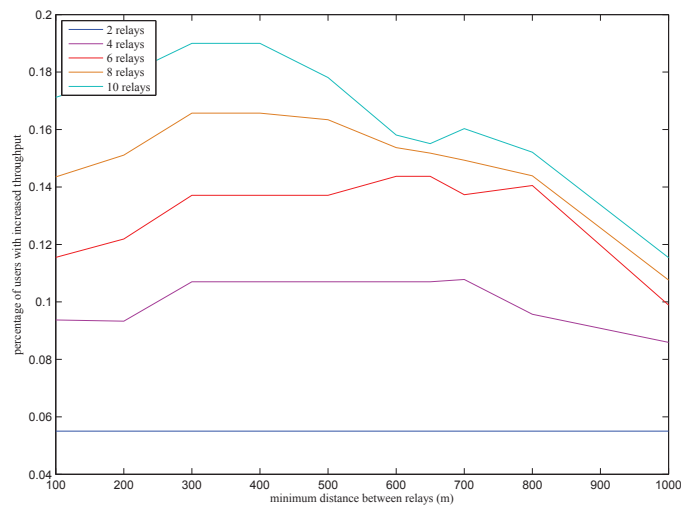
On these figures, a similar behavior is observed: as the number of relays is increasing, and the minimal distance between relays increases, the performance decrease which is due to the cell saturation. Consequently, the achieved performance when the minimal distance is equal to 1000m corresponds to the deployment of 4 or 5 relays, the small difference in performance is generated by different locations of these relays.



(a) Cell edge (5 percentile) throughput.



(b) Mean throughput.



(c) Percentage of users with improved throughput.

Figure 5.4: Throughput according to the number of relays in the cell, and the minimum distance guaranteed between them.

	Cell Edge Throughput (bpcu)	Mean Throughput (bpcu)	% of MSs with improved throughput
No relay	1.0476	2.9463	
Mono. DDF	1.1694	3.0129	11.83
DR DDF	1.1769	3.018	14.30
DA DDF	1.1790	3.0218	15.52

Table 5.2: Particular throughput values over the macro cellular network.

In Fig. 5.4a, is presented the cell edge throughput achieved when the relays use the Monostream DDF protocol for distinct minimal distances between the relays, and different numbers of relays. One can observe that the higher the number of relays in the cell is and the better they are deployed in deeply faded areas, the higher the gains are in terms of cell edge throughput. These gain can be increased by 52% when considering 10 relays deployed with a minimal distance of 100m.

In Fig. 5.4b is presented the mean capacity achieved in the cell when the relays use the Monostream DDF protocol for distinct minimal distances between the relays, and different numbers of relays. For the same reason, the gain can be increased by 3% when considering 10 relays deployed with a minimal distance of 100m.

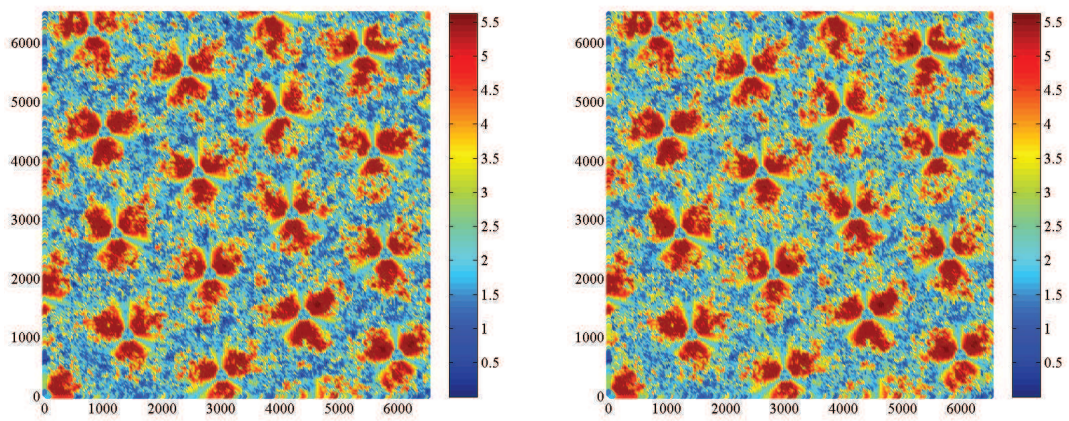
In Fig. 5.4c, the percentage of MSs experiencing an improved throughput of at least 1% when compared to the case without relay is presented according to the minimal distance between each relay pairs, for several number of deployed relays in the cell. The maximum percentage of 19% is not achieved for the highest number of relays and the minimal distance between them but for a minimal distance equal to 300m and 400m. This reveals that relays should not be deployed only at the cell edge in the highly deeply faded areas, but also on cell regions closer from the BS guaranteeing a better BS-RS link, enabling to improve the performance of users with a slightly higher throughput. When this minimal distance is higher than 400m, the performance decrease as relays are deployed in areas where the MSs already achieved the best performance, and cannot be helped by the relays. Consequently, it would be of interest to find the best deployment for each configuration number of relays / minimal distance to maximize the percentage of helped users.

Macro cellular network We now consider that the deployment of 57 BSs generating a macro cellular network helped by 4 relays in each cell. These relays are positioned using the smart positioning method with a minimal distance of 400m between each relay pair.

The performance achieved over such a system are described in Fig. 5.5, where the throughput maps are drawn for the no relay case (Fig. 5.5a) and for the case where the relays use the Monostream DDF relaying scheme (Fig. 5.5b). The gain provided by the relaying technique is sensitive mainly in inter site regions.

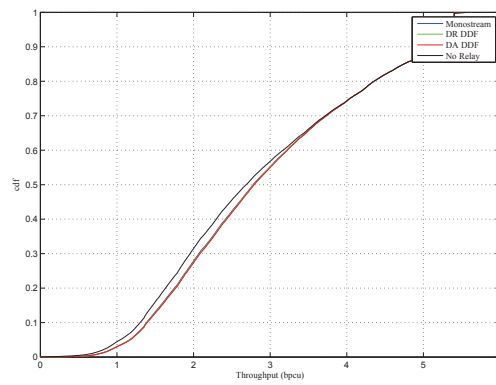
This gain is also shown on the throughput cdf of the users in Fig. 5.5c where the performance of the Monostream, the DA and the DR relaying schemes are compared. These three relaying schemes provide similar gains up to 4.5bpcu which is the highest throughput value which can be achieved through the relay help.

More precisely, the gain provided by the relaying schemes are summarized in Tab. 5.2 describing the cell edge throughput, the mean throughput and the percentage of users with an improved throughput of at least 1% when compared to the case without relay. This table reveals that a minimal cell edge improvement of 11.6% can be achieved using the DDF protocol and that it



(a) Map of throughput without relays.

(b) Map of throughput, Monostream DDF.



(c) Cdf of throughput.

Figure 5.5: Performance over the macro cellular network.

		Pico station (PS)	Femto station (FS)/relay	MS
	Height (m)	1.5	2.5	1.5
Tx	Ntx	2	2	
	Ant. type	Omni	Omni	
	Ant. gain	5	5	
	Carrier frequency (GHz)	2	2	
	Ptmax (dBm)	0	-20	
	Pt (dBm)	-13.98	-33.98	
Rx	Nrx		2	2
	Ant. Type		Omni	Omni
	Ant. gain		5	0
	Noise Power (dBm)		-112.4	-112.4

Table 5.3: Nodes characteristics for indoor deployment.

provides an enhanced mean throughput of 2.2%.

5.1.3 Unicast for indoor small cells

We now consider an indoor deployment of relays using our proposed implementation of the DDF protocol.

a) Deployment

We evaluate the performance of two configurations. On one hand, we consider that the sources and the relays are modeled by Femto Station (FS)s. On the other hand, we consider that the source is modeled by a FS with an increased transmit power and the relays are modeled by FSs. These sources will be called Pico Station (PS)s.

Nodes characteristics The main characteristics of the deployed nodes are described in Tab. 5.3, more details can be found in 3GPP TR 136.931.

Topology We consider the deployment of the different nodes in the MERCE labs located in Rennes, France (48.1164 North, -1.6333 East) whose satellite view is presented in Fig. 5.6.

Four sources are deployed in this building on the same floor: one in the lab center, and the three others in the furthest point of the building. This deployment is presented in Fig. 5.7a where these sources are the four black dots.

Four relays are deployed, each one associated to a source. There are located in the lab in areas experiencing low throughput. In Fig. 5.7b, they are modeled by white dots.

Finally, as we evaluate indoor performance, the considered MSs are located in MERCE lab, and are uniformly deployed over the area.

Propagation model As we consider an indoor deployment, the used propagation model differs from the one used for the macro cellular environment.

On the large scale basis, the path gain is computed according to the Motley Keenan propagation model [71] taking into account the number of wall between the source and the receiver and the



Figure 5.6: Satellite view of MERCE lab (source: google maps).

	Typical Urban	Indoor
Bandwidth (MHz)	5	5
Number of paths	6	17
Attenuation σ^2 (dB)	-7.219, -4.219, -6.219, -10.219, -12.219, -14.219	-0.9463, -7.3400 -19.4778
Delays of arrival	0, 0.2 0.5, 1.6, 2.3, 5	0, 0.015, 0.02, 0.025, 0.03, 0.04, 0.055, 0.06, 0.07, 0.075, 0.09, 0.15, 0.16, 0.17, 0.195, 0.205, 0.225

Table 5.4: Multipath models used for the two considered deployments.

propagation loss between them due to their distance. The wall attenuation is modeled by an deterministic shadowing of 10dB.

The fading coefficients are generated using an indoor model based on the multipath propagation model described in Tab. 5.4.

b) Nodes association and resource allocation

The mobiles are associated to the source providing the best path gain, and to the RS associated to this source.

The MSs are scheduled on the chunk guaranteeing the best short term SNR with the source over the bandwidth. The proposed relaying schemes are designed so that the source is relay-unaware, hence, this scheduling is done as if there were no relays in the system.

c) Simulation results

Pico station assisted by a femto relay The throughput achieved by the indoor users, when the sources are PSs and the relays are FSs, is described in Fig. 5.7.

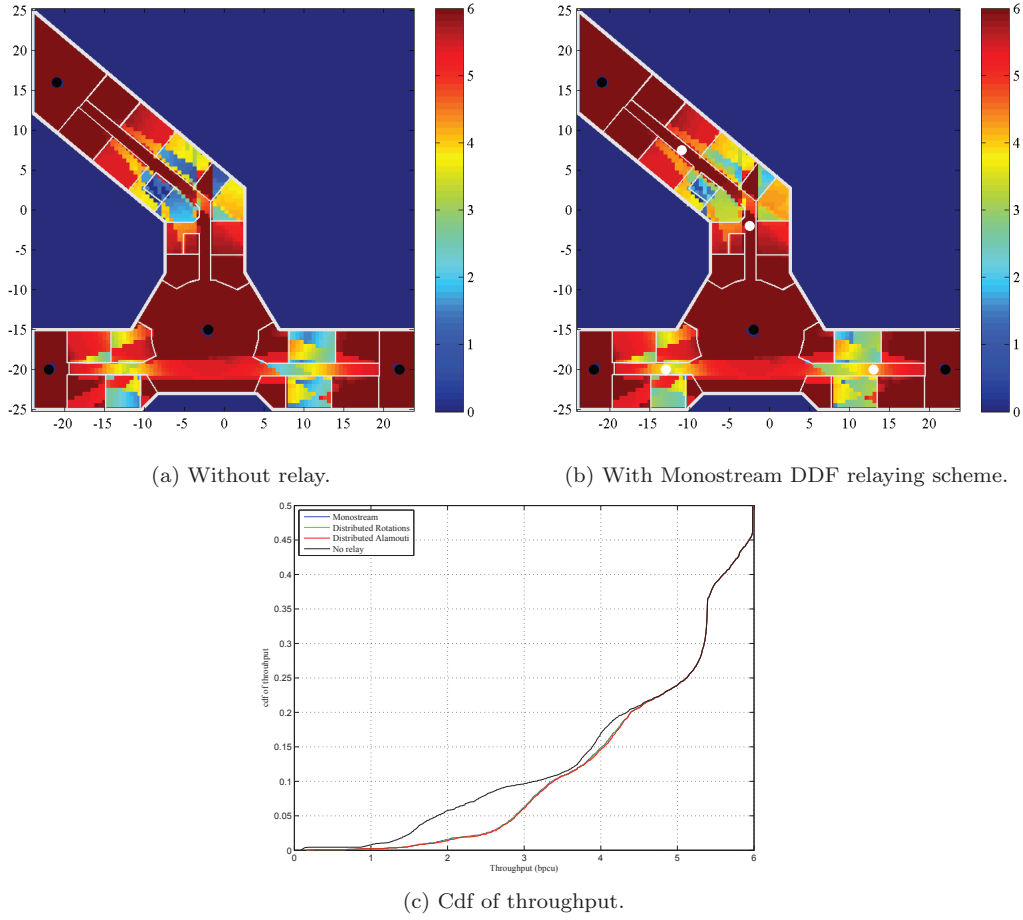


Figure 5.7: Throughput (bpcu) for indoor pico cells (black dots) assisted by femto relays (white dots).

The map of the achieved throughput without the relay in the building is described in Fig. 5.7a. This map shows that there are three areas suffering from low throughput mainly because of wall attenuation.

In Fig. 5.7b, the relays, using the Monostream DDF protocol, are deployed over the area. They provide throughput improvement on the previously mentioned areas which is also revealed by the throughput cdf Fig. 5.7c. The cdf are drawn for the three relaying schemes: the Monostream DDF, the DR DDF and the DA DDF. They all reach almost the same performance, providing a 0.54% improvement of the cell edge (5 percentile) throughput, and a 2% improvement of the mean throughput (see Tab. 5.5).

Femto station assisted by a femto relay The throughput achieved by the indoor users, when the sources are FSs and the relays are FSs, is described in Fig. 5.8.

The map of the achieved throughput without the relay in the building is described in Fig. 5.7a. The performance are worst when compared to the previous case as the transmit power used by the sources is smaller when they are FSs. The three areas suffering from low throughput are consequently wider in this case than in case of PS sources.

In Fig. 5.7b, the relays, using the Monostream DDF protocol, are deployed over the area. They

	Cell Edge Throughput (bpcu)	Mean Throughput (bpcu)	% of MSs with improved throughput
No relay	3.781	5.1991	
Mono. DDF	3.883	5.2979	8.61
DR DDF	3.8967	5.2936	10.64
DA DDF	3.9183	5.2959	13.23

Table 5.5: Particular throughput values when the sources are PSs.

	Cell Edge Throughput (bpcu)	Mean Throughput (bpcu)	% of MSs with improved throughput
No relay	1.5143	4.3005	
Mono DDF	2.6792	4.6537	46.01
DR DDF	2.6792	4.6546	49.08
DA DDF	2.6816	4.6558	49.37

Table 5.6: Particular throughput values when the sources are FSs.

provide throughput improvement on the previously mentioned areas which is also revealed by the throughput cdf Fig. 5.7c. They are drawn for the three relaying schemes: the Monostream DDF, the DR DDF, and the DA DDF. They all reach the same performance, they provide a cell edge (5 percentile) throughput of 1.6 bpcu instead of 0.2 bpcu, and a 8.2% improvement of the mean throughput (see Tab. 5.6).

5.2 Broadcasting

We now consider a second application of the wireless network: the broadcasting, e.g. a video broadcasting. When this application is considered, all sources transmit the same message on the same physical resource and all users intend to decode this unique message.

Consequently, in such a system, the different sources do not generate any interference on the users associated to the other sources.

5.2.1 When users can become relays

In this system, the modulation and coding scheme used to transmit the broadcasted message is chosen in order to achieve a predefined average quality of service at a maximal distance from the source. Then, the users close to the source can potentially decode the message before the end of the transmission, and stop listening to the source till the next message in order to save battery.

However, these users can also use their power in order to assist the transmission by becoming relays for the other users.

Hence, in this section, we propose to study the effect of these relays over the coverage area and the total transmit power used in the system to reach a given coverage.

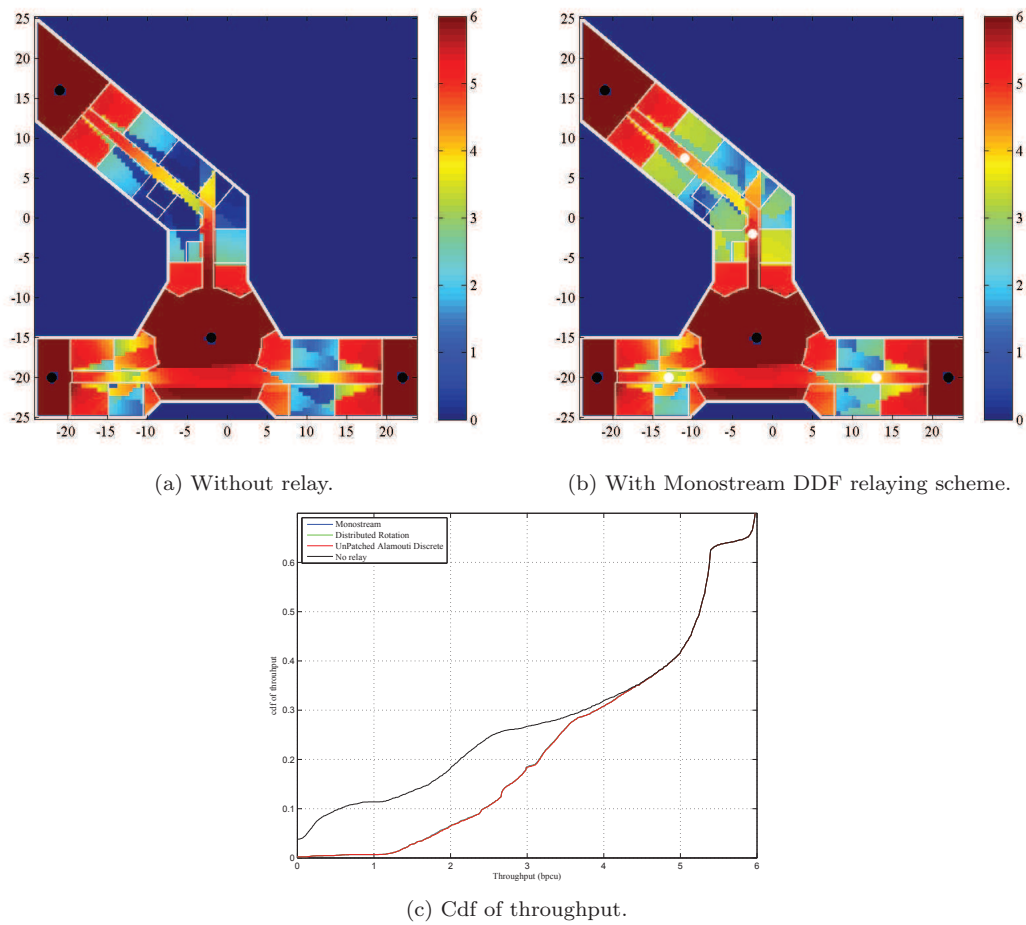


Figure 5.8: Throughput (bpcu) for indoor femto cells (black dots) assisted by femto relays (white dots).

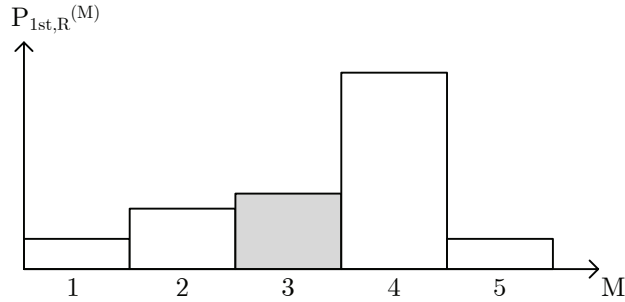


Figure 5.9: Probability of first correct decoding according to the sub-frame index.

a) Activation modes

For a user correctly decoding the message before the transmission ends, we define three activation modes as a relay leading to three different uses of the available power: the systematic mode, the Early Until End (EUE) mode, and the Early Until Average (EUA) mode. In Fig. 5.9 is presented an example of probability of first correct decoding at a node according to the index of the received sub-frames. In this example, we assume that the node has at least 50% chance of correct decoding after receiving the third sub-frame. The different activation modes are illustrated using this example.

Systematic relaying mode The first relaying mode is called systematic as a user turns into relay as soon as it correctly decodes the message and assists this transmission until it ends. Considering the example of Fig. 5.9, whatever the sub-frame index of correct decoding at the node, it will participate in the transmission.

Early Until End relaying mode In order to efficiently use the power resource of each user and thus saving battery, a user will turn as a relay only if its fading coefficient is atypically good, i.e. if it can correctly decode the message before the average instant of correct decoding for its experienced long-term SNR. These relays transmit until the frame ends.

For instance, this will be the case in the example Fig. 5.9 if the node correctly decodes the message after the second sub-frame. It will assist the transmission until the frame's end.

Early Until Average relaying mode The users turn as relays similarly as for the EUE relaying mode, but they stop transmitting at the end of the average block. Indeed, their surrounding neighbors might have correctly decoded the message. Thus, in average, they do not need the help of a relay.

Similarly as for the EUE, this will be the case in the example Fig. 5.9 if the node correctly decodes the message after the second sub-frame but, it will assist the transmission until the end of the third sub-frame.

b) Relaying schemes

After defining these three relaying modes, we focus on the considered relaying schemes for this study of a video broadcasting assisted by relays using our proposed implementation of the DDF protocol.

We consider the Monostream relaying scheme and the DA relaying scheme, which are those requiring less complexity. Indeed, as the relays are users, they do not have high computation abilities.

Distributed Alamouti DDF Because we no longer consider a basic channel study, but a system level evaluation, several relays can assist the transmission simultaneously. Consequently, by using the DA DDF, the relays have the possibility to transmit either the first Alamouti codeword's line, or the second codeword's line. This leads to 3 strategies:

- The relay chooses at random the transmitted line till the transmission ends,
- The relays only transmit the second line of the Alamouti matrix,
- The relays, after sensing the received power of each line of the matrix, sends the line they receive with less power.

5.2.2 Broadcast in a macrocellular network

We consider the deployment of an isolated BS over an urban area as in Section 5.1.2. Consequently, the path gain models, and the multipath model are similar. We assume that there is no shadowing between MSs as they receive signal only from surrounding MSs that are not far enough to suffer from shadowing. The characteristics of the relays are those of the MSs presented in Tab. 5.1.

Moreover, we assume that the transmitted codeword is composed of 5 sub-frames of QPSK symbols, the first sub-frame is three times longer than the others and contains only information bits ($R_{c1} = 1$).

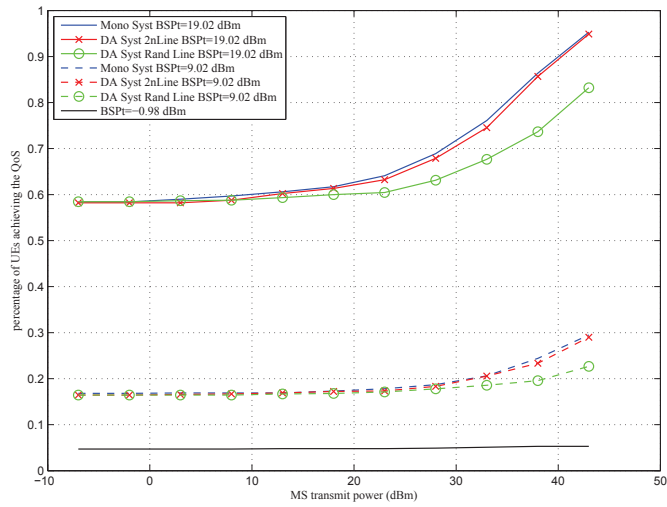
In order to evaluate the power gain provided by the relaying techniques to reach a similar coverage, we make vary the transmission power at the BS in the set $\{-10.98, -0.98, 9.02, 19.02, 29.02\}$ dBm, and at the MSs in the set $\{-7, -2, 3, 8, 13, 18, 23, 28, 33, 38, 43\}$ dBm. A user is said to be under the coverage of the BS if it achieves an average quality of service of 10^{-2} .

a) Evaluation of the systematic activation mode

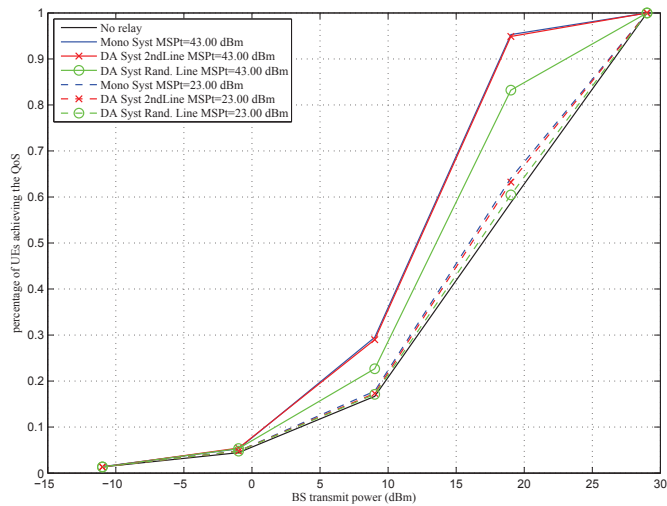
We first consider that the MSs correctly decoding the message before the transmission's end systematically becomes relays.

The achieved performance described in Fig. 5.10 according to two metrics. First, the percentage of users achieving the QoS is plotted according to the transmission power used by the BS, and the transmission power used by the MSs. Then, the total power in the system is represented according to the transmission power used by the MSs. All these results are described for the no relay case, the Monostream systematic case, and the case where the relays use the DA systematic either by transmitting the second line of the Alamouti matrix, or by transmitting a line of this matrix randomly chosen.

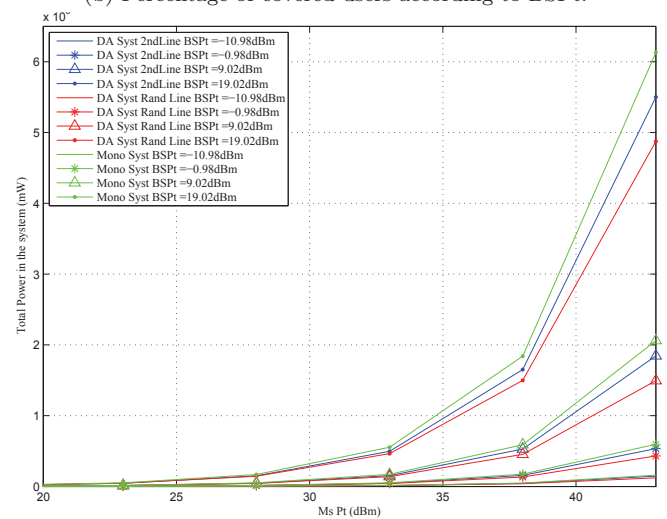
In Fig. 5.10a, the percentage of users achieving the QoS is presented according to the transmission power used by the relays, for several transmission powers at the BS. This Figure reveals that the higher the used transmission powers, and the better the coverage. The relaying protocols impact the coverage as soon as the transmission power used by the relays is higher than 10dBm when $BSPT = 19.02\text{dBm}$, and higher than 23dBm when $BSPT = 9.02\text{dBm}$. The Monostream DDF protocol and the DA DDF protocol in which all relays transmit the second line of the Alamouti matrix achieve almost the same coverage while when the relays transmit a random line of



(a) Percentage of covered users according to MSPr.



(b) Percentage of covered users according to BSPr.



(c) Total power in the system according to MSPr.

Figure 5.10: Performance achieved when the MSs use the systematic activation mode.

this matrix, this coverage is much lower. When the relays use the DA DDF relaying scheme and transmit the matrix line received with less power, the achieved coverage is exactly the same as the performance achieved when transmitting exclusively the second matrix line. Indeed, this line is always received with less power as there is either no relay in the system, or the received power is small when compared to the power received from the BS.

In Fig. 5.10b, the percentage of users achieving the QoS is presented according to the transmission power used by the BS, for several transmission powers at the relays. Similarly, the Monostream DDF protocol and the DA DDF protocol in which all relays transmit the second line of the Alamouti matrix achieve almost the same coverage while but when the relays transmit a random line of this matrix, this coverage is much lower. And, the higher the used power at the relays, and the higher the coverage gain when compared to the case without relay.

In Fig. 5.10c, the total average power in the system is presented according to the transmission power used by the relays, for several transmission powers at the BS. Whatever the considered couples (BSPt, MSPt), the DA DDF 2^{nd} line enables a lower total power in the system than the Monostream DDF even if both protocols provide the same coverage for this couple (BSPt, MSPt). Consequently, this DA DDF protocol allows energy saving to reach the same performance which is due to the coherent combination of the fading coefficients at the users when using this Space Time (ST) code. Finally, when the relays transmit a random matrix line of the Alamouti codeword, the total transmit power in the system is much smaller. Indeed, the achieved coverage is smaller than when the relays use the Monostream relaying scheme, leading to a smaller number of users turning as relays, and consequently less power is used for relaying.

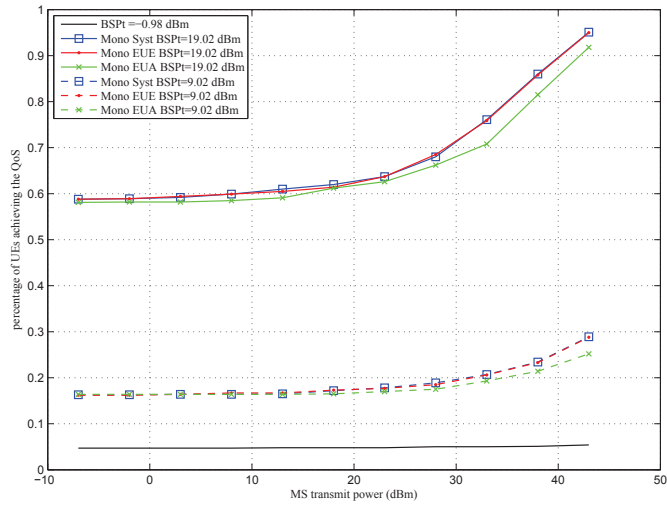
b) Comparison of the activation modes

We now compare the performance achieved by the distinct activation modes when the MSs use the Monostream DDF protocol.

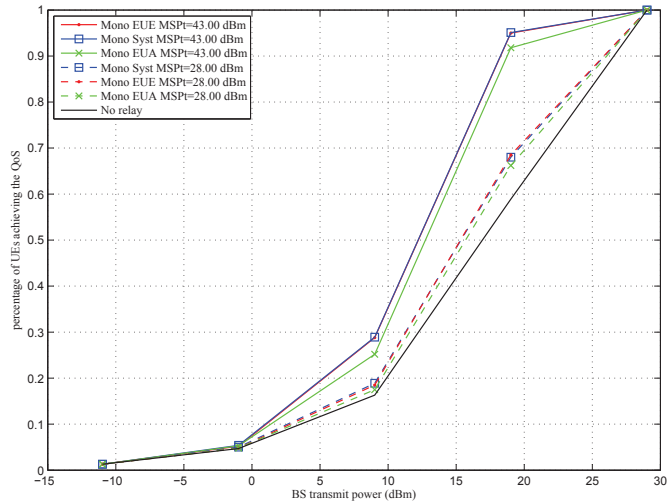
The achieved performance described in Fig. 5.11 in terms of percentage of users achieving the QoS, and total power in the system for the case without relay, the case where the relays use the systematic activation mode, the EUE activation mode and the EUA activation mode.

In Fig. 5.11a, the percentage of users achieving the QoS is presented according to the transmission power used by the relays, for several transmission powers at the BS, and in Fig. 5.11b, the percentage of users achieving the QoS is plotted according to the transmission power used by the BS, for several transmission powers at the relays. These Figures show that the systematic mode and the EUE mode achieve exactly the same coverage. This reveals that the users correctly decoding the message after the average correct decoding time and turning as relays are useless in the system to improve the coverage. They only waste transmission power.

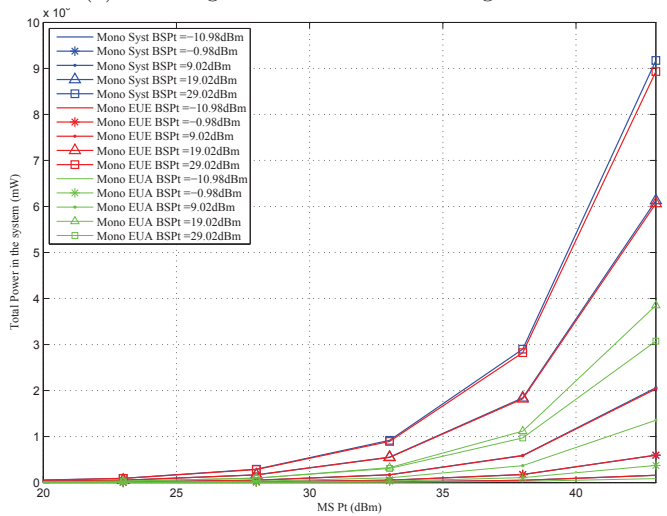
This is reflected in Fig. 5.11c, representing the total average power in the system according to the transmission power used by the relays, for several transmission powers at the BS. Indeed, a slightly smaller amount of power is needed when using the EUE activation mode than when using the systematic mode in order to reach the same coverage. More spectacularly, the power needed when the relays use the EUA mode is much lower than when the systematic and EUE modes are used but still providing similar coverage. Consequently, this transmission mode efficiently uses the available power to achieve a given coverage.



(a) Percentage of covered users according to MSPT.



(b) Percentage of covered users according to BSPT.



(c) Total power in the system according to MSPT.

Figure 5.11: Performance achieved when the MSs using the Monostream relaying scheme and different activation modes.

Conclusion

In this chapter, we studied the performance of the Monostream, the DR and the DA relaying schemes for two applications: a unicast transmission and a broadcast transmission. The performance of these relaying schemes have been evaluated for downlink transmissions in two distinct environments: the macro cellular Typical Urban network, and an indoor transmission in MERCE lab.

The three relaying schemes provide gain when compared to the case without relay. Moreover, these three schemes experience very similar performance. The DA DDF slightly outperforms the Monostream DDF protocol at the system level in term of throughput. Moreover, for the broadcast application, the DA DDF protocol enables to reduce the average power consumption in the network to reach similar coverage.

However, the Monostream DDF protocol still is a promising relaying scheme for the DDF protocol as it enables that both the source and the destination are relay-unaware which guaranteeing backward compatibility, and no additional signaling dedicated for the relaying protocol.

This evaluation must be completed by providing the Patching technique performance at the system level in order to confirm the gain observed at the link level. Moreover, it would be of interest to consider the uplink of these different scenarios in order to reveal the gain provided by the DDF protocol in this context. Indeed, in this case, the relay-unaware source assumption is of particular interest for backward compatibility.

Conclusion and perspectives

In this thesis, we propose and study the performance of a practical implementation of the DDF protocol for plug-and-play relays at the link and system levels.

This practical implementation based on channel coding and codeword segmentation for hybrid automatic repeat request is combined with distinct relaying schemes such as the Monostream scheme, the Distributed Rotation scheme and the Distributed Alamouti scheme.

We show that the three schemes experience the same micro and macro diversity order for a given instant of correct decoding at the relay. The micro diversity order refers to the gain that can be recovered from the short-term channel coefficients. We define the macro diversity order as the number of sources from which the whole information can reliably be recovered even if all other sources experience very poor long-term SNR to the destination. Moreover, we proved that the three schemes outperform the case without relay, and their performance differ thanks to their coding gain: the DA DDF providing better performance than the DR DDF, experiencing better coding gain than the Monostream DDF.

However, the system level studies bring out that this coding gain is meaningless at the system level. This reveals that the pertinent figure of merit to characterize a relaying scheme is the achieved macro diversity order and that the main gain provided by a relaying protocol is at first a long-term SNR gain.

We propose the Patching technique in order to increase the achievable macro diversity order. This technique aims at increasing the number of bits transmitted by the relay up to the number of information bits in the message. When combined with space time block codes, the Patching technique enables to improve both the achievable macro and micro diversity orders.

This Patching technique has also been applied over the Interference Relay Channel where we introduce the use of a precoded DDF protocol at a relay shared by several source/destination pairs. In this case, the Patching technique aims at maximizing the number of precoded symbols at the relay in order to improve the performance achieved by the precoded DDF protocol.

The gain resulting from the use of these various derivations of the DDF protocol are finally observed at the system level for two deployments: a macro cellular network over urban area and an indoor network, and for two applications: a unicast transmission, e.g., web browsing, and a broadcasting transmission, e.g., video broadcasting. The results show that the Monostream relaying scheme for the DDF protocol provides good performance while allowing both the source and the destination to be relay-unaware. Consequently, the Monostream DDF is a promising protocol for the deployment of plug-and-play relays in wireless systems.

The next theoretic step of this work is to prove that, for the multi-relay case, the distributed rotations can provide an increased micro diversity order compared to the Monostream scheme when several relays begin to transmit at the same time.

For future system level evaluations, we will integrate the Patching technique and the precoded DDF protocol in our simulators in order to confirm the gains experienced at the link level.

Our last system study dealing with coverage improvement for a video broadcasting reveals that significant power savings can be done using a particular activation mode at the MSs using the Monostream relaying scheme.

This original way of describing the performance is typical from *green communications*. This concept appeared because of resource scarcity (for instance in a sensor network where sensors work on battery), and because of people increased concern for the impact of electromagnetic waves over health. The aim is to *guarantee a target Quality of Service while minimizing the used resources: time, frequency, and power*. This new way of considering communication system leads to the definition of new metrics, for instance expressed in bit per second per Hertz and per Joule.

We are interested in the future by the design of relaying protocols taking into account a plurality of power optimizations: the transmission power of a device, its computation power (used to encode/decode the signals), or its hardware power consumption.

Appendix A

Recovering diversity from channel coding

A.1 Diversity bound for the uncorrelated block-fading channel

We here recall the proof leading to the diversity bound achieved by the transmission of a codeword generated by a channel encoder of rate R over a block fading channel of N blocks, each block containing L_{BF} symbols. Each channel block is characterized by a fading coefficient, all fading coefficients being independent from one another.

This bound has been derived in [52]:

All codewords of the code can be written as: $\mathbf{c} = (\mathbf{c}_1, \mathbf{c}_2, \dots, \mathbf{c}_N)$ where each \mathbf{c}_i is the portion of the codeword transmitted over the i -th channel block and composed of L_{BF} symbols.

In order to achieve a diversity order equal to ν , for every pair of codewords $(\mathbf{c}_1, \mathbf{c}_2, \dots, \mathbf{c}_N)$ and $(\mathbf{c}'_1, \mathbf{c}'_2, \dots, \mathbf{c}'_N)$, there must be $\mathbf{c}_i \neq \mathbf{c}'_i$ for all but at most $N - \nu$ indexes i . Equivalently, the number of non zero distances $d_i(\mathbf{c}_i, \mathbf{c}'_i)$ must be equal to ν .

By considering that each fraction of the codeword \mathbf{c}_i can be written as an element of a $2^{L_{BF}}$ -element alphabet, i.e. the finite field $\text{GF}(q)$ where $q = 2^{L_{BF}}$. Consequently, the re-written codewords \mathbf{c} are from a q -ary code of length N and of rate RL_{BF} .

Consequently, the achieved diversity order is now the minimal distance d_{min} of this q -ary code. By the Singleton bound [72], we have the property that the number of codewords in the code M is upper bounded by $q^{N-d_{min}+1}$. Moreover, because $M = 2^{RN L_{BF}} = q^{RN}$ and $d_{min} = \nu$, it comes:

$$\begin{aligned} q^{RN} &\leq q^{N-d_{min}+1} \\ RN &\leq N - d_{min} + 1 \\ R &\leq 1 - \frac{\nu - 1}{N} \end{aligned}$$

We now consider the case where $R = 1 - \frac{\nu-1}{N}$, we can find a maximum distance separable code of length $N \leq q + 1$ over $\text{GF}(q)$ with $q^{N-\nu+1}$ codewords.

Consequently, the maximal diversity order achievable over the block fading channel can be expressed according to the coding rate R and the number of channel block:

$$\nu_{max} = \lfloor N(1 - R) \rfloor + 1$$

Consequently, in order to achieve full diversity, the coding rate must be inferior to $1/N$.

A.2 Diversity upper bound for the Matryoshka channel

We now consider another block channel called the Matryoshka channel which has been defined in [57]. After recalling the definition of the Matryoshka channel, we recall the diversity upper bound derived for the transmission of a rate R_c linear code over such a channel.

This channel is defined as follows: We consider ν independent variables (v_1, v_2, \dots, v_ν) providing a total diversity order of ν . The Matryoshka channel is composed of the concatenation of N blocks of lengths $\mathcal{L} = (L_1, \dots, L_N)$, and each block being associated to an intrinsic diversity orders D_i , which results in a vector of diversity orders $\mathcal{D} = (D_1, \dots, D_N)$ in a decreasing order. Consequently, D_1 is the maximal achievable diversity order.

The diversity observed after decoding a rate R_c linear code transmitted over a $\mathcal{M}(\mathcal{D}, \mathcal{L})$ channel is upper bounded by $d = D_i$, where i is given by the following inequality:

$$\sum_{k=1}^{i-1} L_k < R_c \sum_{k=1}^N L_k \leq \sum_{k=1}^i L_k$$

As a result, the full diversity order is achieved as soon as $K \geq L_1$, where L_1 is the length in coded bits of the block of highest diversity order.

We here recall the proof of this result: The transmitted codewords belong to a code of length L and dimension K , where $L = \sum_{k=1}^N L_k$, and $K = LR_c$. If $K > \sum_{k=1}^{i-1} L_k$, whatever the considered code, the puncturing of the last $\sum_{k=i}^N L_k$ bits lead to a zero minimum Hamming distance between all codeword pairs because $\sum_{k=i}^N L_k > L - K$. Consequently, $\nu_{max} \leq D_i$.

Now, by supposing that the code is linear and systematic, if the information bits are transmitted over the blocks of highest diversity order, and if $K < \sum_{k=1}^i L_k$, the Hamming distance after puncturing the last $\sum_{k=i+1}^N L_k$ bits remains strictly positive and induce that $\nu_{max} \geq D_i$.

Bibliography

- [1] E. Van Der Meulen, "Three-terminal communication channels," *Advances in applied Probability*, pp. 120–154, 1971.
 - [2] E. Telatar, "Capacity of multi-antenna Gaussian channels," *European Transactions on Telecommunications*, vol. 10, no. 6, pp. 585–595, 1999.
 - [3] J. Proakis, *Digital communications*, vol. 1221. McGraw-hill, 1987.
 - [4] T. Cover, J. Thomas, J. Wiley, *et al.*, *Elements of Information Theory*, vol. 6. Wiley Online Library, 1991.
 - [5] N. Gresset, L. Brunel, and J. Boutros, "Space Time coding techniques with Bit-Interleaved Coded Modulations for MIMO block-fading channels," *IEEE Transactions on Information Theory*, vol. 54, no. 5, pp. 2156–2178, 2008.
 - [6] V. Tarrokh, N. Seshadri, and A. Calderbank, "Space Time coding for high data rate wireless communication: Performance analysis and code construction," *IEEE Transactions on Information Theory*, vol. 44, pp. 744–765, 1998.
 - [7] C. Berrou, A. Glavieux, and P. Thitimajshima, "Near Shannon limit error-correcting coding and decoding: Turbo-codes. 1," *IEEE International Conference on Communications, Switzerland*, vol. 2, pp. 1064–1070, 1993.
 - [8] R. Palanki and J. Yedidia, "Rateless codes on noisy channels," *IEEE International Symposium on Information Theory, USA*, 2004.
 - [9] S. Alamouti, "A simple transmit diversity technique for wireless communications," *IEEE Journal on Selected Areas in Communications*, vol. 16, no. 8, pp. 1451–1458, 1998.
 - [10] J. Belfiore, G. Rekaya, and E. Viterbo, "The golden code: a 2×2 full-rate space-time code with nonvanishing determinants," *IEEE Transactions on Information Theory*, vol. 51, no. 4, pp. 1432–1436, 2005.
 - [11] W. Hachem, P. Bianchi, and P. Ciblat, "Outage probability-based power and time optimization for relay networks," *IEEE Transactions on Signal Processing*, vol. 57, no. 2, pp. 764–782, 2009.
 - [12] M. Nahas, A. Saadani, and W. Hachem, "Performance of asynchronous two-relay two-hop wireless cooperative networks," *IEEE Transactions on Wireless Communications*, vol. 9, no. 3, pp. 1086–1096, 2010.
 - [13] G. Castagnoli, J. Ganz, and P. Graber, "Optimum cycle redundancy-check codes with 16-bit redundancy," *IEEE Transactions on Communications*, vol. 38, no. 1, pp. 111–114, 1990.
-

-
- [14] D. Chase, "Code combining—a maximum-likelihood decoding approach for combining an arbitrary number of noisy packets," *IEEE Transactions on Communications*, vol. 33, no. 5, pp. 385–393, 1985.
- [15] D. Mandelbaum, "An adaptive-feedback coding scheme using incremental redundancy," *IEEE Transactions on Information Theory*, vol. 20, no. 3, pp. 388–389, 1974.
- [16] S. Lin and P. Yu, "A Hybrid ARQ scheme with parity retransmission for error control of satellite channels," *IEEE Transactions on Communications*, vol. 30, no. 7, pp. 1701–1719, 1982.
- [17] J. Hagenauer, "Rate-compatible punctured convolutional codes (RCPC codes) and their applications," *IEEE Transactions on Communications*, vol. 36, no. 4, pp. 389–400, 1988.
- [18] L. Zheng and D. Tse, "Fundamental tradeoff in multiple-antenna channels," *IEEE Transactions on Information Theory*, vol. 49, no. 5, pp. 1073–1096, 2003.
- [19] M. Bloch, J. Barros, M. Rodrigues, and S. McLaughlin, "An opportunistic physical-layer approach to secure wireless communications," *44th Conference on Communication Control and Computing, Allerton*, 2006.
- [20] A. Nosratinia, T. Hunter, and A. Hedayat, "Cooperative communication in wireless networks," *IEEE Communications Magazine*, vol. 42, no. 10, pp. 74–80, 2004.
- [21] J. Laneman and G. Wornell, "Exploiting distributed spatial diversity in wireless networks," in *Conference on Communications Control and Computing, Allerton*, 2000.
- [22] J. Laneman and G. Wornell, "Distributed space-time-coded protocols for exploiting cooperative diversity in wireless networks," *IEEE Transactions on Information Theory*, vol. 49, no. 10, pp. 2415–2425, 2003.
- [23] T. Cover and A. El Gamal, "Capacity theorems for the relay channel," *IEEE Transactions on Information Theory*, vol. 25, no. 5, pp. 572–584, 1979.
- [24] J. Laneman, D. Tse, and G. Wornell, "Cooperative diversity in wireless networks: Efficient protocols and outage behavior," *IEEE Transactions on Information Theory*, vol. 50, no. 12, pp. 3062–3080, 2004.
- [25] R. Nabar, H. Bolcskei, and F. Kneubuhler, "Fading relay channels: Performance limits and space-time signal design," *IEEE Journal on Selected Areas in Communications*, vol. 22, no. 6, pp. 1099–1109, 2004.
- [26] N. Prasad and M. Varanasi, "Diversity and Multiplexing Tradeoff bounds for cooperative diversity protocols," *IEEE International Symposium on Information Theory, USA*, p. 268, 2004.
- [27] K. Azarian, H. El Gamal, and P. Schniter, "On the achievable Diversity-Multiplexing Tradeoff in half-duplex cooperative channels," *IEEE Transactions on Information Theory*, vol. 51, pp. 4152–4172, december 2005.
- [28] P. Mitran, H. Ochiari, and V. Tarokh, "Space time diversity enhancement using collaborative communications," *IEEE Transactions on Information Theory*, vol. 51, pp. 2041–2057, june 2005.
-

-
- [29] M. Khojastepour, A. Sabharwal, and B. Aazhang, "Lower bounds on the capacity of Gaussian relay channel," in *38th Annual Conference on Information Sciences and Systems*, pp. 17–19, 2004.
- [30] S. Yang and J. Belfiore, "Distributed rotation recovers spatial diversity," *IEEE International Symposium on Information Theory, USA*, pp. 2158–2162, 2010.
- [31] A. Goldsmith, S. Jafar, N. Jindal, and S. Vishwanath, "Fundamental capacity of MIMO channels," *IEEE Journal on Selected Areas in Communications, Special Issue on MIMO systems*, 2003.
- [32] G. Kramer and A. Van Wijngaarden, "On the white Gaussian multiple-access relay channel," *IEEE International Symposium on Information Theory, Italia*, p. 40, 2000.
- [33] T. Rappaport, *Wireless communications, principle and practise*. Prentice Hall PTR, 1996.
- [34] P. Elia and P. Kumar, "Explicit, unified DMG optimal construction for the Dynamic Decode-and-Forward cooperative wireless network," *43rd Conference on Communication Control and Computing, Allerton*, 2006.
- [35] P. Elia and P. Kumar, "Approximately-universal Space-Time codes for the parallel, multi-block and cooperative-Dynamic-Decode-and-Forward channels," *Available Online: <http://arxiv.org/abs/0706.3502>*, 2007.
- [36] K. Kumar and G. Caire, "Coding and decoding for the Dynamic Decode and Forward relay protocol," *IEEE Transactions on Information Theory*, vol. 55, no. 7, pp. 3186 – 3205, 2009.
- [37] A. Murugan, K. Azarian, and H. El Gamal, "Cooperative lattice coding and decoding in half duplex channels," *IEEE Journal on Selected Areas in Communications*, vol. 25, no. 2, pp. 268–279, 2007.
- [38] C. Hucher and P. Sadeghi, "Using distributed rotations for a low-complexity Dynamic Decode-and-Forward relay protocol," *IEEE International Conference on Communications, Japon*, 2011.
- [39] C. Hucher and P. Sadeghi, "Towards a low-complexity Dynamic Decode-and-Forward relay protocol," *Available online: <http://arxiv.org/abs/1012.0599>*, 2010.
- [40] N. Prasad and M. Varanasi, "High performance static and dynamic cooperative communication protocols for the half duplex fading relay channel," in *IEEE Global Conference on Communication, USA*, 2006.
- [41] K. Azarian, H. El Gamal, and P. Schniter, "On the optimality of the ARQ-DDF protocol," *IEEE Transactions on Information Theory*, vol. 54, no. 4, pp. 1718–1724, 2008.
- [42] E. Zimmermann, P. Herhold, and G. Fettweis, "The impact of cooperation on diversity-exploiting protocols," *IEEE 59th Vehicular Technology Conference*, 2004.
- [43] B. Zhao and M. Valenti, "Practical relay networks: a generalization of hybrid ARQ," *IEEE Journal on Selected Areas in Communications*, vol. 23, january 2005.
- [44] J. Castura and Y. Mao, "Rateless coding for wireless relay channels," *IEEE Transactions on Wireless Communications*, vol. 6, no. 5, 2007.
-

-
- [45] R. Hoshyar and R. Tafazolli, "Performance evaluation of HARQ schemes for cooperative regenerative relaying," *IEEE International Conference on Communications, Germany*, 2009.
- [46] E. Braginskii, A. Steiner, and S. Shamai, "Broadcast approach and oblivious cooperative strategies for the wireless relay channel: Part I: Sequential Decode and Forward," *Available online: <http://arxiv.org/abs/1007.4540>*, 2010.
- [47] M. Katz and S. Shamai, "Cooperative schemes for a source and an occasional nearby relay in wireless network," *IEEE Transactions on Information Theory*, vol. 55, no. 11, pp. 5138–5160, 2009.
- [48] R. Bernhardt, "Macroscopic diversity in frequency reuse radio systems," *IEEE Journal on Selected Areas in Communications*, vol. 5, no. 5, pp. 862–870, 1987.
- [49] U. Weiss, "Improving coverage and link quality by macroscopic diversity," in *European Personal Mobile Communications Conference, France*, 1999.
- [50] Y. Tang and M. Valenti, "Coded transmit macrodiversity: Block space-time codes over distributed antennas," in *IEEE 53rd Vehicular Technology Conference*, 2001.
- [51] R. Knopp and H. P.A., "Maximizing diversity on block-fading channels," in *IEEE International Conference on Communications, Canada*, 1997.
- [52] E. Malkamaki and H. Leib, "Coded diversity on block-fading channels," *IEEE Transactions on Information Theory*, vol. 45, no. 2, pp. 771–781, 1999.
- [53] N. Gresset, *Nouvelles techniques de codage spatio-temporel avec des modulations codées à bits entrelacés*. PhD thesis, Telecom ParisTech, 2004.
- [54] M. Plainchault, N. Gresset, and G. Rekaya Ben Othman, "Dynamic Decode and Forward relaying for broadcast transmission by relay-unaware source," *IEEE International Conference on Communication, South Africa*, 2010.
- [55] N. Gresset, M. Plainchault, and G. Rekaya Ben Othman, "Macro and micro diversity improvement with patched Dynamic Decode and Forward relaying," *International Conference on Telecommunication, Qatar*, 2010.
- [56] M. Plainchault, G. Rekaya Ben-Othman, and N. Gresset, "Distributed rotations for the Dynamic Decode and Forward protocol," *Submitted to IEEE International Symposium on Information Theory*, 2012.
- [57] G. Kraidy, N. Gresset, and J. Boutros, "Coding for the Non-Orthogonal Amplify-and-Forward cooperative channel," in *IEEE Information Theory Workshop, USA.*, 2007.
- [58] J. Laneman and G. Wornell, "Distributed Space-Time coded protocols for exploiting cooperative diversity in wireless networks," *IEEE Global Telecommunications Conference*, vol. 1, 2002.
- [59] M. Plainchault, N. Gresset, and G. Rekaya Ben Othman, "Patched Distributed Space Time Block Codes," *IEEE International Conference on Communication, South Africa*, 2010.
-

-
- [60] N. Gresset, "Precoder optimization for user fairness in shared relay channels with interference," *IEEE International Symposium on Personal, Indoor and Mobile Radio Communications*, 2011.
- [61] O. Sahin and E. Erkip, "On achievable rates for interference relay channel with interference cancellation," in *Conference Record of the 41-th Asilomar Conference on Signals, Systems and Computers*, pp. 805–809, 2007.
- [62] A. Chaaban and A. Sezgin, "Achievable rates and upper bounds for the interference relay channel," in *Conference Record of the 44-th Asilomar Conference on Signals, Systems and Computers*, pp. 267–271, 2010.
- [63] R. Tannious and A. Nosratinia, "The interference channel with MIMO relay: Degrees of freedom," in *IEEE International Symposium on Information Theory, Canada*, pp. 1908–1912, 2008.
- [64] O. Sahin, E. Erkip, and O. Simeone, "Interference channel with a relay: models, relaying strategies, bounds," in *Information Theory and Applications Workshop*, pp. 90–95, 2009.
- [65] R. Dabora, I. Marind A. Goldsmith, "Relay strategies for interference forwarding," in *IEEE Information Theory Workshop*, pp. 46–50, 2008.
- [66] A. Panah, K. Truong, S. Peters, and R. Heath, "Interference management schemes for the shared relay concept," *EURASIP Journal on Advances in Signal Processing*, vol. 2011, p. 1, 2011.
- [67] O. Munoz-Medina, J. Vidal, and A. Agustin, "Linear transceiver design in nonregenerative relays with channel state information," *IEEE Transactions on Signal Processing*, vol. 55, no. 6, pp. 2593–2604, 2007.
- [68] N. Lee, H. Park, and J. Chun, "Linear precoder and decoder design for two-way AF MIMO relaying system," in *IEEE Vehicular Technology Conference*, pp. 1221–1225, 2008.
- [69] F.-S. Tseng, W.-R. Wu, and J.-Y. Wu, "Joint source/relay precoder design in Amplify-and-Forward relay systems using an MMSE criterion," in *IEEE Wireless Communications and Networking Conference, Hungary*, pp. 1–5, 2009.
- [70] A. Hjørungnes and D. Gesbert, "Complex-valued matrix differentiation: Techniques and key results," *IEEE Transactions on Signal Processing*, vol. 55, no. 6, pp. 2740–2746, 2007.
- [71] A. Motley and J. Keenan, "Personal communication radio coverage in buildings at 900 MHz and 1700 MHz," *Electronics Letters*, vol. 24, pp. 763–764, jun 1988.
- [72] R. Singleton, "Maximum distance q -nary codes," *IEEE Transactions on Information Theory*, vol. 10, no. 2, pp. 116–118, 1964.
-

List of Publications

Journal Publications

1. M. Plainchault, N. Gresset, and G. Rekaya Ben-Othman, *Macro and micro diversity behaviors of practical Dynamic Decode and Forward relaying schemes*, Arxiv preprint arXiv:1106.5364, To be published in IEEE Transaction on Wireless Communications, 2012.

Conference Publications

Published articles

1. M. Plainchault, N. Gresset, and G. Rekaya-Ben Othman, *Patched Distributed Space Time Block Codes*, IEEE International Conference on Communication, Cape Town, South Africa, 2010.
2. M. Plainchault, N. Gresset, and G. Rekaya-Ben Othman, *Dynamic Decode and Forward relaying for broadcast transmission by relay-unaware source*, IEEE International Conference on Communication, Cape Town, South Africa, 2010.
3. N. Gresset, M. Plainchault, and G. Rekaya-Ben Othman, *Macro and micro diversity improvement with patched Dynamic Decode and Forward relaying*, International Conference on Telecommunication, Doha, Qatar, 2010.
4. M. Plainchault, N. Gresset, and G. Rekaya-Ben Othman, *Dynamic Decode and Forward relaying for broadcast transmission by relay-unaware source* IEEE Global Communication Conference, Houston, United States, 2011.

Articles under review

1. M. Plainchault, G. Rekaya-Ben Othman, and N. Gresset *Distributed Rotations for the Dynamic Decode and Forward protocol* IEEE International Symposium on Information Theory, Cambridge, United States, 2012.
-

Patents

Delivered patents

1. M. Plainchault, N. Gresset, and G. Rekaya-Ben Othman, *Method and a device for determining if an information word transferred by at least a source has to be relayed*, EP 2369760
2. M. Plainchault, N. Gresset, and G. Rekaya-Ben Othman, *Method for transferring by a relay at least one signal composed of complex symbols*, EP2326031
3. M. Plainchault, N. Gresset, and G. Rekaya-Ben Othman, *Method and a device for relaying symbols transferred by a source to a destination*, EP 2293467
4. M. Plainchault, N. Gresset, and G. Rekaya-Ben Othman, *Method and a device for relaying symbols transferred by a source to a destination*, EP 2293466

These European patents have been extended to China and to the USA.

Patents under review

Three other patents are currently under review.
